National Library
of Canada

Canadian Theses Service

Ottawa, Canada
K1A 0N4

Bibliothèque nationale
du Canada

Service des thèses canadiennes

NOTICE

The quality of this microform is heavily dependent upon the quality of the original thesis submitted for microfilming. Every effort has been made to ensure the highest quality of reproduction possible.

If pages are missing, contact the university which granted the degree.

Some pages may have indistinct print especially if the original pages were typed with a poor typewriter ribbon or if the university sent us an inferior photocopy.

Previously copyrighted materials (journal articles, published tests, etc.) are not filmed.

Reproduction in full or in part of this microform is governed by the Canadian Copyright Act, R.S.C. 1970, c. C-30.

AVIS

La qualité de cette microforme dépend grandement de la qualité de la thèse soumise au microfilmage. Nous avons tout fait pour assurer une qualité supérieure de reproduction.

S'il manque des pages, veuillez communiquer avec l'université qui a conféré le grade.

La qualité d'impression de certaines pages peut laisser à désirer, surtout si les pages originales ont été dactylographiées à l'aide d'un ruban usé ou si l'université nous a fait parvenir une photocopie de qualité inférieure.

Les documents qui font déjà l'objet d'un droit d'auteur (articles de revue, tests publiés, etc.) ne sont pas microfilmés.

La reproduction, même partielle, de cette microforme est soumise à la Loi canadienne sur le droit d'auteur, SRC 1970, c. C-30.

NL-339 (r. 88/04)

Canada

THE UNIVERSITY OF ALBERTA

GEOTECHNICAL INVESTIGATIONS OF GLACIOTECTONIC DEFORMATION IN CENTRAL AND SOUTHERN ALBERTA

by

©

Po Chow TSUI

A THESIS
SUBMITTED TO THE FACULTY OF GRADUATE STUDIES AND RESEARCH
IN PARTIAL FULFILMENT OF THE REQUIREMENTS FOR THE DEGREE
OF DOCTOR OF PHILOSOPHY
IN
GEOTECHNIQUE

DEPARTMENT OF CIVIL ENGINEERING

EDMONTON, ALBERTA
FALL 1987

Permission has been granted to the National Library of Canada to microfilm this thesis and to lend or sell copies of the film.

The author (copyright owner) has reserved other publication rights, and neither the thesis nor extensive extracts from it may be printed or otherwise reproduced without his/her written permission.

L'autorisation a été accordée à la Bibliothèque nationale du Canada de microfilmer cette thèse et de prêter ou de vendre des exemplaires du film.

L'auteur (titulaire du droit d'auteur) se réserve les autres droits de publication; ni la thèse ni de longs extraits de celle-ci ne doivent être imprimés ou autrement reproduits sans son autorisation écrite.

ISBN 0-315-41001-9

THE UNIVERSITY OF ALBERTA

RELEASE FORM

NAME OF AUTHOR Po Chow TSUI

TITLE OF THESIS GEOTECHNICAL INVESTIGATIONS OF GLACIOTECTONIC DEFORMATION IN CENTRAL AND SOUTHERN ALBERTA

DEGREE FOR WHICH THESIS WAS PRESENTED DOCTOR OF PHILOSOPHY

YEAR THIS DEGREE GRANTED FALL 1987

Permission is hereby granted to THE UNIVERSITY OF ALBERTA LIBRARY to reproduce single copies of this thesis and to lend or sell such copies for private, scholarly or scientific research purposes only.

The author reserves other publication rights, and neither the thesis nor extensive extracts from it may be printed or otherwise reproduced without the author's written permission.

(SIGNED) ....

PERMANENT ADDRESS:

Department of Civil Engineering,
University of Alberta, Edmonton,
Alberta, Canada T6G 2G7

DATED May 6, 1987

THE UNIVERSITY OF ALBERTA

FACULTY OF GRADUATE STUDIES AND RESEARCH

The undersigned certify that they have read, and recommend to the Faculty of Graduate Studies and Research, for acceptance, a thesis entitled GEOTECHNICAL INVESTIGATIONS OF GLACIOTECTONIC DEFORMATION IN CENTRAL AND SOUTHERN ALBERTA submitted by Po Chow TSUI in partial fulfilment of the requirements for the degree of DOCTOR OF PHILOSOPHY.

DR. D.M. CRUDEN ....
Supervisor

DR. S. THOMSON S Thomson ....

DR. N.R. MORGENSTERN ....

DR. J.D SCOTT ....

DR. N.W. RUTTER ....

DR. M.M. FENTON ....
External Examiner

Date April 24, 1987

ABSTRACT

The study of the ice-thrust terrains found in central and southern Alberta indicates that macroscopic deformations due to ice thrusting include concentric folds, fault-bend folds, disharmonic folds, normal faults, strike-slip faults, thrust faults with stair-case geometry, sole thrusts or decollements in the form of shear zones, and duplex structures.

The ice-thrust argillaceous sediments found in the shear zone or sole thrust in Highvale mine were studied by means of the polarizing microscope and the scanning electron microscope. The observed fabric indicates that in addition to glaciotectonism, the ice-thrust sediments found in Highvale mine probably have been disturbed by permafrost, cycles of loading and unloading, and surface weathering. Laboratory work on fissured and brecciated ice-thrust sediments sampled from a bentonitic mudstone in the mine, indicates that the strength of these brecciated deposits is below the peak and, in general, close to residual. Slope stability problems found in the mine are related to the local joint systems and the horizontal shear zone or sole thrust formed by ice thrusting. The intersection of the steeply-inclined local joint sets with the flat-lying shear layer, which has a strength close to residual, permits slope failure to take place readily.

Facies and fabric models were applied to show the relationship between the regional bedrock topographic configuration and the occurrence and attitudes of ice-thrust features. Three glaciotectonic facies are recognized in central and southern Alberta: (1) Escarpment, (2) Valley, and (3) Plains.

Field observations and stability analyses suggest that glaciotectonism in the study areas is caused by foundation failure at the snout of a subpolar ice sheet when its marginal stagnant and frozen area is compressed by the active-flowing upglacier ice and the corresponding earth pressure in the strata.

Applications of glaciotectonics include ice direction indicators, site investigations, interpretation of laboratory test results, slope stability problems, and mechanics on glacier surge and ice-rock avalanches.

ACKNOWLEDGEMENTS

The author wishes to thank Emeritus Professor, Dr. Stanley Thomson, for providing this challenging topic and instructing the author throughout this research. The author would like to express his gratitude to his supervisor, Dr. David Cruden, who guided and discussed the topic with the author during the past four years. The criticism and guidance that the author received from Dr. Thomson and Dr. Cruden are sincerely appreciated. Thanks are also given to Dr. Norbert Morgenstern who first introduced ice-thrust bedrock and its related problems in Alberta to the author. Field work was supported by a Boreal Institute of the University of Alberta grant (#55-30207) to the author and by a Natural Sciences and Engineering Research Council of Canada (NSERC, A3559) grant to Dr. Thomson.

Special thanks are presented to Dr. Andre Chan, who was a former graduate student in this Department and shared the same office with the author, and who gave valuable ideas and assistance to the author during field sampling in the mine at Highvale and laboratory testing. Thanks are given to Dr. Dave Chan who permitted the author to use his computer programs on stress analysis and plotting. The author wishes to express his appreciation to Mr. Lal Samarasekera and Dr. David Sego who showed patience in discussions and willingness to help.

The writer is indebted to TransAlta Utilities Corporation and Alberta Research Council for the release of

their drillhole data of the mine in Highvale. The permission granted by Dr. Dennis Nikols to allow the author to perform field work in Highvale mine is acknowledged. The shear zone in Pit 2 in the mine was introduced to the author by Dr. Mark Fenton, and the rose diagrams of the joint sets measured in Pit 3 in the mine were provided by Dr. Willem Langenberg. The information on the date when the slides occurred was provided by Carolyn Jones and John Pawlowicz of Alberta Research Council, and Harry Laleune of TransAlta Ltd. The author is grateful to Dr. Fenton, Dr. Langenberg, and Mr. Pawlowicz who were always willing to discuss the geological problems observed in the mine. The key maps, logs, and reports of the mine were located with the help of Mr. Conrad Journault of TransAlta Ltd. and Mr. Brian Lyons of Monenco Ltd.

The CANMET reports were offered by Mr. Keith Kosar, and Dr. Kenneth Barron allowed the writer to access to the computer program MBPSSF. The author is grateful to Mr. Bill Kirtley for the permission to enter his ranch and grain farm in Lowden Lake area, and to I.X.L. Industries Ltd. for the permission to enter the clay pits near Eagle Butte area.

Discussions with Dr. R.A. Burwash on the optical properties of minerals and the polarizing microscope were helpful. Thanks are given to Dr. Joszef Toth who took time to discuss the groundwater basics with the author. Mr. Heinrich Heinz translated a German geology article for the writer and his help is much appreciated. Thin sections were made by Mr. Campbell Kidston and Mr. Max Baaske of Alberta Research Council. SEM samples were prepared with the help of Mr. George Braybrook. X-Ray diffraction analysis was performed by Susan Putz and Lora Swensen of Alberta Research Council. The writer is also grateful to Mr. Steve Gamble and Mr. Jay Khajuria for laboratory instrument preparation. Mr. J. Rogers assisted in taking some of the laboratory photographs. Mr. John Fekete of Alberta Transportation provided bench mark information and road sections along Highway 56 south of Lowden Lake. Thanks are given to Dr. Stephen Moran and Charlotte Mougeot who pointed out the location of suspected ice-thrust features near McDonald Lake and Vermilion areas to the writer.

At last, the deepest gratitude is given to Mr. J.A. Proudfoot, an instructor of Red Deer College, who exposed the fascinating worlds of Geography and Geological Sciences to the author through his idea-stimulating and encouraging lectures and field trips, and had influenced the latter to shift his major field of interest from Business Administration to Earth Sciences.

Table of Contents

Chapter Page

1. INTRODUCTION 1

1.1 Thesis Topic and Purpose of Investigation 1

1.2 Scope and Organization of Thesis 2

2. BACKGROUND OF GLACIOTECTONISM AND METHODS OF INVESTIGATION 4

2.1 Definition of Ice-Thrust Ridges and Glaciotectonism 4

2.2 Literature Review 5

2.3 Characteristics of Ice-Thrust Features 8

2.3.1 Morphology 8

2.3.2 Topography of Occurrence 9

2.3.3 Stratigraphy and Lithology 10

2.3.4 Structure 12

2.3.4.1 Folds 12

2.3.4.2 Faults 12

2.3.4.3 Thrust Sheets 13

2.3.4.4 Scars 14

2.3.5 Glacial Origin 15

2.4 Methods of Investigation 16

3. DESCRIPTION OF THE STUDY AREAS 18

3.1 Location and Accessibility of the Study Areas .18

3.2 Regional Physiography 20

3.3 Regional Bedrock Geology 21

3.3.1 Stratigraphy 21

3.3.2 Geological History 21

3.4 Physiography, Surficial Geology, and Glacial History of the Study Areas 23

3.4.1 Introduction 23

3.4.2 Conclusions 24

4. MORPHOLOGY AND SURFICIAL GEOLOGY OF ICE-THRUST TERRAIN 26

4.1 Method of Study 26

4.2 Identification of Ice-Thrust Features 27

4.2.1 Description and Classification of Morainal Features 27

4.2.2 Examples 30

4.3 Terrain Analysis 31

4.3.1 Definition 32

4.3.2 Results 33

4.3.2.1 Ice-Thrust Terrain Unit 33

4.3.2.2 Ice-thrust Terrain Pattern 35

4.4 Discussion 39

4.5 Conclusion 40

5. MACROFABRIC 42

5.1 Faults 42

5.1.1 Sole Thrusts or Shear Zones 42

5.1.1.1 Field Description 42

5.1.1.2 Subsurface Investigation 53

5.1.1.3 Observation and Interpretation of the Subsurface Cross-Sections 63

5.1.2 Thrust Faults 67

5.1.3 Strike-Slip Faults 68

5.1.4 Normal Faults 70

5.2 Folds 71

5.2.1 Description 71

5.2.2 Concentric Folds 75

5.2.3 Fault-Bend Folds 77

5.3 Scars 80

5.3.1 Genesis 80

5.3.2 Method of Study 82

5.3.3 Calculation of Depth to Decollement 83

5.3.4 Discussion 86

5.4 Jointing 88

5.4.1 Field Description 88

5.4.1.1 Joint Orientation 88

5.4.1.2 Joint spacing and roughness ...89

5.4.2 Discussion 91

5.5 Kinematic Analysis of the Formation of Glaciotectonic Macrofabric 95

6. MESOFABRIC, MICROFABRIC AND SUBMICROFABRIC OF ICE-THRUST SEDIMENTS 102

6.1 Introduction 102

6.2 Mesofabric 103

6.2.1 Fold Structure 103

6.2.2 Displacement Shear 105

6.3 Microfabric 110

6.3.1 Observation (for bentonitic mudstone only) 110

6.3.1.1 Texture 112

6.3.1.2 Structure 117

6.4 Submicrofabric 125

6.4.1 Observation 126

6.4.1.1 Elementary Particle Arrangements 126

6.4.1.2 Particle Assemblages 131

6.4.1.3 Pore Spaces 134

6.4.1.4 Shear Structure 135

6.4.1.5 Permafrost and Freeze-Thaw Features 138

6.5 General Discussion 138

6.6 Shear Subzones 148

6.7 Genesis of the Microfabric and Submicroscopic of Ice-Thrust Sediments 153

6.7.1 Deformation Agents 154

6.7.2 Evolution of the Microfabric and Submicrofabric of the Ice-Thrust Sediments 157

6.8 Geological Conditions of the Sediments During Ice Thrusting 162

7. GEOTECHNICAL PROPERTIES OF ICE-THRUST SEDIMENTS ...165

7.1 Introduction 165

7.2 Laboratory Work 166

7.2.1 Classification Tests 166

7.2.2 Consolidation Test 171

7.2.3 Triaxial Tests 174

7.2.4 Direct Shear Test 182

7.3 Discussion 191

7.4 Conclusion 196

8. GLACIOTECTONIC FACIES 199

8.1 Introduction and Definition 199

8.2 Method of Study 200

8.3 Glaciotectonic Facies 202

8.3.1 Escarpment Type 202

8.3.2 Valley Type 206

8.3.3 Plains Type 207

8.4 Discussion 209

9. MODELS OF ICE THRUSTING 214

9.1 Introduction 214

9.2 Thermal Conditions of the Late Pleistocene Ice Sheet in the Study Region 214

9.3 Mechanics of Glaciotectonism 216

9.3.1 Introduction 216

9.3.2 Ice Surface Profile and Permafrost 217

9.3.3 Geometry of a Glaciotectonic Rupture Surface 221

9.3.4 Strength Properties 223

9.3.5 Stability Analysis 225

9.3.5.1 Plains Type Glaciotectonic Facies 227

9.3.5.2 Escarpment/Valley Type Glaciotectonic Facies 237

9.4 Discussion 242

9.5 Models of Ice Thrusting 244

10. APPLICATIONS OF GLACIOTECTONICS 251

10.1 Geological Applications of Glaciotectonics ...251

10.1.1 Ice Direction Indicator. Case Study: Lowden Lake and Beltz Lake Areas 251

10.1.1.1 Introduction 251

10.1.1.2 Field Descriptions 252

10.1.1.3 Discussion 256

10.1.1.4 Analysis of the Direction of Ice Movement 259

10.1.1.5 Glacial History 263

10.1.2 Applications to Surficial Deformation .265

10.1.3 Applications to Log Interpretation 266

10.2 Geotechnical Applications of Glaciotectonics .267

10.2.1 Applications to Slope Stability Problems. Case Study: Analysis of Two Landslides in Highvale Mine, Wabamun Lake Area 267

10.2.1.1 Introduction 268

10.2.1.2 Geology of the Slide Area 269

10.2.1.3 Geometry of Rupture Surface ..269

10.2.1.4 Water table 273

10.2.1.5 Strength Properties 278

10.2.1.6 Stability Analysis 278

10.2.1.7 Discussion 285

10.2.1.8 Conclusions 291

10.2.2 Applications to Site Investigation and Laboratory Testing 292

10.3 Glaciological Applications of Glaciotectonics 294

10.3.1 Ice-Rock Avalanches 294

11. CONCLUSIONS 296

11.1 Conclusions 296

11.2 Recommendations for Future Research 302

11.2.1 Strength of Ice-Thrust Sediments 302

11.2.2 Field Mapping and Classifying an Ice-Thrust Terrain 304

11.2.3 Local Joint System due to Ice Thrusting 305

11.2.4 Thrust System of Ice-Thrust Terrain ...305

11.2.5 Regional Studies of the Occurrence of Ice Thrusting 306

11.2.6 Models of Ice Thrusting 306

REFERENCES 308

Appendix A - Location and Accessibility of the Outcrops and Ice-Thrust Features in the Study Areas 333

A.1 Wabamun Lake Area 333

A.2 Edmonton Area 333

A.3 Red Deer - Stettler Area 334

A.4 Hanna - Sedgewick Area 335

A.5 Cypress Hills Area 336

Appendix B - Physiography, Surficial Geology, and Glacial History of the Study Areas 337

B.1 Wabamun Lake Area 337

B.1.1 Physiography 337

B.1.2 Surficial Geology 337

B.1.3 Glacial History 338

B.2 Edmonton Area 339

B.2.1 Physiography 339

B.2.2 Surficial Geology 340

B.2.3 Glacial History 341

B.3 Red Deer - Stettler Area 342

B.3.1 Physiography 342

B.3.2 Surficial Geology 344

B.3.3 Glacial History 345

B.4 Hanna - Sedgewick Area 347

B.4.1 Physiography 347

B.4.2 Surficial Geology 349

B.4.3 Glacial History 350

B.5 Cypress Hills Area 352

B.5.1 Physiography 352

B.5.2 Surficial Geology 353

B.5.3 Glacial History 355

Appendix C - Airphotograph Interpretation, Field Observations, Terrain Units, Terrain Pattern, and Measured Sections of the Study Areas 358

C.1 Wabamun Lake Area 358

C.1.1 Southern Shore of Wabamun Lake 358

C.1.2 Southern Shore of Isle Lake 364

C.2 Edmonton Area 372

C.2.1 Nisku 372

C.2.2 Gibbons 373

C.3 Red Deer - Stettler Area 375

C.3.1 Lowden Lake Area 375

C.3.2 Beltz Lake Area 386

C.3.3 Northwest of Sullivan Lake Area 391

C.3.4 Nevis Area 396

C.4 Hanna - Sedgewick Area 398

C.5 Cypress Hills Area 401

Appendix D - Calculation of Interbed Slip along Highwall due to Excavation 408

Appendix E - Location and Procedures for Block Sampling, Pit 3, Highvale Mine 411

Appendix F - Microfabric: Laboratory Preparation and Method of Study 414

F.1 Preparation of Samples for Thin Sectioning 414

F.2 Preparation of Thin Sections 416

F.3 Optical Theory Used to Study the Microfabric of Clay 418

F.4 Method of Study 421

Appendix G - Submicrofabric: Laboratory Preparation and Method of Study 422

G.1 Preparation of SEM Samples 422

G.2 Method of Study 423

Appendix H - Laboratory Tests Results 425

Appendix I - Examples of Glaciotectonic Facies 438

I.1 Escarpment Facies 438

I.1.1 Wabamun Lake Area 438

I.1.2 Nisku Area 441

I.1.3 Lowden Lake Area 443

I.1.4 Cypress Hills Area 443

I.2 Valley Facies 446

I.2.1 Edmonton City Area 446

I.3 Plains Facies 450

I.3.1 Hanna - Sedgewick Area 450

I.3.2 Northwest of Sullivan Lake Area 452

List of Tables

Table Page

4.1 Characteristics of Morainal Transverse Features 29

7.1 Classification Test Results of Bentonitic Mudstone and Bentonite 169

9.1 Material Properties of the Frozen Toe Area of a Glacier 230

9.2 Results of Stability Analysis on Glacier Stagnant Toe with Proglacial Permafrost, Plains Glaciotectonic Facies 234

9.3 Results of Stability Analysis on Glacier Stagnant Toe without Proglacial Permafrost, Plains Glaciotectonic Facies 235

9.4 Results of Stability Analysis on Glacier Stagnant Toe with Proglacier Permafrost, Escarpment/Valley Glaciotectonic Facies 240

10.1 Soil Strength along the Highwall Adjacent to Slides 1 and 2, Pit 3, Highvale Mine 280

10.2 Results of the Stability Analysis, Slides 1 and 2, Pit 3, Highvale Mine 283

H.1 Atterberg Limits of Bentonitic Mudstone* in Highvale Mine 426

H.2 Summary of Consolidation Tests on Bentonitic Mudstone 427

H.3 Summary of Consolidated Undrained Triaxial Tests on Bentonitic Mudstone 429

H.4 Summary of Unconsolidated Undrained Traxial Tests on Bentonitic Mudstone 430

H.5 Summary of Drained Direct Shear Tests on Bentontic Mudstone 431

H.6 Summary of Drained Direct Shear Tests on Bentonte 432

H.7 Summary of Drained Direct Shear Tests on Bentonitic Mudstone Core Samples*, Highvale Mine 433

H.8 Geological Descriptions of Core Samples, Highvale Mine 434

Table Page

H.9 Summary of Drained Direct Shear Test on Bentonite Core Samples*, Highvale Mine 436

H.10 Strength Properties of Suspected Ice-Thrust Sediments 437

List of Figures

Figure Page

3.1 Location and Accessibility of the Study Areas and the Outcrops Studied 19

4.1 Classification of Morainal Features of Continental Glacier 28

4.2 Ice-Thrust Ridges and Ridges of Undetermined Origin at and between Lowden Lake and Beltz Lake Areas 38

5.1 Location of the Line of Sections and Boreholes in Pit 3, Highvale Mine 56

5.2 North-South Oriented Line of Sections in Pit 3, Highvale Mine 57

5.3 East-West Oriented Line of Sections in Pit 3, Highvale Mine 58

5.4 A Diagrammatic Sketch of the Formation of Fault-Bend Folds and Ice-Thrust Ridges 79

5.5 Topographic Cross-Section of Ice-Thrust Ridges, Lowden Lake Area 84

5.6 Rose Diagram of Joint Sets measured in Slides 1 and 2, Pit 3, Highvale Mine 90

5.7 A Sketch of the Formation of Ice-Thrust Ridges due to Folding and/or Thrusting 98

6.1 Location References of the Thin Section 111

6.2 A Diagrammatic Sketch of The Fabric Units 113

6.3 Histograms of Inclination Measurements of Conjugate Sets of Microscopic Lineations 122

6.4 Spatial Relationship and Distribution of the Submicrofabric Units 127

6.5 Predicted and Observed Width/Displacement of Shear Zone Due to Ice Thrusting 146

6.6 Lithological and Mineralogical Characteristics of Shear Subzones, Pit 3, Highvale Mine 149

6.7 Evolution of Connectors and Aggregations in the Ice-Thrust Sediments 161

Figure Page

6.8 A Diagrammatic Drawing of the Evolution of the Submicrofabric of Brecciated Sediments, Pit 3, Highvale Mine 163

7.1 Grain Size Distribution of Bentonitic Mudstone 167

7.2 Grain Size Distribution of Bentonite 168

7.3 Consolidation Curves of Bentonitic Mudstone, Highvale Mine 173

7.4 Deviator Stress vs Axial Strain Plot of CU Triaxial Tests on Bentonitic Mudstone 176

7.5 p - q Plot of CU Triaxial Tests on Bentonitic Mudstone 177

7.6 Mohr Circle Plot of Triaxial Tests and Direct Shear Tests on Bentonitic Mudstone 178

7.7 Deviator Stress vs Axial Strain Plot of UU Triaxial Test on Bentonitic Mudstone 180

7.8 Mohr Circle Plot of UU Triaxial Tests on Bentonitic Mudstone 181

7.9 Shear Stress vs Displacement Plot of Drained Direct Shear Test on Bentonitic Mudstone 184

7.10 Shear Stress vs Displacement Plot of Drained Direct Shear Test on Bentonite 185

7.11 Effective Shear Strength vs Effective Normal Stress Plot of the Bentonite 186

7.12 Effective Shear Strength vs Effective Normal Stress Plot of Drained DS Tests on Bentonitic Mudstone, Highvale Mine 187

7.13 A Subsurface Profile of Highvale Mine 190

8.1 Symbols Used in Fabric Diagrams 201

8.2 Fabric Diagram of Escarpment Type Glaciotectonic Facies, Wabamun Lake Area 204

8.3 Fabric Diagram of Escarpment Type Glaciotectonic Facies, Lowden Lake Area 205

Figure Page

8.4 Fabric Diagram of Plains Type Glaciotectonic Facies, Hanna - Sedgewick Area 208

9.1 Surface Profile of the Glacier and Thermal Conditions of the Subglacial Sediments 220

9.2 Glaciotectonic Conditions of the Marginal Stagnant Area of a Subpolar Ice Sheet, Plains Type Glaciotectonic Facies 228

9.3 Free-Body Diagram: a - Plains Type Glaciotectonic Facies, b - Escarpment/Valley Type Glaciotectonic Facies 229

9.4 Glaciotectonic Conditions of the Marginal Stagnant Area of a Subpolar Ice Sheet, Escarpment/Valley Type Glaciotectonic Facies 238

9.5 Model of Glaciotectonism, Escarpment/Valley Glaciotectonic Facies 246

10.1 Histogram of the Frequency of Giant Grooves Observed in Beltz Lake Area 254

10.2 Plan View and Profile of Slide 1, Pit 3, Highvale Mine 270

10.3 Plan View and Profile of Slide 2, Pit 3, Highvale Mine 271

10.4 Piezometric Surfaces in the Bentonitic Sandstone and Coal Layers, Pit 3, Highvale Mine 275

10.5 Piezometric Readings taken at Borehole #HV-83-005 near Slide 1, Pit 3, Highvale Mine 276

10.6 Probable Configurations of Water Tables in Slide Area, Pit 3, Highvale Mine 279

10.7 Pore Water Pressure Distribution along the Rupture Surface of Slide 1, Pit 3, Highvale Mine 282

C.1 Explanation of ELUC Symbols 359

C.2 Symbols Used in Terrain Analysis 361

Figure Page

C.3 Symbols Used in Geologic Sections and Stratigraphic Columns 362

C.4 Terrain Pattern at the Southern Shore of Wabamun Lake 363

C.5 Location Map of Pit 3, Highvale Mine 365

C.6 Location Map of the Two Slides in Pit 3, Highvale Mine 366

C.7 Stratigraphic Section of Slide 1, Pit 3, Highvale Mine 367

C.8 Stratigraphic Section of Slide 2, Pit 3, Highvale Mine 368

C.9 Stereographic Plots of Deformed Beds: a - Pit 2, Highvale Mine, b - Southern Shore of Isle Lake 369

C.10 Terrain Pattern at the Southern Shore of Isle Lake 371

C.11 Terrain Pattern at Nisku Area 374

C.12 Terrain Pattern at Lowden Lake Area 376

C.13 Stereographic Plot of Deformed Beds Exposed in Sections Ea, Eb and Fa, Lowden Lake Area 377

C.14 Stereographic Plot of Deformed Beds Exposed in Sections 1 and D, Lowden Lake Area 378

C.15 Stereographic Plot of Deformed Beds Exposed in Sections B and Gb,Lowden Lake Area 379

C.16 Section D, Lowden Lake Area 380

C.17 Section Fa, Lowden Lake Area 381

C.18 Section Gb, Lowden Lake Area 382

C.19 Terrain Pattern at Beltz Lake Area 387

C.20 Stereographic Plot of Deformed Beds Exposed in Sections 3 and 4, Beltz Lake Area 388

Figure Page

C.21 Stereographic Plot of Deformed Beds Exposed in Sections 5 and 7, Beltz Lake Area 389

C.22 Terrain Pattern at Area Northwest of Sullivan Lake 392

C.23 Section Exposed in Area Northwest of Sullivan Lake 394

C.24 Stereographic Plots of Deformed Beds: a - Section 1, Area Northwest of Sullivan Lake, b - Sections 3, 4a, 4b and 5, Hanna - Sedgewick Area 395

C.25 Terrain Pattern at Nevis Area 397

C.26 Stereographic Plot of Deformed Beds, Nevis Area 399

C.27 Terrain Pattern at Hanna - Sedgewick Area 400

C.28 Terrain Pattern at Cypress Hills Area 403

C.29 Stratigraphic Section of Pit 45, Cypress Hills Area 404

C.30 Stereographic Plot of Deformed Beds, Pits 39 and 45, Cypress Hills Area 405

F.1 Locations in Block Samples for Thin Sectioning and SEM Samples 415

H.1 Lithological and Structural Descriptions of Triaxial Test Samples, Bentonitic Mudstone 428

I.1 Escarpment Type Glaciotectonic Facies, southern shore of Wabamun Lake 439

I.2 Escarpment or Valley Type Glaciotectonic Facies, southern shore of Isle Lake 439

I.3 Escarpment Type Glaciotectonic Facies, Nisku Vicinity, Edmonton area 442

I.4 Escarpment Type Glaciotectonic Facies, Lowden Lake area 442

I.5 Escarpment Type Glaciotectonic Facies, Cypress Hills area 445

Figure Page

I.6 Escarpment Type Glaciotectonic Facies, Cypress Hills area 445

I.7 Valley Type Glaciotectonic Facies, City of Edmonton, Edmonton area 448

I.8 Valley Type Glaciotectonic Facies, City of Edmonton, Edmonton area 448

I.9 Plains Type Glaciotectonic Facies, Hanna - Sedgewick Area 451

I.10 Plains Type Glaciotectonic Facies, Hanna - Sedgewick Area 451

List of Plates

Plate Page

5.1 Shear Surfaces within the Shear Zone Exposed in Pit 2, Highvale Mine 44

5.2 Shear Zone Exposed in Pit 3, Highvale Mine 46

5.3 Minor Shears within the Shear Zone, Pit 3, Highvale Mine 47

5.4 Minor Thrust within Shear Zone, Pit 3, Highvale Mine 47

5.5 Coal Fragments in the Bentonite, Pit 3, Highvale Mine 51

5.6 Gentle Folds in the Bentonitic Sandstone, Pit 3,Highvale Mine 73

5.7 Open to Close Folds Observed in the Bentonitic Sandstone, Pit3, Highvale Mine 74

5.8 Brecciated Coal Lamination Observed in Pit3, Highvale Mine 74

6.1 Monoclinal Structure Observed in the Bentonite, Pit 3, Highvale Mine 104

6.2 Hand Specimen Obtained at Slip Surface of the Shear Zone , Slide 1, Pit 3, Highvale Mine 104

6.3 Hand Specimen of the Bentonite, Slide 2, Pit 3, Highvale Mine 107

6.4 Thin Section of the Bentonite, Slide 2, Highvale Mine 109

6.5 Nodules and Conjugate Sets of Lineations in Clay Matrix, crossed nicols, 42x 115

6.6 Angular to Subangular Peds, crossed nicols, 42x 116

6.7 Sheared Nodules at the Slip Surface, crossed nicols, 42x 116

6.8 Inclined Displacement Shear, crossed nicols, 42x 119

6.9 Compacted Partly Discernible Groups of Clay Platelets 128

Plate Page

6.10 Compacted Partly Discernible Groups of Clay Platelets in Core and Onion Skin of Aggregation 128

6.11 Loosely compacted Partly Discernible Groups of Clay Platelets 129

6.12 Individual Clay Particles Interact with Groups of Clay Particles 129

6.13 Stack Structure and Diamond-shaped Aggregations 130

6.14 Stack Structure and Oval-Shaped Aggregaion 130

6.15 Elliptical-Shaped Aggregations 130

6.16 Contact of the Cores and the Onion Skins of Aggregations 133

6.17 Minor shears Extend through the Onion Skins 133

6.18 Absent of Aggregations at Major Principal Displacement Shear 133

6.19 Submicroscopic Shear Zone 136

6.20 Fractured Clay Platelets at the Shear 136

6.21 Trans-assemblage Pores and Fractures 136

10.1 Set I NE-SW Trending Giant Grooves, Beltz Lake Area 255

C.1 Macrofabric Exposed in Pit 45, Cypress Hills area 407

E.1 Sampling the Bentonitic Mudstone by a Direct Shear Test Mould, Pit 3, Highvale Mine 413

I.1 Looking South Toward Eagle Butte District, Cypress Hills Area 447

1. INTRODUCTION

1.1 Thesis Topic and Purpose of Investigation

This thesis studies the characteristics and distribution of the geological features and their associated geotechnical properties due to glacial deformation in the Lower Tertiary to Upper Cretaceous sedimentary formations that underlie central and southern Alberta. This investigation is performed because:

1. Although ice-thrust features are known to be widespread on the Prairie region in North America and their mechanics of formation have been suggested (Moran et al., 1980; Kupsch, 1962), the macroscopic to submicroscopic fabric of ice-thrust features have neither been fully studied nor reported. This study will document the entire range of scale of the fabric of a heavily overconsolidated ice-thrust sediment and the geological traits to identify them from aerial photos, in the field and in laboratory samples.
2. Glacially-disturbed sediments are weakened and are probably related to many geotechnical problems such as landslides (Morgenstern, 1977; Sauer, 1978; Christiansen and Whitaker, 1976), however, the geotechnical properties of these ice-deformed sediments have not been studied in detail. Recently, slope instability occurred along the highwall of the open strip Highvale coal mine in the Wabamun Lake area, which is known to be in an

ice-thrust terrain (Fenton et al., 1983; Andriashek et al., 1979). This instability had endangered the dragline that operated close to the crest of the slope. Indeed, a safe and economic design of any engineering structure in ice-thrust terrain cannot be attained without a full understanding of the strength properties of the deformed sediments.

3. Most of the literature concerning ice-thrust features on the Prairies are either regional studies (Moran et al., 1980) or local reports (Slater, 1927a; Hopkins, 1923; Byers, 1959). No detailed investigation has been undertaken of the local appearance of ice-thrust features in different parts of central and southern Alberta which relates them to the regional occurrence and distribution of ice thrusting. The comprehension of this relationship will help to indicate the possible locations of ice-thrust terrain in the country and the types of deformations that may exist in the area. This is useful information to any geological or geotechnical investigation that will be undertaken in that region.

1.2 Scope and Organization of Thesis

In Chapter 2, the terminology of glaciotectonism is defined and the background of glacial deformation reviewed. The methods of study used in this thesis are also delineated in this Chapter. Chapter 3 describes the locations, physiography, surficial geology, and glacial history of the areas studied by the author in southern and central Alberta. Field observations and aerial photograph interpretation of these areas are shown in Chapter 4. Macroscopic glacial-deformed structures are described and interpreted in Chapter 5 and the mesoscopic to submicroscopic features observed in the ice-disturbed sediments are indicated in Chapter 6. The processes other than glaciotectonism that might have deformed the sediments in the study areas are also considered in Chapter 6. The types of laboratory work performed on the ice-disturbed sediments and their measured geotechnical properties are presented in Chapter 7. The facies concept applied to glaciotectonism is introduced in Chapter 8 and is used to explain and predict the occurrence of ice thrusting and distribution of ice-deformed features in the region. In Chapter 9, the information on glaciotectonism and ice-deformed features presented in the previous Chapters are used to develop a theory on the mechanics of ice thrusting. The geological, geotechnical, and glaciological applications of glaciotectonics are shown in Chapter 10. Examples are given for certain applications. Finally, conclusions and recommendations for future research on ice thrusting make up Chapter 11.

2. BACKGROUND OF GLACIOTECTONISM AND METHODS OF INVESTIGATION

2.1 Definition of Ice-Thrust Ridges and Glaciotectonism

According to Bates and Jackson (1980), an ice-thrust ridge is an asymmetrical ridge of local, essentially non-glacial material that has been pressed up by the shearing action of an advancing glacier. It is typically 10 - 60 m high, 150 - 300 m wide, and as much as 5 km long. The term is sometimes used incorrectly as a synonym for push moraine, which is an accumulation of glacial drift. An ice-thrust ridge is also known as an ice-contorted ridge, a glacial pressure ridge, a pressure ridge or an ice-pushed ridge.

Ice-thrust ridges are commonly parallel to the margin of the glacier that formed them but may lie perpendicular to the direction of the glacier movement. They have been referred to as ice-thrust features, glaciotectonic features, pseudo-moraines, push moraines, thrust moraines, and push ridges.

Although ice-thrust ridges have been well described, the processes that form them have not. These processes, called glaciotectonism (also known as ice thrusting, ice shoving, glacial tectonics, ice pushing, glaciotectonic deformation) are glacial disturbances of bedrock and glacial sediments near the margin of a glacier by folding, fracturing and faulting, often followed by overthrusting and shearing. They may form topographic highs or lows such as ice-thrust ridges and related depressions on the ground surface due to stresses exerted by the glacier that resulted in drag and/or pushing.

2.2 Literature Review

In Europe, an ice-pressure hypothesis was developed to explain the deformed sediments observed in coastal cliffs of Denmark by Johnstrup (1869; reference of Petersen, 1977). In 1894, Geikie (1894, p. 338 - 340) described the deformation in glacial sediments along the coast of Norfolk, England, and stated that the contorted drift and the incorporated Cretaceous chalk erratics up to 165 m long displaced from the adjacent beds were due to the pressure and movement of an ice sheet. Glaciotectonic disturbances were found in Lias clay, Oxford clay, and other Mesozoic and Tertiary strata in eastern England, the chalk and lignite in Germany, and sediments in Switzerland, Iceland and Russia (Charlesworth, 1957, p. 255). This is followed by Rutten (1960) who described the distribution of ice-pushed ridges on the northwestern European plain (Holland and Germany). Recently, ice-deformed glaciofluvial and glaciomarine sediments have been found in Sweden (Konigsson and Linde, 1977) and in western Norway (Sonstegaard,1979). In southeastern Denmark, glacially contorted pre-Quaternary and Quaternary sediments were noted exposed along coastal cliffs (Berthelsen, 1979). In east Greenland, Quaternary marine and glaciolacustrine sediments have been deformed by the Holocene glacier (Funder and Petersen, 1980). Ice pushed Lower and Middle Pleistocene deposits in the Netherlands have been investigated by Ruegg (1981), Wateren (1981), and Zandstra (1981); and Maarleveld (1981) studied the sequence of ice pushing in Central Netherlands. Most recently, Jaroszewski (1984) reported the glacial disturbed Tertiary sediments of Poland.

In North America, glacial thrust features were first mentioned by Sardeson (1898, 1905, 1906) after he had investigated the deformed Cretaceous sedimentary deposits in southeastern Minnesota. He was followed by Hopkins (1923) and Slater (1926, 1927a) who studied the structure of Mud Buttes and Tit Hills in Alberta and thought that the Pleistocene glaciation has disturbed the uncemented Upper Cretaceous sediments. Later, Lamerson and Dellwig (1957) pointed out that the superficial structures developed in the sedimentary Pennsylvanian rocks exposed in south-central Iowa were due to ice pushing. Mackay (1959) investigated glaciotectonic features in sediments of Pleistocene or earlier age along the Yukon coast. Detailed mapping of the deformed Upper Cretaceous strata in the vicinity of Claybank, Saskatchewan, indicated that the structures were produced by the subglacial drag of a Pleistocene ice sheet (Byers, 1959). Kupsch (1962) summarized the ice-thrust ridges in western Canada with a detailed description of the uncemented Upper Cretaceous rocks which are exposed on the Missouri Coteau Upland that extends from southern

Saskatchewan to east central Alberta. Ice-pushed deformation in northeastern Kansas and North Dakota have been studied by Dellwig and Baldwin (1965) and Bluemle (1966, 1970) respectively. Thomson and Matheson (1970a) noted ice-shoved features in the Upper Cretaceous Eastend Formation which is exposed in the clay pits in the Medicine Hat area, southeastern Alberta; and ice-thrust gravels in central Alberta were observed by Babcock et al. (1978). Subsequently, Sauer (1974, 1978), and Christiansen and Whitaker (1976) studied glaciotectonic features in southern Saskatchewan and stated their effects on slope stability, stratigraphic correlation, seepage problems, and the criteria used to identify subsurface ice-thrust features based on drilling (Christiansen, 1971). Recently, Moran (1971), Clayton and Moran (1974), and Moran et al. (1980) reviewed the genesis and distribution of the glacial-thrust terrain in North America and developed models to explain the mechanism and criteria for ice thrusting. Surficial and geologic maps indicating the distribution of ice-thrust features in central and eastern Alberta have been constructed by Andriashek et al. (1979), Green (1982), and Fenton and Andriashek (1983). Bluemle and Clayton (1984) recognized glacial thrust forms composed of Cretaceous and Tertiary sediments in North Dakota; and uncemented Cretaceous and Tertiary strata and other glacial deposits deformed by the readvances of the Late Wisconsinan ice had been found along the coasts of eastern Massachusetts and southern New York (Oldale and O'Hara, 1984; Mills and Wells, 1974). Hicock and Dreimanis (1985) discussed the glaciotectonically deformed structures in uncemented sediments found in British Columbia and southern Ontario. Most recently, ice-push Ordovician limestone was observed in southern Quebec (Schroeder et al., 1986).

2.3 Characteristics of Ice-Thrust Features

The general geological characteristics of ice-thrust features are briefly outlined below.

2.3.1 Morphology

In map view, ice-thrust features may express themselves as a series of linear to curvilinear, parallel and generally sharply crested ridges with the concave side facing the direction of local ice flow, heights up to 200 m, and a basal width up to 5 km (Rutten, 1960; Christiansen and Whitaker, 1976; Clayton and Moran, 1974). Depressions of a similar size and shape may be present upglacier from the ice-thrust ridges, that is, in a direction opposite to the ice movement causing these ridges. Ice-thrust features may also appear as equidimensional hills up to 50 m high and 5 km across and with or without an elongate or sub-circular depression of similar dimension upglacier (Clayton and Moran, 1974; Sauer, 1978; Moran et al., 1980; Bluemle and Clayton, 1984). Generally, the depression is within 2 km upglacier from the hills. In some places, there may be no depression; in this case, the ice-thrust feature is a hill on the preglacial surface and is simply moved to a new location (Moran et al., 1980, p. 461 - 462). Sometimes ice thrusting may form a series of hills that are aligned parallel to the ice flow direction and decrease in size downglacier from a source area.

2.3.2 Topography of Occurrence

Ice-thrust features in the form of ridges or hills with associated source depressions upglacier have been found mainly in three kinds of topographical configurations: (1) escarpment, (2) valley, and (3) plain. Examples of ice-thrust features found on escarpments are a glacial-thrust hill (surface area = 0.6 km^2) and source depression (surface area = 0.5 km^2) observed on the downglacier crest of a meltwater channel which lies normal to the direction of the ice flow (Moran et al., 1980, fig. 1), and ice-thrust features are also found at and near the Missouri Coteau Escarpment against which the last glacier flowed (Hopkins, 1923; Slater, 1927a; Byers, 1959; Gravenor and Bayrock, 1955; Gravenor et al., 1960, p. 22; Kupsch, 1962; Bluemle, 1970; Bluemle and Clayton, 1984). Glaciotectonic features have been found along the slopes of cuesta escarpments and valleys that faced against the direction of the ice flow (Oldale and O'Hara, 1984; Andrews, 1980; Mills and Wells, 1974). Ice-disturbed sediments have also been found situated on projecting spurs on the sides of the preglacial Gipping Valley which forms part of the margin of the London Basin (Slater, 1927b); a marked correlation of ice-pushed structures with valleys are also noted by Rutten (1960), Jahn (1973), and Wateren (1985). The structure of the ridges in the walls of these valleys indicate that they have been pushed from the valley thalweg outwards. An example of ice-thrust features found on a plain is Herschel Island which is about 11 km long and 180 m high and with a volume of about 8 km^3, and the Herschel Basin upglacier which is about 19 km long and 70 m deep and with a volume of about 6.3 km^3, found on the flat Arctic coastal plain along the Yukon coast (Mackay, 1959, fig. 6). These source depressions formed by ice thrusting are indeed scar structures and will be described in detail later.

2.3.3 Stratigraphy and Lithology

Ice-thrust Pennsylvanian limestones and shales are observed in south-central Iowa (Lamerson and Dellwig, 1957); and in southern Manitoba, glacial drag features occur in the gypsiferous Amaranth Formation of Jurassic age (Wardlaw et al., 1969; Bannatyne, 1971).

In southern Saskatchewan and eastern Alberta, exposures show that ice-thrust ridges are composed mainly of complexly folded and faulted ~~un~~cemented Cretaceous shales, silts, and sands (Kupsch, 1962, p. 583). The ice-deformed Upper Cretaceous Eastend Formation, which is composed chiefly of sands, silts and clays, is exposed in some clay pits near

Claybanks in Saskatchewan (Byers, 1959) and the Cypress Hills in southeastern Alberta (Thomson and Matheson, 1970a). Deformation of Pleistocene deposits, the Sutherland Group, is exposed at Fort Qu'Appelle in southern Saskatchewan (Sauer, 1974). In addition, ice thrusting occurred in the Paleocene Ravenscrag Formation (clays, silts, sands and lignite) and the Upper Cretaceous Judith River Formation (sandstone, clays or clayshale) in southeastern and south-central Saskatchewan respectively (Sauer, 1978). Moreover, the Upper Cretaceous Horseshoe Canyon Formation which is part of the Edmonton Group (coal, shales, sandstones) and the Lower Tertiary Paskapoo Formation (sandstones, minor shales) have been deformed by the ice in the Wabamun Lake district in central Alberta (Pearson, 1959; Andriashek et al., 1979; Green, 1982). Local deformation in the Cretaceous bedrock due to the overriding ice is observed between Innisfail and Morningside in the Red Deer - Stettler area (Stalker, 1960a). In southeastern Alberta, ice-deformed deposits are observed in the Neutral Hills, which are composed of Upper Cretaceous bentonitic shales and sandstones (Gravenor et al; 1960, p. 22) and in the Mud Buttes and Tit Hills, which consist of the Upper Cretaceous Belly River Formation (Hopkins, 1923; Slater, 1927a).

To conclude, ice-thrust features in central and southern Alberta are mainly found in till, marine to continental uncemented sediments (clay, silt, sand) and weakly cemented to cemented sedimentary bedrock (shale, siltstone, sandstone, coal) with a strength that ranged from extremely weak to extremely strong, that lie near to the ground surface of the region. The terms used to describe the strength of the bedrock follow the Canadian Foundation Engineering Manual (1985).

2.3.4 Structure

Ice-thrust structures chiefly include: (1) Folds, (2) Faults, (3) Thrust Sheets, and (4) Scars. They are described in the following paragraphs.

2.3.4.1 Folds

The folds generally are isoclinal, overturned, asymmetrical with an absence of the lower part of the inverted limbs, and associated with imbricate thrusts which always dip against the recent glacial direction at about 30° - 45° (Byers, 1959; Kupsch, 1962, p. 586; Wateren, 1981). Shales may form cores of anticlines and are commonly squeezed into fissures (Lamerson and Dellwig, 1957; Dellwig and Baldwin, 1965).

2.3.4.2 Faults

Thrust faults usually lie along the clay-sand contacts (Zandstra, 1981), within the clay sediments (Slater, 1927a), or follow limestone and shale fractures (Lamerson and Dellwig, 1957). Shearing along these thrust planes forms brecciated and slickensided zones (Christiansen and Whitaker, 1976; Sauer, 1978; Clayton and Moran, 1974).

Kupsch (1962) stated that ice usually thrust or plucked the competent beds (sandstone) over the incompetent beds (clay or shale). Field observation indicated that drag folding is common in incompetent beds and thrust planes usually lie within or adjacent to these beds. Indeed, the thrust planes originated in one horizon or plane of failure which represents the decollement, and the depth to the decollement from the surface is related to the thickness of the permafrost during ice thrusting (Kupsch, 1962, p. 591). The thrusts were reported to steepen upglacier up to 90° as noted by Brinkmann (1953), Slater (1927a, 1927b), and Kupsch (1962, fig. 4).

2.3.4.3 Thrust Sheets

Thrust sheets have a thickness up to 200 m with an average of about 60 m and an area up to 400 km^2 (Mathews and Mackay, 1960; Sauer, 1978; Moran et al., 1980; Eyles and Menzies, 1983; Wateren, 1985), and may have been transported and accumulated as glacial-thrust hills and ridges. In general, they can be recognized on aerial photographs and in the field; however, in some places the thrust sheets and glacial-disturbed structures show no features on the ground surface and can only be determined by drilling (Moran 1971; Christiansen and Whitaker, 1976). Most often they are imbricated, that is, the thrust sheets may be broken into imbricate slabs by imbricate thrust faults. The estimated displacements of the thrust sheet range between 0.01 to 2 km (Byers, 1959; Lessig and Rice, 1962; Mills and Wells, 1974; Moran et al., 1980).

2.3.4.4 Scars

A scar is the so-called 'source depression' found behind the ice-thrust features such as glacial-thrust ridges and hills or thrust blocks. This glaciotectonic scar structure is believed to be bounded by a sole thrust or shear zone at the bottom, tension fractures at the sides that face upglacier and downglacier, and strike-slip faults at the adjacent sides. They are probably formed when layers of bedrock were thrust or dragged forward by the glacier, the thrust block pulls apart at its rear, compresses at its front, and shears along its bottom and the sides. Subsequently, a scar structure, or the source depression that has been described above is left behind the thrust block which may be expressed as ice-thrust ridges or hills.

A glaciotectonic scar structure is rarely reported in the literature probably because a scar structure is an enclosed negative structure and most often is either filled by glacial and/or post-glacial deposits or appears as a shallow depression or water body at the ground surface; thus, the related faults of the structure are seldom exposed. As a result, it is very difficult to recognize this structure on outcrops or drill logs and its presence is mainly inferred from the distribution and configuration of other ice-thrust features, for example, the Herschel Island and Basin discussed in Section 2.3.2. Nevertheless, glaciotectonic 'riftlike' structures up to 11 - 18 m wide and 9 - 15 m deep have been observed along the slopes of a valley where the ice had flowed over and moved away from them (Lessig and Rice, 1962). Field studies indicate that the thrust block that lies in front of this riftlike structure has a surface area of about 8,000 m^2 and a thickness of approximately of 15 m (Lessig and Rice, 1962). In the Lowden Lake area, a scar structure was observed on a slope that the glacier flowed against (see Chapter 5).

2.3.5 Glacial Origin

Many workers (Slater, 1927b; Byer, 1959; Kupsch, 1962; Wateren, 1981) reported that the exposed deformation in ice-thrust terrain are superficial in nature as noted by the presence of low-angle thrust faults, disharmonic folds, and detachment in depth. Moreover, Hopkins (1923, p. 426) noted that within or adjacent to the ice-thrust area, there is no intense local uplift for no old rocks are brought to the surface and no regional tectonic movement could have produced these local deformations. Furthermore, the intimate intermixing of the deformed units with glacial till (Lamerson and Dellwig, 1957), the deformation of uncemented sediments in a solid state (Catto, 1984), the glacial striae which are observed in these features with their trend normal to the fold axes of the deformations, the deformed ridges oriented roughly parallel to the glacier margin, and the thrust hills and source depressions aligned approximately parallel to the ice direction of movement, point to glacial ice as the only source of the deformation force for these ice-thrust features.

Studies also show that ice thrusting occurred within 5 km upglacier from the ice margin due to the location of permafrost zone beneath the glacier (Moran et al., 1980; Moran, 1971, p. 135 - 136; Clayton and Moran, 1974).

2.4 Methods of Investigation

1. Several locations with exposed ice-thrust features in central and southern Alberta were selected for field mapping and airphotograph interpretation in order to investigate the macrofabric of these deformations, their spatial relationships with the adjacent surficial deposits, the direction of recent ice movement, and their distribution in these parts of the region. Bedrock and surficial geology maps, and bedrock and surficial topographical maps of these ice-thrust areas were studied to identify certain stratigraphy and topographic configurations that are especially susceptible to glaciotectonism. The attitudes of fabric elements (such as folds, faults, and strike of the regional bedrock

surface) and the glacier direction of motion observed in the ice-thrust terrains studied would be assembled in Schmidt nets to demonstrate the trends of these fabric elements in the region with respect to each other.

2. Geotechnical laboratory testing, petrographic and scanning electron microscopic studies were performed on samples obtained from one of the sites that had been covered by detailed field investigations. The fabric of the sediments studied at different scales was used to interpret the engineering behavior of the ice-thrust materials in laboratory tests and in natural environments.
3. Limit equilibrium methods were used to indicate that under the thermal conditions of the ice sheet that glaciated the study areas and the properties of the subglacial sediments deduced from the ice-thrust terrains studied, the frozen toe of the glacier would fail and caused glaciotectonic deformation.
4. Backanalysis of two slope movements that occurred in one of the ice-thrust terrains studied based on limit equilibrium methods was used to show that the fundamental understanding of the fabric and strength properties of the ice-thrust sediments deduced from this investigation is valid.

3. DESCRIPTION OF THE STUDY AREAS

3.1 Location and Accessibility of the Study Areas

Five regions situated in central and southern Alberta were visited during the summers of 1983, 1984 and 1985. They are : (1) Wabamun Lake area, (2) Edmonton area, (3) Red Deer - Stettler area, (4) Hanna - Sedgewick area, and (5) Cypress Hills area. Figure 3.1 shows the locations of these regions and the outcrops studied. Within the regions, glacial-disturbed sediments in the Wabamun Lake area and the Edmonton city area have been described by Fenton and Andriashek (1983), Andriashek et al. (1979), and Kathol and McPherson (1975). Stalker (1960a) studied the surficial geology of the Red Deer - Stettler area and produced maps indicating the recent ice-movement direction and the location of some ridges with undetermined origin. Stalker (1973) also documented ridges composed of mixed contorted deposits due to ice movement along the Red Deer River Valley near the town of Drumheller and along Highway 56 south of Lowden Lake. The ice-thrust features exposed in Nisku and Gibbons of the Edmonton area, near Beltz Lake and Nevis in the Red Deer - Stettler area, along Highway 36 and adjacent to the Sullivan Lake in the Hanna - Sedgewick area, and Cypress Hills area were investigated for the first time. Appendix A describes the location and accessibility of the outcrops of the ice-thrust features in these regions studied by the author.

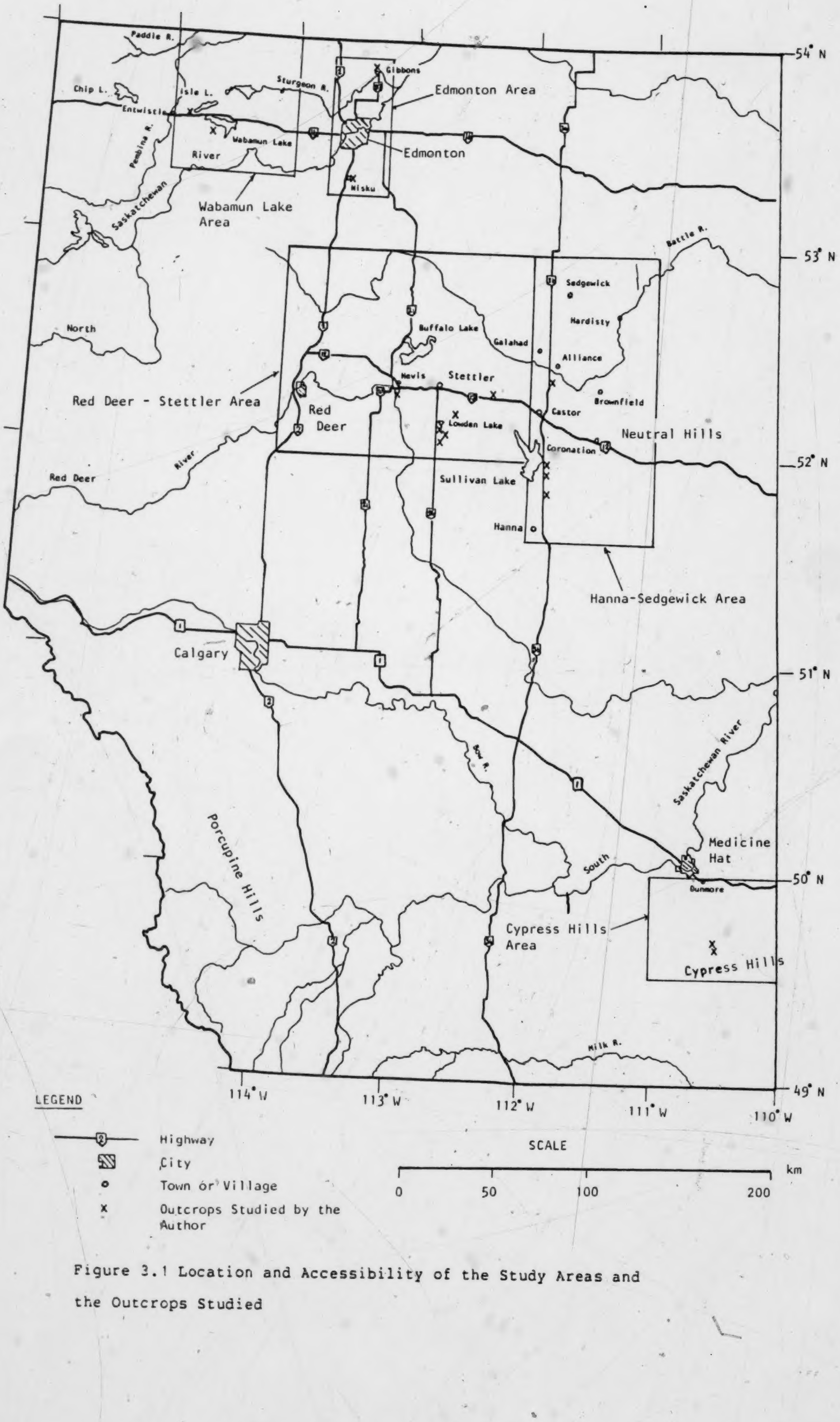
Paddle R.
Chip L.
Isle L.
Entwistle
Pembina R.
Sturgeon R.
Gibbons
Edmonton Area
Edmonton
Wabamun Lake
River
Wisku
Wabamun Lake Area
Saskatchewan
North
Battle R.
Sedgewick
Hardisty
Buffalo Lake
Galahad
Alliance
Nevis
Stettler
Brownfield
Red Deer - Stettler Area
Red Deer
Castor
Lowden Lake
Coronation
Neutral Hills
Red Deer
River
Sullivan Lake
Hanna
Hanna-Sedgewick Area
Calgary
Bow R.
Saskatchewan River
Porcupine Hills
South
Medicine Hat
Dunmore
Cypress Hills Area
Cypress Hills
Milk R.
54° N
53° N
52° N
51° N
50° N
49° N
114° W
113° W
112° W
111° W
110° W
LEGEND
Highway
City
Town or Village
Outcrops Studied by the Author
SCALE
0
50
100
200
km

Figure 3.1 Location and Accessibility of the Study Areas and the Outcrops Studied

3.2 Regional Physiography

Physiographically, the study areas are located in the Alberta Plains which are a subdivision of the Interior Plains Physiographic Province. The Interior Plains are bordered by the Shield on the east and the Cordillera on the west. The Plains are underlain by nearly horizontal strata that range in age from late Proterozoic to Recent. Although virtually the continuation of the Alberta Plateau, the Alberta Plains have a more even topography, with a few widely separated groups of hills such as the Neutral, the Cypress, and the Porcupine Hills (Figure 3.1). Generally, the Plains are at an elevation of 750 m with hills occasionally rising to 1100 m or more (Douglas, 1970, p. 20). The Alberta Plains are tree-covered to semi-arid grassland.

In central and southern Alberta, the general trend of preglacial and modern drainage is eastward or east-northeastward toward the city of Saskatoon and Lake Winnipeg (Stalker, 1961, p. 2). The bedrock topography of Alberta was mainly formed by erosion during Tertiary and early Pleistocene time. Except for certain locations which have been under intense glacial and recent fluvial erosion, most of the preglacial landforms of the area have been preserved beneath the glacial deposits. It is thought that the preglacial bedrock topography of Alberta is in general similar to the bedrock topography observed today. These relatively unmodified preglacial landforms, which are used to deduce the glaciotectonic facies in central and southern Alberta, will be shown in Chapter 8.

3.3 Regional Bedrock Geology

3.3.1 Stratigraphy

This thesis concentrates on the Lower Tertiary to Upper Cretaceous argillaceous and arenaceous deposits and volcanic ashes that crop out discontinuously along roadcuts, ditches, excavations, and river banks in central and southern Alberta. The formations which are exposed in Alberta have been described in detail by Green (1982). The regional attitude of the Horseshoe Canyon Formation has a gentle dip of 0.16° W or SW in the Red Deer-Stettler area (Stalker, 1960a) and a dip of about 0.30° W in the Alberta Plain (Carrigy, 1971).

Most of the strata in the area are bentonitic. Locker (1973, p. 35) reported that both the Horseshoe Canyon and the Belly River Formations contain an average of 23% by weight (of total rock) of montmorillonite with a range of 5 - 75%. Generally, montmorillonite is present as a sandstone cement and also as a main component of the claystones.

3.3.2 Geological History

The Upper Cretaceous - Tertiary bedrock formations of central Alberta were deposited in a subsiding basin flanking highlands to the south and west of the present Rocky

Mountains (Locker, 1973, p. 17).

During the Late Cretaceous Epoch, the highlands to the west were uplifted while the basin to the east subsided. As a result, the highlands acted as the source area and provided debris which was transported to the basin by streams that flowed eastward over a gently sloping depositional surface. The debris that was deposited in the western portion of the continental basin formed the Horseshoe Canyon Formation (formerly the Edmonton Formation) which consists of interbedded sands, silts, clays, organic matter and volcanic tephra; while the debris that was deposited in the eastern portion of the basin below sea level formed the Bearpaw Formation which is mainly composed of silty clays.

In late Cretaceous or early Tertiary time, broad regional uplift occurred and probably was accompanied by orogenic uplift along the Rocky Mountain belt (Webb, 1951, p. 2312). The marine regression in the east and the rejuvenated erosion in the west caused rapid accumulation of fresh-water sediments across the present Foothills and spread eastward onto the Plains. These non-marine deposits formed the Paskapoo Formation. The orogeny caused widespread uplift and the onset of erosion which continues to the present. This post-Tertiary regional erosion is reflected in the Upper Cretaceous beds outcropping in the eastern part of the basin and the broad topographic outlines of the Alberta Plains as observed today. The Tertiary beds are preserved only in the western Plains and adjacent Foothills.

The Late Wisconsinan, Laurentide-Keewatin ice sheet glaciated the Interior Plains of western Canada during the Pleistocene Epoch (Prest, 1984). After this glaciation, the resumed drainage might or might not follow the preglacial drainage system. Most of the post-glacial rivers incised deeply into the glacial deposits and bedrock and formed steep-sided valleys with a depth of 60 m to 90 m below the general Plains level (Locker, 1973).

3.4 Physiography, Surficial Geology, and Glacial History of the Study Areas

3.4.1 Introduction

The discussion of the characteristics of ice-thrust features in Chapter 2 (section 2.3) indicate that the occurrence of ice thrusting and its associated deformation in an area are intimately related to the factors such as the lithology of the surficial bedrock and the topographic configuration of that particular area, and probably the position of the margin of the glacier that caused ice thrusting. Thus, a complete understanding and interpretation of the occurrence and distribution of the ice-thrust features in an area cannot be attained without a full knowledge of these factors. As a result, a detailed picture of the physiography, surficial geology, and glacial geology of each of the study areas is a necessity for this investigation and these are described in Appendix B.

3.4.2 Conclusions

Some important conclusions are obtained after the examination of the physiography, surficial geology, and glacial history of the study areas where ice-thrust features were found (Appendix B). These conclusions are listed below and they are in general consistent with the geologic and topographic characteristics on the occurrence of ice-thrust features observed in other parts of the continent (Chapter 2, Section 2.3).

1. All the study areas are underlain by uncemented to cemented, non-marine to marine sediments of the Lower Tertiary to Upper Cretaceous age which are deposits susceptible to glaciotectonic deformation. Most of these sediments belong to the Belly River, Bearpaw, Wapiti, Horseshoe Canyon, Eastend, Whitemud, Battle, Frenchman, and Paskapoo Formations.
2. All the study areas are located near or within preglacial valleys, meltwater channels, or along the slopes of escarpments or plateaus. Moreover, the slopes of these topographic features in general face against the flowing direction of the last Wisconsinan glacier that invaded the region. For example: the Cypress Hills Plateau.
3. The presence of the glacial features such as hummocky disintegration moraine, glaciolacustrine deposits, and

meltwater channels in the study areas seem to indicate that the last glacier had stagnated with its margin at or close to the study areas. For example: in the Wabamun Lake area, the presence of a relatively thick hummocky disintegration moraine north of Isle and Wabamun Lakes and the presence of meltwater channels along the southwestern shore of the former seem to show that the stagnant ice margin had remained still in the area just north of these lakes for some period of time.

4. Rejuvenation and minor advances seem to have occurred (at least locally) during deglaciation in a few of the study areas. For example: the Red Deer - Stettler and the Hanna - Sedgewick areas, which are composed of till-filled stream trenches and ice-flow markings, suggest that there were rapid (?) readvances after the stagnation of the glacier in these regions.

4. MORPHOLOGY AND SURFICIAL GEOLOGY OF ICE-THRUST TERRAIN

This Chapter investigates the morphology and distribution of ice-thrust features in the study areas and their relationships with the adjacent glacial deposits and topographic features.

4.1 Method of Study

Terrain analysis, which chiefly consists of aerial photograph interpretation and field mapping, is used in this investigation. Typical ice-thrust ridges are found in an arcuate belt that consists of parallel to sub-parallel steep-sided curvilinear ridges with their concave side facing the direction of ice movement (Gravenor et al., 1960, p. 25; Mollard, 1982, p. 32) and typical ice-thrust hills appear as a series of aligned mounds which decrease in size downglacier from a source area (Moran et al., 1980). However, it is noted that, unlike well-known ice-thrust features which are quite distinct on aerial photographs, many ice-thrust features are often expressed as linear forms on the ground and may be easily misinterpreted as other morainal ridges such as end moraines (Kupsch, 1962; Rutten, 1960; Bluemle and Clayton, 1984; Stalker, 1973, plate 18; Oldale and O'Hara, 1984). Thus, a classification method is developed and described below to differentiate ice-thrust features from other glacial features appearing on aerial photographs and in the field.

4.2 Identification of Ice-Thrust Features

4.2.1 Description and Classification of Morainal Features

Figure 4.1 shows that, basically, morainal features can be broadly divided into (1) parallel to ice-flow, (2) transverse to ice-flow, (3) non-oriented. Since this thesis is concerned with ice-thrust ridges which lie transverse or perpendicular to the direction of ice movement, only the morainal features that are transverse to ice-flow are described. They are further classified into features deposited by actively-flowing ice or stagnant ice. Further classification may be based on the composition and morphology of these transverse features. Table 4.1 indicates the morphological characteristics, the dimensions, and composition of these transverse features. The terminology used here mainly follows the nomenclature of moraine and ice-flow features applied to the glacial map of Canada (Prest et al., 1968). Descriptions of these features include the work done by Prest (1968), Gravenor and Kupsch (1959), Gravenor et al. (1960), Stalker (1960b), and Kupsch (1962).

Based on the depositional environment, morainal transverse ridges are classified (Figure 4.1) as:

(i) Live-ice, depositional, transverse features which include: (a) Ice-thrust ridges, (b) Push moraines which are a type of end moraine, (c) ribbed moraines which are also known as Rogen moraines and, (d) De Geer moraines or cross valley moraines. Subclasses (a) and (b) are composed chiefly

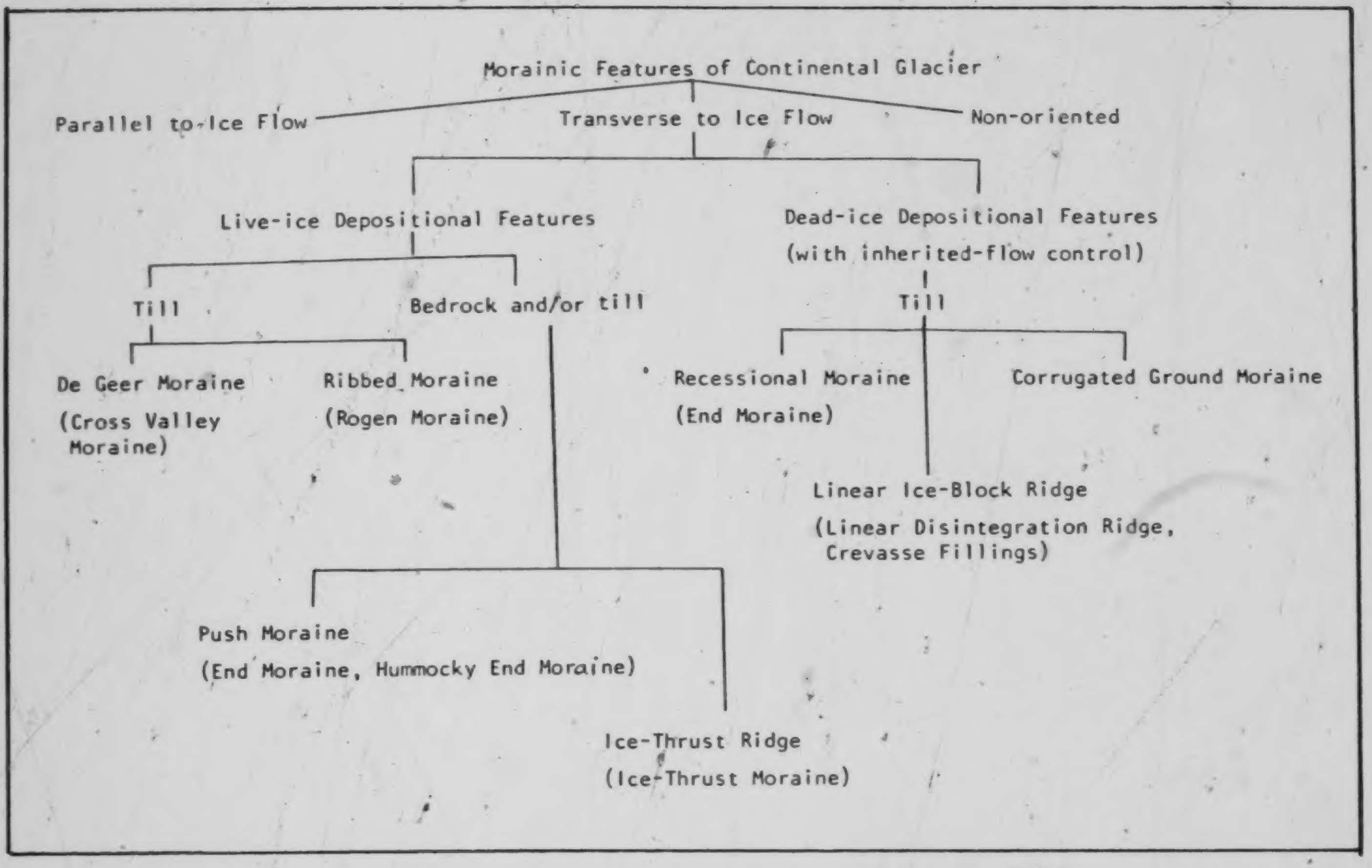
Morainic Features of Continental Glacier
Parallel to-Ice Flow
Transverse to Ice Flow
Non-oriented
Live-ice Depositional Features
Dead-ice Depositional Features
(with inherited-flow control)
Till
Bedrock and/or till
Till
De Geer Moraine
(Cross Valley Moraine)
Ribbed Moraine
(Rogen Moraine)
Recessional Moraine
(End Moraine)
Corrugated Ground Moraine
Linear Ice-Block Ridge
(Linear Disintegration Ridge, Crevasse Fillings)
Push Moraine
(End Moraine, Hummocky End Moraine)
Ice-Thrust Ridge
(Ice-Thrust Moraine)

Figure 4.1 : Classification of Morainic Features of Continental Glacier (alternate terminology used to indicate the classified moraines is shown in brackets)

Morainal Feature	Composition	Morphological Characteristics	Dimension	Genesis	References
Push Moraine (hummocky end moraine)	Unindurated material, till and bedrock	- Transverse ridges, or a group of ridges, that are arcuate in outline, regularly spaced, and are emphasized by intervening depressions; outline a former ice margin - Composed of structures that show pushing, ploughing or overriding action in the unconsolidated material in a generally unfrozen state	Ht.= 3.1 to 152 m or more L. = over 0.81 km	- Glaciated material produced at the front of actively flowing glacier, or a ridge of pre-existing material structurally disturbed by the ice push	Prest, 1968; Gravenor and Kupsch, 1959; Mollard, 1982
Recessional Moraine	Till	- Transverse ridge that outline a former ice margin	As above	- Construction of a transverse ridge at the stagnant ice snout during a halt in glacier retreat	Prest, 1968
Corrugated Moraine	Mainly basal till, but sorted material or bedrock may be locally found	- Low relief ground moraine that consists of short to elongate, irregular transverse ridges with troughs that form a broad arcuate system that outlines the position of former ice lobe - Form a corrguated or washboard like pattern on an airphoto and on the ground	Ht. = 0.3 - 3.1 m L. = 91 m to over 1.61 km W. = 76 - 274 m S. = 30.5 - 91 m	- Subglacial thrusting, pushing, squeezing of material into subglacial fracture system or zone of weakness in an ice marginal zone and were preserved because of subsequent stagnation of the local ice - Deposited subglacially at the base of thrust planes in the ice during ultimate stagnation	Prest, 1968; Gravenor and Kupsch, 1959; Gravenor et al, 1960
De Geer Moraine (cross valley moraine)	Stony, sandy to silty till, may be gravelly	- A succession of discrete, narrow ridges from short and straight, to long and undulatory - Found in areas of former lake or sea cover. Best develops and commonly restricted to low areas	Ht. = less than 12.2 m L. = 1 km W. = 2 or 3 times the height S. = a few hundred to thousand metres	- Formed at the base of an ice cliff grounded in a glacial lake - Formed underneath a glacier lobe that extended into water	Prest, 1968; Sugden and John, 1976; Mollard and Janes, 1984
Ribbed Moraine (Rogen moraine)	Bouldery till	- Relatively large scale lineaments that are often gently arcuate, slightly concave and gentler upstream, and give a ribbed pattern on the ground - Depressions between ridges may be occupied by elongated and multifingered lakes - Ridges crests are often fluted and drumlinized. Ridges in places are connected by cross ribs - Better developed in lowlands and shallow depressions	Ht. = 9.1 - 27.4 m L. = up to 4.83 km S. = crests of ridges 91 to 305 m apart	- Formed near the margin beneath an actively flowing glacier, and the individual ribs represent thrust plates and folds that formed in a zone of compressive flow - Formed subglacially in a region of compressive glacier flow, possibly where obstructions to glacier flow caused the formation of shear planes in the basal zone of the glacier and upward thrusting and stacking of slices of debris-laden basal ice	Prest, 1968; Sugden and John, 1976; Mollard and Janes, 1984
Linear ice-block ridge (crevasse fillings, linear disintegration ridges)	Till, may include pockets of stratified material	- Small, elongate ridges transverse to parallel to ice-flow direction - Generally there are two sets of ridges intersect at acute or at right angles	Ht. = 0.91 - 10.7 m L. = a few m to a few km W. = 15.2 m	- Either by squeezing of till from beneath the ice or by the slumping of debris from the ice surface into a crevasse system - Occur in stagnant ice	Prest, 1968; Gravenor and Kupsch, 1959; Gravenor et al., 1960; Stalker, 1960b

Table 4.1 : Characteristics of Morainal Transverse Features (Ht. = Height, L.= Length, W. = Width, S.= Spacing)

of bedrock and/or till while (c) and (d) are usually made up entirely of till.

(ii) Dead-ice, depositional, tranverse features which can be classified as: (a) recessional moraines which are a type of end moraine, (b) linear ice-block ridges which are also known as linear disintegration ridges and crevasse fillings, (c) corrugated ground moraines

The classification and descriptions of these transverse features noted above have suggested the basis for identifying ice-thrust ridges with topographic expression and outcrops on aerial photographs and on the ground.

The following examples show the use of this classifying method to recognize ice-thrust ridges in a glacial terrain.

4.2.2 Examples

On aerial photographs, transverse ridges showing 2 sets of ridges intersecting each other probably indicate that the ridges are linear ice-block ridges. A sequence of broad ridges separated by depressions in the form of multifinger lakes (Mollard and Janes, 1984, plates 3.16 and 3.17) may indicate ribbed moraines (Prest, 1968). When a succession of narrow and discrete ridges with spacing of a few hundred metres (Mollard and Janes, 1984, plate 3.15) and are found on a broad open depression, such as a former lake bed, it is probable that they are De Geer moraines. If the transverse ridges do not belong to any of the above categories, the features may be ice-thrust ridges, end moraines or corrugated ground moraines. This is because in plan view, ice-thrust ridges, end moraines and corrugated moraines may show similar morphological features, that is, linear to arcuate ridges near the front of the former ice and with their concave side facing the ice direction. Thus, ground checks and subsurface data are needed to distinguish ice-thrust ridges, which are mainly composed of deformed bedrock, from end moraines and corrugated ground moraines which are chiefly composed of till. It needs to be noted that live-ice depositional features (end moraines and ice-thrust ridges) and dead-ice depositional features (corrugated ground moraines) may occur adjacent to each other along the margin of a glacier as the formation of these features is governed by local topography, surficial geology, and local thickness and flow of the ice.

4.3 Terrain Analysis

Based on the classifying method described above, aerial photograph analysis outlining an area which is composed of a single morphologic feature, for example, an ice-thrust ridge, defines a land form unit (Grant, 1975a, 1975b). Subsequent field work provides field data on the dimensions, surficial deposits and subsurface structure of the morphologic features within the land form units and checks on the boundaries and descriptions of the land form units outlined during the preliminary aerial photo analysis. After all the characteristics of the morphologic feature within a land form unit and its boundary with other units are clearly known and modified to be consistent with the field data, the land form unit is termed a terrain unit (Grant, 1975a, 1975b).

4.3.1 Definition

When terrain analysis is performed on a glaciotectonic area, the terms ice-thrust terrain unit and ice-thrust terrain pattern are more representative of the ice-thrust features in the areas. These terms are defined as follows.

1. An ice-thrust terrain unit is an area in which the surficial and subsurface structures are made up mainly of bedrock deformed by glaciotectonism. The deformed bedrock may be expressed as a topographic feature such as an ice-thrust ridge that can be detected on an aerial photograph on a scale of about 1 : 10^4. This study found that photo sets, with a scale of 1 : 30,000 to 1: 60,000 and covering an area with stereoscopic view of about 48 km^2 to 190 km^2 respectively, would provide suitable coverage and resolution for detecting ice-thrust features and their relationship with the surrounding deposits. However, sometimes no topographical expression of the ice-thrust features are visible on the ground. It is to be noted that Moran et al. (1980, p. 460) have defined glacial-thrust terrain as a region consisting of ice-thrust features with topographic expressions.
2. An ice-thrust terrain pattern is the association and

spatial relationship of the ice-thrust terrain unit with other (glacial) terrain units forming a specific terrain pattern which indicates the occurrence and distribution of glaciotectonism and ice-thrust features in a particular area.

This pattern, unit terminology basically follows Grant (1975a, 1975b)

4.3.2 Results

Airphotograph interpretation and field observations of the ice-thrust features, the adjacent glacial deposits, and topographic features of the study areas are shown in Appendix C. Ice-thrust terrain units and other glacial terrain units and the associated ice-thrust terrain pattern of each of the study areas are also indicated in Appendix C. For illustrative purposes, the terrain units observed at Lowden Lake and Beltz Lake areas are described particularly in detail in Sections C.3.1 and C.3.2.

The general characteristics of these ice-thrust terrain units and patterns observed in the study areas are described below.

4.3.2.1 Ice-Thrust Terrain Unit

1. The ice-thrust features in the ice-thrust terrain units observed in the study areas may:
   a. express themselves as distinct topographic forms such as ice-thrust ridges, for example, the southern shore of Isle Lake and Lowden Lake area

(Appendix C, Figures C.10 and C.12).

b. express themselves as some indistinct topographic forms such as gently rolling hills and ridges, for example, southern shore of Wabamun Lake, Beltz Lake area, and area northwest of Sullivan Lake (Appendix C, Figures C.4, C.19, and C.22).

c. not express themselves as any distinguishable topographic forms related to ice thrusting, for example, the gently rolling plain observed in Nisku area, and Hanna - Sedgewick area (Appendix C, Figures C.11 and C.27).

Ice-thrust features with poor to no topographic expressions cause the boundaries of the ice-thrust terrain units to be difficult to trace except in the immediate vicinity of exposures, for example, Beltz Lake area.

2. Despite the diffuse and indistinct boundaries of most of the ice-thrust terrain units and the lack of knowledge on the areal extent of subsurface deformation due to ice thrusting in most of the study areas, the ice-thrust terrain units and their associated ice-thrust ridges found along the southern shore of Isle Lake and Lowden Lake areas seem to form an arcuate-shaped belt of deformation with its concave side facing the direction of ice flow (Appendix C, Figures C.10 and C.12).

3. It is noted that most of the ice-thrust features in the ice-thrust terrain units in the study areas are overlain by ground moraine and/or hummocky disintegration moraine. For example: Wabamun Lake area, Lowden Lake area, Nevis area, and Cypress Hills area (Appendix C, Figures, C.4, C.10, C.12, C.25, and C.28). The three areas, the Nisku area, Beltz Lake area, and Hanna - Sedgewick area, are found covered by glaciofluvial and/or glaciolacustrine deposits (Appendix C, Figures C.11, C.19, and C.27). This shows the occurrence of glacial and/or postglacial erosion and deposition in the ice-thrust terrain units after glaciotectonic deformation, resulting the reduction and/or destruction of the topographic expression of most of the ice-thrust features in the study areas.

4.3.2.2 Ice-thrust Terrain Pattern

1. In general, the ice-thrust terrain pattern of the study areas are made up of four main types of terrain units: (1) ice-thrust terrain unit, (2) meltwater channel, (3) ground moraine and/or hummocky moraine terrain unit, and (4) glaciofluvial and/or glaciolacustrine terrain unit.
2. Examination of the spatial relationship of the ice-thrust terrain unit and the meltwater channel with respect to the glacial direction in the study areas indicate that most of the ice-thrust terrain

units are located on the downglacier slopes or edges of the meltwater channels that face the direction of ice movement, for instances, Wabamun Lake area, Nisku area, Nevis area, and the area northwest of Sullivan Lake. Moreover, it has been noted that the trends of the meltwater channels and the ice-thrust ridges within the ice-thrust terrain units observed in the study areas often were approximately parallel to each other and both seemed to lie roughly perpendicular to the direction of the ice movement inferred from the adjacent glacial features. For example: Wabamun Lake area, Lowden Lake area, and the area northwest of Sullivan Lake (Appendix C, Figures C.4, C.10, and C.22; Figures 8.2 and 8.3). Furthermore, the ice-thrust terrain unit and the meltwater channel are chiefly surrounded by ground moraine and/or hummocky moraine terrain units (Appendix C, Figures C.4, C.10, C.12, C.22, and C.28); however, two areas were found in which the ice-thrust terrain units were mainly bounded by a glaciofluvial and/or glaciolacustrine deposits (Appendix C, Figures C.11 and C.27). One area was seen in which the ice-thrust terrain unit was surrounded by glaciofluvial, glaciolacustrine, and hummocky moraine terrain units (Appendix C, Figure C.25).

3. Preliminary aerial photograph studies have also been

performed by the writer over the region between and adjacent to the Lowden Lake and Beltz Lake areas that covers a total area of about 400 km². This investigation indicates that there are many linear to curvilinear ridges present in the region (Figure 4.2). However, ridges with distinct outcrops and ground checked to be ice-thrust features (see Appendix C) are only found at the Lowden Lake and Beltz Lake areas. Since no exposures were found on the linear features located outside the areas, it is uncertain whether they are features due to ice thrusting or only some other kind of glacial form. Indeed, the lineated ridges found adjacent to the moraine plateau at the Lowden Lake area (Appendix C, Figure C.12) closely resemble moraine ridges formed by ice-pressing process (Stalker, 1960b, plate XII, XIII). Nevertheless, the presence of linear forms between ice-thrust terrains with distinct ice-thrust terrain units suggests the following:

a. When ice-thrust terrains are found only tens of km apart, terrain studies should also be performed in the area between these 'closeby' ice-thrust terrains.

b. The differences in the morphology and trends of the ice-thrust features within the ice-thrust terrain units (Figure 4.2) and the distribution of the associated glacial terrain units within

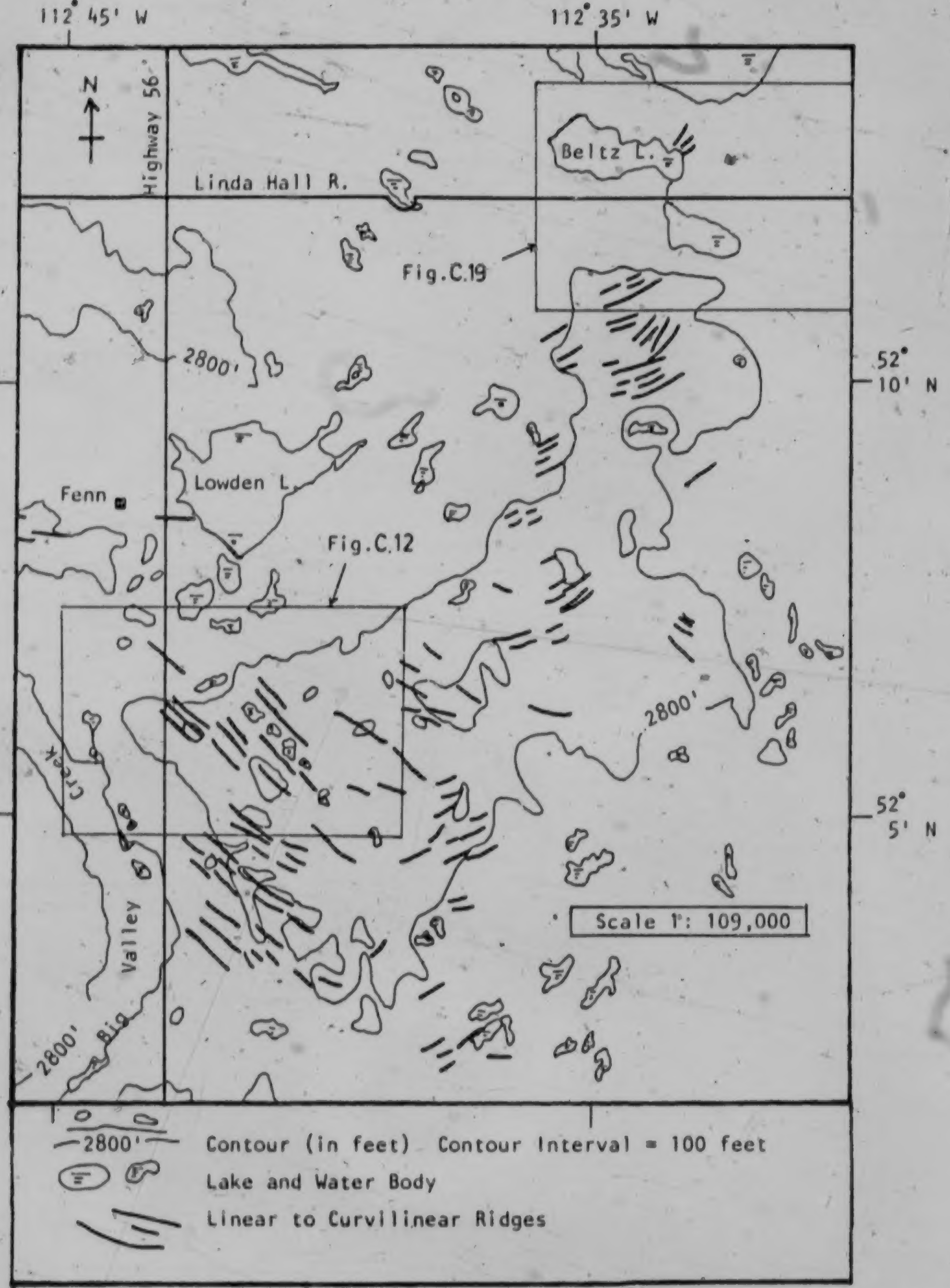
112° 45' W
112° 35' W
N
Highway 56
Linda Hall R.
Beltz L.
Fig.C.19
2800'
52° 10' N
Lowden L.
Fenn
Fig.C.12
2800'
52° 5' N
Creek
Valley
Big
2800'
Scale 1": 109,000
2800'
Contour (in feet) Contour Interval = 100 feet
Lake and Water Body
Linear to Curvilinear Ridges

Figure 4.2 : Ice-Thrust Ridges and Ridges of Undetermined Origin Found at and between Lowden Lake and Beltz Lake Areas (Interpreted and Traced from Airphoto AS 1532-132,133,134; AS 825-78,79,80; C661-5202-4151-32,34,5203-4143-71,73, 5204-4143-27,29,31,5202-4151-75,76; Scale 1;31,680)

the ice-thrust terrain patterns in Lowden Lake area and Beltz Lake area (Appendix C, Figures C.12 and C.19) indicate that the morphologic information obtained from an ice-thrust terrain may not be applied to its immediate adjacent ice-disturbed region.

4.4 Discussion

1. The arcuate-shaped ice-thrust ridges and ice-thrust terrain units with their concave side facing the flowing direction of the glacier in the study areas (Appendix C, Figures C.10 and C.12) which resemble the push moraines that were formed at the snout of the glacier (Gravenor et al., 1960, p. 22 and 25) suggest that they were ice-marginal phenomena (Moran et al., 1980; Aber, 1982). Thus, the meltwater channel which the ice-thrust terrain units are located close to or within, has its trend roughly parallel to the linear to curvilinear direction of the units and their associated ice-thrust ridges and is identified as a proglacial channel.
2. The general occurrence of the ice-thrust terrain units near or within a proglacial meltwater channel and surrounded or covered by dead-ice disintegration moraines, glaciofluvial and glaciolacustrine deposits (Appendix C, Figures C.4, C.10, C.12, C.22, C.27, and C.28) indicate that ice-thrust features in the study areas are formed near or at the margin of a stagnant and

downwasting glacier. This is an area of ablation which would provide large amounts of meltwater to form spillways or meltwater channels. Moreover, ice-thrust ridges could also channel meltwater flow.

3. The location of most of the ice-thrust terrain units in the study areas at or close to proglacial channels which are formed on the slopes of preglacial valleys or escarpments (Chapter 3, Appendix B), seems to indicate that both the regional sloped surface and local topographic barrier that lie parallel and at or close to the margin of a glacier affect the occurrence of ice thrusting. This will be discussed in Chapters 8 and 9.
4. Glacial rejuvenation or readvance had occurred along the margin of the stagnant glacier in some of the study areas. This is shown by the linear glacial erosional features (giant grooves) that incised the ice-thrust ridges near the eastern shore of Beltz Lake (Appendix C, Figure C.19; Chapter 10, Section 10.1.1.), and the presence of till-filled channels and flutings in the study areas of Red Deer - Stettler and Hanna - Sedgewick (Chapter 3 and Appendix B).

4.5 Conclusion

The investigation discussed in this Chapter suggests glaciotectonism in the study areas was probably associated with rapid (?) readvances of the margin of a stagnant and downwasting glacier which was located on the slopes of preglacial valleys or near local topographic troughs such as proglacial meltwater channels. Dead-ice disintegration moraines, glaciofluvial and glaciolacustrine sediments were left adjacent and/or covered the ice-thrust features in the study areas after this rejuvenated glacier had melted.

5. MACROFABRIC

In this thesis, macrofabric is defined as the soil or rock features that are too large to be directly observed in their entirety in outcrops (modified after Bates and Jackson, 1980).

The macrofabric due to glaciotectonism found in the study areas is described below.

5.1 Faults

5.1.1 Sole Thrusts or Shear Zones

In the summer of 1984, the mapping of the geology of two landslides, which occurred in Pit 3, and a joint survey in Pit 2 in Highvale mine, which is located in an ice-thrust terrain at the southern shore of Wabamun Lake (Appendix C, Figure C.4), have enabled the author to observe and describe ice-thrust shear zones and their related structures exposed in these pits in detail. Figures C.5, C.6, C.7, and C.8 in Appendix C show the locations and the stratigraphic sections of the two slides in the mine surveyed by the author.

5.1.1.1 Field Description

(A) In Pit 2, which is about 8 km southeast of Pit 3, a horizontal shear zone was exposed near the bottom of the highwall and could be traced for about 1000 m.

The observed shear zone is about 0.3 - 0.46 m thick, composed mainly of dark grey to dark brown grey, soft to very soft mudstone which could be moulded by fingers. The zone is overlain by deformed light grey sandstone to siltstone and is underlain by undeformed light brownish sandstone to siltstone, and shale. The contact of the shear zone with the strata above and below is sharp and distinct. The bottom of shear zone is about 3.7 m above the top of the main coal seam #1 of the mine. Coal seams #1 to #6, which are exposed 670 m northwest of the observed shear zone, are in general flat-lying and undeformed but are orthogonally jointed. Most of this shear zone is flat and tends to run parallel to the overlying and underlying horizontal bedding.

Three to four slickensided and polished planes that can be traced for several metres were found within the shear zone (Plate 5.1). Anticlinal structures with a wavelength of 2.5 cm could be seen within the shear zone. Two imbricate thrust faults splay off the shear zone with a separation of at least 0.46 m, and an apparent dip of 30°. The beds that have been displaced by the imbricate thrust faults have a dip/dip direction of about 30°/ 355°, and two shear planes within the shear zone also show an average dip/dip direction of about 56°/ 357° (Appendix C, Figure C.9a). The intersection of the shear zone with the imbricate thrusts in Pit 2 have caused some small slumps and wedge failures along the highwall. Langenberg (1985, p. 5) measured four folds and twelve imbricates present in the

Plate 5.1 Shear Surfaces within the Shear Zone Exposed in Pit 2, Highvale Mine

neighbourhood of the shear zone in Pit 2 and obtained a mean trend/plunge of about 065°/ 13° NE for the fold axes and a mean dip/dip direction of about 23°/ 012° for the imbricate thrusts. The attitudes of the deformed structures observed in Pit 2 suggest that they are due to compression originating from approximately north.

(B) In Pit 3, the shear zone is exposed on the highwall near the slide regions. The structural geology of this zone is described in detail by the author. It is composed mainly of two layers (Plate 5.2).

1. Bentonitic Mudstone layer

The layer is about 3.4 m and 0.4 m thick at Slides 1 and 2 respectively. Abundant coal lenses and root remains up to 2.5 cm wide and 12.7 cm long were found near the lower portion of the layer in Slide 1. The presence of these carbonaceous remains has caused the layer at this level to be stiff, highly fractured and shattered. Approaching the top of the layer, the amount of carbonaceous remains decreased to become totally absent and the layer became soft and plastic. Here, undulatory, wavy and randomly orientated planes were observed, they ranged from a few cm to 60 cm long and had smooth and shiny surfaces (Plate 5.3). Slickensides were found on some of them. These wavy planes were formed in material that was crumbly and in lump form (about 1.5 cm in diameter); however, the lumps could easily

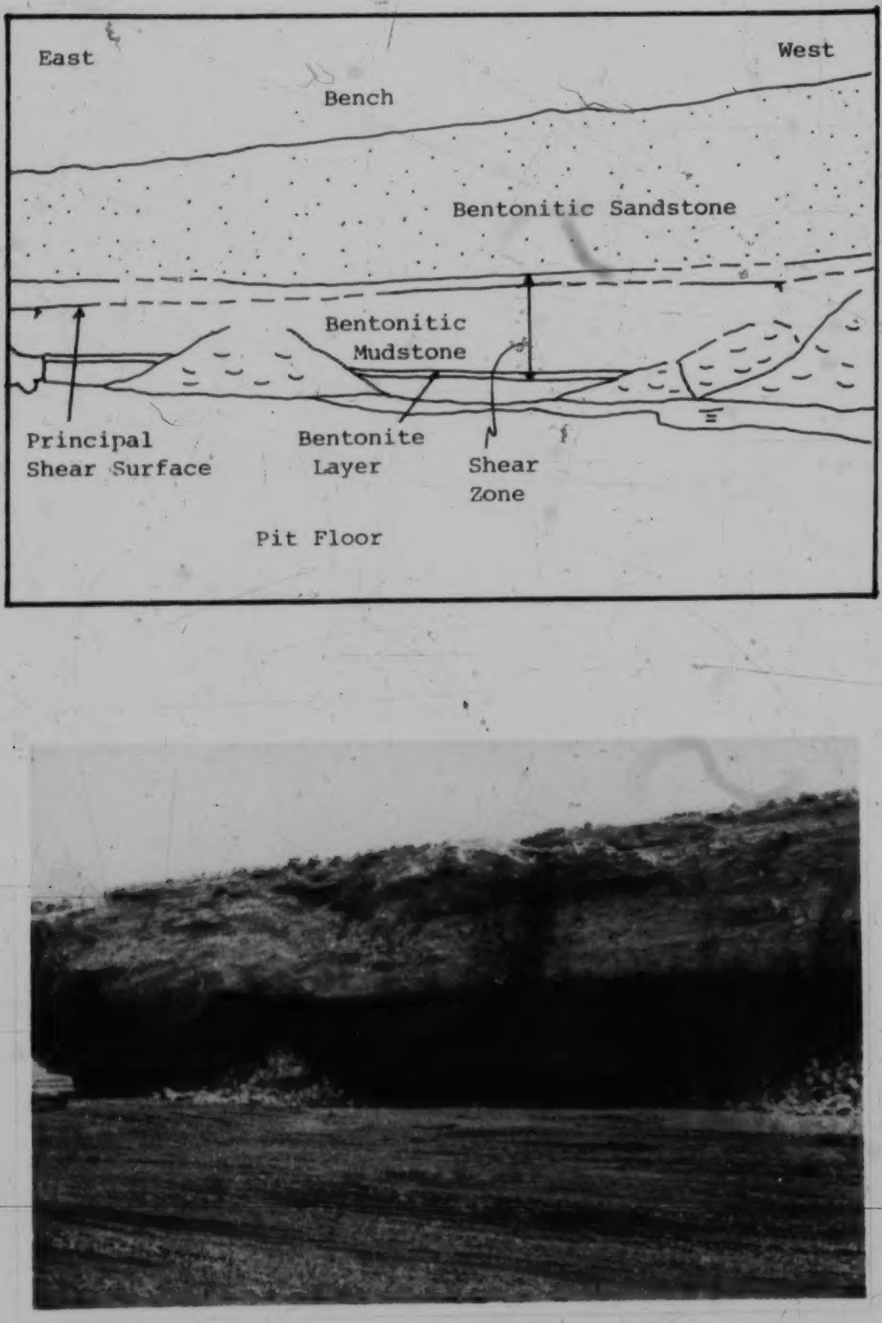
East
West
Bench
Bentonitic Sandstone
Bentonitic
Mudstone
Principal
Shear Surface
Bentonite
Layer
Shear
Zone
Pit Floor

Plate 5.2 Shear Zone Exposed in Pit 3, Highvale Mine

Plate 5.3 Minor Shears within the Shear Zone, Pit 3, Highvale Mine

Plate 5.4 Minor Thrust within Shear Zone, Pit 3, Highvale Mine

be remoulded by finger pressure when moist. The contact between the bentonitic mudstone and the overlying bentonitic sandstone was sharp and undulatory.

At Slide 1, about 1 m below the contact with the overlying bentonitic sandstone, a horizontal shear plane was found within the mudstone. It has been inferred as one of the principal slip surfaces caused by ice thrusting and was also considered to be the failure surface of the slide mass. This major shear plane could be traced across the stable portion of the north-facing highwall for almost 300 m west of Slide 1 (Plate 5.2). A close examination of this shear plane revealed that it was located in a zone of very soft and moist clay bounded between two distinct, crumbly, fissured, layers of bentonitic clay. The mesoscopic and microscopic characteristics of these layers will be investigated in detail in Chapter 6. Many randomly orientated wavy surfaces diverged upward and downward from this major slip plane (Plate 5.3). Digging into this major shear surface west of Slide 1 revealed that this surface is planar with distinct slickensides perpendicular to the strike of the east-west mine wall. The measured dip/dip direction of this shear plane are 8°/ 011°, 6°/ 000°, and 6°/ 320° with an average of 6°/ 355°. However, the accuracy of these measurements is doubtful because of operator errors involved in measuring the small strike and dip of a bedding plane with small inclination with respect to the horizontal (less than 10 degrees) using a geologic compass (Cruden and Charlesworth, 1976; Ragan, 1985).

2. Bentonite Layer

This layer was overlain and underlain by two thin coal beds about 15 to 25 cm thick. In Slide 2, the contact between the upper coal and the top of the bentonite was wavy and it was common for the upper coal to intrude down into the bentonite. The coal also intruded into the overlying bentonitic mudstone with displacements from 0.46 m to 0.76 m (Plate 5.4). On the other hand, the contact between the bentonite and the lower coal bed was undulatory, and no invasion of the beds was observed. Folding in the lower coal bed usually had a wavelength and amplitude of 15.2 cm and 10.2 cm respectively. Seepage occurred locally at the contact between the coal beds and the bentonite. As in Pit 2, field observations showed that the main coal seams in Pit 3, which were located below the two slides, were horizontal and undeformed. It was concluded that the bentonite formed at least part of the basal portion of the zone of decollement on which most of the movement due to ice thrusting had taken place.

In Pit 3, the top of the shear zone is distinct and is at the contact of the bentonitic mudstone with the overlying gently deformed bentonitic sandstone (Appendix C, Figures C.7 and C.8). The contact, which is undulatory and with pebbles found locally in the sandstone, is interpreted as a erosional surface or an unconformity. The base of the shear zone is defined as the boundary between the thin coal bed that underlies the bentonite and the carbonaceous shale that overlies the the main coal seams. This is because the deformation and shearing were quite intense in the bentonite and the argillaceous strata above. This is evident as the presence of at least three principal slip surfaces in the bentonite, the thin coal bed which immediately overlies the bentonite has been intruded into the mudstone and the underlying bentonite (Plate 5.4), and the bentonite sampled in the field was found to contain many angular coal chips and mudstone fragments (Plate 5.5) which are believed to have been intruded into the bentonite from the overlying mudstone and thin coal layer during shearing. However, the degree of deformation decreases when the bottom of the bentonite and the underlying main coal beds are approached where only small concentric and disharmonic folds are found. The occurrence of these disharmonic folds and thrust faults with depth indicate that at a particular depth, the overlying deformed beds must have been completely

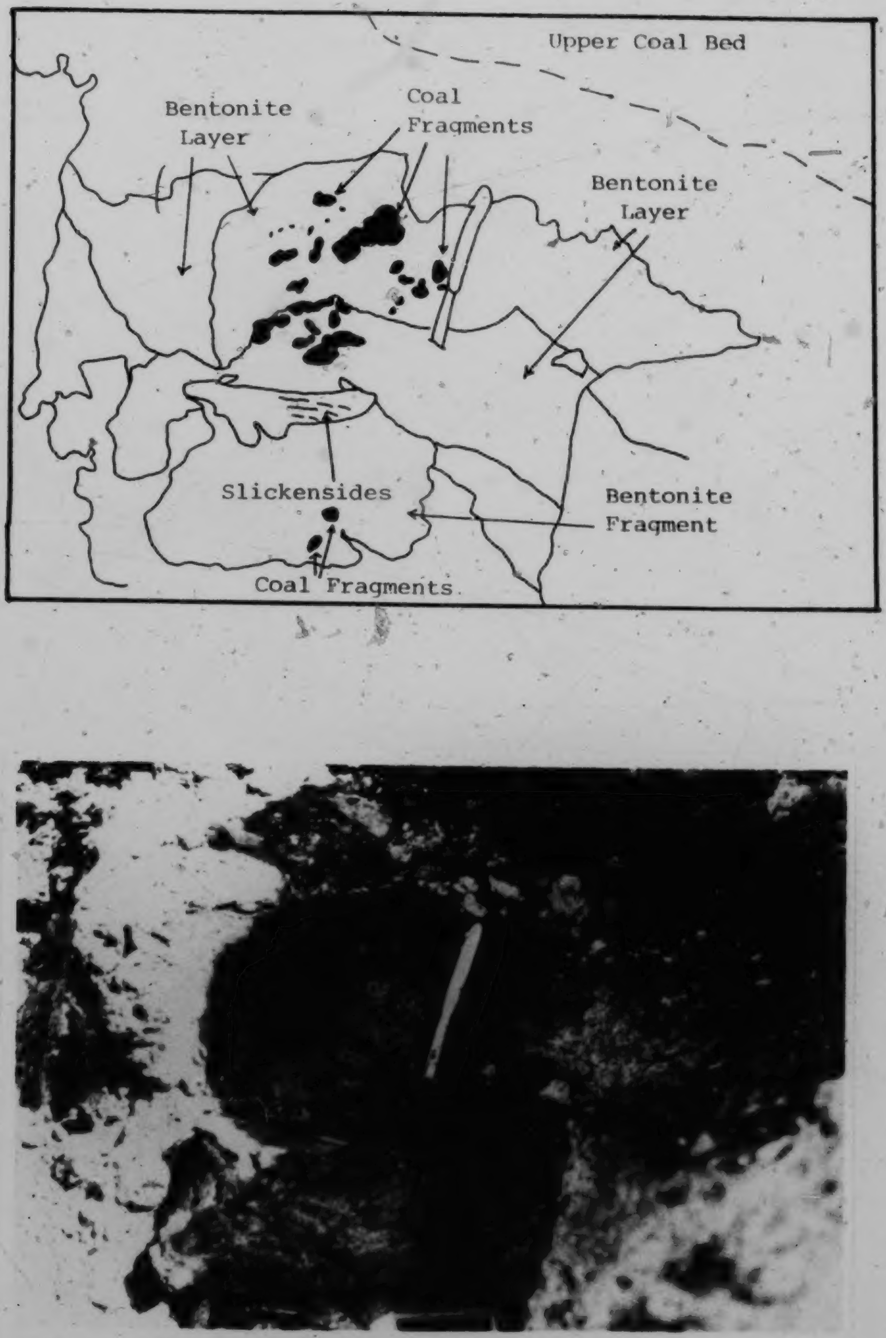
Upper Coal Bed
Bentonite Layer
Coal Fragments
Bentonite Layer
Slickensides
Bentonite Fragment
Coal Fragments

Plate 5.5 Coal Fragments in the Bentonite, Pit 3, Highvale Mine

detached from the underlying strata. This requires a shearing-off or decollement at the base (Ragan, 1985, p. 230). Thus, it is concluded that the deformed bentonite and the thin coal beds immediately below form the base of the shear zone or the decollement and are comparable to the ice-thrust fabric observed by Slater (1927b), Mackay (1959), Hansen et al. (1961), and Wateren (1981). Moreover, the top of the shear zone or decollement in Pit 3, Highvale mine, is at a depth of about 8.7 - 27.0 m below the ground surface, compared with the depth (25 m) of glaciotectonic deformation observed in other ice-thrust terrains (Wateren, 1981). Ice thrusting has also been reported to cause deformation up to a depth that exceeds 60 m (Sauer, 1978) to 150 - 183 m (Byers, 1959; Brinkmann, 1953); however, the reliability of these values cannot be ascertained at present. This is because field investigations (this Chapter) and theoretical consideration (Chapter 9) on glaciotectonism suggest that glaciotectonic deformation tends to occur at a depth less than 30 m below the ground surface.

It has also been considered that the shear zones in Highvale mine were formed by the excavation of the mine. Since it is known that unloading due to a large excavation into layered sequence of rock, either artificial or natural, would cause an upward rebound of the excavation floor and an inward movement of the excavation walls, resulting flexural slip between beds (Matheson, 1972). As a result, an analysis of the displacement along the layered bedrock due to rebound caused by excavation was performed (Appendix D). Appendix D shows that the shearing in the strata at the highwall due to rebound after the excavation in Highvale mine is not sufficient to produce a shear zone in the mine.

5.1.1.2 Subsurface Investigation

A 300 m long, flat-lying shear zone has been observed on the E-W trending highwall in Pit 3, Highvale mine, Wabamun Lake area (Plate 5.2). Unfortunately, only a section of the shear zone is exposed and the other sides or the plan view which shows the area of the zone are still unknown. Since a number of boreholes have been drilled in Pit 3 of the mine where the shear zone is exposed, a detailed analysis of the log data and the construction of subsurface cross-sections of the area will show the geometry of the shear zone and its related deformations in this ice-thrust terrain. Moreover, it is believed that the information of the subsurface deformed structures obtained from this study can be applied to other ice-thrust terrains.

1. Drill Hole Data

Drillings (include auger drilling, rotary drilling and rotary coring) in the mine were performed by Monenco Ltd. and Alberta Research

Council (Monenco Ltd., 1983a, 1983b; Alberta Research Council, 1983; Pawlowicz et al., 1985). The errors that may be involved when interpreting these drill log data were investigated and are listed below.

a. Dry auger drilling and rotary drilling can supply information on the subsurface lithology but not on the underlying structure such as shear zone (Fenton et al., 1983). As a result, the interpretation of these logs is always accompanied by speculation and/or control from adjacent cored drill holes (if any).

b. Knowing the presence of shear zones in the mine, the boreholes were logged by the consultants (Monenco Ltd. and Alberta Research Council) and the logs hence are second hand information.

c. The shear zone in Pit 3 is believed to occur above the top of the main coal seam #1; however, some logs were obtained from boreholes which ended above the top of these coal layers. This is especially true for all auger drill holes which cannot penetrate the 'hard' mudstone layers.

d. A few logs were taken from the simplified cross-sections drawn by the consultant in which the information on structure is missing.

With these drawbacks of the drill log data in mind, the construction and interpretation of the cross-sections of the shear zone in Pit 3, Highvale mine, follows.

2. Location of Line of Sections

In general, the line of section of a basal thrust should be chosen to lie parallel to the slip or movement direction of the structure so that the sections can be balanced and the minimum displacement on the thrust may be estimated (Elliott and Johnson, 1980; Elliott, 1983). Field investigation of ice-thrust features that are exposed in Pits 2 and 3 in the mine indicate that the last glacier entered the area mainly from the north (Appendix C, Figure C.9a; Section 5.1.1.1) and probably caused a north-south slip motion in some of the underlying materials. Because of this, eight section lines, four oriented north-south (N-S) and four oriented east-west (E-W), were constructed (Figures 5.1, 5.2, and 5.3). The N-S sections show the true lateral view of thrust sheets and the related discontinuities; while the E-W sections display the existence of transverse structures. The combination of these sections would produce a 3-D perspective of the subsurface structures in the ice-thrust terrain in Wabamun Lake area.

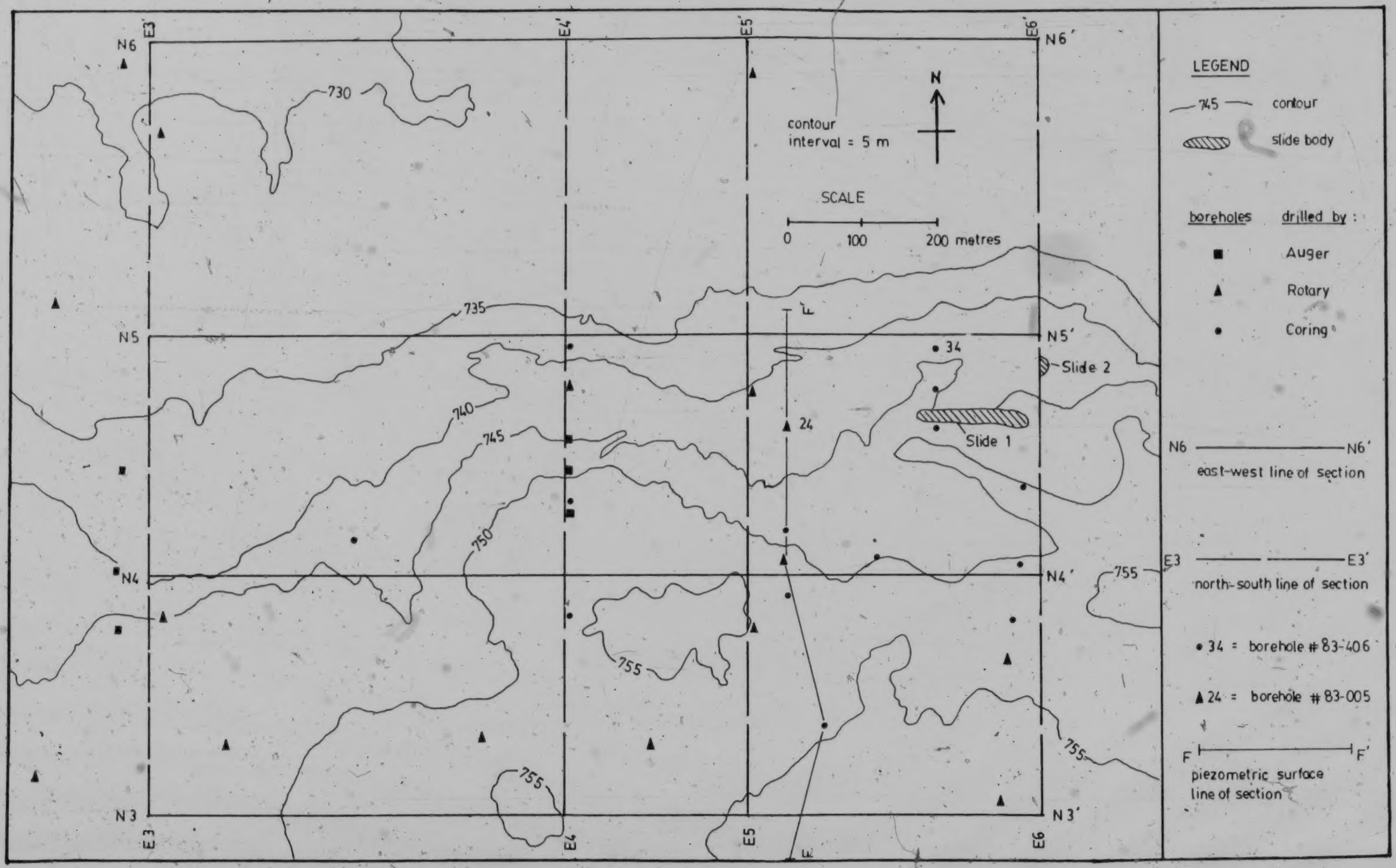
N6
E3
E4'
E5'
E6'
N6'
730
contour
interval = 5 m
N
SCALE
0
100
200 metres
735
F'
N5
N5'
34
Slide 2
740
24
745
Slide 1
750
N4
N4'
755
755
755
755
N3
N3'
E3
E4
E5
E6
F
LEGEND
745 contour
slide body
boreholes
drilled by :
Auger
Rotary
Coring
N6 N6'
east-west line of section
E3 E3'
north-south line of section
• 34 = borehole # 83-406
▲ 24 = borehole # 83-005
F F'
piezometric surface
line of section

Figure 5.1 : LOCATION OF LINE OF SECTIONS AND BOREHOLES, PIT 3, HIGHVALE MINE

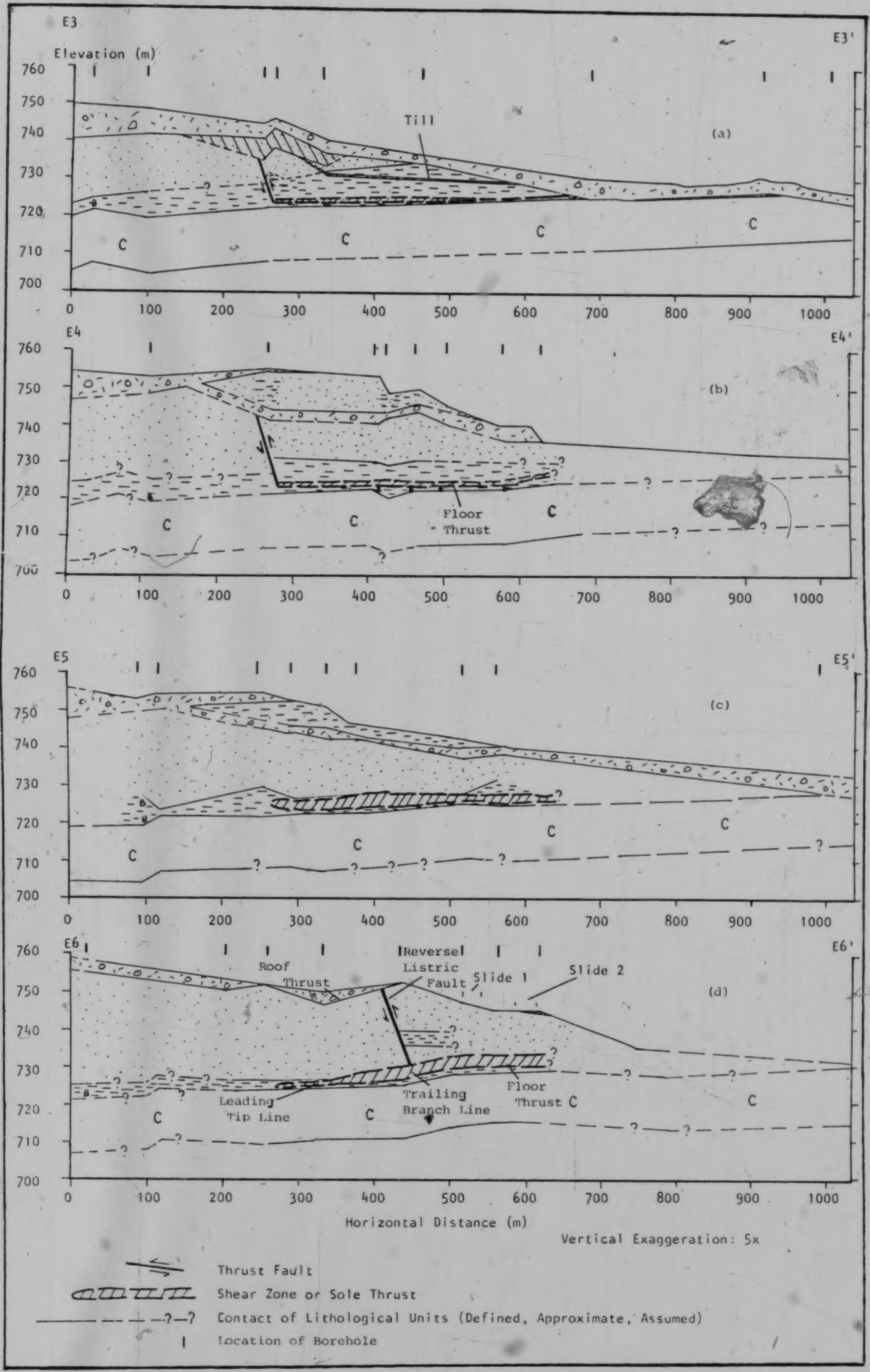
E3
Elevation (m)
E3'
Till
(a)
C
E4
E4'
(b)
Floor Thrust
C
E5
E5'
(c)
C
E6
E6'
Roof Thrust
Reverse Listric Fault
Slide 1
Slide 2
(d)
Leading Tip Line
Trailing Branch Line
Floor Thrust
C
760
750
740
730
720
710
700
0
100
200
300
400
500
600
700
800
900
1000
Horizontal Distance (m)
Vertical Exaggeration: 5x
Thrust Fault
Shear Zone or Sole Thrust
Contact of Lithological Units (Defined, Approximate, Assumed)
Location of Borehole

Figure 5.2 North-South Oriented Line of Sections in Pit 3, Highvale Mine

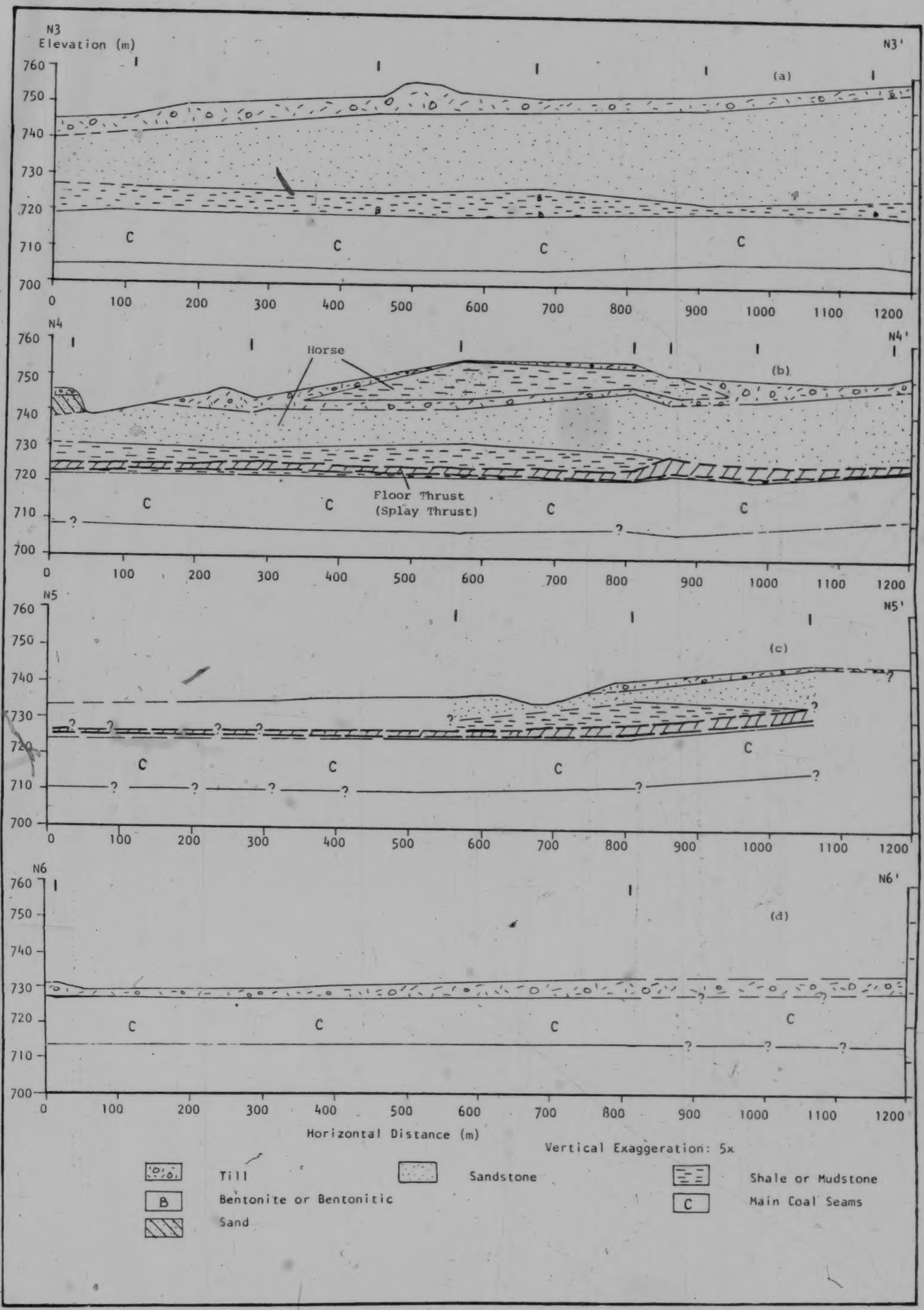
N3
Elevation (m)
N3'
(a)
N4
N4'
(b)
Horse
Floor Thrust
(Splay Thrust)
N5
N5'
(c)
N6
N6'
(d)
C
?
760
750
740
730
720
710
700
0
100
200
300
400
500
600
700
800
900
1000
1100
1200
Horizontal Distance (m)
Vertical Exaggeration: 5x
Till
Bentonite or Bentonitic
Sand
Sandstone
Shale or Mudstone
Main Coal Seams

Figure 5.3 East-West Oriented Line of Sections in Pit 3, Highvale Mine

The construction of these sections is based on the logs of 36 drill holes which covered 1.24 km² of the eastern portion of Pit 3. Most of these drill holes are not aligned with the sections and are projected onto the sections with a distance varied from 5 m (Hole #11 on E4-E4') to 150 m (Hole #1 on E3-E3') with an average of about 54 m (Figure 5.1).

As shown in the following paragraphs, the correlation between boreholes are mainly based on the main coal seams and the structure of the shear zone which are extensive horizontal features (Section 5.1.1.1.); as a result, the construction of the lines of sections based on some of the boreholes that are 54 m away from the sections can still be justified.

3. Recognition and Correlation of a Ice-Thrust Shear Zone in Drill Hole Logs

(A) Recognition

Field evidence shows that the bedrock in Highvale mine at the southern shore of Wabamun Lake formed mainly in a deltaic and fluvial depositional environment where interfingering and pinchout of strata are common (Monenco Ltd., 1984). Except for the main coal seams, lithology changes over a short distance, for example, less than 100 metres, both in the vertical and lateral directions. Marker beds are absent. In this case, a detailed stratigraphy cannot be drawn and correlation of boreholes based on lithology is difficult.

Despite this shortcoming in strata correlation, a shear zone can be identified in boreholes. This involves knowledge of the structure of the shear zone, the lithology in which a shear zone is likely to occur and the materials that are usually found above and below a shear zone. The following describes the criteria and procedures for the identification of the shear zone in borehole logs of the Highvale mine, Wabamun Lake area. These criteria are based on studies by the author of many log data and outcrops in the area.

a. A control or reference borehole should be carefully cored and logged with detailed lithological and structural descriptions that show the characteristic signature of the shear zone and its adjacent stratigraphic units in the area. Borehole #HV-83-406, which is located 125 m northwest of Slide 1 where the shear zone is exposed, serves as the control log for identifying and correlating the shear zone in the study area (see Figure 7.13).

b. The control log and field observations indicate that the shear zone in Pit 3 tends to have a lithology described as "brecciated, shattered, crushed, rubbled, highly fractured, numerous slickensides, and very high degree of internal fracture". Although these terms have been used quite loosely by drillers and site geologists to describe a disturbed layer, these descriptions found in other logs of the area probably indicate the occurrence of a shear zone in the associated drill hole as far as the study area is concerned.

c. The rock quality of the shear zone, which has a RQD that ranged from 50 to 100 %, is usually described as poor to excellent. As a result, RQD alone does not seem to be a good indicator of the shear zone formed by ice thrusting. However, when the lithologic descriptions of the cores are accompanied with RQD, the confidence in identifying the shear zone increases.

d. The mudstone layer that overlies coal seam #1 in the mine is the most probable horizon where the shear zone is expected to be found. This is based on field observations in Pits 2 and 3 where the flat-lying shear zones at least 300 m long were found in the mudstone to bentonitic mudstone about one to a few metres above the top surface of coal seam #1.

e. The top of coal seam #1 is treated as the lowest elevation where a shear zone may be found. The main coal seams (#1 to #6) and the strata underlying them are expected to be undeformed or only slighty deformed. This conclusion was reached after field observation and examination tens of borehole logs which show that, in general, the main coal seams are undisturbed. The strata below also do not show any significant disturbance.

(B) Correlation

Based on the five criteria stated above, lines of sections were constructed that show the configuration of the shear zone and its deformed environment. The sections of E3-E3', E4-E4', E5-E5', E6-E6', N4-N4', N5-N5' show the presence of a shear zone (Figures 5.2a, 5.2b, 5.2c, 5.2d, 5.3b, and 5.3c). The absence of a shear zone in sections N3-N3', and N6-N6' (Figures 5.3a, 5.3d) may be due to: (a) the types of drill holes (auger and rotary cuttings which may not be able to detect a brecciated zone), (b) the actual irregular shape of the shear zone (which may not be encountered by the pattern of the line of sections used in this study).

The deformed subsurface structures observed in the cross-sections of Pit 3, Highvale mine, are decribed and interpreted below.

5.1.1.3 Observation and Interpretation of the Subsurface Cross-Sections

The terminology used in describing the thrust system in the area follows McClay (1981) and Boyer and Elliott (1982).

1. Monoclinal and gentle anticlinal structures were found in the main coal seams (Figures 5.2a, 5.2b, 5.2c, and 5.2d) though folding and faulting in the mine seem to be restricted to strata overlying these coal layers. Nevertheless, the deformation of the seams in general is slight and the coal can be generalized as the rigid basement that has not been involved in glacial deformation.
2. A shear zone with a thickness that ranges from 0.5 to 4.2 m with an average of about 2.3 m, a length of about 395 m or greater, and a width of at least 1200 m is found just above the top of the main coal seams (Figures 5.2 and 5.3). The shear zone observed in the study area is a planar structure with an E-W major axis and a N-S minor axis. The E-W axis of the shear zone tends to remain at the same stratigraphic horizon along the entire length of the sections. The N-S axis of the shear zone seems to originate from the northward-dipping bedrock slope of the interglacial North Saskatchewan Valley at the southern shore of Lake Wabamun and extends southward along the flat-lying mudstone layer for a distance

before it terminates either in the form of thrust faults which cut across the overlying sandstone and siltstone beds upward to reach the surface, or die out into the horizontally-lying incompetent bed (Figures 5.2a, 5.2b, 5.2c and 5.2d).

Considering the presence of disharmonic folds and minor thrusts in the shear zone (Section 5.1.1.1), the close contact of this zone with its underlying rigid and apparently undeformed basement (that is, the main coal seams) and the presence of thrust faults that splay upward from it, this shear zone can be regarded as a sole thrust, a floor thrust, or a decollment fault of the thrust system of the area. The contact between the bottom of the uppermost layer of till and the underlying thrust nappe which is mainly composed of shale can be treated as the roof thrust of the thrust system in the mine. It needs to be noted that masses of bedrock "floating" within surficial material appear in drill logs and were interpreted as due to gravity glide action by Monenco Ltd. (1979, p. 2). However, according to the stratigraphic setting and the size of the deformed bedrock which is shown on the cross-sections (Figures 5.2a, 5.2b, 5.2c), it is more reasonable to interpret the displaced blocks as originating from the underlying shale layer that has been thrust along the shear zone southward and upward into its present position due to ice thrusting instead of mass movement.

3. The lateral view of the thrust system in the area (Figures 5.2a, 5.2b, and 5.2c) show a hinterland dipping duplex structure which had caused shortening and thickening of strata, and thrust older beds over younger beds. The transverse view of the thrust system of the area (Figure 5.3b) shows the floor thrust, two horses of the duplex structure and thickening of the strata.
4. Reverse listric faults (RLF) are observed in Figures 5.2a, 5.2b and 5.2d that connect the floor thrust with the roof thrust forming horses resting on a frontal ramp. (The apparent absence of a footwall ramp or RLF in Figure 5.2c may be because the borehole data, which were obtained by the rotary and auger drilling methods, could not preserve the shear and faulted structure in the weakly cemented sandstone.) Because of the truncation of the upper horses by the till layer, it is not possible to determine whether enough slip has occurred on the subsidiary fault to produce a duplex with an anticlinal stack.

Figures 5.2c and 5.2d indicate that the shear zone continues to extend horizontally beyond the base of the lower horse, forming a structure analogous to a splay thrust with a trailing branch-line on the reverse listric fault (or trailing thrust fault) and a leading tip-line (Boyer and Elliott, 1982, figs. 19; Hossack, 1983, p. 104). This splay observed in the study area is interpreted as an incipient fracture or developing thrust generated by ice thrusting and has not fully developed into another RLF that joined with the roof thrust to form another horse. This also suggests that the portion of the shear zone that formed the leading tip-line should develop later than the portion of the shear zone that occupied the basal portion of the RLF. In this case, the duplex in the area is a piggyback structure with the sequential branches becoming older toward the hinterland. This seems to indicate that during glaciotectonism, thrusts develop in the footwall of the first thrust and in sequence forwards.

5. Cross-sections show that the shear zone and the overlying thrusts in the study area are in general planar structures and have not undergone any large-scale folding after failure, suggesting all these structures are probably contemporary and formed during the same period of glaciotectonism.
6. In the thrust system of the area, the minimum distance of travel of the upper thrust blocks due to folding and thrusting is estimated to be at least 280 - 860 m (Figures 5.2a, b, c). The displacement

along the sole thrust is at least 355 - 395 m if the 'arrow and bow' rule of Elliott (1976, p. 289) is followed. Depth to the basal decollement in the study area (which is dependent upon the elevation of the erosional surface) range 8.7 - 27.0 m and it is always found 0.5 - 3.3 m above the main coal seams. Langerberg (1985) has also estimated that the movement along the shear zone or sole thrust in Pit 2 of the mine can be balanced with 50 - 80 m of shortening by folding (20 m) and imbricate thrusting (30 - 60 m).

7. The occurring thrusts are blind because due to the presence of a till layer that covered the whole thrust system in the area (Appendix C, Figure C.4). The combination of poor lithological correlation and the surficial cover in the area prevent the identification of strike-slip faults which may be present in an ice-thrust terrain (see Section 5.1.3 in this Chapter) on aerial photographs and drill logs.

5.1.2 Thrust Faults

Reverse listric thrust faults are found in the ice-thrust terrain at the southern shore of Wabamun Lake studied by the author and they tend to originate from a principal horizon or layer which is mainly composed of incompetent, fine-grained sediments such as shale and clay

(Figure 5.2, Plate 5.1). The studies agree with the descriptions of the thrusts related to glaciotectonism described by Kupsch (1962), Wateren (1981), Mills and Wells (1974), Byers (1959), Lessig and Rice (1962), and Slater (1927a).

The exposures in Lowden Lake area and the subsurface sections of Highvale mine at the southern shore of Wabamun Lake also show that thrust faults in ice-thrust terrains might have a stair-case geometry which appears as steeply-inclined at depth but become nearly horizontal when approaching the surface (Figure 5.2b; Appendix C, Figure C.18). The steeply-inclined portion of the the thrust often overlies competent layers while the nearly horizontal portion overlies incompetent layers thus indicating that the thrust fault changes from a diagonal, cross-cutting shear to a bedding-plane thrust (Appendix C, Figure C.16). The stair-case geometry of the thrust faults in the study areas indicates that they have not undergone subsequent horizontal deformation after thrust faulting, although vertical deformation such as normal faulting has occurred. Moreover, thrust faults in the ice-thrust terrains studied sometimes appear as an imbricate structure (Appendix C, Figure C.23).

5.1.3 Strike-Slip Faults

In all the ice-thrust terrains studied in this thesis, a strike-slip fault is found only in the Lowden Lake area and is based chiefly on aerial photograph interpretation.

In that area, a similar distribution pattern of ice thrust-ridges is found immediately adjacent to the strike-slip fault (Appendix C, Figure C.12) probably indicating that folding occurred prior to the strike-slip faulting. It is believed that the strike-slip fault separates the thrust sheet, which is composed of ice-thrust ridges, into two sheets with a differential displacement along their floor thrust. The occurrence of the strike-slip fault within one thrust sheet and subsequent to the folding and thrusting, indicates that it is a secondary feature and comparable to the secondary tranverse tear faults in the eastern margin of the Canadian Rocky Mountains (Dahlstrom, 1970, p. 375). Tear faults or strike-slip faults are common features in a thrust belt because of the impossibility of translating a huge rock mass as a single unit (Davis, 1984, p. 285; Price et al., 1978). The thrust sheets in the ice-thrust terrains studied are composed mainly of sedimentary strata with non-uniform material properties because pinchouts and facies changes are common. Thus, the uneven compressive forces applied on the ends of the sheets during thrusting would result in a differential stress distribution within the thrust sheets. This would cause unequal amount of shortening or forward movement of the sheets and thus the formation of a strike-slip fault.

The occurrence of strike-slip faulting in ice-thrust terrain is believed to be more common than it is found in this study. However, the fact that it is rarely observed is probably because that marker beds are in general absent in the deltaic facies in the ice-thrust terrains studied and this has made the identification of strike-slip faulting by surficial mapping nearly impossible. Thus, the recognition of strike-slip faulting in ice-thrust terrains must depend entirely on the relative movement of distinct ice-thrust ridges appearing on aerial photographs. However, glacial and postglacial erosion and deposition may have disguised many ice-thrust features and their associated strike-slip faults. Moreover, many ice-thrust features are subsurface structures and their detection is difficult.

5.1.4 Normal Faults

In the Lowden Lake area and Cypress Hills area, normal faults (apparent dips of 51° - 80°) were found which cut across the fold and thrust structures and tilted beds, indicating that they were formed later than the latter deformations (Appendix C, Figures C.16 and C.18, Plate C.1).

Normal faulting appears to be the last deformation to occur in ice-thrust terrain probably because ice-thrust features are formed in a frozen state (Berthelsen, 1979; Clayton and Moran, 1974) and deformed as a rigid body. Deglaciation and decay of the permafrost causes thawing in the ice-thrust features, thus resulting in differential settlement and normal faulting. This is similar to the development of a supraglacial system which shows that, during deglaciation, the ice-cores or lateral support of the trough fillings would be removed, leading minor faulting or flexure in the fillings (Paul, 1983, p. 85; fig. 3.7). Moreover, it has been suggested that when a block of subsurface material was thrust above the foreland of an inland glacier, the material would fail due to the reduction in confining pressure and in the stress level, and a rotation of the principal stress directions, resulting in the formation of the relaxation structures such as normal faults (Rotnicki, 1976; Wateren, 1981).

5.2 Folds

Within the study areas, aerial photograph interpretation and field observations indicate that the surficial bedrock has been deformed into symmetrical to asymmetrical, plunging inclined, gentle to tight folds. Field measurements and descriptions of the fold structures found in the study areas have been shown in Appendix C. In the following sections, the folds which are exposed at the southern shore of Wabamun Lake and the Lowden Lake areas are further described and interpreted.

5.2.1 Description

In the Highvale mine, which is located at the southern shore of Wabamun Lake (Appendix C, Figure C.4), gentle folds were observed in the bentonitic sandstone that outcropped near the top of the highwall in the mine (Plate 5.6), and open to close folds, with a wavelength of 4.8 m and an amplitude of 1.8 m, were exposed near the base of the highwall about 45 m north of Slide 2 (Plate 5.7). The folds are composed mainly of weakly cemented bentonitic sandstone and siltstone. A coal layer about 2.5 cm thick was found lying between the open- to close- folded sandstone bedding (Plate 5.8). The former has been crumpled into angular fragments with particle sizes generally less than 3 mm in diameter. It is believed that the brecciation is due to flexural slip during folding. A joint with a dip/dip direction of 76°/ 094° was noted cutting into the anticlines. The fold axis trends 099° and 287° azimuth with a plunge of 12° E and 4° W respectively, that is, more or less perpendicular to the highwall where Slide 2 occurred, but parallel the highwall at Slide 1 (Figures 10.2 and 10.3).

In the Lowden Lake area, the ice-thrust ridges recognized on aerial photographs represent roughly the general shape of the folded strata (Appendix C, Figures C.17 and C.18) and show a wavelength of about 160 m and an amplitude of about 10 m. In plan view, the deformations appear as folds with their axial traces approximately parallel to each other (Appendix C, Figure C.12). The folds observed were deformed by thrust faults, and die out along their axes by plunging and/or becoming conical folds, though the latter cannot be proved at present due to insufficient exposures. A stereographic plot of the poles to the bedding planes and fold axes measured in seven sections in the

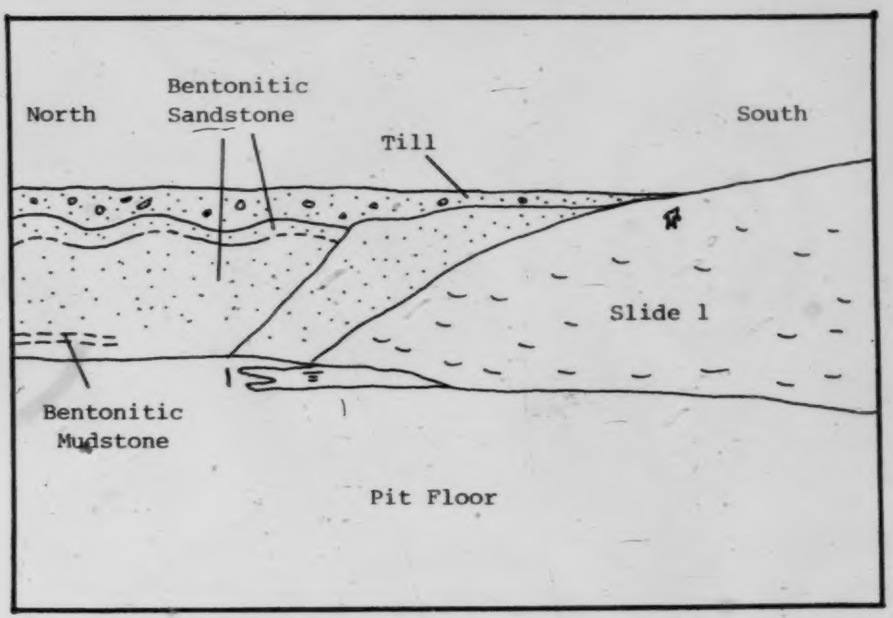
North
Bentonitic Sandstone
Till
South
Slide 1
Bentonitic Mudstone
Pit Floor

Plate 5.6 Gentle Folds in the Bentonitic Sandstone, Pit 3,Highvale Mine

Plate 5.7 Open to Close Folds Observed in the Bentonitic Sandstone, Pit3, Highvale Mine

Plate 5.8 Brecciated Coal Lamination Observed in Pit3, Highvale Mine

Lowden Lake area is shown in Figure 8.3.

It is noted that the orientations of fold axes of the fold structures in the areas mentioned above are rougly perpendicular to the inferred direction of ice movement in the areas. This relationship between ice-flow direction and the trends of ice-deformed fabric will be discussed in Chapter 8.

All the macroscopic folds observed in the study areas can be categorized into two main types: (1) concentric fold, and (2) fault-bend fold.

5.2.2 Concentric Folds

The field observations in Pit 3, Highvale mine, southern shore of Wabamun Lake, indicate that near the surface the fold is open and seems to have a constant orthogonal thickness (Plate 5.6); however, when approaching the top surface of the main coal seam, the folds are tightened and crumpled with a varied shape and thickness (Plate 5.7). Thrust faults are seen splaying out just above the top of the main coal seams or the decollement into the folded layers (Plate 5.4). Plate 5.8 also shows the occurrence of interbed slip in the folded strata. In general, the deformation ceases at and below the top of the main coal seam. The folds in the area are characteristic of concentric folds, a special case of parallel folding in which the thickness of the layers, measured normal to the bed is constant. The folded surfaces, as seen in profile, define circular arcs and deformation is mainly by bedding-plane slip, that is, shear parallel to bedding (Hobbs et al., 1976, p. 174; Carey, 1962; Ragan, 1985).

The conservation of volume in concentric folds implies that beyond the centres of curvature of concentric folds at depth, the mechanism of parallel folding failed, and complex crenulation and/or faulting would form instead in order to accommodate the excess bed length and volume that develop beyond the centres of curvature of the concentric folds. This would result in the formation of disharmonic folds and thrust faults, detachment of the folded strata from the underlying beds along a surface which would undergo shearing and sliding and is known as a decollement (Dahlstrom, 1969b). This horizon of detachment in the Highvale mine at the southern of Wabamun Lake has already been discussed in Section 5.1.1. Plates 5.4 and 5.7 show the presence of thrust faulting and disharmonic folds near the top of main coal seam (decollement) in the mine. The occurrence of the disharmonic folds and thrust faults below the concentric fold sequence exposed on the highwall are not uniform mainly because they depend on the mechanical properties of the strata at that elevation. Nevertheless, the presence of circular arc concentric folds about 10 m above the shear zone (sole thrust) exposed in the mine (Plate 5.6), the increase in complexity in these folds together with the appearance of imbricate thrusts with depth toward the shear zone indicate that the deformation in the area probably was initiated by the formation of concentric folds and thrust faults, and the horizon of detachment (decollement) formed afterwards when compression, folding, and shortening continued hence causing the amplitude to increase and wavelength to decrease. Continued shearing along the horizon of detachment also caused the bedding along this plane to deform into a shear zone or sole thrust.

Thus, concentric folding would cause the formation of anticlinal and synclinal structures, ridged topographical expressions, and complicated structures such as imbricate thrusts faults and asymmetrical folds to exist at depth before a horizon of detachment or decollement has been reached.

The absence of smooth, circular-arc concentric folds and the presence of imbricate thrusts and disharmonic folds in some of the exposures found in other ice-thrust terrains studied such as Lowden Lake area and area northwest of Sullivan Lake (Appendix C, Figures C.17 and C.23) are probably due to glacial and postglacial erosion which has eroded the concentric folds and exposed the complicated structures that overlie the decollement.

5.2.3 Fault-Bend Folds

Fault-bend folds are found in exposures in the Lowden Lake area (Appendix C, Figure C.18).

Fault-bend folds are formed when a thrust fault migrates by bedding-plane slip along a rather gently inclined incompetent bedding plane (such as shale) for some distance; however, due to local lithological variation, the frictional resistance increases where further horizontal spreading of the thrust become difficult. Thus, the thrust began to incline upward and when it cuts diagonally up (typically at about 30° to the horizontal) across a competent layer such as sandstone, a ramp is formed. This ramp may connect with a higher horizontal incompetent layer and the thrust may grow and follow this layer for some distance before it cuts diagonally up through a higher competent bed to connect with another higher incompetent layer (Rich, 1934; Park, 1983). The resulting thrust has a stair-case geometry; and fault-bend folds form when the thrust sheet slides along the thrust fault with a stair-case geometry. Figure 5.4 is a sketch which shows the formation of fault-bend folds and the resulting ice-thrust ridges. Generally, the bedding within the thrust sheets will be parallel to the flats and ramps except at the point where a ramp connects with a higher flat. In this area the bedding in the overlying thrust sheet will be bent toward the foreland (Figures 5.2a(?) and 5.4). Subsequent sliding of thrust sheets over the fault bend fold will produce imbricate slices or duplex structure (Boyer and Elliott, 1982, fig. 19).

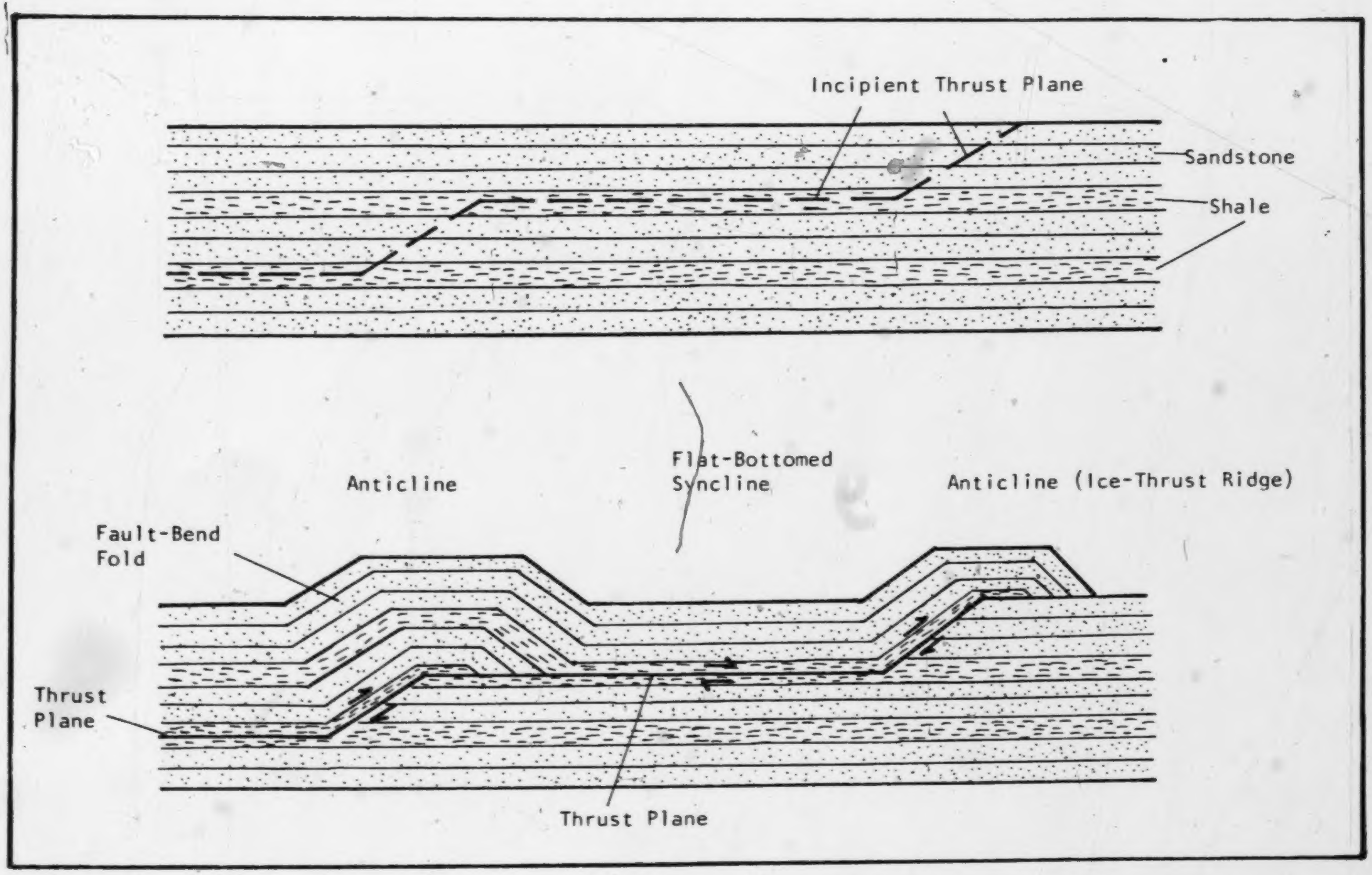
Incipient Thrust Plane
Sandstone
Shale
Anticline
Flat-Bottomed Syncline
Anticline (Ice-Thrust Ridge)
Fault-Bend Fold
Thrust Plane
Thrust Plane

Figure 5.4 : A Sketch of the Formation of Fault-Bend Fold (After Rich, 1934; Douglas, 1950)

5.3 Scars

Airphoto interpretation and field studies indicated that the ice-thrust ridges found in Lowden Lake area are located downglacier of a shallow depression which is probably a scar formed by ice thrusting (Photo AS 1532-133; Appendix C, Figure C.12). This is the only area studied where a scar due to ice thrusting was detected. The following section describes the genesis of a scar in the study area formed due to ice thrusting, and the methods used to estimate the depth of the structure, that is, the depth to decollement.

5.3.1 Genesis

As pointed out in the proceding sections, ice thrusting caused thrust faulting and concentric folding and the deformation should involve external and internal deformation in the horizontal and the vertical directions. The friction existing within the thrust sheet and along the thrust fault and the effect of obstacles appearing at the front of the thrust sheet may cause the front of the thrust sheet to move relatively more slowly than the back of the sheet. This uneven motion will lead to horizontal and vertical internal deformation of the thrust sheet. Horizontal internal deformation, which includes interbed slip in the parallel folds, the imbricate thrusting in the lower portion of the disharmonic folds, and compaction near the front, would cause horizontal shortening and result in vertical internal deformation such as folding. Horizontal shortening also causes tension near the back of the sheet. However, unless the front of the thrust sheet is fully rigid, thrusting always involves horizontal external deformation or translation of the thrust sheet along the thrust fault and the decollement. On the other hand, if the overall inclination of the thrust fault is very small, the amount of vertical external deformation, that is, the rising of the thrust sheet when it moves up the thrust fault, would be relatively small. As a result, in an area underlain by a horizontal decollement at shallow depth, it is believed that thrusting mainly involves horizontal internal and external deformation, and vertical internal deformation.

The tensile strength of a rock mass (especially jointed rock) is relatively low; and thus, the ends of the thrust sheets, which are under tension during horizontal internal and external deformation, would detach from the terrain behind and be displaced forward. The tensile fracture would soon be enlarged and a depression or scar would form at the location where the fracture of the thrust sheet took place. The scar would have its depth and length equal to the original thickness and length of the thrust sheet before deformation, while its width would depend on the amount of horizontal internal deformation (shortening) and/or horizontal external displacement (translation). After thrusting, this scar may be filled with water and become a lake or be occupied by streams, or filled with glacial and postglacial sediments and becomes featureless. The trace of the dimensions of these depressions would provide information concerning the amount of displacement and/or shortening that the thrust sheets have undergone, the original geometrical shape of the ends of the deformed blocks, and the depth of decollement.

5.3.2 Method of Study

The area balance technique was used to calculate the amount of shortening and displacement and the depth of decollement when the scar was formed in the Lowden Lake area. This technique is based on the assumptions that the volume of the thrust mass is conserved and a plane strain condition is considered, that is, the amount of material uplifted (whether folded or thrust) must be equal to the area of the scar formed by shortening and/or displacement. Once the amount of shortening or displacement is known, depth of deformation or the decollement can then be calculated (Goguel, 1962; Dahlstrom, 1969b, fig. 12; Ragan, 1985).

A section profile of Highway 56, that passes through the Lowden Lake area from Sections 12 to 24 of Township 36, Range 24 and cuts through the ice-thrust ridges south of the lake, has been obtained from Alberta Transportation Department. At the location where the Highway cuts through the ice-thrust ridges, altimeter survey measurements were also performed in order to obtain topographic control of these ridges. Bench marks in the towns of Stettler and Erskine were used as the reference points for the survey. The section profile indicates that the bedrock surface before deformation was probably located at 2757 ft (840 m) above sea level. Since the Highway section is not oriented perpendicular to the trend of the ice-thrust ridges nor parallel to the ice direction, the resulting profile is projected 52° from its original north-south trend in order to obtain a true section perpendicular to the trend of these glaciotectonic ridges (Figure 5.5).

5.3.3 Calculation of Depth to Decollement

The depressions found behind the ice-thrust ridges in the study area should be approximately equal to the total uplifted area due to ice thrusting which is represented by the ice-thrust ridges found in the ice-thrust terrain unit south of Lowden Lake (Appendix C, Figure C.12). The minimum shortening due to horizontal internal deformation was obtained by comparing the horizontal distance of these ice-thrust ridges and the length of the external outline of the ridges shown on the true section (Figure 5.5). Three different approaches were used to calculate the depth of deformation or decollement.

1. Thrust sheet with an immovable front and a horizontal decollement at depth - the front of the thrust sheet fixed. During thrusting, only shortening due to horizontal internal deformation and the resulting

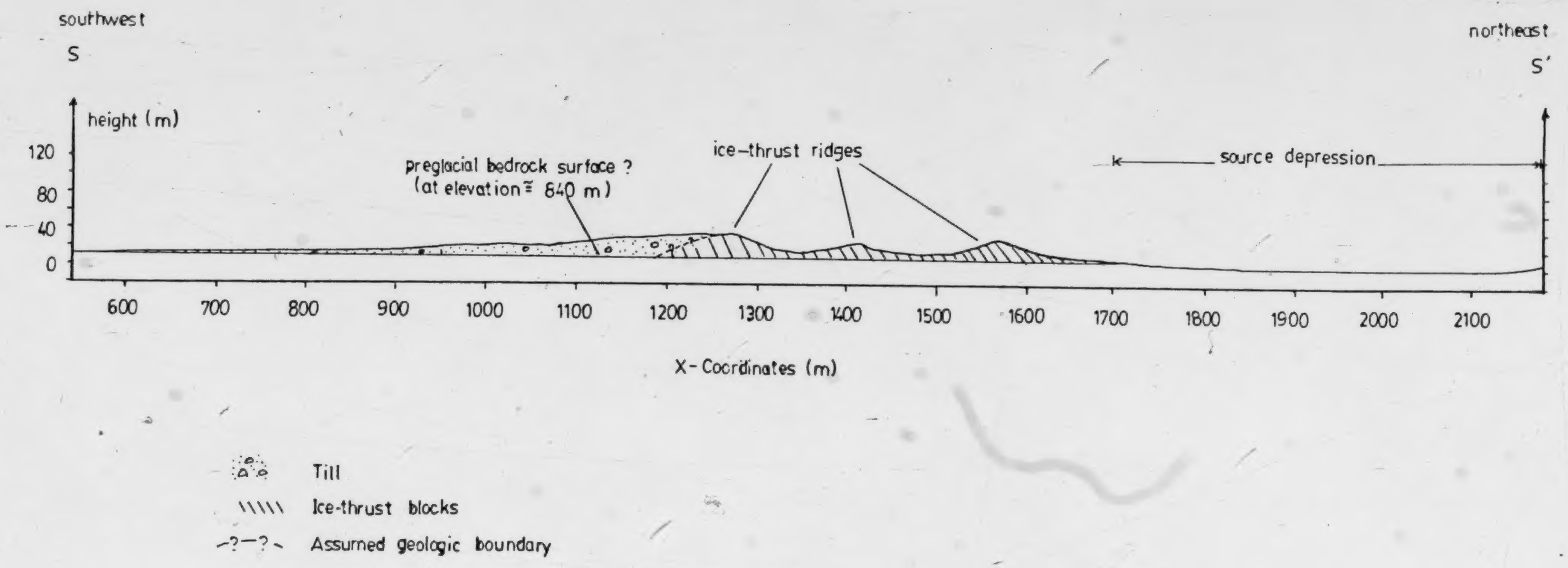
southwest
S
northeast
S'
height (m)
120
80
40
0
preglacial bedrock surface ?
(at elevation ≅ 840 m)
ice-thrust ridges
source depression
600
700
800
900
1000
1100
1200
1300
1400
1500
1600
1700
1800
1900
2000
2100
X-Coordinates (m)
Till
\\\\\ Ice-thrust blocks
-?-?- Assumed geologic boundary

Figure 5.5 : CROSS-SECTION OF ICE-THRUST RIDGES, LOWDEN LAKE AREA

vertical internal deformation or uplifting would occur. An uplifted area and 16 - 20 m of shortening were obtained from the cross-section (Figure 5.5). Area balance indicates that the depth of deformation due to ice thrusting was 335 - 574 m.

2. Thrust sheet with an immovable front and an inclined decollement - a floor thrust with a hindward dip as described by Williams (1984) was considered. With 16 - 20 m of shortening and the uplifted area indicated in Figure 5.5, the inclination of the thrust is 26° - 32° with respect to the horizontal and the estimated maximum depth of deformation is about 340 - 577 m.
3. Thrust sheet with a movable front and a horizontal decollement at depth - the front of the thrust sheet was allowed to move freely along a horizontal decollement. At the Lowden Lake area, a depression of about 484 m wide is found behind the ice-thrust ridges which appeared to act as the source area of the thrust masses (Appendix C, Figure C.12; Figure 5.5). This is comparable to the transverse-ridge form of Bluemle and Clayton (1984, fig. 9) which consists of tranverse ridges perpendicular to the direction of the last glacier and a source depression upglacier. When considering the sheet was only deformed by folding but without imbricate thrusting, the thrust sheet that comprises the ice-thrust ridges would have an undeformed width and thickness of about 528 m and 10 m respectively

which should be equivalent to the dimensions of the depression that is considered as the source area for the thrust masses. In the field, the depression shows a width of only 484 m. The width of the scar would be equal to 528 m if 44 m of it is covered by sediments, while the width of the decollement would be larger than this amount if part of it is covered by the thrust masses. In either case, the maximum amount of sliding along the decollement is equal to the width of the scar. The total deformation of the ice-thrust rock masses would be made up by about 16 m of shortening due to horizontal internal deformation and about 528 m of translation due to horizontal external deformation. This approach also indicates that the height of the ice-thrust ridges and the depth of the scar with respect to the ground surface before ice thrusting occurred has a maximum ratio of 3.5 : 1 and a minimum ratio of 2.4 : 1.

5.3.4 Discussion

1. The thrust sheet with an immovable front yielded a depression and depth to decollement hundreds of metres below the ground surface and is not comparable to the depth of the decollement observed in other ice-thrust terrain units, for example, in the Highvale Mine at the Wabamun Lake area where the depth and movement along the sole thrust due to ice thrusting are found to be 9 - 27

m and 355 - 395 m respectively (Figures 5.2 and 5.3). Although the maximum thickness of a thrust sheet due to ice thrusting documented in literature is about 200 m, the average thickness of the deformed layer is about 60 m (Mathews and Mackay, 1960; Sauer, 1978; Moran et al., 1980; Eyles and Menzies, 1983). Ice-deformed thrust sheets at Lowden Lake area with a freely movable front which show a depth of decollement of about 10 m, 16 m of shortening and 528 m of translation during ice thrusting, seem to be close to the truth.

2. The ice-thrust ridges found at the Lowden Lake area are believed to have formed when, under ice thrusting, a rock mass about 528 m wide and 10 m thick was folded, thickened and thrust onto the surface to form ice-thrust ridges, leaving a depression or a scar structure behind which is partially covered by till at present. For comparison, a scar structure with a width of about 11 m and a depth of about 9 m formed due to glacial drag on Pennsylvanian bedrock is entirely filled by debris (Lessig and Rice, 1962, fig. 3).
3. Area balance is based on the assumption that the volume of the deformed block is conserved. However, because of the actual volume reduction of the deformed strata due to compaction and stretching perpendicular to the fold axis, the area balance may give a low estimate of the depth of decollement.
4. Scar structures should be common features behind

ice-thrust ridges and hills. The fact that they are rarely found in the ice-thrust terrain studied is thought to be because, as with strike-slip faulting in ice-thrust terrain, the scar is usually covered by glacial and/or postglacial deposits and is hardly noticeable on aerial photographs and in the field.

5.4 Jointing

This section concerning joint structure in ice-thrust terrain is based entirely on the information obtained from Highvale mine, Wabamun Lake area.

5.4.1 Field Description

A joint survey was undertaken in Pits 2 and 3 in Highvale mine at the southern shore of Wabamun Lake by the personnel of Alberta Research Council and the author during the summer of 1984. Terrain analysis indicate that the pits are located in an ice-thrust terrain unit (Appendix C, Figure C.4). In Pit 3, 101 and 50 joints were measured in Slides 1 and 2 respectively. The results are as follows.

5.4.1.1 Joint Orientation

Three major joint sets were found in Slide 1. The strike/dip of the sets of joints are: 075°/ 82° SE, 155°/ 80° NE, 090°/ 84° S with the second set varying between 135° and 175° azimuth. Five joint sets were found in Slide 2 with strike/dip of : 020°/ 83° NW, 045°/ 85°NW, 075°/ 85° NW, 150°/ 80° NE, 175°/ 90°.

W. Langenberg of the Alberta Research Council has constructed rose diagrams of the joint sets measured in Slides 1 and 2 respectively (Figure 5.6). It is to be noted that the observed joint sets may not precisely represent the actual number of joint sets present in the area because of the existence of a blind zone for joints which are parallel to any 2-dimensional exposures (Terzaghi, 1965; Ragan, 1985, p. 284). More joint measurements taken from highwalls with a variety of orientations in the mine are needed before the problems can be completely solved. Nevertheless, careful digging into the highwall in Pit 3 seemed to indicate that the blind zone problem is not severe in the highwall examined since the two major joint sets found are almost parallel to the exposed planes (Figures 10.2 and 10.3).

5.4.1.2 Joint spacing and roughness

In Slide 1, joint set 1 has a spacing of 13 - 19 cm and set 3 has a spacing of 10 - 19 cm. Both have tight to extremely narrow separation and the nature of these joint surfaces are rough with asperities tending to match each other, indicating that no shearing has occurred. In Slide 2, set 1 has a wide spacing of about 20 cm while set 2 also has a wide spacing of about 18 - 30 cm. The nature of their surfaces are similar to those found in Slide 1. The descriptions of the joint sets followed Rawlings (1977).

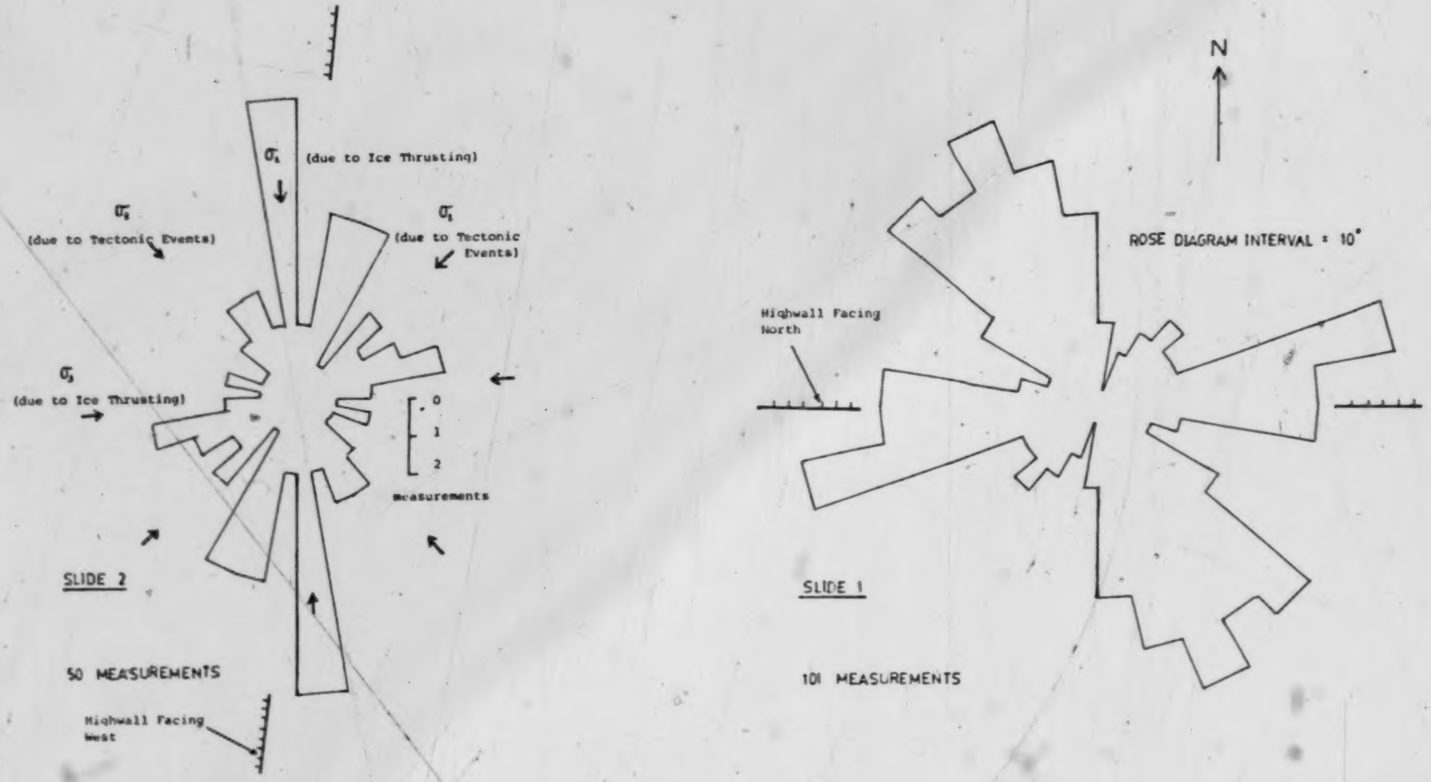

Figure 5.6 Rose Diagram of Joint Sets measured in Slides 1 and 2, Pit 3, Highvale Mine

5.4.2 Discussion

According to the Navier-Coulomb criterion of brittle failure, the angle which the plane of failure makes with the major principal stress axis is

$$\theta = 45 - \phi / 2 \quad \ldots\ldots\ldots\ldots\ldots\ldots\ldots\ldots \quad (5.1)$$

where $\tan \phi = \mu$, the coefficient of internal friction of material.

When conjugate planes are developed in an isotropic material, the acute angle 2θ will be bisected by the axis of σ_1 , and the line of intersection of the shear plane will be parallel to the axis of σ_2 (Price, 1966, p. 60). Price (1966) suggested that brittle and semi-brittle rock under tectonic compression and uplift would generally develop 4 sets of joints, in which the sets which are perpendicular and parallel to the direction of compression are tension joints, the other two or conjugate sets, which are bisected by the axis of compression are shear joints.

Gough and Bell (1981, 1982) performed studies on stress orientations from oil fractures in Alberta and northern Canada and discovered that the orientations of the principal horizontal stresses in the bedrock are in harmony within the entire western Canadian sedimentary basin. The regional stress field is essentially a strike-slip type, with σ_2 vertical, σ_1 NE-SW, σ_3 NW-SE. Investigations of the azimuthal distributions of breakouts in the six oilwells near the west Pembina oilfield (about 55 km southwest of Highvale mine, Wabamun Lake area) indicate the σ_1 direction is at about 42° - 51° azimuth (Gough and Bell, 1981, fig 3). Indeed, the general trend of σ_1 is at right angles to the strike of the thrusts of the Rocky Mountains. Fordjor et al. (1983) suggested that the uniform stress field in the Alberta Plain may be due to the contemporary tectonic traction on the underside of the lithosphere of the North American Plate.

By combining the stress field in the Alberta Plains, the failure criterion of brittle rock, and field observations of the orientations of the joint sets and lineaments in western Canada, a regional stress field may be derived; that is, σ_1 is at about 42° - 51°, σ_3 lies in the same horizontal plane but at right angles to σ_1 , and σ_2 is vertical. As a result, a theoretical regional joint system, having two tension joint sets striking at 42° - 51° and 132° - 141° and two shear joint sets strike at about 12° - 21° and 72° - 81°, is presumed to develop when considering the overburden has a internal angle of shearing resistance of about 30°. In contrast, field investigation of the regional joint system in late Cretaceous to Paleocene rocks in central and southern Alberta shows joint sets strike approximately 55°- 65°, 140° - 155°, 5°, and 95° (Babcock, 1973, 1974).

When this regional joint system is compared with the joint system observed in the deformed sediments that overlies the shear zone in Pit 3, Highvale mine (Figure 5.6), it is noticed that there are two joint sets which deviate from this regional joint system. These deviating local joint sets strike about 090° and 175°.

Local joint system formed due to ice advance have been suggested. For examples, Trainer (1973) performed a joint set survey on glaciated igneous and sedimentary rocks and suggested that the joint system found seem to show two sets of shear joints which flank the direction of ice advance and strike at about 40° to it, two sets of extension joints which flank the direction of advance and strike within about 10° of it, and two sets of release joints which are nearly normal to the sets of extension joints (Trainer, 1973). He believed that these joints were opened by glaciation and most were formed along preexisting zones of weakness following the regional joint system while some new joints were formed in sound rock when the older zones of weakness do not occur near the required positions for fracturing under the stress applied by the moving glacier. Moreover, systematically-distributed and steeply-inclined fissures oriented parallel and/or perpendicular to the direction of ice movement have also been found in boulder clays and quartzite (Pusch, 1973a; Barden, 1973; Broster et al., 1979).

From Pit 2 (about 8 km southeast of Pit 3), field measurements in the ice-deformed bedding such as imbricate faults which diverged from a horizontal shear zone or sole thrust, seem to indicate that the recent glacial direction was about 175° azimuth (Appendix C, Figure C.9a). Treating this direction as the direction of the major principal stress (due to ice thrusting) with σ_2 vertical (due to the weight of the ice), and σ_3 parallel to the ground and orthogonal to σ_1, the local stress field in the mine during recent glaciation is obtained. According to the brittle failure criterion (Equation 5.1), the theoretical joint system from this local stress field should consist of at least two tension joint sets which strike about 085° and 175° azimuth, and two shear joint sets which strike at 175° $\pm \theta$, that is, 020° and 150° azimuth (since the internal angle of shearing resistance of the bentonitic sandstone in the Pits is about 40°, quoted from Monenco Ltd., 1983c).

The field data on the orientation of the joint sets (which strike at about 020°, 150°, 175°) observed in study area match reasonally well with the preceding theoretical calculations. However, the joint set which strikes at 090° azimuth is about 5° off the theoretical consideration. This may be due to: (a) insufficient number of field measurements to obtain the true mean orientation of this set, and (b) other fissures due to stress release and weathering caused by the erosion of the thick overburden in the geological past and the retreat of the glacier. It must be noted that no shear joints have actually been observed in the bentonitic sandstone that overlies the shear zone in Pit 3, Highvale mine. The weakly cemented sandstone probably has prevented the preservation of shear features on its joint surfaces. Thus, the interpretation of the genesis of the joint system in the study area is mainly based on the orientations rather than the surface nature of the joint sets observed in the field.

The arguments presented above suggest that the local joint system in the study area formed due to ice thrusting is different from the regional joint system in central Alberta formed due to the past tectonic events, and the direction of the glacial advance can be estimated once the local and regional joint systems of the area in an ice-thrust have been mapped. However, this conclusion should be treated as tentative because it is mainly deduced from a small number of joint measurements (Figure 5.6) obtained from two particular sites in an ice-thrust terrain. More joint studies must be performed in the mine and in other ice-thrust terrains before a definite conclusion can be reached.

5.5 Kinematic Analysis of the Formation of Glaciotectonic Macrofabric

The thrust system found in the ice-thrust terrains studied chiefly consists of:

1. Decollements or sole thrusts.
2. Concentric folds and fault-bend folds.
3. Strike-slip faults and normal faults.
4. Imbricate thrusts.
5. Piggy-back thrust sequences.
6. Scars.

7. Local joint systems.

Field observation and scale models indicate that excepting their smaller scale, the types and geometry of the macrofabric appeared in glaciotectonic thrust systems resemble closely the thrust systems observed in the foreland margins of orogenic tectonic terrains (Dahlstrom, 1969a, 1969b, 1970; Boyer and Elliott, 1982; Elliott, 1976; Ussing, 1907; Berthelsen, 1979; Koster, 1957; Bucher, 1956). This is probably because both the gravitational spreading of supracrustal rocks which is responsible for the foreland orogenic deformation (Price, 1973) and the gravitational spreading of a continental ice sheet which is responsible for the ice thrusting have applied a similar mode of stress system in the surficial sediments and deformed them. Thus, it seems reasonable that a kinematic analysis of the glaciotectonic macrofabric, that is, the reconstruction of the movements that take place during the formation of ice-thrust ridges and its associated macrofabric, can be performed based on the available understanding of the orogenic tectonics. The kinematic analysis, which mainly applies to the ice-thrust terrains found along the southern shore of Wabamun Lake and Lowden Lake areas, is described below.

1. During ice thrusting, horizontal compressional force was applied to the ends of horizontal layers of surficial bedrock in an ice-thrust terrain. Deformation probably started as an initial fracture which subsequently spread

horizontally along bedding toward the foreland, following the zone of bedding plane slippage as described by Douglas (1950).

2. Depending on the lithology and defects in the sediments, further compression of these layers of bedrock probably led to the following cases (Figure 5.7):
   a. Formation of bedding plane step thrust (Figure 5.7-1) - Depending on the amount of sliding of the thrust sheet on a stair-case thrust fault, a broad, flat-topped anticline or a narrow anticline with a rounded crest would be formed at the location where the thrust breaks upward from the lower glide plane while a flat-bottomed syncline would be formed between these thrust breaks (Rich, 1934; Douglas, 1950, fig. 17, p. 81). Thus, the ice-thrust ridges are the topographic expressions of a series of fault-bend folds.
   b. Formation of concentric folds, imbricate faults, and decollement (Figure 5.7-2) - Obstacles appear at the front of a thrust sheet that prevent further movement of the sheet toward the foreland; thus, the continued pushing of the thrust sheets from behind will cause the displaced mass to be further folded, crumpled and faulted, and detached from its underlying rigid basement. In this case, the ice-thrust ridges are the topographic expressions of a series of concentric folds and/or disharmonic

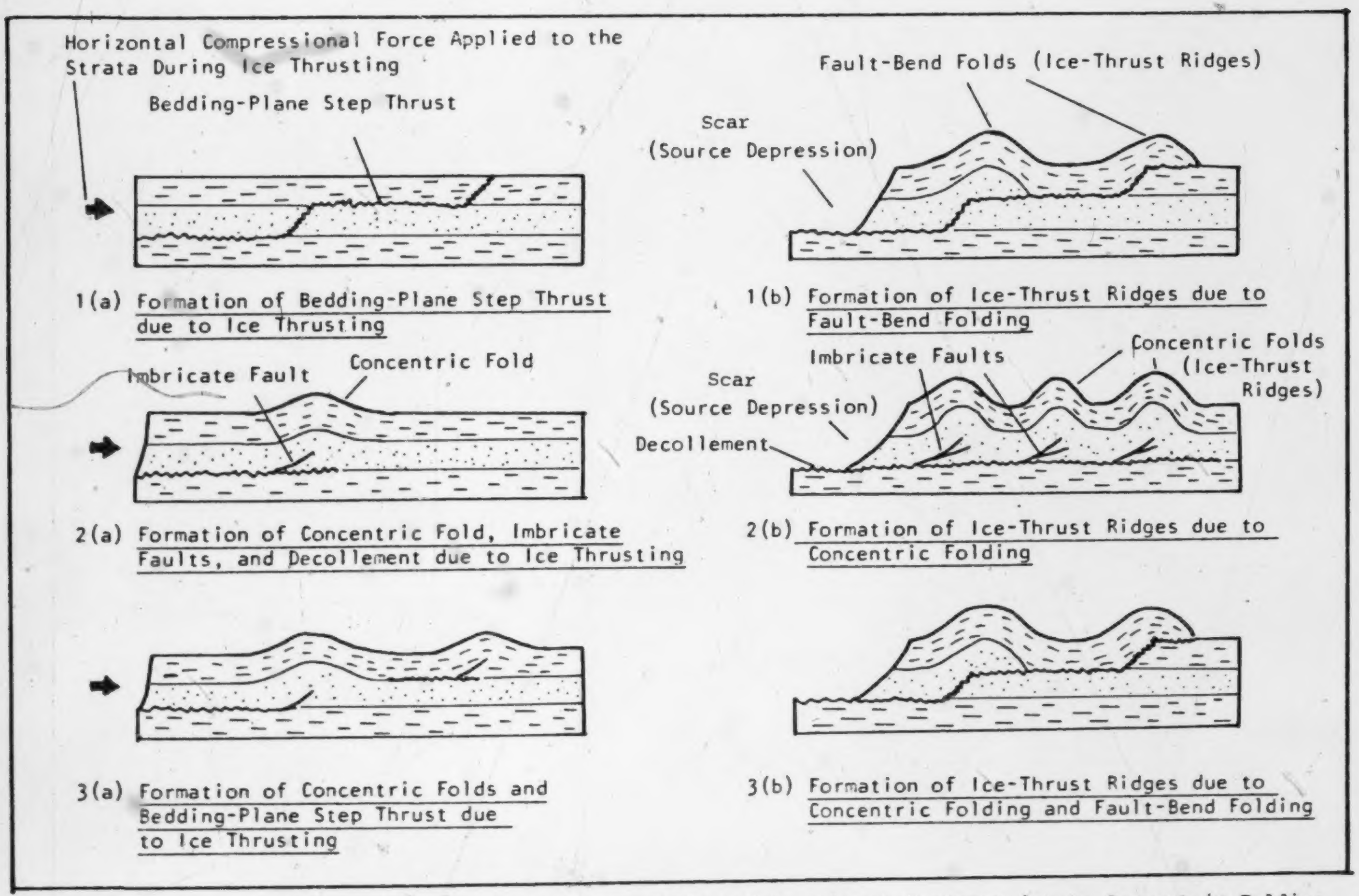
Horizontal Compressional Force Applied to the Strata During Ice Thrusting
Bedding-Plane Step Thrust
Scar (Source Depression)
Fault-Bend Folds (Ice-Thrust Ridges)
Imbricate Fault
Concentric Fold
Scar (Source Depression)
Decollement
Imbricate Faults
Concentric Folds (Ice-Thrust Ridges)

1(a) Formation of Bedding-Plane Step Thrust due to Ice Thrusting

1(b) Formation of Ice-Thrust Ridges due to Fault-Bend Folding

2(a) Formation of Concentric Fold, Imbricate Faults, and Decollement due to Ice Thrusting

2(b) Formation of Ice-Thrust Ridges due to Concentric Folding

3(a) Formation of Concentric Folds and Bedding-Plane Step Thrust due to Ice Thrusting

3(b) Formation of Ice-Thrust Ridges due to Concentric Folding and Fault-Bend Folding

Figure 5.7 : A Diagrammatic Sketch of the Formation of Ice-Thrust Features due to Concentric Folding and/or Thrust Faulting

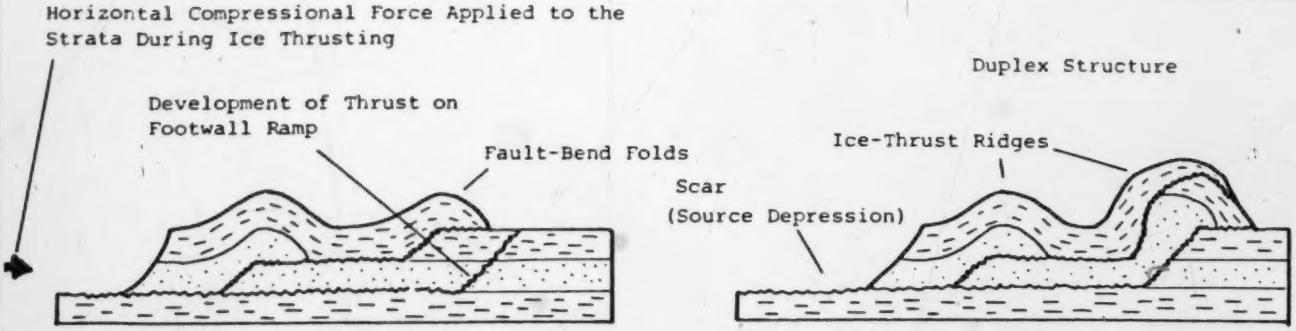
Horizontal Compressional Force Applied to the Strata During Ice Thrusting
Development of Thrust on Footwall Ramp
Fault-Bend Folds
Duplex Structure
Ice-Thrust Ridges
Scar (Source Depression)

4(a) Formation of Thrust on the Footwall Ramp due to Ice Thrusting

4(b) Formation of Ice-Thrust Ridges and Duplex Structure

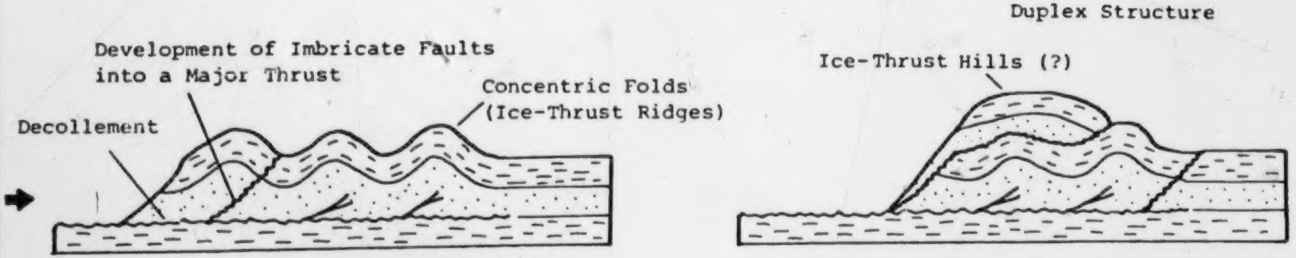
Duplex Structure
Development of Imbricate Faults into a Major Thrust
Ice-Thrust Hills (?)
Concentric Folds (Ice-Thrust Ridges)
Decollement

5(a) Formation of Thrust within the Concentric Folds due to Ice Thrusting

5(b) Formation of Ice-Thrust Hills (?) and Duplex Structure

Figure 5.7 (continued) : (1) and (3) are modified after Dahlstrom (1970, fig. 29) and Verrall (1968); (2), (4) and (5) are suggested by the Author folds.

c. Formation of concentric folds and bedding-plane step thrust (Figure 5.7-3) - Stair-case thrust fault and concentric folds were formed simultaneously. Continued forward pushing will cause the sliding of the concentric folded thrust sheet along the stair-case thrust fault and formaton of anticlines and synclines at the ramps and flats of the stair-case thrust fault. In this case, ice-thrust ridges are the topographic expressions of a series of concentric folds and fault-bend folds.

d. Formation of duplex structure (Figure 5.7-4,-5) - The collapse of the footwall ramp of the bedding plane step thrust terrain or the growth of the imbricate thrust onto the ground surface in the concentric fold terrain under the continued forward pushing would result in the overriding and stacking of concentric fold and/or fault-bend fold thrust sheets, resulting in the formation of duplex structure. In this case, the ice-thrust features are the topographic expressions of a series of concentric folds and fault-bend folds of the duplex structure.

3. A scar would form behind the thrust sheet and its formation has been described in detail in Section 5.3. Moreover, the lateral discontinuities of the glaciotectonic thrust sheet in the ice-thrust terrains

were probably completed by opening and connecting the near-vertical joints formed in sound rock or along pre-existing zones of weakness such as a regional joint set under the stress applied by the moving ice.

The first and/or third cases (Figures 5.7-1, -3) are probably equivalent to the subsurface folding and faulting deformation and formation of ice-thrust ridges in the Lowden Lake area as shown by the thrust faults with a stair-case geometry and the fault-bend folds exposed in the area (Appendix C, Figure C.16 and C.18); furthermore, the topographic cross-sections of the area indicate that the glaciotectonic thrust sheet was deformed with a freely moveable front (Figure 5.5).

The second and fourth cases (Figure 5.7-2, -4, -5) are probably equivalent to the glaciotectonic deformation in Pit 3, Highvale mine, Wabamun Lake area, as shown by the well-developed decollement, concentric folds, disharmonic folds, imbricate thrusts (Plates 5.2, 5.4, 5.6 and 5.7), and the presence of duplex structure (Figures 5.2 and 5.3).

6. MESOFABRIC, MICROFABRIC AND SUBMICROFABRIC OF ICE-THRUST SEDIMENTS

6.1 Introduction

In this thesis, mesofabric refers to the soil or rock features that are large enough to be observed without the aid of a microscope yet small enough that they can still be observed directly in their entirety. Microfabric is defined as the features of the soil that require at least a standard light microscope to identify them. Submicrofabric comprises the soil units and arrangements that can only be seen under an electron microscope.

This study involves the investigation of mesoscopic fabric of ice-thrust clayey sediments appearing in outcrops and hand specimens, and the recognition of the microscopic and submicroscopic fabric within the clay matrix such as the particular pattern of arrangement of the sand and silt grains and clay aggregates and deformed structures appearing under a polarizing microscope and a scanning electron microscope (SEM).

The hand specimens and samples used in this study (for petrographic and SEM studies and for the geotechnical property tests) were from block samples collected at the horizon where a continuous horizontal slip surface was located within the shear zone that was about 3.4 m thick exposed in Pit 3, Highvale mine, Wabamun Lake area (Plate 5.2; Section 5.1.1.1). Appendix E describes the location and method of block sampling.

6.2 Mesofabric

6.2.1 Fold Structure

Small-scale folds and monoclinal structures were found in the bentonite and the thin coal layers which overlie and underlie it (Plate 6.1) in the Highvale mine. These beds are rather undulatory and wavy with fold axes approximately perpendicular to the direction of recent ice movement in the area (Appendix C, Figure C.9a). Both the bentonite and the thin coal layers are located at the bottom of the shear zone or sole thrust of the area (see Chapter 5, Section 5.1.1.1).

Many highly deformed sideritic nodule layers were found embedded in the exposed gently folded strata in the ice-thrust terrains studied. For example, in the Nisku area, the sideritic nodule layers were commonly deformed into gentle to tight folds with amplitudes and wavelengths of about 0.3 - 1.0 m and 0.3 - 1.5 m respectively; while the beds above and below the nodule layers still maintain gentle folds. The deformed nodular layers are similar to the convolute folds and ptygmatic folds which sometimes are associated with concentric folds and are characteristic folds of high-grade metamorphosed rocks (Hobbs et al., 1976, p. 174). The presence of these kinds of folds in the study areas indicates that the beds might have behaved in a ductile manner during the period of glaciotectonism. Indeed,

METRIC 1 2 3 4 5 6 7 8
Ben. #3
13 14

Plate 6.1 Monoclinal Structure Observed in the Bentonite, Pit 3, Highvale Mine

SLIDE #1
MUDSTONE
8
7
6
5
4
3
2

Plate 6.2 Hand Specimen Obtained at Slip Surface of the Shear Zone , Slide 1, Pit 3, Highvale Mine

small-scale glaciotectonic structure in subtill beds that resemble metamorphic sediments have been found in the Edmonton area (Shaw, 1982, fig. 19).

6.2.2 Displacement Shear

The exposed shear zone adjacent to Slide 1, Highvale mine, chiefly consists of bentonitic mudstone that contains a few continuous and horizontal slickensided surfaces with one happening to coincide with the present failure surface of the slides in the area. These shear surfaces are known as the principal displacement shears that develop in a shear zone after large movements from at least several to 10 cm or more have occurred (Skempton and Petley, 1967). Examination of the hand specimens obtained from the block samples collected at this flat-lying slip surface in the shear zone adjacent to Slide 1 indicates that the portion above the slip surface is a light grey to dark grey, very fine-grained, moist and plastic layer while the bottom portion is a dark brown to dark greyish brown, stiff, fissured, relatively dry layer with many angular clay lumps (Plate 6.2). These two layers are separated by the flat-lying horizontal slip plane observed in the field. The specimens can easily be split along this discontinuity.

Examination of the thin sections made from these hand specimens by the unaided eye show that this slip surface also appears horizontal to gently undulating. Figure F.1 in Appendix F shows the locations in the block samples for thin sectioning. The thin sections also show that, immediately adjacent to the slip surface, there is a mixture of light grey to brown nodules or lumps varying from less than 1 mm to 3 mm in length, and vertical to inclined fractures diverging upward and downward from the shear surface. Above the slip plane or toward the top of the thin sections, the material is chiefly a light grey to light brown clay matrix with scattered nodules. There is a tendency toward a decrease of size and number of fissures and nodules. Below the slip surface or toward the bottom of the thin sections, the material is composed essentially of dark brown to light greyish brown angular lumps and peds up to 7 mm long. The size of fissures or cracks are relatively larger and may be up to 1 mm wide.

Hand specimens were also obtained from a bentonite layer, which is 13 - 20 cm thick with at least three undulatory principal displacement shear surfaces, exposed near the base of a shear zone about 0.9 m thick in Pit 3, Highvale mine. Examination of the samples indicates that the shear planes generally are overlain and underlain by a black, brownish grey to dark grey, moist, plastic, and dense clay layer which is 0.5 to 3.5 cm thick (Plate 6.3). Many angular coal fragments were found in the layer. Away from the shear plane, the material becomes a light brown, light greyish white to light grey, dry, stiff, crumbly and porous clay. At the shear surfaces, angular coal fragments with length of less than 1 mm to 8 mm were noted with their sides

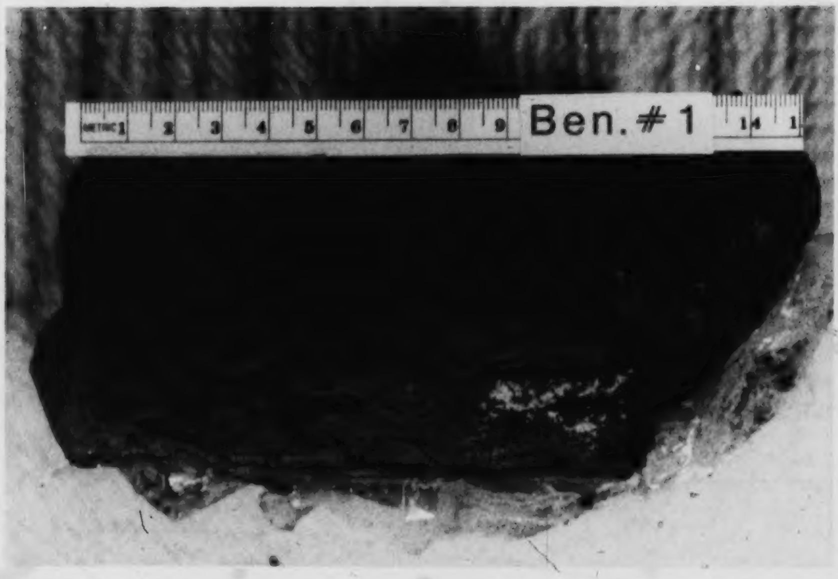

Plate 6.3 Hand Specimen of the Bentonite, Slide 2, Pit 3, Highvale Mine

oriented parallel to the plane; however, the grains become randomly oriented about 5 mm below the shear plane (Plates 6.4 and 5.5).

Between the principal slip surfaces observed in the shear zone exposed in the mine, the sediment is relatively dry, porous and crumbly with many inclined to horizontal fissures, clay lumps or lenses (Plates 6.2 and 5.3). These are probably the minor shears, which included 'displacement shears' or 'slip surfaces', Riedel- and thrust-shears, as termed by Skempton and Petley (1967). It is believed that the porous and crumbly zone between the principal slip surfaces within the shear zone observed in the study area is equivalent to the zone of minor shears. The relative movement along individual minor shears is small and probably of the order of a few millimetres at most since generally they are polished but are seldom slickensided. This is comparable to the sheared features observed in tectonic shear zones by Fookes (1965), Skempton (1966), and Skempton and Petley (1967).

No mapping was performed on the minor shears observed in the study area because of the difficulties involved in measuring the true attitudes of these undulating surfaces that were exposed on a steeply inclined plane.

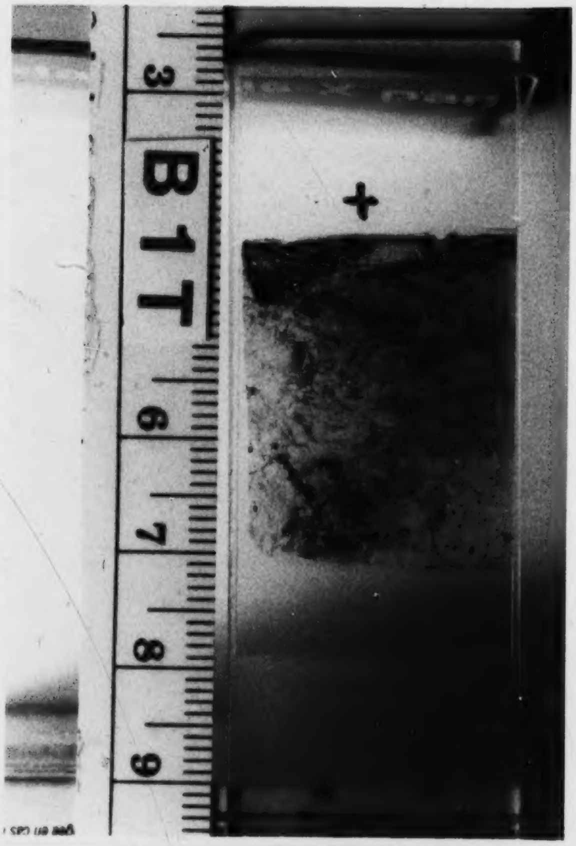

Plate 6.4 Thin Section of the Bentonite, Slide 2, Highvale Mine

6.3 Microfabric

The laboratory preparation and the method used in the investigation of the microfabric of ice-thrust sediments are described in Appendix F.

The characteristic microscopic features found in this investigation are shown below.

6.3.1 Observation (for bentonitic mudstone only)

The continuous horizontal slip surface observed in Pit 3 (Plate 5.2) and also in the thin sections was used as the plane of reference to describe the microfabric observed. Thus, the upper portion and the lower portion of the thin section which are mentioned in the following paragraphs refer to the materials that lie above and below this horizontal slip surface respectively. All the thin sections studied were oriented with their top normal and away from the ground surface and the bottom normal and toward the ground (Figures 6.1 and F.1).

The terminology used to describe the texture of the features observed in the thin sections are outlined below. This is after the modification of the work of Brewer (1964) and Yong and Sheeran (1973) by the author.

Peds (aggregates or crumbs) are mesoscopic fabric units visible to the unaided eye and are defined as an individual natural soil aggregate, separated from adjoining peds by surface of weakness which are recognized as natural discontinuities. Natural soil aggregates are composed

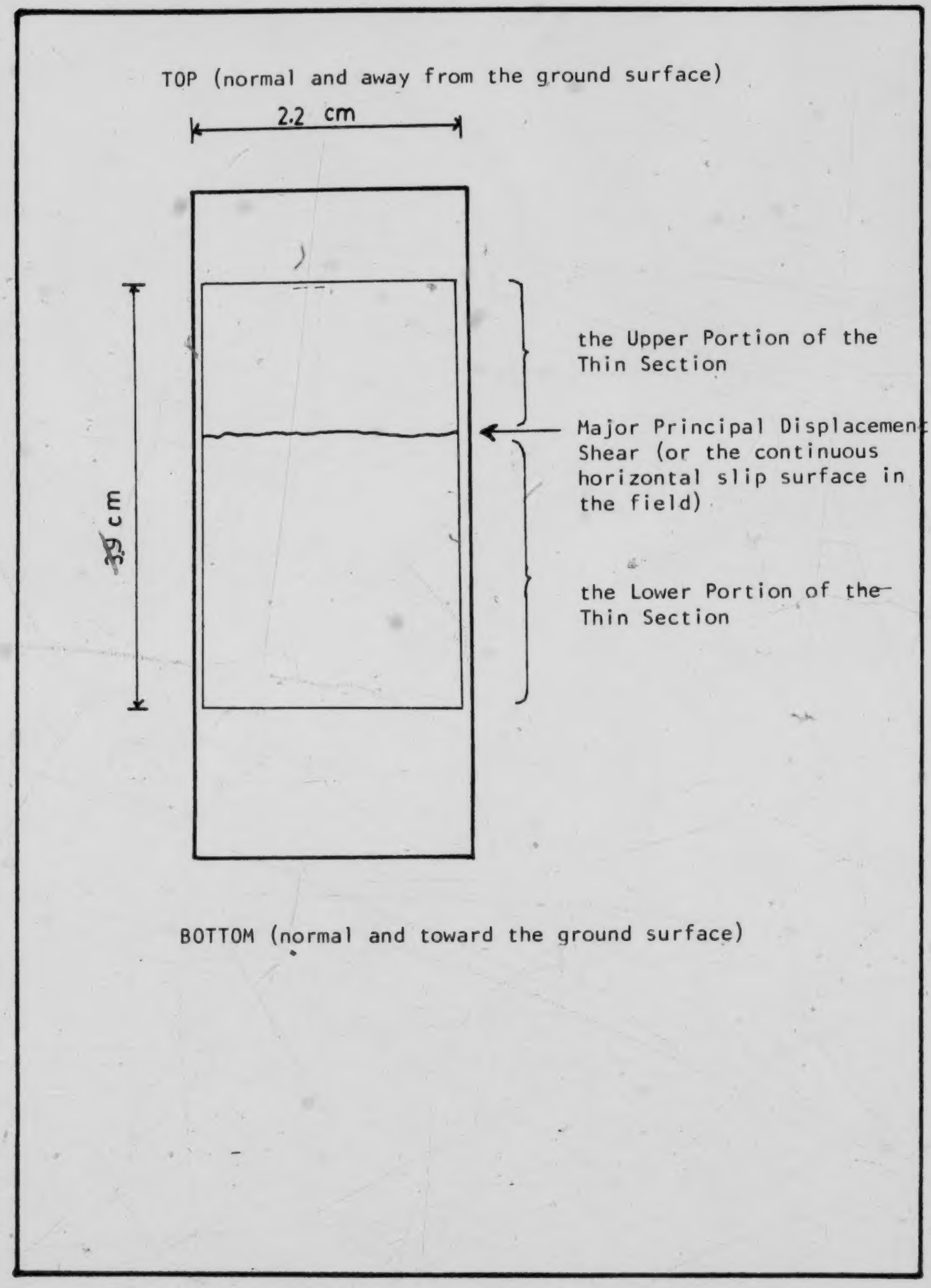
TOP (normal and away from the ground surface)
2.2 cm
3.9 cm
the Upper Portion of the Thin Section
Major Principal Displacement Shear (or the continuous horizontal slip surface in the field)
the Lower Portion of the Thin Section
BOTTOM (normal and toward the ground surface)

Figure 6.1 Location References of the Thin Section

chiefly of microscopic fabric units visible under the light microscope such as nodules (skeleton grains and organic inclusions), fractures (voids), and clay matrix (domains or plasma). Clay matrix consists of individual or groups of clay particles which are submicroscopic fabric units and are only visible under electron microscope. Figure 6.2 shows a diagrammatic sketch of these fabric units. The observed texture of the ice-thrust sediments is now described.

6.3.1.1 Texture

1. Grain Size and Shape - Examination of the thin sections show that basically the ice-thrust sediments sampled consist four main components: peds, nodules, fractures and clay matrix. It was observed that peds and nodules were angular to rounded in shape and ranged from 0.08 mm to 2.7 mm in length or in diameter. A clay matrix composed mainly of microscopic to submicroscopic clay particles surrounded the nodules or the space between peds. Organic inclusions were mainly organic remains with irregular shape usually distributed randomly within the clay matrix. (Particles with outlines of spicules were observed under high magnification which resemble relict glass shards in altered tuff found in the fine-grained rocks in centra Alberta (Locker, 1973, plate 5, figs. 1 and 2). No photographs were taken due to the difficulties in focusing these particles under high

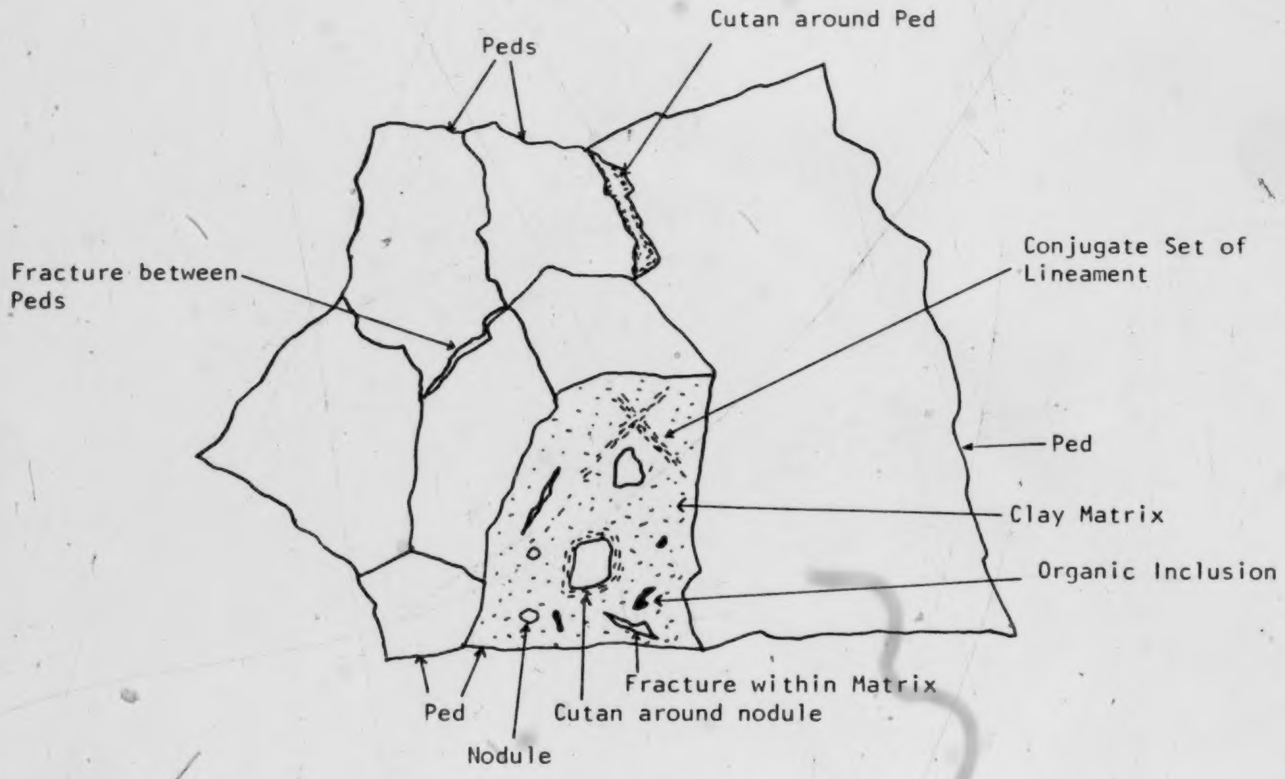
Cutan around Ped
Peds
Fracture between Peds
Conjugate Set of Lineament
Ped
Clay Matrix
Organic Inclusion
Fracture within Matrix
Cutan around nodule
Ped
Nodule

Figure 6.2 : A Diagrammatic Sketch of the Fabric Units

magnification.)

In the upper portion of the thin section a few nodules were found and were always scattered widely in the clay matrix (Plate 6.5). These nodules were rounded to very rounded and some have boundaries so diffuse that it was difficult to distinguish whether they were nodules or clay matrix. On the other hand, the lower portion of the thin section was mainly made up of peds that were angular to subangular and had definite boundaries (Plate 6.6). The boundaries or edges of these peds usually matched the adjacent ones thus forming an interlocking framework. This seemed to indicate that the latter were broken from the former and very little displacement had taken place between them. Near the middle of the thin section, that is, at and immediately adjacent to the horizontal slip surface, both angular and rounded nodules were found embedded in a clay matrix. The sides of the nodules that were in direct contact with the slip surface tended to be smooth and flat, suggesting they had been moved and sheared along this plane (Plate 6.7).

2. Grain Sorting - In the upper portion of the thin section, clay matrix dominated and fewer nodules were present and in general were randomly oriented and not in contact (Plate 6.5). Organic inclusions were often found scattered in the clay matrix. In

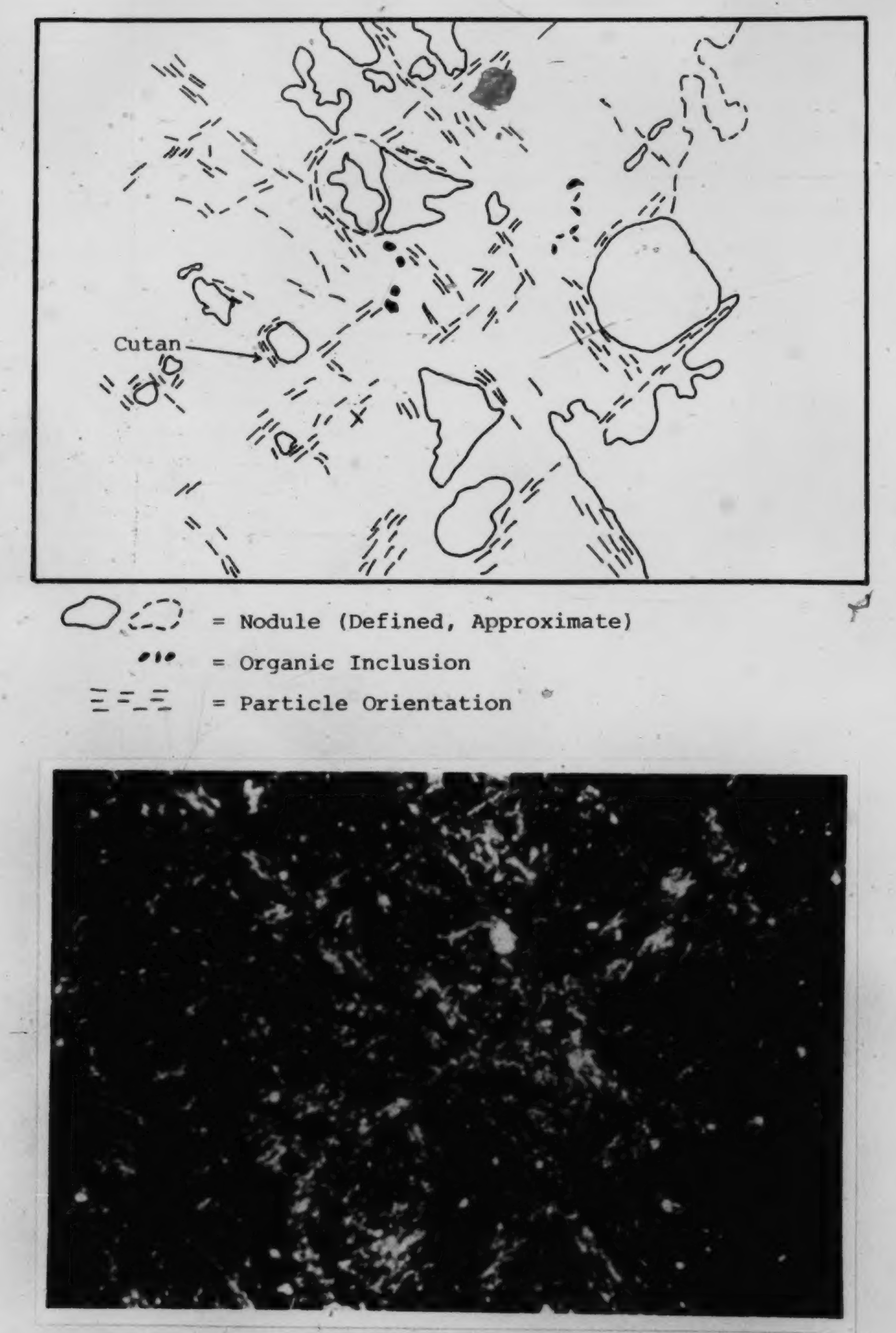
Cutan
= Nodule (Defined, Approximate)
= Organic Inclusion
= Particle Orientation

Plate 6.5 Nodules and Conjugate Sets of Lineations in Clay Matrix, crossed nicols, 42x

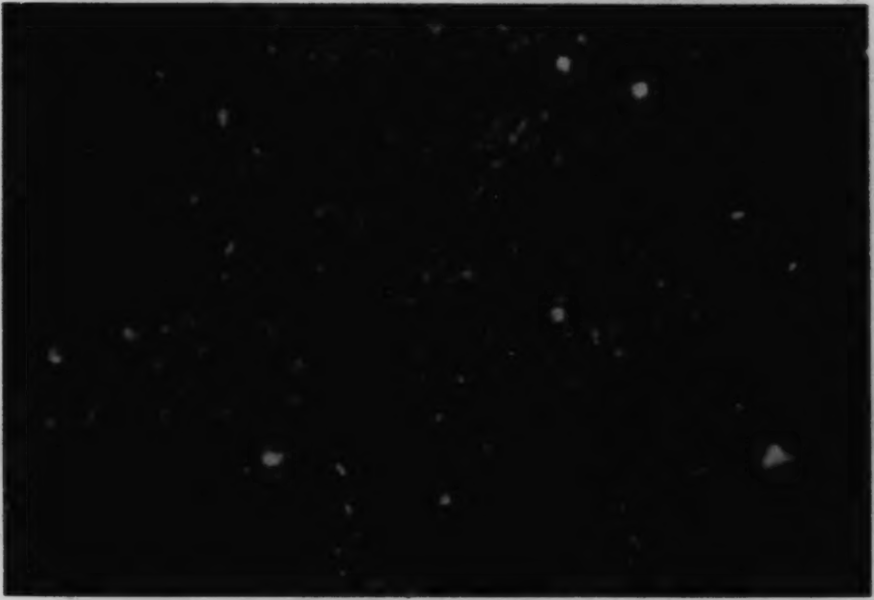

Plate 6.6 Angular to Subangular Peds, crossed nicols, 42x

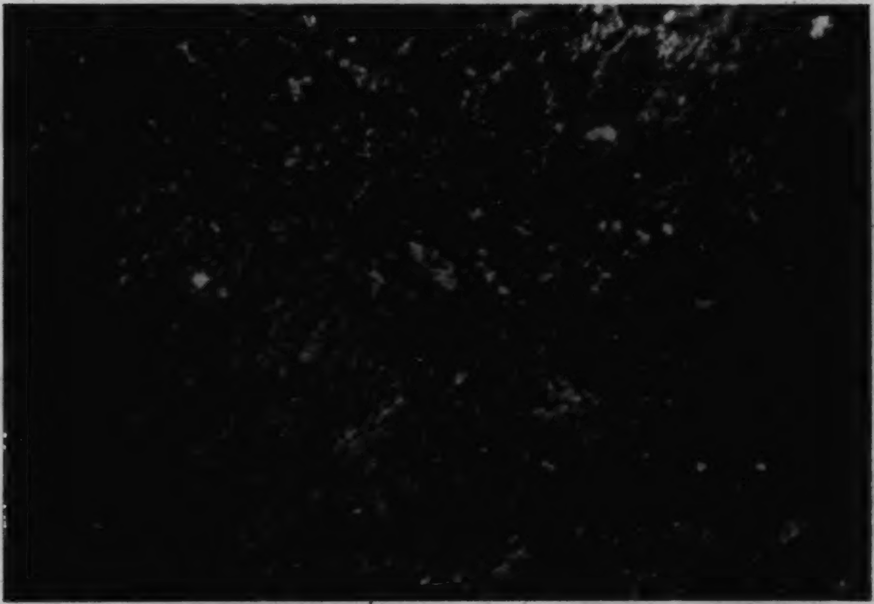

Plate 6.7 Sheared Nodules at the Slip Surface, crossed nicols, 42x

contrast, the lower portion of the thin section was composed chiefly of peds with very little clay matrix and few organic inclusions. The clay matrix was essentially absent or was in a minute amount between these peds (Plate 6.6). The peds were usually in contact with each other and the space between the larger peds was often filled by relatively smaller angular to subangular peds. At approximately the middle of the thin section, a thin layer about 7 to 15 mm thick was distinguished both by naked eye and under microscope; it seems to consist of equal amounts of nodules, clay matrix, and organic inclusions. The horizontal slip surface was at or near the middle of this layer. In general, the amount of nodules was inversely proportional to the distance up and directly proportional to the distance down the horizontal slip surface. This middle layer will be described in detail later.

6.3.1.2 Structure

The terminology used in describing the discontinuities and microstructure observed in the ice-thrust sediments follows Skempton (1966) and Brewer (1964).

1. Discontinuities

Principal displacement shear - A horizontal and flat-lying discontinuity with smooth surfaces bounded by a thin layer of clay particles oriented parallel to the surfaces and about 12 to 300 μm thick was observed near the middle of all the thin sections. This was the principal displacment shear and sheared nodules were found along it (Plate 6.7); furthermore, inclined fissures and lineations resembling Riedel and thrust shears were noted to diverge upward and downward away from this shear plane. In fact, the distinct, continuous, flat-lying slip surface observed in the field was located exactly at the position where this principal displacement shear was found in the centre of the thin sections.

Other shear planes which bear similar structural features to that just described were found in the upper portion of the thin sections although in general the layers of clay particles that were parallel to these planes were relatively thinner and had a thickness of 15 - 60 μm. Moreover, these planes usually did not remain horizontal all along their length and sometimes became inclined (Plate 6.8). Because of this, the continuous and flat-lying principal displacement shear that was found near the middle of the thin sections was referred to as the major principal displacement shear in order to distinguish it from other continuous and horizontal/inclined shear planes in the specimens. The observed major principal

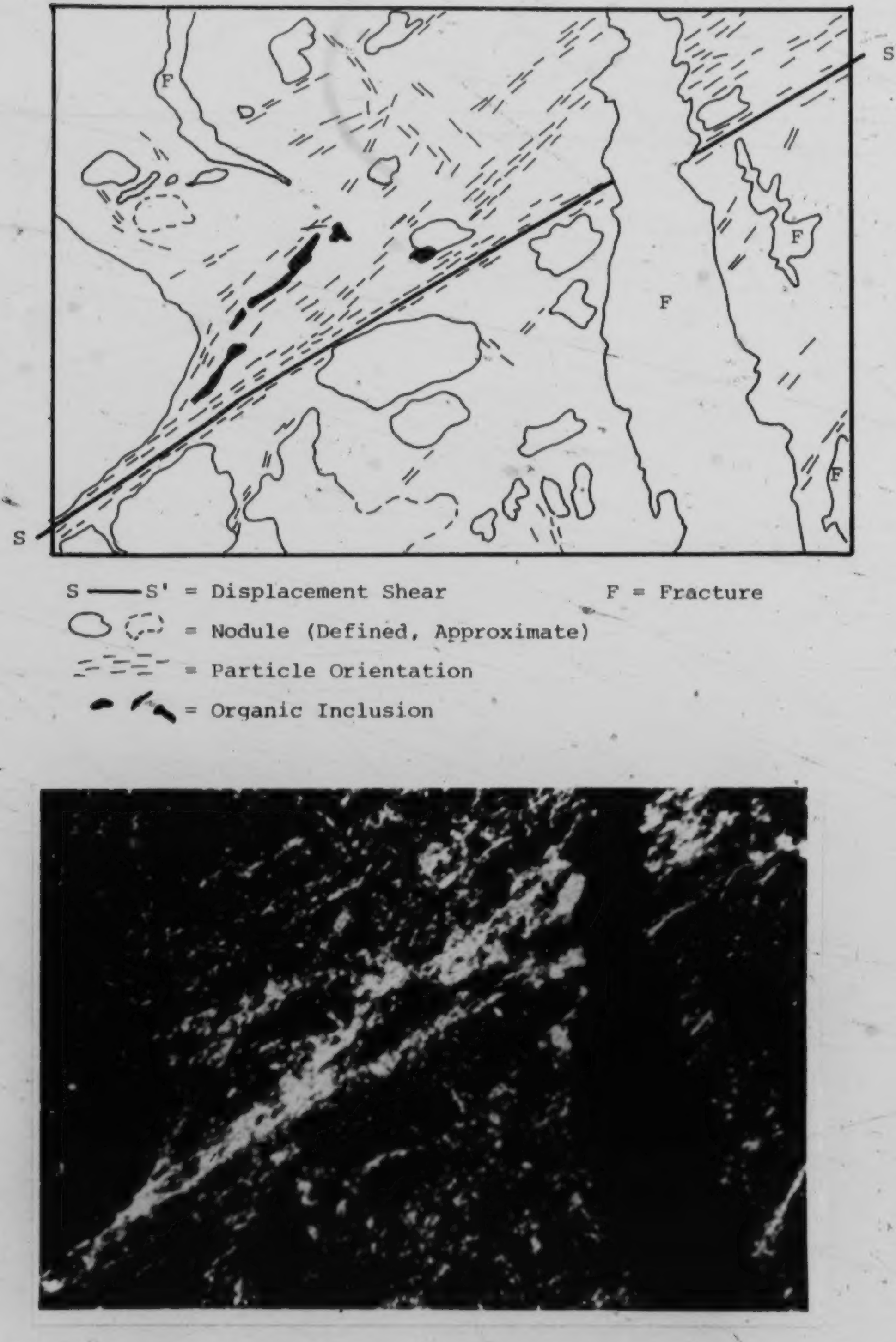
S
S'
F
F
F
F
S ——— S' = Displacement Shear
F = Fracture
= Nodule (Defined, Approximate)
= Particle Orientation
= Organic Inclusion

Plate 6.8 Inclined Displacement Shear, crossed nicols, 42x

displacement shear was in general tightly closed although locally it opened up.

Riedel and thrust shears - During the rotation of the stage of the polarized microscope between crossed-nicols, preferred orientation of clay particles, sometimes appearing as conjugate sets of lineations, were found in the clay matrix (Plate 6.5). Generally, these lineations were 0.45 to 1.13 mm long and 4 to 24 μm thick and with a density of about 8 lineations per millimetre. They occurred within the clay matrix, followed along the boundaries of the nodules and shear planes, or extended through aggregates of clay particles and other deformed structures (Plates 6.5).

Those microscopic lineations, which diverged from the principal displacement shears and had an inclination of 16° - 30° and about 130° from the horizontal, are believed to be the Riedel and thrust shears. These shear discontinuities usually have a length of 0.3 to 1.65 mm and a width of 4 to 80 μm. Other lineations in the clay matrix found in the upper portion of the thin sections were relatively more discontinuous than the Riedel and thrust shears described above; and often occurred as conjugate sets as well. Nearly 20 inclination measurements of these lineaments found in the upper portion of each thin sections were taken and the resulting data show that basically these conjugate discontinuities can be divided into two sets (Figure 6.3). The first set had an inclination that ranged from 12° - 64° with respect to the horizontal with most inclined at 35° - 46°; the inclination of the second set ranged from 110° - 168° with respect to the horizontal and most were inclined at 127° - 144°. Thus, these lineations intersected each other at approximately right angles to acute angles. The relatively discontinuous nature and general orientations of most of these conjugate sets of lineations (Figure 6.3) which differ from the configuration of the Riedel and thrust shears observed in the specimen studied (Plate 6.8), and their abundance in clay matrix without distinct shear discontinuities (Plate 6.5), resemble closely of the right bimasepic fabric and clino-bimasepic fabric in soil formed due to shrinkage and swelling (Brewer, 1964, p. 336).

Generally, shear discontinuities appearing in the clay matrix were found adjacent to the major principal displacement shear and in the upper portion of the thin sections, and rarely appeared in the lower portion of the thin section which were composed mainly of angular peds.

Cutan and Argillan - Cutan is defined as a modification of the fabric at natural surfaces in soil materials due to concentration of particular

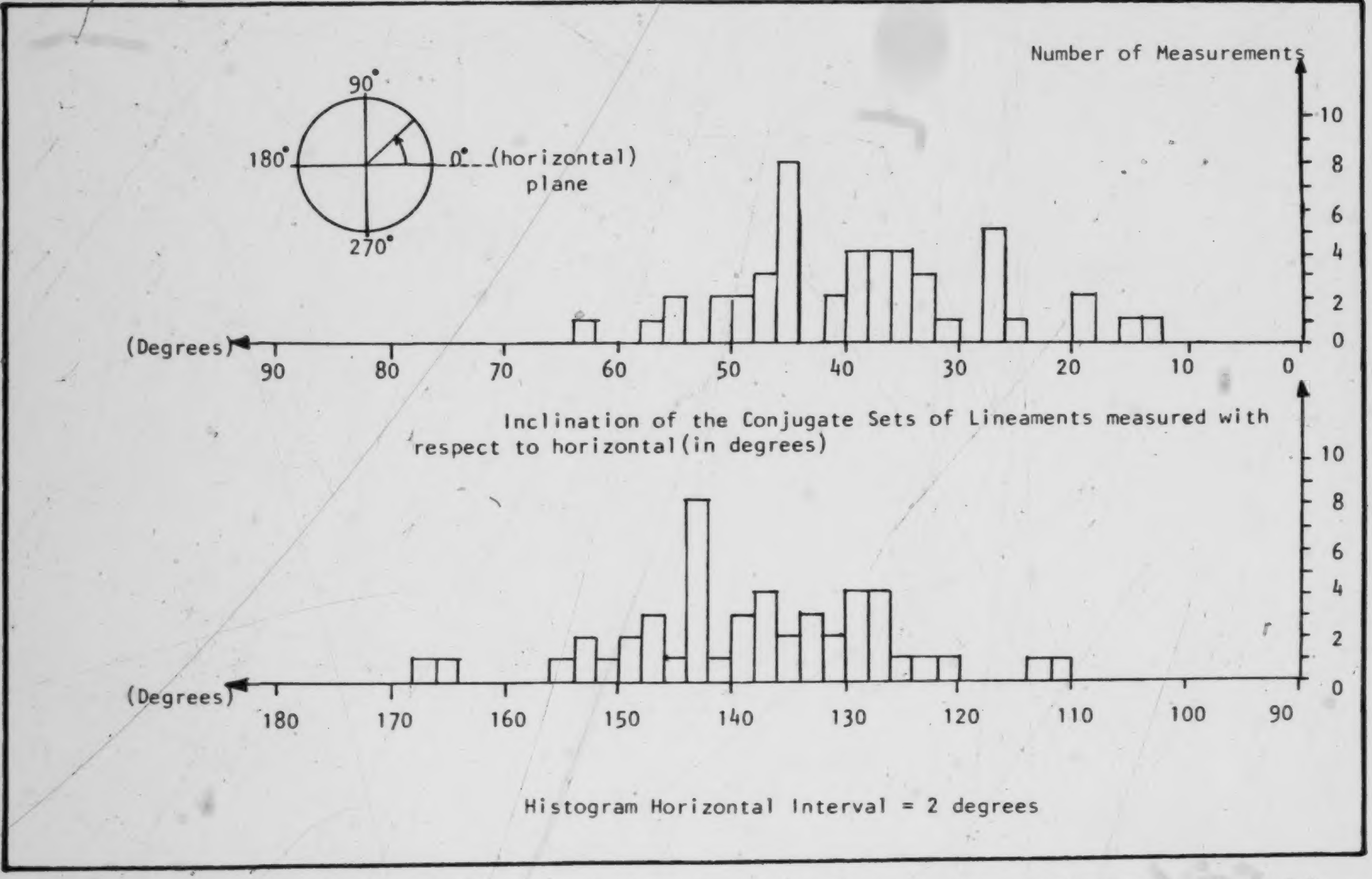

Figure 6.3 : Histograms that show the Inclination of the Conjugate Sets of Lineaments Appeared in Thin Sections

constituents or insitu modification of the clay matrix (plasma); and it is called argillan when the constituents are composed essentially of clay particles (Brewer, 1964).

The study of the microfabric of the ice-thrust sediments show that embedded grain argillans, which are layers of preferred oriented clay particles with a thickness of 4 - 7 µm lying parallel and/or around the boundaries of nodules, were commonly found within the clay matrix in the upper portion of the thin section (Plate 6.5). On the other hand, the lower portion of the thin section was composed of peds with none or a very small amount of nodules; and argillans were usually found around peds forming ped argillans or free grain argillans. Embedded grain argillans were common in the upper portion of the thin sections and near the major principal displacement shear where nodules are surrounded by clay matrix and the clay particles might orient themselves around the features during compression.

Cutans also found bordering fractures and shear planes.

Fractures and Voids - The fractures found in the upper portion of the thin sections were relatively short, narrow, and skewed, and generally had a length and a width of 0.6 - 1.65 mm and 0.015 - 0.3 mm respectively. Commonly these fractures were clean, with no infilling. However, the fractures in the lower portion of the thin section were relatively longer and wider, and had a length of 0.08 mm to greater than 5.4 mm and a width of 0.03 to 0.3 mm (Plate 6.6). These fractures were, in general, filled by well-packed angular to subangular aggregates often with their asperities matching the sides of adjacent peds, suggested that no to very little displacement had occurred along them. The fractures found in the lower portion of the thin sections actually delineated the sides of the peds and were probably formed by the connection of numerous short, flat and/or curved planes which resemble crazing planes formed due to irregular drying (Brewer, 1964, p. 204, fig. 42).

Horizontal and slightly inclined fractures were found at and adjacent to the major principal displacement shear at the middle of the thin sections. The fractures were rather continuous with smooth fracture surfaces and had a width of about 0.20 mm. It is believed that these fractures were formed due to the opening of the displacement shears and/or due to the coalescence of shear lenses.

2. Fold structure - About 4 mm below the major principal displacement shear, an organic lamination (coal) about 6.4 μm thick was deformed into anticlinal and synclinal structure. Conjugate

lineations (Riedel and thrust shears?), which seems to act as micro-thrusts, had segmented the fold structure into many tiny uneven pieces.

6.4 Submicrofabric

The SEM studies of the submicrofabric of the clay lumps, peds, and shear discontinuities found under the optical microscope may reveal evidence of deformation due to permafrost, weathering, and past high overburden pressure which have not been found at lower magnifications (Tovey and Wong, 1977, 1980; Marsland et al., 1983). This information will throw light on the submicrofabric of the sediments in the study area before ice thrusting occurred and the ground conditions such as the presence permafrost when ice thrusting took place. This knowledge is essentially for the understanding of the ice thrusting mechanism.

Due to the quality of the block samples and consistent with the petrographical studies described in the previous sections, SEM investigation were only performed on the bentonitic mudstone collected adjacent to the major principal displacement shear in the shear zone of Slide 1, Pit 3, Highvale mine

The laboratory preparation and method used in the investigation of the submicroscopic of ice-thrust sediments are described in Appendix G. The characteristic submicrofabric found in this study are shown below.

6.4.1 Observation

The general spatial relationship and distribution of the submicrofabric observed in the ice-thrust sediments are indicated in Figure 6.4. The terminology used to describe the submicroscopic sediment units mainly follows Collins and McGown (1974).

6.4.1.1 Elementary Particle Arrangements

The elementary particle arrangements of the clay studied can be described as densely compacted, random to preferred oriented, partly discernible groups of clay platelets (Plates 6.9 and 6.10). However, these groups of clay platelets may be in an open arrangement locally (Plate 6.11). Particle interaction, such as cardhouse arrangements were not seen although at the shear discontinuities, individual clay platelets were found interacting with groups of clay particles (Plate 6.12). In general, interactions between small groups of clay platelets are the dominant elementary particle arrangements in the sample studied. The group of clay platelets may have a length of 3 - 6 μm (Plate 6.9) though single clay platelet with length up to 10 - 20 μm were seen (Plate 6.11). Sometimes perfectly oriented platelets were piled up to form a large particle resembling a book or a stack structure with a length of 15 μm and a thickness of 2 - 3 μm (Plate 6.13).

Generally, the highly compacted and oriented groups of clay platelets were similar to the turbostratic

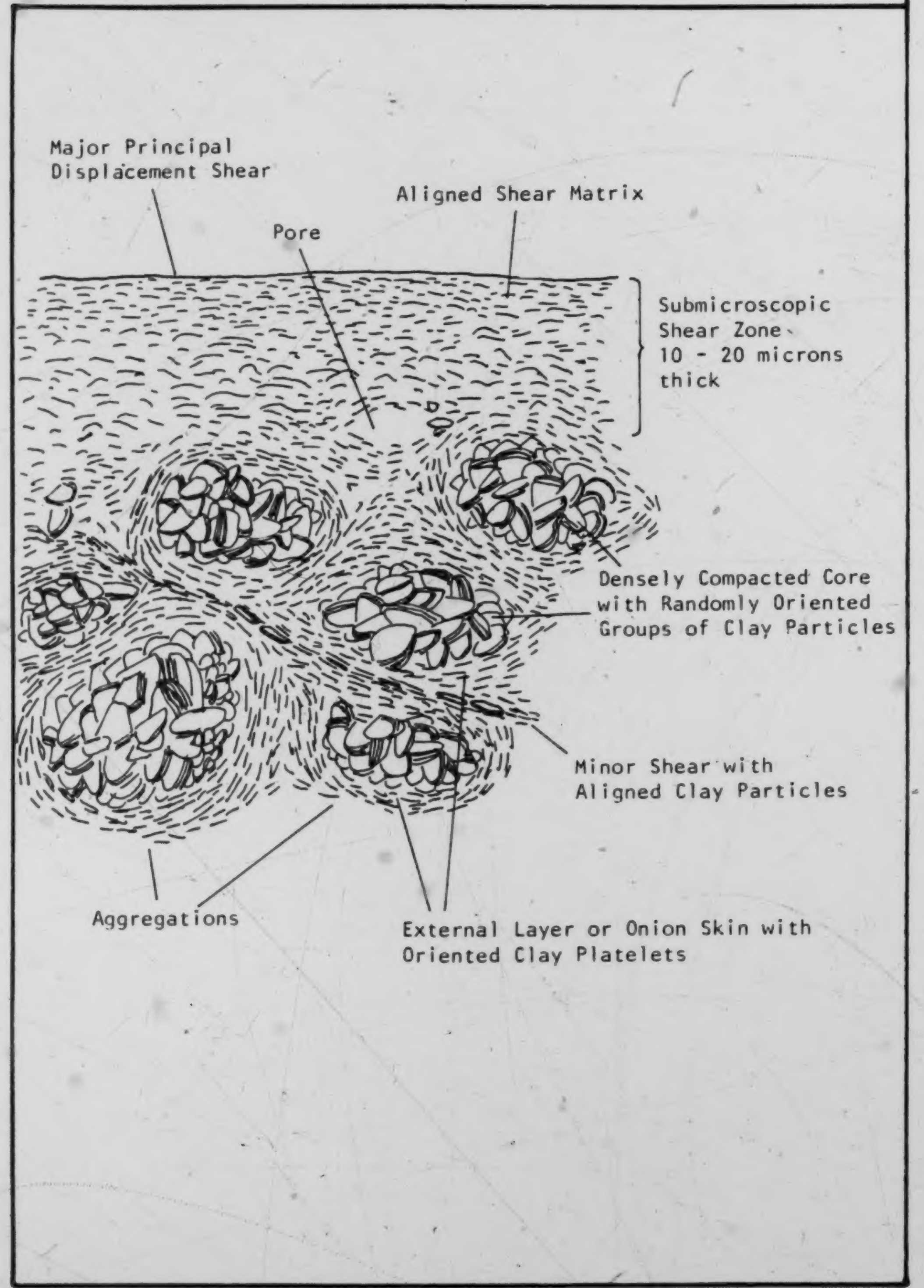
Major Principal
Displacement Shear
Aligned Shear Matrix
Pore
Submicroscopic Shear Zone 10 - 20 microns thick
Densely Compacted Core with Randomly Oriented Groups of Clay Particles
Minor Shear with Aligned Clay Particles
Aggregations
External Layer or Onion Skin with Oriented Clay Platelets

Figure 6.4 : Spatial Relationship and Distribution of the Submicrofabric Units in the Ice-Thrust Sediments

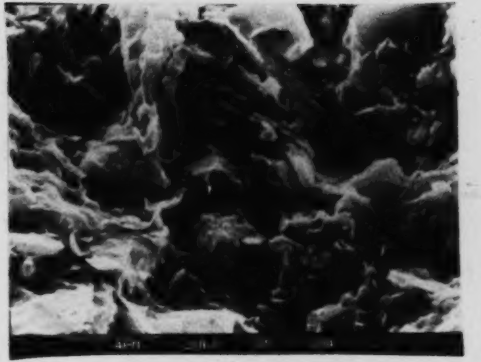

Plate 6.9 Compacted Partly Discernible Groups of Clay Platelets

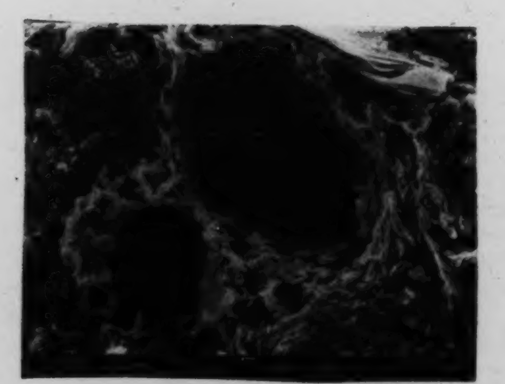

Plate 6.10 Compacted Partly Discernible Groups of Clay Platelets in Core and Onion Skin of Aggregation

Plate 6.11 Loosely compacted Partly Discernible Groups of Clay Platelets

Plate 6.12 Individual Clay Particles Interact with Groups of Clay Particles

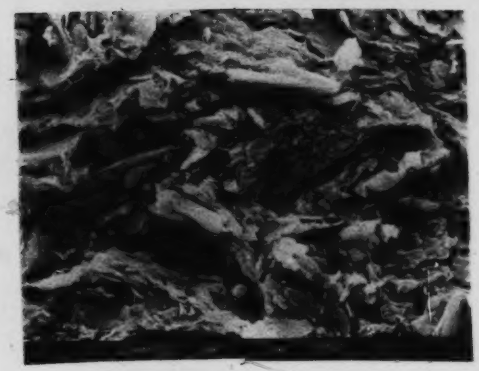

Plate 6.13 Stack Structure and Diamond-shaped Aggregations

Plate 6.14 Stack Structure and Oval-Shaped Aggregaion

Plate 6.15 Elliptical-Shaped Aggregations

arrangements proposed by Aylmore and Quirk (1960). The compacted and randomly oriented groups of clay platelets that were largely made up by face-face association of clay plates (Plate 6.13) can be visualized as the resulting submicrofabric after the collapse and compaction of the edge-edge, edge-face floccuated and aggregated arrangement, the bookhouse arrangement, and the stepped cluster arrangement suggested by Van Olphen (1963), Sloane and Kell (1966) and Smalley and Cabrera (1969). The strong tendency for clay platelets to form face-to-face arrangements is supported by this study.

6.4.1.2 Particle Assemblages

Particle asemblages are defined as the units of particle organization that consist of definable physical boundaries and a specific mechanical function (Collins and McGown, 1974). The types of particle assemblages observed in the clay examined are as follows.

1. Aggregations - Except at the major principal shear, densely compacted, oval-, cellular-, diamond-, to irregular-shaped aggregations were found in all samples obtained from the middle and lower subzones (Plates 6.13, 6.14, and 6.15). The aggregations observed were composed of: (a) a dense internal core made up of randomly oriented groups of clay platelets tightly compacted together (Plates 6.10 and 6.13), and (b) an external shell, which resembles onion skins, usually made up of dense

layers of clay platelets in a turbostratic arrangement oriented approximately parallel to the surfaces of the aggregations (Plates 6.10 and 6.15). This external shell or onion skins vary from a few to tens of clay platelets thick. The observed length of the major and minor axes of these aggregations are 29 - 68 μm and 15 - 42 μm respectively, with a common ratio of about 1.2 : 1 to 2.4 : 1.

The studies show that at the contacts of the cores and the onion skins of most of the aggregations, the clay platelet groups of these two units intimately touch each other but without linkage or fusion (Plate 6.16). The randomly oriented and turbostratic arrangements of the groups of clay platelets within the cores and the onion skins of the aggregations respectively and the close but disconnected contact between these two features seem to suggest that the onion skins and the cores of the aggregations were two different microfeatures before they were united into aggregations.

The mode of interaction of these aggregations with other microfabric features is essentially by the contact of their onion skins (Plate 6.14). Minor shears may appear between these contacts as evident by the particle alignment along these discontinuities that extended through the onion skins (Plates 6.12, 6.15, and 6.17).

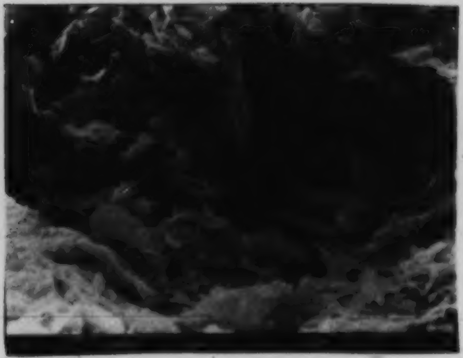

Plate 6.16 Contact of the Cores and the Onion Skins of Aggregations

Plate 6.17 Minor shears Extend through the Onion Skins

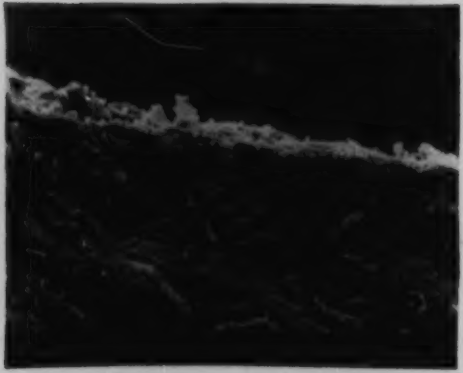

Plate 6.18 Absent of Aggregations at Major Principal Displacement Shear

2. Connectors - Connectors are elongated clay and fine silt assemblages that form between silt and sand grains (Collins and McGown, 1974). No connectors were found between the silt size aggregations of the ice-thrust sediments studied. However, connectors made by a partly discernible particle system that linked groups of clay platelets were found within a few of the cores of aggregations with an open structural arrangement (Plate 6.11).
3. Interweaving Bunches and Particle Matrices - It was observed that aggregations were often densely compacted and their onion skins tended to connect and fuse with each other, forming an interwoven system that consisted of interweaving bunches of oriented groups of clay platelets wrapped around aggregations (Plate 6.14). Except at the major principal displacement shear, where aggregations are absent (Plate 6.18), the interweaving bunches are the main particle matrix that bound the aggregations together and also acted as the background of the submicrofabric of the SEM samples.

6.4.1.3 Pore Spaces

In general, the submicrofabric of the soil studied was made up of densely compacted groups of clay platelets. Thus, intra-elemental pores such as interparticle pores were absent. However, intergroup pores were found surviving in a few aggregations (Plate

6.11). Intra-assemblage pores, which are irregular spaces found within aggregations such as between its external layers (onion skins) and cores were more common than the intergroup pores (Plate 6.11).

Inter-assemblage pores are an elongated space that was observed between aggregations in the samples studied. Some of these inter-assemblage pores were connected to each other and form trans-assemblage pores which were fractures that extended across several aggregations (Plate 6.21). However, the submicrofabric sometimes is so compact that only densely compacted interweaving bunches and shears were found between aggregations (Plates 6.13, 6.15, and 6.17).

6.4.1.4 Shear Structure

A submicroscopic shear zone 10 - 20 μm thick and composed mainly of aligned clay platelets was found immediately below the major principal displacement shear (Plate 6.19).

Away from the major principal displacement shear and this microscopic shear zone, the matrices of the samples varied from porous to compact, and clay platelets that coalesced into aggregations were common (Plate 6.19). Minor shears sometimes were found at the contacts of the external layers (or onion skins) of the aggregations which may have been deformed into undulatory discontinuities attached by aligned clay platelets (Plates 6.12, 6.15, and 6.17). The

7

Plate 6.19 Submicroscopic Shear Zone

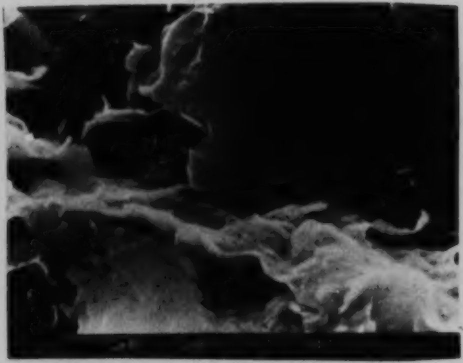

Plate 6.20 Fractured Clay Platelets at the Shear

Plate 6.21 Trans-assemblage Pores and Fractures

displacements along these minor shears varied and probably were small, usually only a few clay platelets were found oriented parallel or inclined along these discontinuities (Plate 6.12). This seems to indicate that there was insufficient movement and deformation along the minor shears to cause the reorientation of clay particles along their full length. Plate 6.20 shows that the platelets that lie normal to a minor shear were fractured and have angular edges in contact with the shear which is about 0.5 cm below the major principal displacement shear. About 1 cm below the major principal displacement shear, a fold structure overturned in the direction of the slickenslide was observed.

Aggregations, which were a common submicrofabric in the sample, were absent in the immediate vicinity of the major principal displacement shear. However, about 10 - 20 μm away from the principal shear, aggregations, folds and minor shears were common. Some of these aggregations seemed to have their major axes oriented in the direction of the slickenslides observed on the principal displacement shear (Plates 6.13 and 6.15). This seems to show that at principal shear, the shearing was strong enough to break down the dense cores of the aggregations into aligned shear matrices, but the deformation rapidly diminished and became unevenly distributed (about 10 - 20 μm) away from the major principal displacement shear, although fracturing and shearing of clay platelets in local areas might still have taken place.

6.4.1.5 Permafrost and Freeze-Thaw Features

The trans-assemblage pores and fractures that traversed the aggregations (Plate 6.21) with a densely compacted nature in general are comparable to the close-packed aggregations and large cracks within the peds of a clayey soil after being subjected to freezing-thawing-drying-wetting cycles (Smart and Tovey, 1981, fig. 12.2). However, it is to be noted that the discontinuities suspected of being formed by freeze-thaw action cannot be differentiated from those fractures and minor shears caused by ice thrusting. It is believed that both might have occurred simultanously in the deposits in the study area.

6.5 General Discussion

1. In the ice-thrust sediments studied, single particle arrangement or individual particle interaction is absent and clay particles always appear in groups aggregated into aggregations of various shape and size (Plates 6.13 and 6.15). The presence of submicroscopic fractures and minor shears, that extended through the onion skins (Plates 6.15 and 6.17) which are composed of roughly compacted aligned clay platelets wrapped around the dense cores of these aggregations, are probably the reason for the sediments having a granular nature and a tendency to break into large irregular lumps or

aggregates under finger pressure. At the same time, the compacted and rigid nature of the silt size aggregations between these submicroscopic discontinuities and some of these individual particles which are the size of a silt grain (Plates 6.14 and 6.20) have obviously created difficulty in breaking the sediments down mechanically (even accompanied with blenderizing, see Section 7.2.1) into primary individual clay platelets for grain size analysis. Indeed, grain size classification tests (Figure 7.1) have shown that the bentonitic mudstone studied is a silt although the SEM studies indicate that most of the material seem to comprise clay platelets. This type of phenomenon is not uncommon for heavily overconsolidated soils. X-ray analysis on the heavily overconsolidated Triassic Keuper Marl has shown up to 80 % of clay mineral particles while standard sedimentary tests show the percentage of clay size varying from 10 % for the unweathered material to 50 % for the weathered material (Barden and Sides, 1971b). Studies suggest that the unweathered Kueper Marl is composed essentially of clay particles aggregated into silt size clusters with a number of clay minerals larger than 2 μm (Barden and Sides, 1971b; Chandler, 1969). Another example is that the silt content of the Paskapoo Formation determined by the hydrometer tests always exceeds that measured by thin section point count method, and it is believed that this is due to the difficulty in breaking down the rocks into their primary particles mechanically for the conventional sedimentary techniques in grain size analysis (Locker, 1973)

2. The sediments studied by the author from a non-marine heavily overconsolidated sedimentary deposit that have been subjected to extremely high overburden pressure up to 11,900 - 15,700 kPa (Carrigy, 1971; Nurkowski, 1984), show poor to absent fissility and tend to disintegrate into small angular clay lumps or peds (Plate 6.2). Petrographic studies have indicated that randomness of clay flakes dominates in non-fissile claystone while in shale with moderate to poor fissility, the particles are in general parallel but composed of certain domains with other oriented particles (O'Brien, 1970; Odom, 1967). SEM studies indicate that the absence of fissility in the samples studied is mainly because the portion of the clay platelets that are oriented instead of being arranged into horizontal layers, formed interweaving bunches made up of compacted and preferentially oriented groups of clay platelets between aggregations (Plate 6.14). Moreover, relict volcanic glass was observed in the sediments studied which indicates that some of the clay minerals in the aggregates have a diagenetic origin. Locker (1973, p. 31) suggested that the subsequent alteration of volcanic ash to montmorillonite would not lead to the formation of oriented aggregates. Thus, the soil studied show poor to absent fissility

although composed of many oriented clay particles (Plates 6.10 and 6.15). Indeed, London clay and many other heavily overconsolidated clays, which exhibit a turbostratic microstructure of domains formed by clay plates locally oriented around silt grains in an onion skin arrangement (Barden, 1972a, figs. 12 and 14), always show a tendency to disintegrate into peds, crumbs and aggregates (Barden, 1972b). It seems that these turbostratic microstructure and onion skin arrangements of the aggregations often form local planes of weakness which microshears and other fractures are most likely to follow.

3. Petrographic and SEM studies indicate that compression texture and kink band structure, which are found in natural and laboratory prepared clay soils subjected to direct shear (Morgenstern and Tchalenko, 1967b, 1967c; Tchalenko, 1968b, 1970), were not seen in the ice-thrusted sediments exposed in Highvale mine, Wabamun Lake area (Plates 6.5 and 6.8). Foster and De (1971) postulated that the absence of kink band structure in the heavily overconsolidated kaolinitic clay (OCR = 19) after being subjected to direct shear was because the degree of the initial preferred orientation parallel to the shear direction was insufficient to allow kinking to occur. The ice-thrust sediments studied are stiff and compact submicroscopic aggregates (Plate 6.10). The shearing along the major principal displacement shear in

the ice-thrust sediments investigated during ice thrusting seems to be strong enough to break down the microfabric immediately at this shear plane into an aligned shear matrix. However, the magnitude of deformation, which diminished rapidly away from the major shear as is evident from the presence of minor shears and slightly deformed aggregations only tens of microns away from this shear plane (Plate 6.19), was probably not capable of breaking down the densely compacted aggregations orient the clay platelets adjacent to the shear into a kink band structure.

4. The engineering behavior of the heavily overconsolidated ice-thrust sediments in the study area at present is controlled by the macrofabric and mesofabric such as joints and principal displacement shears (Plate 5.3); however, the location and occurrence of these planes of weakness caused by deformations such as ice thrusting, loading and unloading, and weathering are believed to be governed by the submicrofabric of the soils, for example, the onion skins of the aggregations which are made up by oriented clay platelets in a turbostratic arrangement (Plate 6.15) are potential breaks during deformation.

The ice-thrust sediments compose many horizontal to inclined mesoscopic, microscopic and submicroscopic fissures, fractures, and shear planes which are opened locally (Plates 5.3 and 6.19) and are expected to have a secondary permeability higher than other undeformed bentonitic mudstones in the area. This is shown by the field measurements which indicate that the hydraulic conductivities of the disturbed and undisturbed mudstone in the study area are 0.0064 cm/s and 0.0002 - 0.00074 cm/s respectively (Monenco, 1984, vol. 1, table 3-5).

5. It is noted that the meso- and microfabric such as Riedel shears and principal displacement shears observed in the sole thrust due to ice thrusting are in general similar to those found within shear zones of different magnitudes caused by tectonic activities such as landslides, earthquake faulting and flexural slip, or by laboratory shear experiments such as direct shear tests or ring shear tests (Morgenstern and Tchalenko, 1967a, 1967b; Tchalenko, 1968a, 1968b, 1970; Garga, 1973). Tectonism (such as earthquakes) and glaciotectonism are able to produce shear zones less than a metre to tens of metres thick; while other tectonic activities such as landslides and laboratory shear tests generally produce shear zones a millimetre to a few centimetres thick (Morgenstern and Tchalenko, 1967a, 1967b; Tchalenko, 1968a, 1968b, 1970; Stimpson and Walton, 1970; Skempton and Petley, 1967; Skempton, 1966; Garga, 1973). It has been suggested that the structural evolution within shear zones formed by earthquakes, Riedel experiments and shear box tests follow a similar pattern (Tchalenko and Ambraseys, 1970; Morgenstern and Tchalenko, 1967b;

Tchalenko, 1968b, 1970). This is probably because all these shear zones were formed under a similar mode of kinematic restraint during shearing. For example, in the direct shear test, the kinematic restraints are imposed upon the samples by the boundaries of the apparatus; for tectonic faulting, the restraints are the surrounding strata and rock masses; while for glaciotectonism, the kinematic restraints that act upon the underlying shear zone include both the glacier which lies directly above the sheared sediments and the surrounding strata that enclose the shear zone.

Since shear zones formed by strike-slip faulting and ice thrusting are believed to be under the similar kinematic restraints, the empirical equation developed by Otsuki (1978) to relate width/displacement of strike-slip faults may be applicable to the prediction of the width/displacement of a shear zone formed by ice thrusting. The predicted displacement of the shear zone observed (with a maximum thickness of about 4.2 m) in Highvale mine based on Otsuki's equation is about 240 m; compared with the displacement of 355 - 395 m estimated from borehole correlation (Figure 5.2). When the 355 - 395 m of displacement of the shear zone in the study area are used in the equation, the predicted thickness of the shear zone has a range of 6.2 - 6.9 m. Thus, the error in the width and the displacement prediction on the shear zone due to ice thrusting found in the study area based on Otsuki's empirical equation are 32 - 39 % and 48 - 64 % respectively (Figure 6.5). Some of these errors may have arisen from mis-identification of the sheared materials in the borehole logs thus leading to an error in correlating and estimating the movement along the shear zone. Nevertheless, the Otsuki's equation seems to provide an upperbound for the width and lowerbound for the displacement of the shear zone due to ice thrusting. Thus, glaciotectonic sole thrusts and tectonic strike-slip faults are probably formed under similar modes of kinematic restraints.

6. The study of the microfabric and submicrofabric of the shear zone indicates that the magnitude of straining and deformation such as the breakdown of peds and the orientation of clay particles, are unevenly distributed except along the principal displacement shears where there are microscopic clay layers with particles oriented parallel along the traces of the shear planes (Plates 6.8 and 6.18). It is not uncommon that regions with random and preferred orientation of clay particles are present within shear zones (Morgenstern and Tchalenko, 1967a; Garga, 1973). Laboratory work and field investigations suggested that this is because, during the initial stage of shearing, the entire shear zone was deformed in simple shear and many local strains and faults such as Riedel and conjugate Riedel shears were produced (Morgenstern and Tchalenko, 1967b;

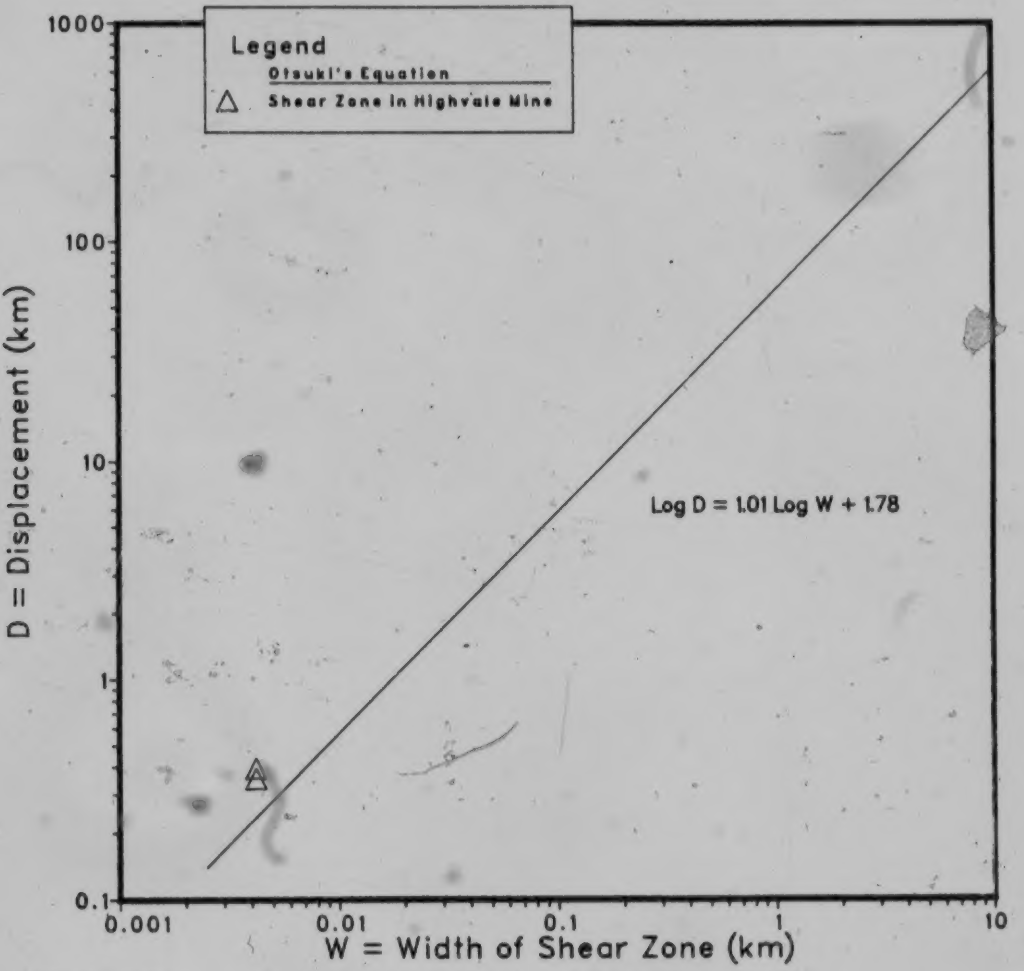

Figure 6.5 Predicted and Observed Width/Displacement of Shear Zone Due to Ice Thrusting (after Otsuki, 1978)

Tchalenko, 1970). However, due to the kinematic restraints imposed upon the shear zone by the surrounding material, the mode of deformation of the strata was tranformed from a simple shear to a direct shear condition. Subsequent deformation mainly occurred in the central portion of the shear zone where the Riedel shears were interconnected by discontinuities known as thrust or P shears. At large strains, all the deformation or displacement of the shear zone was concentrated along a horizon less than a few millimetres thick, that is, the principal displacement shear; while leaving the rest of the shear zone essentially undisturbed (Skempton, 1966; Tchalenko, 1968b, 1970; Morgenstern and Tchalenko, 1967b; Tchalenko and Ambraseys, 1970). The preservation of loosely compacted groups of clay platelets near a principal displacement shear in the ice-thrust sediments studied (Plate 6.11) seems to support this view.

7. The microfabric of ice-thrust sediments discussed in this Chapter, for example, the densely compacted oval-to irregular-shaped aggregations, are based on the examination of 15 - 20 hand specimens, 9 thin sections (3.9 x 2.2 mm^2 per section), and 12 SEM samples from block samples collected at a horizon in a specfic site in Highvale mine, Wabamun Lake area. Although field observations show that the samples from a shear zone seem to represent the typical deformed material caused

by ice thrusting, the sampling size is small compared to the large volumes of rock masses and the different types of materials affected by glaciotectonism in the study area. More studies should be performed on different horizons in the shear zone and ice-disturbed sediments in other sites before the microfabric of ice-thrust sediments are fully known, for instance, whether aggregations are a common feature in heavily overconsolidated ice-thrust clayey sediments.

6.6 Shear Subzones

The studies of the mesofabric, microfabric, submicrofabric, and the mineral composition of the shear zone found in Highvale Mine show that the portion of the shear zone where the principal slip surface located can be further divided into three subzones (Plate 5.2 and Figure 6.6). The recognition of these subzones is important because: (a) it would provide information on the mesoscopic, microscopic, and submicroscopic geological features that indicate the possible location of a principal displacement shear within the ice-thrust sediments in an ice-thrust terrain, (b) the understanding of the variation and distribution of fabric and strength properties within a shear zone, which influence most of the engineering properties (such as permeability, consolidation, and shear strength) of the sediments and the degree of anisotropy of these properties in the rock mass, would help future site

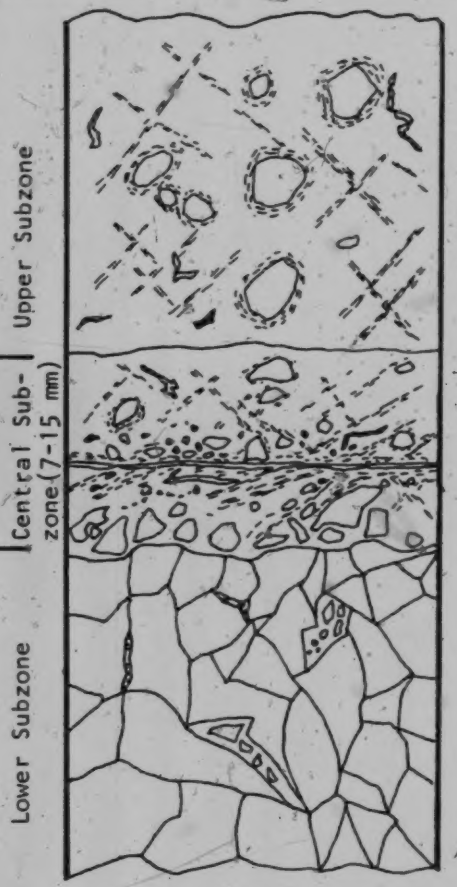

- Light grey to grey
- Scattered and randomly oriented nodules resembling lithorelicts, cutans around nodules or lithorelicts; lithorelicts engulfed by clay matrix
- Conjugate sets of lineaments in clay matrix
- narrow fractures and small voids

- Montmorillonite content : 60 - 65 % (average = 62 %)
- Illite content : 10 - 30 % (average = 18 %)
- Kaolinite content : 5 - 25 % (average = 18 %)
- Chlorite content : absent to 5 %

- Light grey, brown to dark brown
- Many inclined lineaments (Riedel, conjugate Riedel and thrust shears?)
- Major Principal Displacement Shear, clay particles oriented parallel to the shears
- Fractures with smooth surfaces, presence of fold structure
- Montmorillonite content : 65 - 85 % (average = 73 %)
- Illite content : 5 - 24 % (average = 15 %)
- Kaolinite content : 5 - 15 % (average = 12 %)
- Chlorite content : absent to trace amount

- Brown to dark brown
- Angular to subangular peds
- clay matrix is confined to peds
- Fractures are wide and with irregular surfaces; crazed planes

- Montmorillonite content : 35 - 68 % (average = 48 %)
- Illite content : 11 - 45 % (average = 30 %)
- Kaolinite content : 15 - 21 % (average = 19 %)
- Chlorite content : about 5 %

Figure 6.6 : Lithological and Mineralogical Characteristics of the Shear Subzones, Pit 3, Highvale Mine

investigation in the area in selecting appropriate field sampling techniques and insitu and laboratory testing methods, and assist the interpretation of the test results of these disturbed materials (McGown et al., 1980; McGown, 1982; Marsland and Butler, 1967). The characteristics of these subzones which are shown in Figure 6.6 are described as follows.

1. Lower Subzone - This subzone is equivalent to the lower portion of the thin sections examined or the sediments below the horizontal slip surface observed in the field. This is a brown, dark brown to dark greyish brown subzone which is composed mainly of angular to subangular peds with roughly matching asperities, indicating that the material has undergone brittle failure. Fractures are relatively larger, longer and more irregular than those found in the overlying subzones. The clay mineral content includes 35 - 68 % montmorillonite with an average of about 48 %, illite that ranges 11- 45 % with an average of about 30 %, 15 - 21 % kaolinite with an average of 19 %, and about 5 % chlorite. The top of this subzone is 0.75 to 6 mm below the major principal displacement shear.
2. Central Subzone - The central subzone is the very thin layer of material found approximately in the middle of the thin sections and is equivalent to the sediments that lie at and immediately adjacent to the horizontal slip surface observed in the field (Plates 5.2 and E.1).

This is a light grey, brown to dark brown horizontal layer about 7 to 15 mm thick. The major principal displacement shear is situated at the middle to near the bottom of this subzone. Many inclined lineations (displacement shears, Riedel and thrust shears) and fractures with smooth surfaces were found lying parallel or inclined to the major principal displacement shear. It is believed that most of these discontinuities have been sheared and slickensided because layers of clay particles with preferred orientation are always found along these discontinuities (Plates 6.7, 6.12, and 6.17). The central subzone is believed to have been formed during ice thrusting when the material at the contact of the overlying and underlying subzones were sheared and mixed together. The clay mineral content of this subzone is composed of 65 - 85 % montmorillonite with an average of about 73 %, 5 - 24 % illite with an average of approximately 15 %, 5 - 15 % kaolinite with an average of 12 %, and a trace amount of chlorite.

3. Upper Subzone - This subzone is the material found at the upper portion of the thin sections or the sediments above the horizontal slip surface in the field. This subzone is essentially light grey to dark grey in color and is composed of nodules or aggregates of clay particles scattered in a clay matrix and not in contact with each other. These nodules resemble lithorelicts and tend to have diffused sides. Closed and small fractures

together with a conjugate set of lineations are common in the clay matrix (Plate 6.5). About 60 - 65 % montmorillonite, 10 - 30 % illite, 5 - 25 % kaolinite, and 0 - 5 % chlorite are found in the clay size particles in this subzone (Figure 6.6). The bottom of the upper subzone is at 6 - 9 mm above the major principal displacement shear.

The presence of lithorelicts and peds above and below the central subzone seems to suggest that the horizontal slip surface observed in the field was located at the contact that was overlain by a weathered layer and underlain by a relatively less weathered layer. During ice thrusting, deformation and shear displacement probably were concentrated along the contact between the weathered layers. This resulted in shearing, dilation, and breakdown of the peds and nodules that were located adjacent to the contact, and migration and mixing of the material both from the overlying and the underlying layers, forming a highly deformed layer (central subzone) that was composed of a mixture of sheared peds and lithorelicts and a principal displacement shear (Plate 6.7). Moreover, it has been shown that the presence of a clear separable shear plane bounded with strongly oriented clay on either side such as the middle subzone mentioned here is an indication that sliding was the dominant mode of shear behavior during the residual state of deformation of this subzone (Lupini et al., 1981, figs. 18, 23).

Examination of the mineralogical content also indicates that there is more montmorillonite and less illite in the central subzone than in the underlying and overlying subzones (Figure 6.6). This is probably because there was a rapid increase and decrease in the amount of volcanic ash deposition in that particular period of the geological past which produced a bentonitic clay layer with relatively distinct difference in the amount of bentonite content.

6.7 Genesis of the Microfabric and Submicroscopic of Ice-Thrust Sediments

Chapter 5 has shown that ice thrusting could produce macroscopic deformation such as principal displacement shears, folds, and fractures; however, brecciation and nodules resembling lithorelicts in the ice-thrust sediments found in Highvale mine indicate that in addition to glaciotectonism, the materials in the shear zone in that area have also undergone other kinds of deformation. For example, brecciation could be formed by valley bulging (Hollingworth et al., 1944), the decay of permafrost (Chandler, 1972), or glaciotectonics (Geike, 1889; Sauer, 1978). By examining the field evidence and the geological history of the study area, four possible deformation processes other than glacial thrusting that may be responsible for the development of some of the fabric observed in the bentonitic mudstone in Pit 3, Highvale mine are discussed below.

6.7.1 Deformation Agents

1. Permafrost - It has been suggested that the formation and/or subsequent melting of ground ice lenses might have caused internal crumbling and brecciation in argillaceous sediments which would result in a microfabric with shattered peds or lithorelicts in a matrix of brecciated, disturbed, remoulded, and structureless soft clay (Chandler, 1972, fig. 15; Marsland et al., 1983, fig. 24). The appearance of rounded nodules in the clay matrix found in the upper subzone (Plate 6.5) and the broken ped structure (Plate 6.6) in the lower subzone within the shear zone in the study area resemble the brecciation due to permafrost. During and after the Pleistocene glaciation, permafrost, which probably formed and decayed in the Wabamun Lake area and other ice-thrust terrain in the region, had caused disturbance in the underlying argillaceous sediments.
2. Loading history - It has been suggested that unloading might be the cause of the microscopic shear planes in the stiff overconsolidated clay (Morgenstern, 1967; Bjerrum, 1967). Unloading occurred in the study area due to the erosion of thick layers of Tertiary sediments

before Pleistocene time (Nurkowski, 1984; Locker, 1973); while loading and unloading ocurred again during the last glaciation when the continental glacier advanced and retreated from the study area. Minor shears must have been developed in the underlying strata due to the uneven straining caused by these cycles of loading and unloading (Plates 6.12, 6.15, and 6.17), although those that appear near the principal displacement shears were probably formed due to shearing by ice thrusting.

3. Surface weathering - The presence of an erosional surface near the top of the shear zone in the Highvale mine shows that the bentonitic mudstone had been under subaerial erosion before glaciotectonism (Plate 5.2; Section 5.1.1.1). Since the mudstone was once close to the ground surface, it had probably been disturbed by weathering due to seasonal and annual water content changes and/or freeze-thaw action. Moreover, microstructure, which is closely analogous to the rounded nodules, clay matrix and conjugate sets of micro-lineations found in the upper subzone within the bentonitic mudstone in the study area (Figure 6.5), has been found in London clay which has undergone surface weathering (Tchalenko, 1968a, fig. 4). Brewer (1964, p. 232, 340) also commented that weathering such as disintegration, physical softening, shrinkage and swelling, would cause compression, tension and shearing in the clay matrix and form a striated orientation

pattern; while rotation and/or translocation of nodules and skeleton grains under pressure such as swelling may shear the adjacent clay matrix and cause embedded grain or nodule cutans to develop. Indeed, embedded grain cutans are a common features in the ice-thrust sediments studied (Plate 6.5). Furthermore, the presence of trans-assemblage pores and fractures in the lower subzone within the shear zone in the study area indicate the probable occurrence of freeze-thaw action (Plate 6.21).

4. Sample preparation - The size and shape of the fractures and infills suggest that some of the fractures in the upper and lower portions of the thin sections may be due to shrinkage upon drying (Plate 6.6). However, the amount of fracturing in the samples caused by sample preparation for thin sectioning is considered to be small because the natural moisture content of the bentonitic mudstone was at or near its shrinkage limit during the preparation of the thin sections (Appendix F). Nevertheless, cracks formed during thin sectioning should tend to follow existing planes of weakness such as microshears in the samples. Thus, most of the fractures and voids found in the thin sections are believed to follow existing planes of weakness formed by geological processes such as permafrost, weathering and ice thrusting.

To summarize, it is inferred that before the last glaciation, surface weathering and removal of the overburden are the main deformation processes that were responsible for the development of some of the microfabric in the bentonitic mudstone in the study area. During the stage of glaciotectonism in Pleistocene time, ice thrusting deformed the sediments in the area and the loading and unloading due to the advance and the retreat of the continental glacier should have further deformed the underlying strata; and finally, permafrost should have caused more disturbance in the ice-thrust sediments observed in the study area during and probably before the glaciotectonism.

6.7.2 Evolution of the Microfabric and Submicrofabric of the Ice-Thrust Sediments

Pusch (1973b) proposed a soil model for natural sedimentary clays and postuated that soils consist of stiff aggregates of closely spaced particles connected by links or bridges of particle network. Under sufficiently high external shear stress or stresses exceeding the preconsolidation pressure, a number of these links will collapse into groups of oriented particles (domains) in connection with a movement of the aggregates into stable positions (Pusch, 1973b, fig. 3). This view of the primary microfabric of clayey soils is supported by the SEM studies of post-glacial normally consolidated to lightly overconsolidated clays (not subjected to high overburden pressure, shearing, and weathering) which have shown aggregations chained to each other by relatively narrow and elongated assemblages made up by fine silt to clay particles to form large pore spaces (Collins and McGown, 1974, fig. 10e). Studies by Pusch (1973c) and Barden and Sides (1971b) also show that the general microfabric of natural clayey soil is that of interconnected particle aggregates or silt size grains separated by voids of varying size. On the other hand, other SEM studies on heavily overconsolidated, stiff fissured clay such as the London clay (erosion of about 330 m of overburden) and the Upper Lias Gretton clay (erosion of about 1000 m of overburden) have shown that the large silt size particles are wrapped with a closely-packed dispersed turbostratic clay structure and have a tendency for horizontal orientation (Barden, 1972a, fig. 12 - 15; Barden, 1972b). Barden (1972a) concluded that the microfabric observed in the stiff fissured clays seems to have originated from an originally flocculated structure that subsequently collapsed into a turbostratic arrangement. In contrast, the ice-thrust sediments studied, which are heavily overconsolidatd, also show an overall compact structure without connectors or large pore spaces between aggregations (Plates 6.10 and 6.15). The connection and fusion of the onion skins of these aggregations have produced an image of a braided stream network of oriented clay particles flowing around the dense cores of aggregations (Plate 6.14), resembling the turbulent microstructure proposed by Sergeyev et al. (1980, fig. 5) which is believed to be formed during the course of lithogenesis by compacting clay sediments containing honeycomb and possibly matrix microstructures.

Comparison of the submicrofabric observed in the samples obtained from the Highvale mine, Wabamun Lake area, with the microstructure found in other normally consolidated, lightly overconsolidated to heavily overconsolidated soils mentioned above suggest that the original microfabric of the ice-thrust sediments studied were probably composed of silt size aggregations that consisted of flocculated groups of clay platelets linked by narrow and elongated chains of clay platelets (Plate 6.11). Under high overburden pressure, these chains collapsed and were turned into groups of oriented particles (domains) as suggested by Pusch (1973b, fig. 3c). Since the primary aggregations are relatively dense and stiff, compression caused the groups of clay platelets in the aggregations to compact but not to realign probably because of the lack of space for the groups of particles to reorient in the direction normal to the major principal stress. On the other hand, the chains between these aggregations are relatively fragile and are located in a space that is much freer and allows rotation to the preferred orientation. Prolonged compression should have caused the domains to press tightly onto the surface of the aggregations and subsequently compact into a dense matrix. This is probably accompanied by weathering which cause (a) uneven breakdown of the silt size flocculated aggregates of clay particles as noted in Keuper Marl (Barden and Sides, 1971b), and (b) particle intergrowth that bound individual clay platelets into patches as evidenced by the difficulty in recognizing individual clay particles. Subsequently, ice thrusting caused the formation of submicroscopic deformed features such as the principal displacement shear (Plate 6.18) and further compressed and moulded the groups of clay particles into aggregations. Thus, the final products are densely compacted secondary aggregations that are composed of a dense core of randomly oriented groups of clay platelets surrounded by an onion skin that is made up of groups of oriented particles with a turbostratic arrangement (Plates 6.14 and 6.15). The presence of the open and flocculated structure in local areas of the sediments studied (Plate 6.11) is believed to be the original microfabric of the material that survived the post-depositional processes probably due to the arching effect (Barden, 1973).

Figure 6.7 indicates the configuration of the observed particle assemblages in the ice-thrust sediments at present and the postulated particle assemblages before the sediment was subjected to the high overburden pressure, weathering, and glaciotectonic deformation. Figure 6.8 is a diagrammatic drawing that illustrates the evolution of the submicrofabric of the ice-thrust sediments studied subjected to the

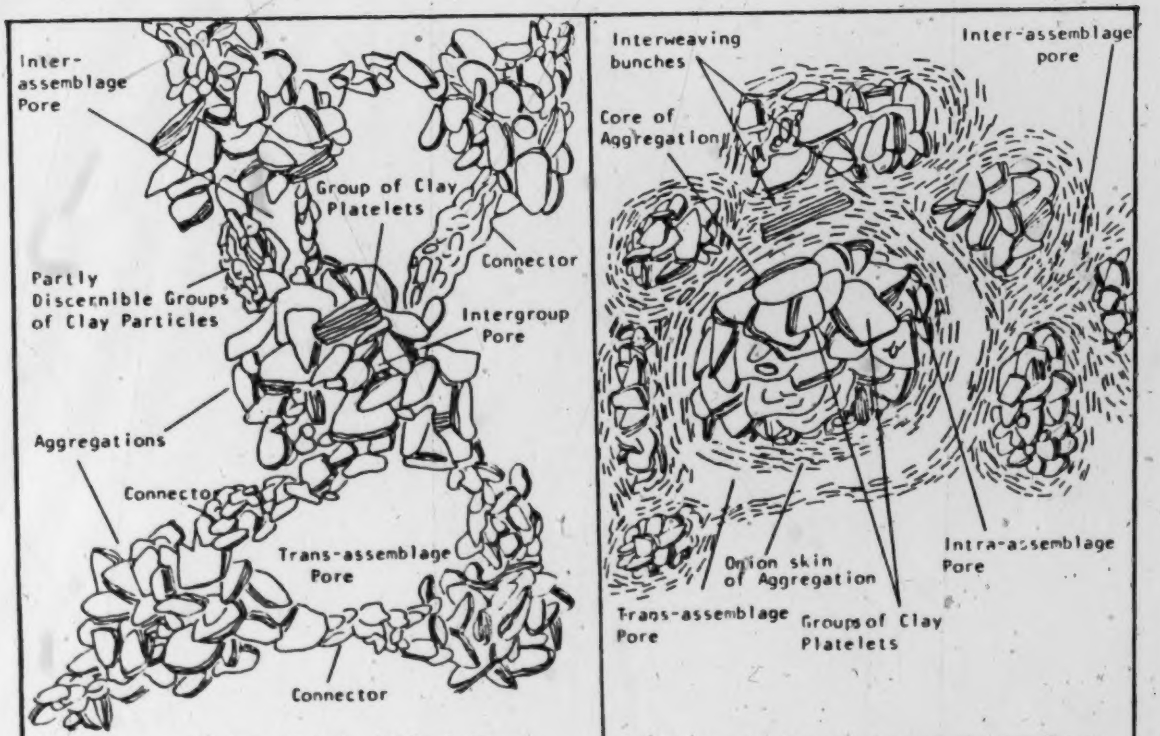
Inter-assemblage Pore
Group of Clay Platelets
Connector
Partly Discernible Groups of Clay Particles
Intergroup Pore
Aggregations
Connector
Trans-assemblage Pore
Connector
Interweaving bunches
Inter-assemblage pore
Core of Aggregation
Intra-assemblage Pore
Onion skin of Aggregation
Trans-assemblage Pore
Groups of Clay Platelets

(a) Postulated Submicrofabric of the Sediments Studied before Diagenesis

(b) Observed Submicrofabric of the Ice-Thrust Sediments Studied by the Author

Figure 6.7 : Characteristics of the Submicrofabric Units of the Sediments Studied Before and After Subjected to High Overburden Pressure and Glaciotectonic Deformation. (a) is Modified After Collins and McGown (1974) and (b) is Observed by the Author.

post-depositional processes.

6.8 Geological Conditions of the Sediments During Ice Thrusting

1. The existence of permafrost related features such as lithorelicts in a matrix of brecciated clay and the trans-assemblage pores and fractures in the ice-thrust sediments studied (Plate 6.21), and the formation of ice-thrust features near or at the margin of a stagnant glacier (Chapter 4) where permafrost tends to occur (Rutten, 1960; Mathews, 1964; Clayton and Moran, 1974) seem to indicate that the ice-thrust sediments in the study areas were under permafrost during glaciotectonism. That sediments were frozen during ice thrusting seems to be supported by the studies of the ice-rich permafrost soil along the Great Bear River where ice-deformed glaciofluvial deposits of Pleistocene age were observed in the area with a maximum depth of permafrost about 61 m at present (Savigny, 1980, p. 120), and by the presence of massive ice in glacially deformed sediments observed along the western arctic coast (Mackay, 1971).
2. Prior to ice thrusting, most of the argillaceous sediments in the study areas were already disturbed and composed of minor shears, fractures, and lithorelicts due to the post-depositional processes such as cycles of loading and unloading, surface weathering and permafrost

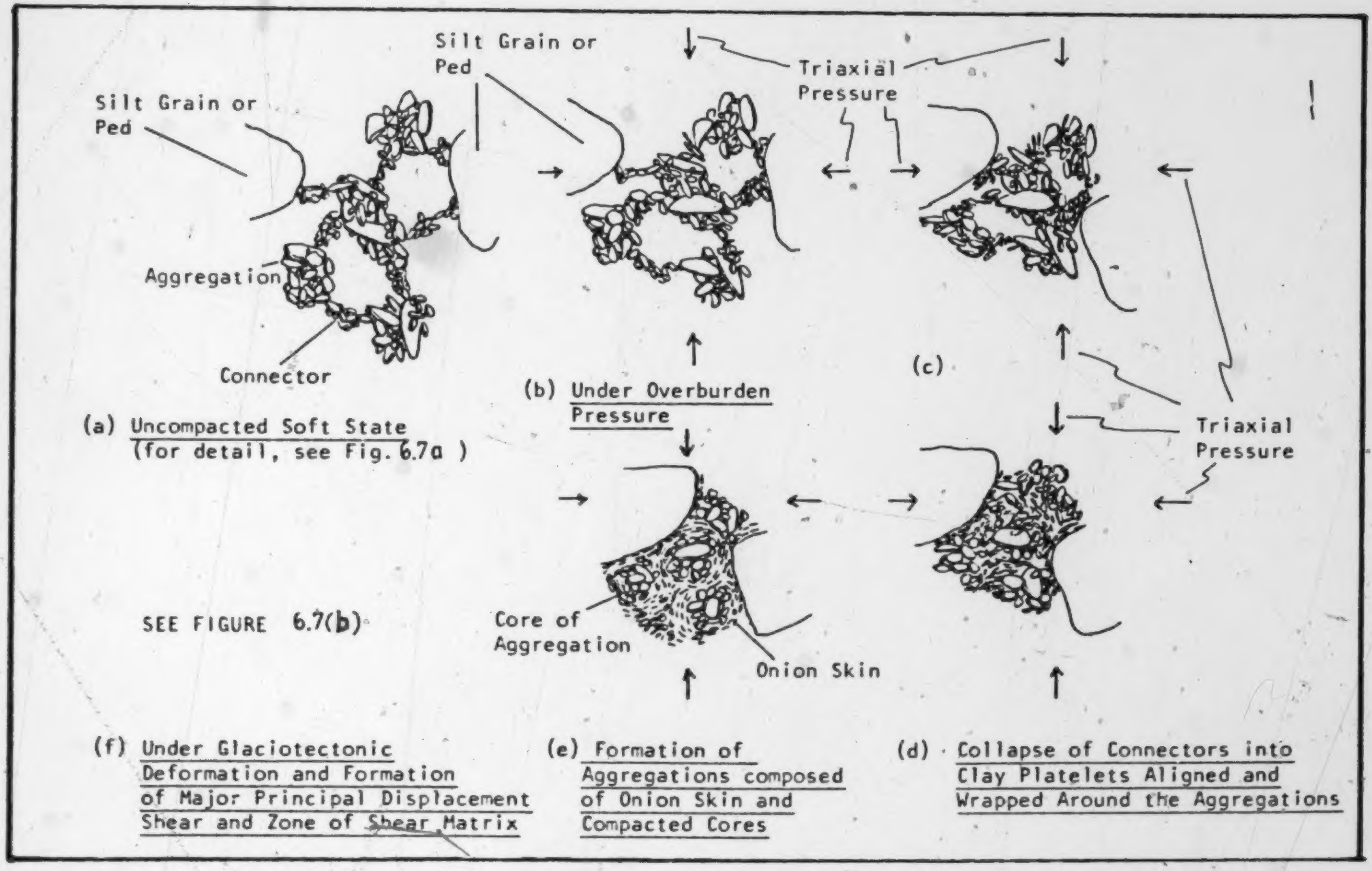
Silt Grain or Ped
Aggregation
Connector
Silt Grain or Ped
Triaxial Pressure
(c)
Triaxial Pressure
SEE FIGURE 6.7(b)
Core of Aggregation
Onion Skin

(a) Uncompacted Soft State (for detail, see Fig. 6.7a)

(b) Under Overburden Pressure

(c)

(d) Collapse of Connectors into Clay Platelets Aligned and Wrapped Around the Aggregations

(e) Formation of Aggregations composed of Onion Skin and Compacted Cores

(f) Under Glaciotectonic Deformation and Formation of Major Principal Displacement Shear and Zone of Shear Matrix

Figure 6.8 : Evolution of the Submicrofabric Units of the Sediments Studied Subjected Under High Overburden Pressure and Glaciotectonic Deformation. (a), (b) and (c) are modified after Pusch (1973b), (d), (e) and (f) are Suggested by the Author.

that occurred in central and southern Alberta (Chapter 3).

3. As far as the sole thrust in the glaciotectonic thrust system is concerned, the sediments within the fault during ice thrusting were kinematically restrained by the overlying ice sheet and the surrounding rock masses.

7. GEOTECHNICAL PROPERTIES OF ICE-THRUST SEDIMENTS

7.1 Introduction

The geotechnical properties of ice-thrust sediments discussed in this thesis are based chiefly on the geotechnical laboratory tests performed by the author on the block samples collected within a shear zone near two slide masses (Slides 1 and 2) in Pit 3, Highvale mine, Wabamun Lake area (Appendix C, Figure C.4). The locations and the procedures for the block sampling and the fabric of the samples have been described in detail in Chapter 6, and the geology of the site and the shear zone has been delineated in Chapter 5.

The cost of insitu drilling in the mine to obtain core samples for examination and testing exceeds the funding of this project. Fortunately, in the past few years, many boreholes had been drilled by consultants in the mine. Figure 5.1 shows the location of the boreholes with respect to the slide masses in Pit 3. A number of these boreholes were logged both geologically and geophysically, and core samples were taken for geotechnical laboratory testing. In particular, borehole #HV-83-406 had been drilled and logged carefully by the consultants in the summer of 1983 about 150 m northwest of the 1984 slides where detailed field mapping and block sampling were performed subsequently by the author.

The test results of the core samples together with the geologic and geophysical logs of boreholes have enhanced the interpretation and generalization of the geotechnical properties of the ice-thrust sediments obtained from laboratory tests on the block samples performed by the author. Moreover, the analysis of these subsurface log data, field observations and tests results of the ice-thrust sediments in the study area have also enabled a subsoil profile of an ice-thrust terrain to be presented. The laboratory work on the block samples carried out by the author are described in the following paragraphs.

7.2 Laboratory Work

Laboratory tests were performed by the author on the block samples of bentonitic mudstone and bentonite.

7.2.1 Classification Tests

For grain size classification, in order to break down the lumps and aggregations in the bentonitic mudstone and bentonite, the samples were subjected to high-speed blenderizing following the procedures suggested by Heley and Maclver (1971) before analysis according to the methods outlined in ASTM Standards (1986). Figures 7.1 and 7.2 show the grain size distribution of the samples. The results of the classification tests on the bentonitic mudstone and bentonite are summarized in Table 7.1. The distribution of clay minerals in the bentonitic mudstone has been given on

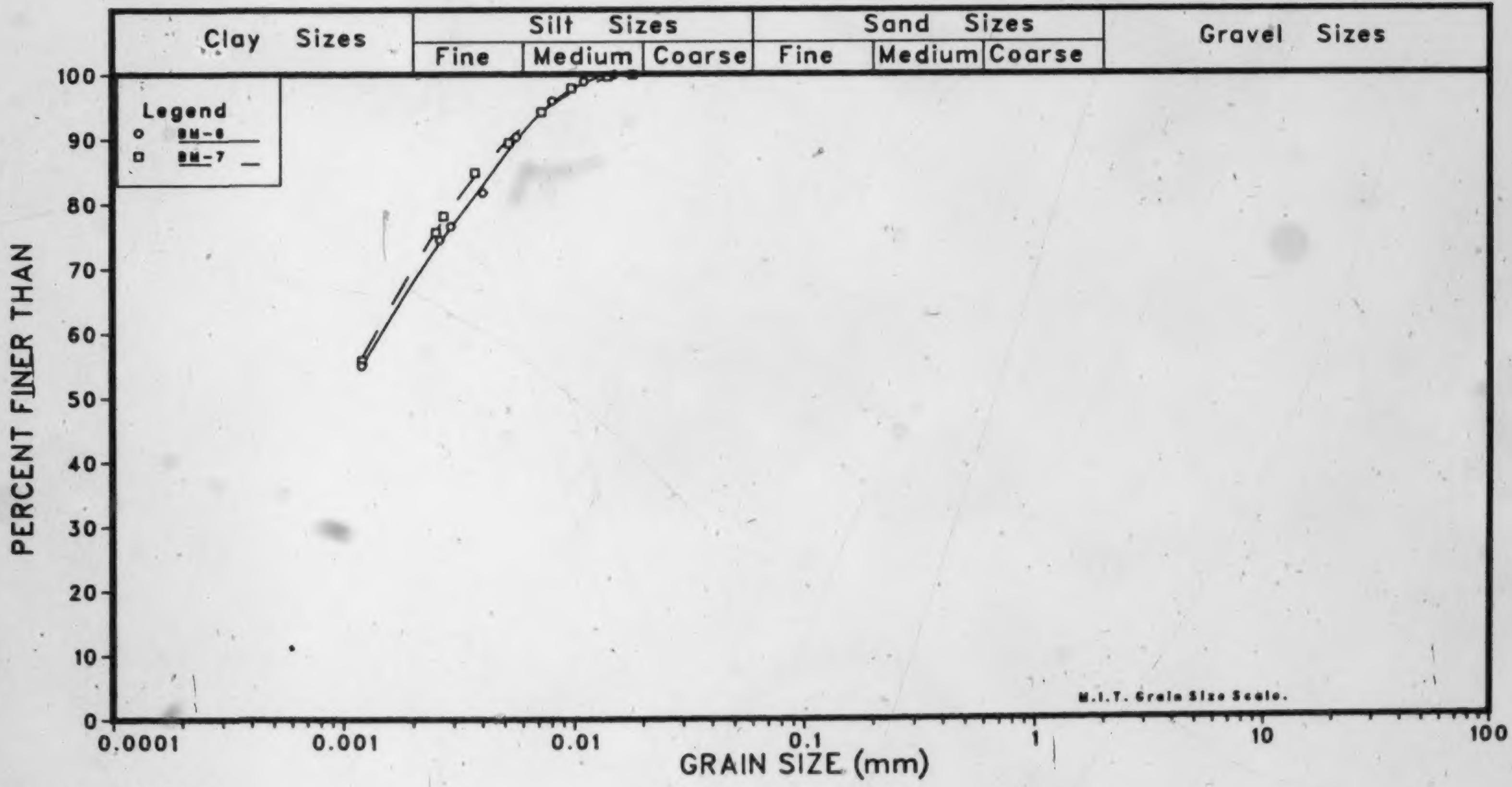

Figure 7.1 Grain Size Distribution of Bentonitic Mudstone, Pit 3, Highvale Mine

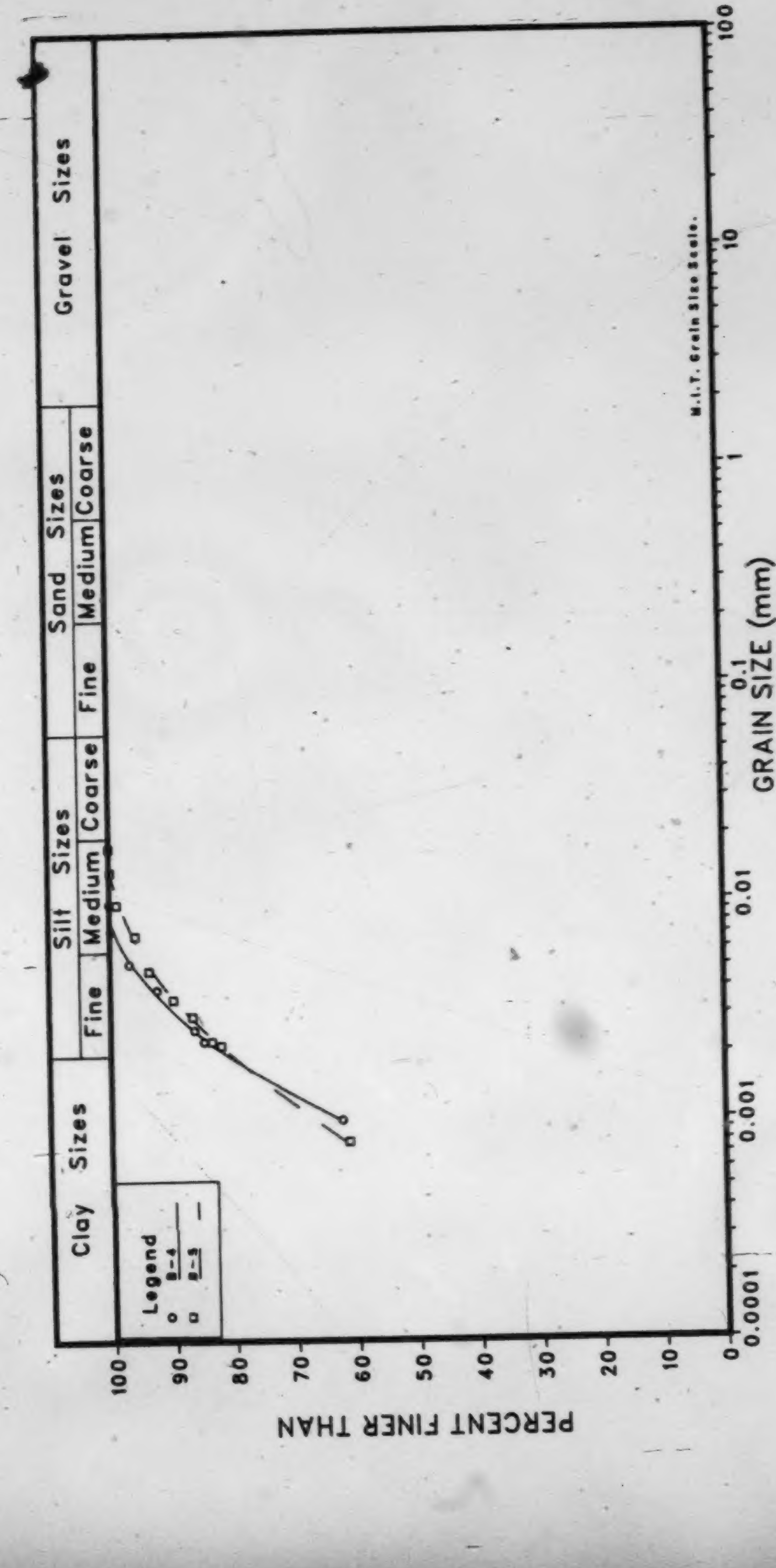

Figure 7.2 Grain Size Distribution of Bentonite, Pit 3, Highvale Mine

Table 7.1 Classification Test Results of Bentonitic Mudstone and Bentonite

Lithology	Depth (m)	w (%)	P_L (%)	L_L (%)	I_P (%)	I_L	C.F. (%)	A
Bentonitic Mudstone	14	22.9 to 32.1	39.8	76.5	36.7	-0.46 to -0.21	63 to 70	0.52 to 0.58
Bentonite	17.2	53.2	59.5	176.5	117.0	-0.05	80 to 80.5	1.45 to 1.46

C.F. = Clay Fraction (less than 2 microns)

A = Activity

Figure 6.6.

Based on the Unified Soil Classification System, the samples described as bentonitic mudstones are classified as inorganic silt (MH) and the bentonites are classified as inorganic clay (CH). It is to be noted that most of the silt-size particles are probably clay lumps and/or coal chips which appeared to remain in the soil mixture after at least 10 minutes of blenderizing. Indeed, the petrographical and SEM studies on the block samples (Chapter 6) indicate that the silt-size particles in the sediments investigated mainly are clay platelets. The bentonitic mudstone has an undrained shear strength ranging from Cu equal to 65 to 107 kPa (discussed in the triaxial test section below) which is characteristic of a clay rather than mudstone according to the classification of argillaceous material suggested by Morgenstern and Eigenbrod (1974), who proposed a Cu of 1,800 kPa as the upper and lower limit for clay and mudstone respectively. However, the mudstone in the study area, which has a Cu less than 300 kPa and a plasticity below the Casgrande's A-line, would be classified as a silt according to Grainger (1984). Nevertheless, for simplicity and consistent with the terminology adopted by other workers in the study area and in central Alberta (Locker, 1973; Fenton et al., 1983; Pawlowicz et al., 1985; Monenco Ltd., 1984), the terms bentonitic mudstone and bentonite will be retained in the remainer of this thesis.

The values of Atterberg Limits of the bentonitic mudstone studied (Table 7.1) agree with the physical properties of the mudstones found in other parts of the pit which have a liquidity index varying from 0.58 to -1.41 with most falling between 0 and -0.3. The plasticity index varies from 21 to 195 % with most the ranging of 30 to 74 % (Appendix H, Table H.1).

X-ray diffraction analysis indicate that the clay fraction of the bentonite consists of 100 % montmorillonite, while the clay minerals in the clay fraction of the bentonitic mudstone varied from relatively higher montmorillonite and lower illite and kaolinite contents at the continuous shear surface within the shear zone to relatively lower montmorillonite and higher illite and kaolinite contents away from this surface (Figure 6.6).

7.2.2 Consolidation Test

Conventional one-dimensional incremental consolidometer tests were performed on the bentonitic mudstone sampled from the brecciated zone containing the continuous failure plane. Two samples were tested, one was collected 1 cm above the principal shear plane and the other was from the upper subzone (Figure 6.6) about 5 cm above the first sample. The natural moisture content for the former was 28.2 and for the latter was 17.8 %. The low moisture content is believed to be partly due to the nature of the material and partly due to drying during sampling and storage. The Casagrande Method was used to estimate the insitu preconsolidation pressure P_c'. In order to obtain a well-defined virgin curve to calculate P_c', the samples were carried to a stress level equal to about 8 times P_c' as suggested by Brumund et al. (1976). The test data are presented as vertical strain vs effective stress rather than void ratio vs the effective stress because this enabled the consolidation data of the direct shear samples to be plotted on the same graph and to compare the disturbance between samples. Figure 7.3 is the ϵ vs log P' plot for the samples and shows a P_c' of 320 and 370 kPa, and an overconsolidation ratio (OCR) of 1.8 and 2.1; indicating that the bentonitic mudstone tested is slightly overconsolidated at present. The summary of the consolidation tests is shown in Table H.2 (Appendix H).

Nurkowski (1984, fig. 13, table 3, p. 292) studied the relation between the coal rank variation and the overburden pressure of the Upper Cretaceous and Tertiary Plains coals in Alberta and calculated that 1,176 - 1,548 m of overburden was needed to mature coal to a rank of subbituminous B. The coal of the mine is ranked as subbituminous B (Pearson, 1959), and the samples for the consolidation tests are about 3.8 m above the top of the main coal seams and about 14 m below the present ground surface. Assuming the eroded overburden has a total unit weight of 20 KN/m^3, the samples collected in the area are presumed to have an effective preconsolidation pressure of 11,945 - 15,735 kPa. Since the present insitu pressure P_0' is about 176 kPa, the OCR of the

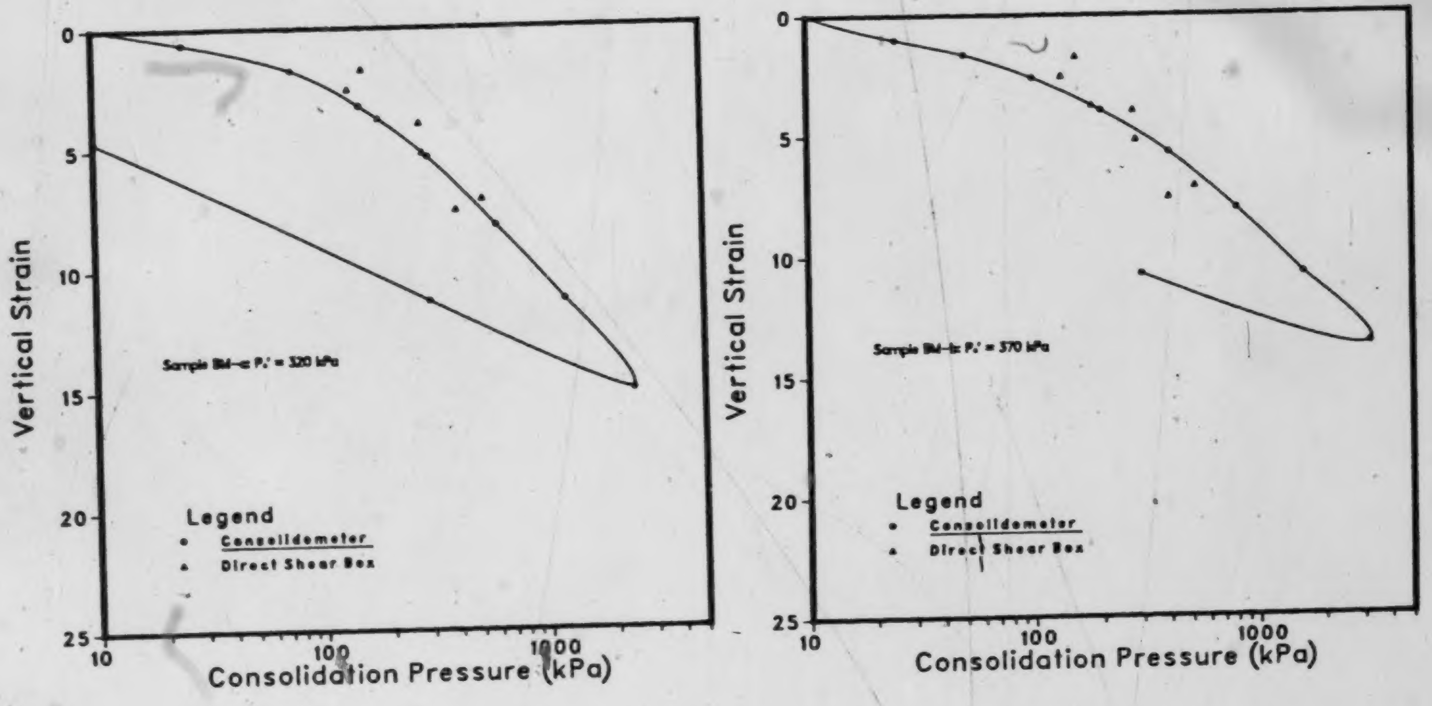

Figure 7.3 Consolidation Curves of Bentonitic Mudstone, Highvale Mine

samples based on geologic evidence ranges from 68 to 89.

7.2.3 Triaxial Tests

Triaxial tests were performed on the bentonitic mudstone samples following the standard procedures delineated by Bishop and Henkel (1962). The diameter of the samples was 37.8 mm and had a height of 71.2 - 76.4 mm. The samples were porous and consisted of angular lumps 1 - 15 mm long, and many horizontal to inclined fissures 2 to 15 mm long and from closed to 1 mm wide. All samples show light to pale grey, relatively plastic, soft bands with wavy boundaries resembling a flowage structure. The bands were 6 - 15 mm thick and at least 0.38 m long, and were underlain or/and overlain by a relative dark brownish grey to yellowish grey, crumbly, silty layer. Figure H.1 shows the lithological and structural descriptions of these triaxial samples before and after the tests (Appendix H).

The samples were stage consolidated isotropically to an effective confining pressures of 400, 526 and 701 kPa. Two rubber membranes with a thickness of 0.5 mm and 0.25 mm for the outer and inner membranes respectively were used to enclose the samples, with grease on the surface of the inner membrane. A 200 kPa back pressure was applied to all samples to ensure full saturation and to de-air the volume measuring device. The pore pressure coefficient B after the final consolidation stage varied from 0.95 to 1.00. Radial and one end drainage were used for the dissipation and equalization of pore water pressure during shear. The samples were tested with a rate of strain of approximately 0.002 - 0.003 mm/min and pore pressure was measured during shearing. The samples failed mainly by bulging with shear planes inclined 30° - 55° from the horizontal which tend to follow the orientation of the relatively plastic laminations and fissured surfaces. The rupture patterns of the samples after the triaxial tests are shown in Appendix H (Figure H.1). Figure 7.4 shows the change of the deviator stress vs vertical strain during shearing. Figure 7.5 is a p'- q' plot which shows the stress path of the triaxial tests. The pore pressure coefficient A of the soils at failure ranged from 0.38 to 0.52 which are typical values for a slightly overconsolidated soil to normally consolidated sandy clay (Bishop and Henkel, 1962, table 5, fig. 8; Skempton, 1954, table 2). The sediments failed at an axial strain of about 6.0 % for $\sigma_c' = 400$ kPa, 10.7 % for $\sigma_c' = 526$ kPa, and 3.05 % for $\sigma_c' = 701$ kPa. Figure 7.6 is the σ' vs τ' plot obtained from CU tests and shows the sediments have an effective strength of $c' = 0$ kPa and $\phi' = 22.5°$. The results of the triaxial tests are shown in Table H.3 (Appendix H).

Due to the lack of test samples, only one unconsolidated undrained test was performed to measure the undrained strength of the sediments. The sample had a diameter of 37.8 mm and a height of 70.9 mm. The sample was mainly dark grey to dark brownish grey; however, a light grey, relative plastic zone of about 0.5 cm thick and

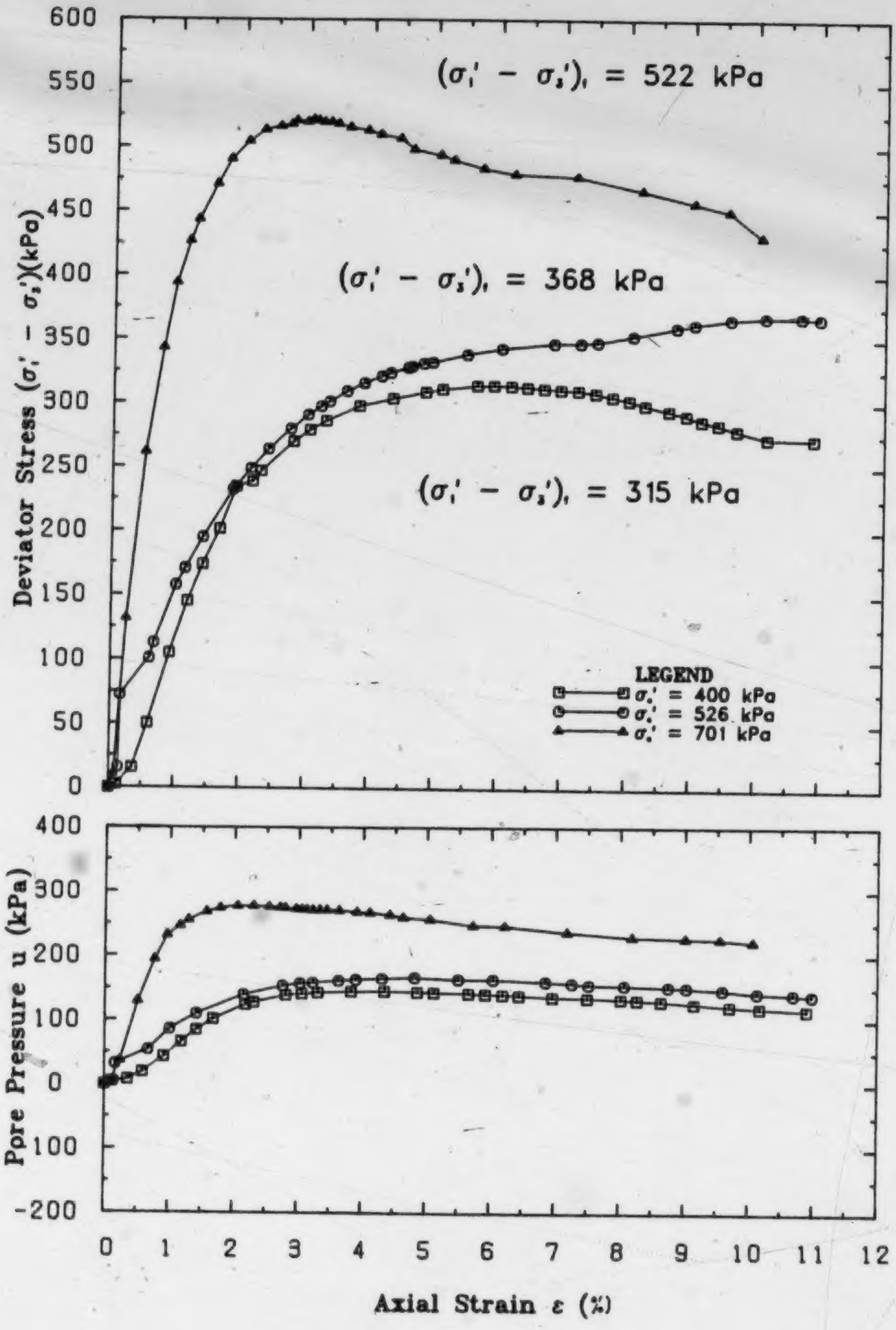

Figure 7.4 Deviator Stress vs Axial Strain Plot of CU Triaxial Tests on Bentonitic Mudstone

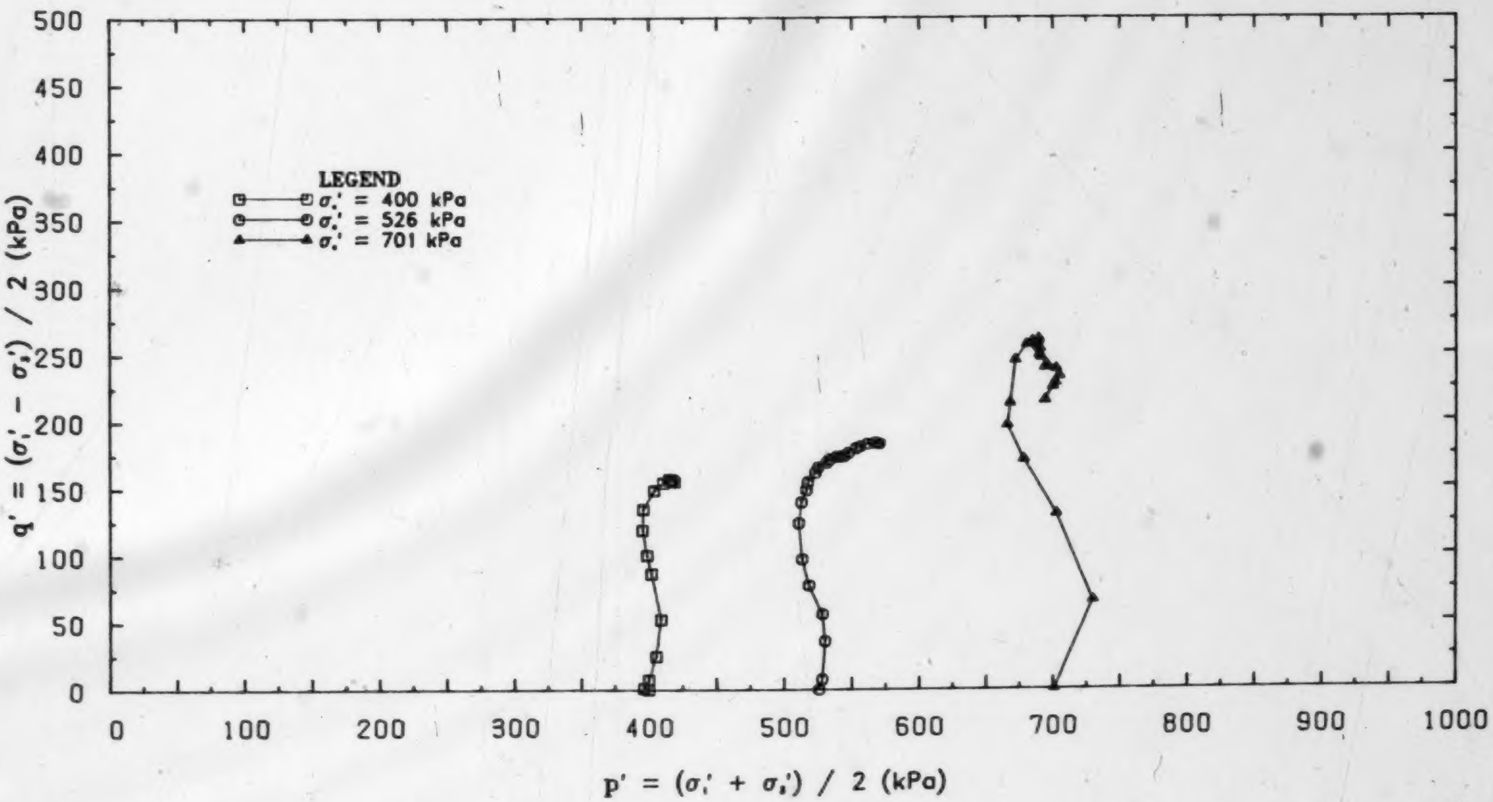

Figure 7.5 p' - q' Plot of CU Triaxial Tests on Bentonitic Mudstone

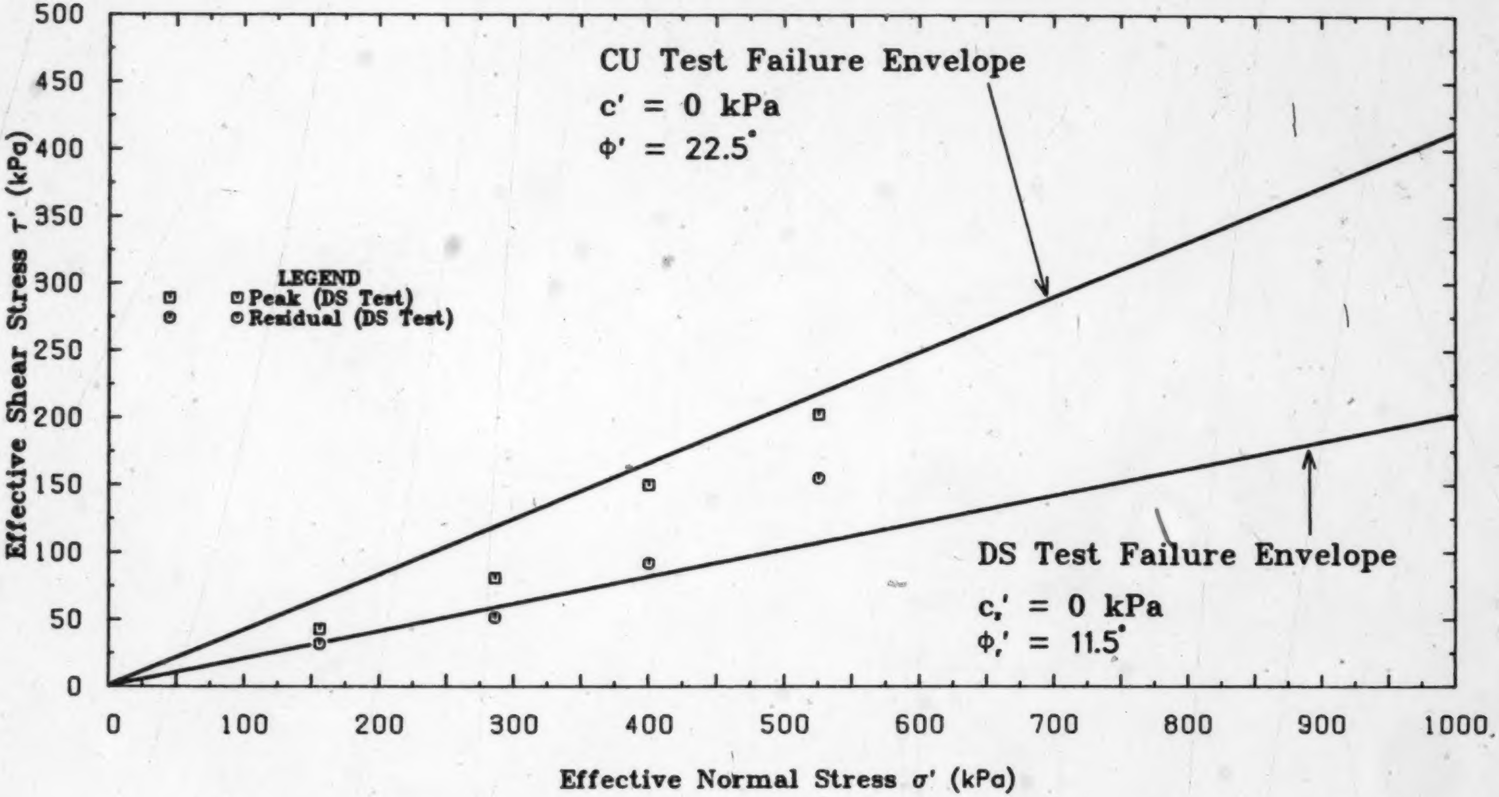

Figure 7.6 Mohr Circle Plot of Triaxial Tests and Direct Shear Tests on Bentonitic Mudstone

inclined about 30° from the horizontal was found near the bottom of the sample. In order to decrease the influence of jointing and fissuring in this soft and friable material, a strain rate of 0.35 mm/min (0.49 % strain per min) and a confining pressure of 350 kPa were used in this UU test as suggested by Morgenstern and Eigenbrod (1974, p. 1143). No back pressure was applied. Failure occurred after 5.5 % axial strain and the deviator stress ($\sigma_1 - \sigma_3$) remained constant beyond this strain (Figure 7.7). Two shear planes were developed at failure (Appendix H, Figure H.1). One of these shear planes was mainly along the light grey plastic zone with an inclination of about 20° - 25°. The other developed within the relatively crumbly zone and inclined at about 35° - 45° from the horizontal.

The UU test result in this study together with two other UU tests performed by Hardy Associates on the materials with similar lithologic descriptions are indicated in Figure 7.8 and Table H.4 (Appendix H). The resulting Cu varied from 65 - 107 kPa. The variation probably is due to the difference in lithology, mineralogy, the degree of saturation, and structure between samples and the amount of disturbance during sampling and the orientation of the fissures relative to the plane of the maximum shear stress (Marsland and Butler, 1967, fig. 6).

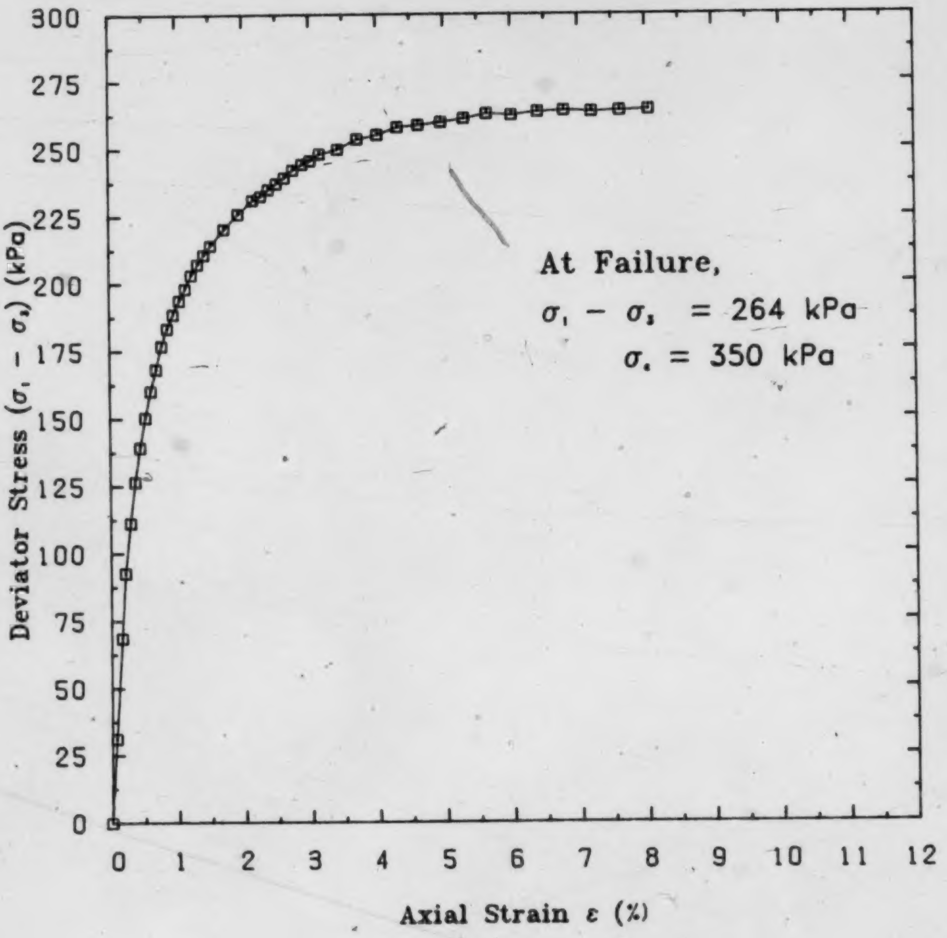

Figure 7.7 Deviator Stress vs Axial Strain Plot of UU Triaxial Test on Bentonitic Mudstone

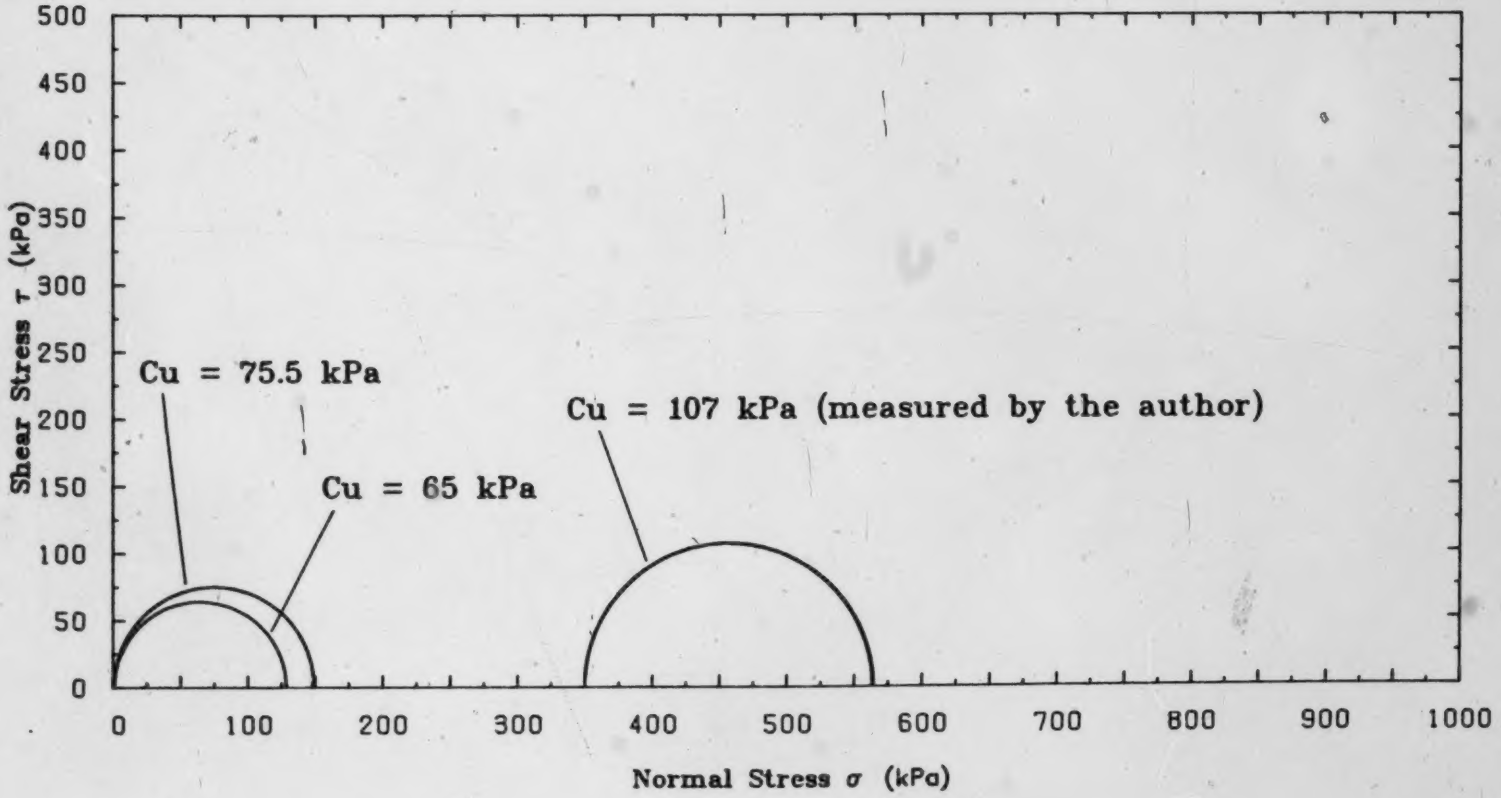

Figure 7.8 Mohr Circle Plot of UU Triaxial Tests on Bentcnitic Mudstone

7.2.4 Direct Shear Test

The samples used in the shear test were 152.4 mm square and were 24.0 to 38.2 mm thick. Difficulties were involved in trimming the samples due their brittle and crumbly nature. As a result, some disturbance due to sample preparation was expected. On the other hand, Townsend and Gilbert (1976) noted that residual strength is independent of specimen preparation procedures and comparable values have been obtained from intact, precut, and remoulded specimens of clayshale; hence, the effects on ϕ_r' of the different testing procedures and types of test are considered to be small. The rate of displacement for the bentonitic mudstone in the test was 0.00065 to 0.0049 mm/min, and for the bentonite was 0.00195 to 0.0096 mm/min. These rates of shear, which ensure complete drainage, were determined from the consolidation tests performed on the samples in the direct shear box before the shear tests began. These rates fall within the range of displacement used in other drained direct shear tests performed on the similar kinds of clayey deposits such as the Edmonton and the Paskapoo Formations (Locker, 1973; Sinclair and Brooker, 1967). The maximum displacement for the direct shear test apparatus is not large enough to allow the soil to reach a residual value. Thus, the shear box was hand crank advanced at least 4 complete cycles to align the soil particles along the shear plane. Figures 7.9 and 7.10 show the shear stress vs displacement relationships of the bentonitic mudstone and the bentonite. The summary of the drained direct shear tests are shown in Tables H.5 and H.6. All the samples tested during shearing showed a contraction or a decrease in volume with strain, and a plastic mode of deformation.

Figures 7.6 and Figure 7.11 are the σ' vs τ' plots of the test results for the bentonitic mudstone and the bentonite. The peak strengths for the mudstone and bentonite studied are scattered; however, both show an average residual of $c_r' = 0$ kPa, $\phi_r' = 11.5°$.

The shear test results of the bentonitic mudstone (Figure 7.6) are compared with other direct shear test results on mudstone core samples obtained from boreholes #HV-83-406 (about 125 m northwest of Slide 1), #HV-83-008 (about 100 m southeast of Slide 1 and about 160 m south of Slide 2), #HV-83-2, -3, -6, -7, -8, -9, -10, -17 near the slide area in Pit 3, and other core samples collected from other pits within the mine (Monenco Ltd., 1984) (Figure 7.12). Figure 5.1 shows the location of some of these boreholes. These mudstone core samples are described as weathered, brecciated or sheared or a combination and were tested within a normal stress range of 100 - 1200 kPa. The strength parameters, the normal stresses used in the tests, Atterberg Limits, geologic descriptions, depth and the corresponding borehole number of these core samples are shown on Tables H.1, H.7 and H.8 (Appendix H). The peak and the residual strengths of the mudstone samples in the mine are scattered (Figure 7.12). However, close examination of

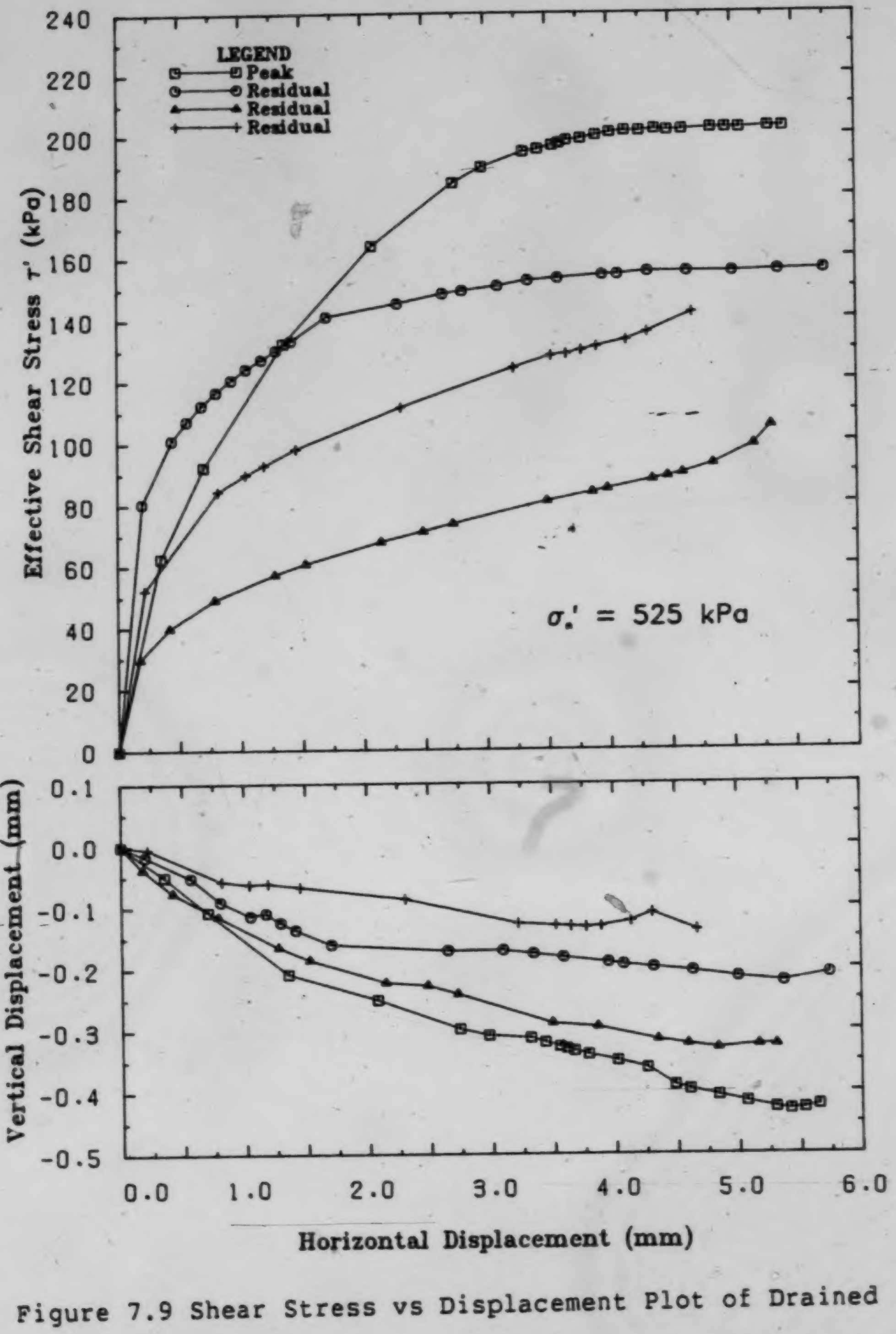

Figure 7.9 Shear Stress vs Displacement Plot of Drained Direct Shear Test on Bentonitic Mudstone

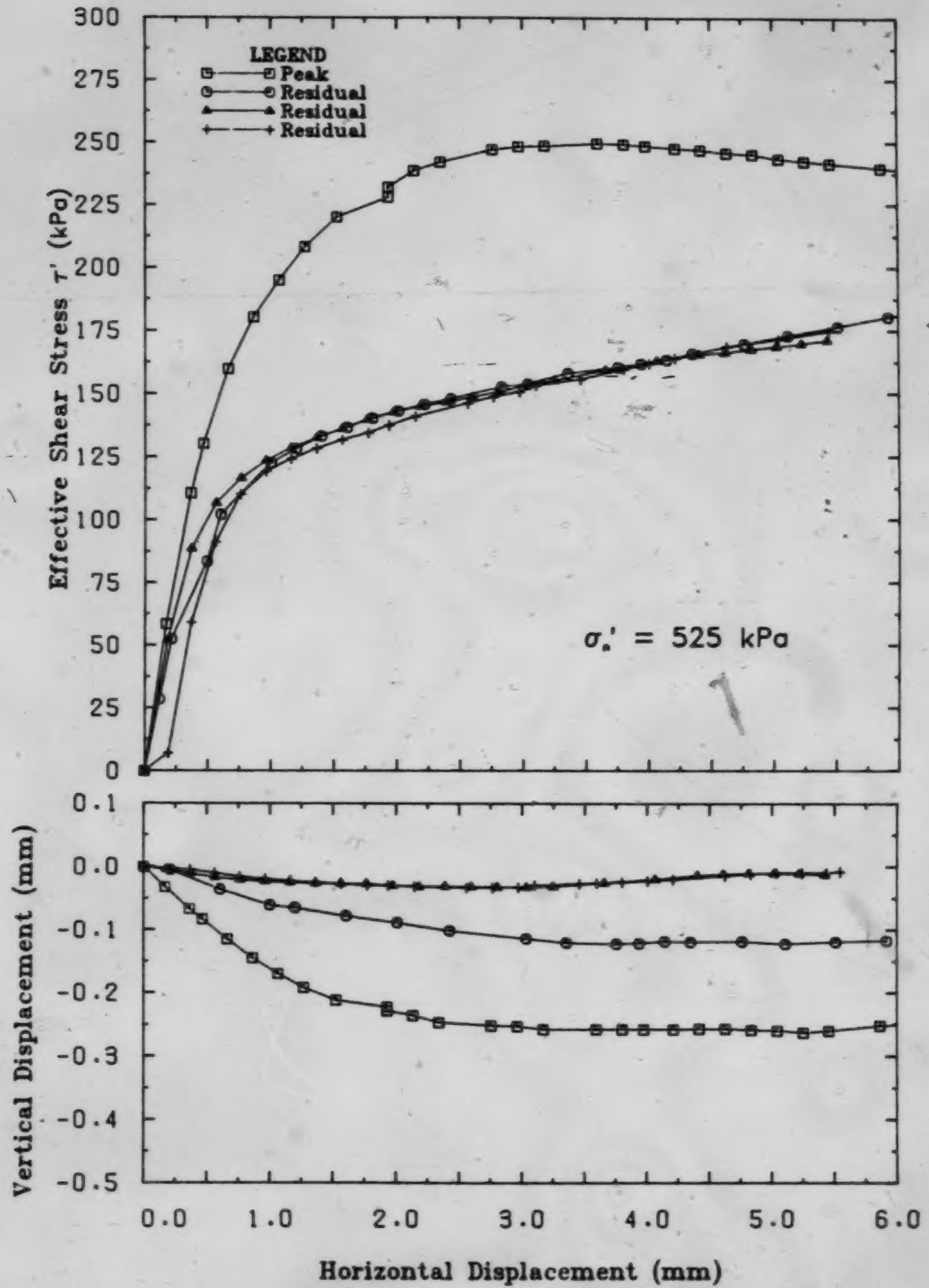

Figure 7.10 Shear Stress vs Displacement Plot of Drained Direct Shear Test on Bentonite

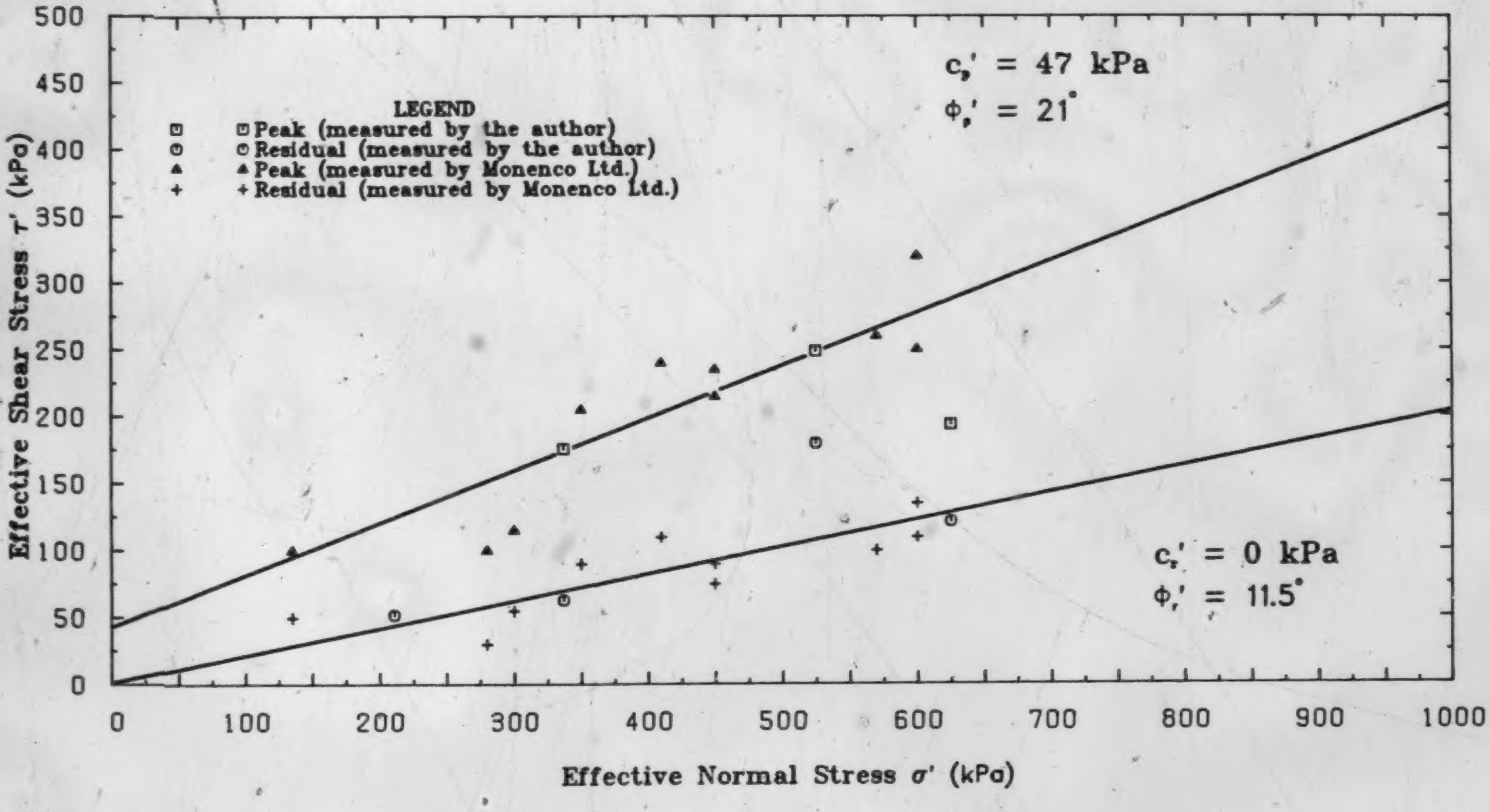

Figure 7.11 Effective Shear Strength vs Effective Normal Stress Plot of the Bentonite

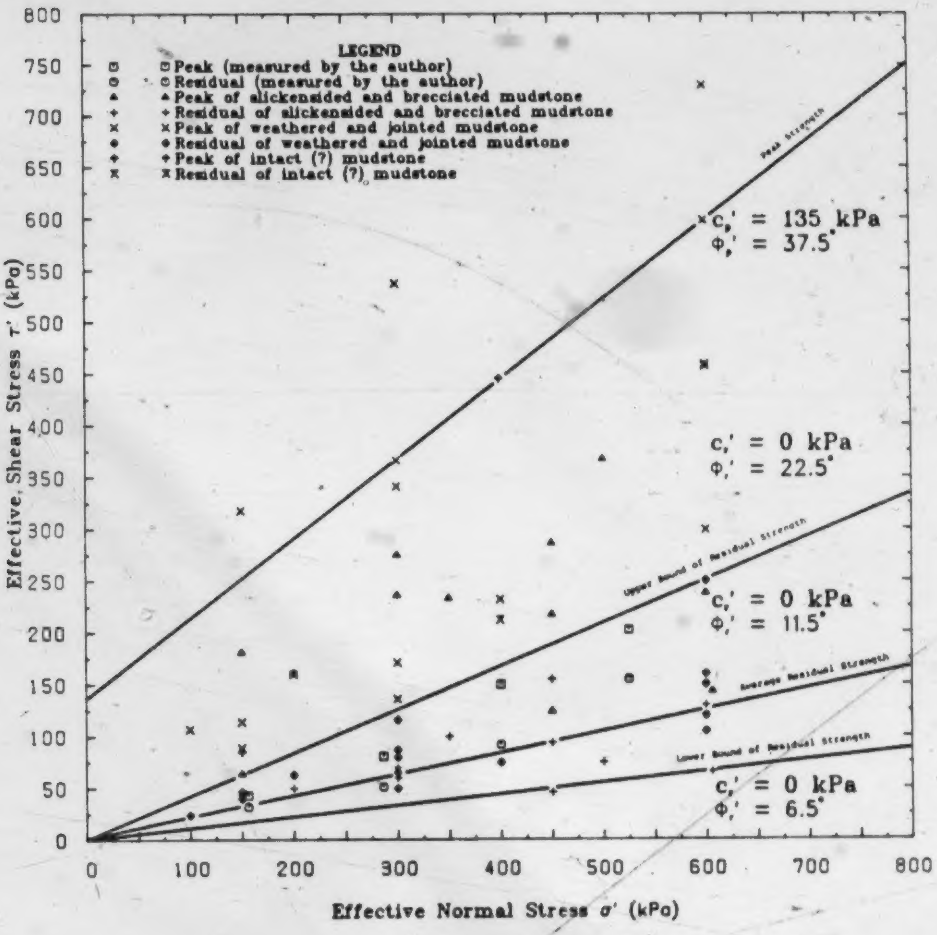

Figure 7.12 Effective Shear Strength vs Effective Normal Stress Plot of Drained DS Tests on Bentonitic Mudstone, Highvale Mine

the geologic descriptions of these samples indicate that trends can be drawn based on their geologic fabric described in Table H.8. Indeed, the maximum peak strength of this bentonitic mudstone in Highvale mine can be represented by three silty, jointed, carbonaceous and bentonitic clays with coal stringers as:

$c_p' = 135$ kPa, $\phi_p' = 37.5°$

Compared to the above, the remaining samples were relatively more fractured, jointed, and slickensided and show a peak strength less than the above values.

The residual strength of the mudstone showed a wide range with an upper bound of (Figure 7.12):

$c_r' = 0$ kPa, $\phi_r' = 22.5°$

and a lower bound of:

$c_r' = 0$ kPa, $\phi_r' = 6.5°$

Despite this range, most of the test results seem to fall on a residual failure envelope having:

$c_r' = 0$ kPa, $\phi_r' = 11.5°$

The shear test results on the core samples of bentonite are also plotted in Figure 7.11. The peak strength has a c_p' = 47 kPa, $\phi_p' = 21°$, and the residual strength has a $c_r' = 0$ kPa, $\phi_r' = 11.5°$.

In contrast, the bentonite of the Upper Cretaceous Edmonton Formation has a ϕ_r of about 8.5° (Sinclair and Brooker, 1967). Table H.9 shows the geotechnical properties of the bentonite tested by the consultants (Appendix H).

Figure 7.13 is a subsurface profile of Highvale mine based on the laboratory tests, field mapping, and drill hole logs performed by the author and the consultants.

To conclude, the mudstone tested by the author, collected from Pit 3 where slope instability occurred, has a maximum strength near the upper bound of the residual strength (Figure 7.12); while the maximum strength of the bentonite varied from peak to between the peak and the residual (Figure 7.11). Laboratory examinations of the mode of shear behavior and the structure in the failure zone of remoulded cohesive soils at residual have shown that when a fine-grained sediment (clay fractions exceeding about 30 %) which consists of large amount of platy clay minerals and a lesser amount of equi-dimensional particles, has undergone large strain, the shear stress vs displacement relationship would be brittle and a shear plane with strongly oriented clay particles would form. Moreover, subsequent re-shearing on the same deformed zone would only show a non-brittle shear stress vs displacement behavior and a measured low shear strength (Lupini et al., 1981, figs. 15 and 18). The heavily overconsolidated ice-thrust clay sediments in the study area of the Highvale mine, which show a very low maximum shear strength (Figures 7.6 and 7.12), a non-brittle, plastic mode of deformation with a small volume change during shear (Figure 7.9), low OCR (Figure 7.3), together with the presence of minor shears and distinct

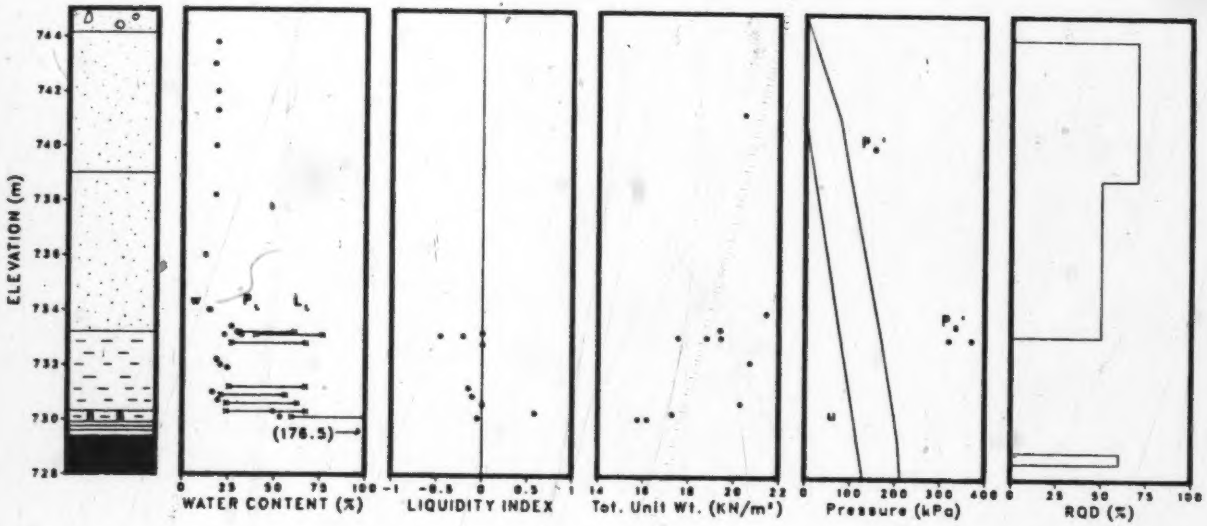

Figure 7.13 A Subsurface Profile of Highvale Mine

principal displacement shears bounded by a narrow zone of aligned platy clay particles (Plates 6.7, 6.12, 6.15, 6.17, and 6.18), indicate that the present laboratory shear tests were a reshearing of pre-sheared materials.

7.3 Discussion

1. Besides minor shears, the remoulded clay matrix in the shear zone of Highvale mine should also have a low strength and represent local areas of weakness since studies indicate that the water content is in general higher in the remoulded clay compared to the brecciated clay aggregates or lithorelicts (Chandler, 1973). This is proven by the cross-sections of triaxially sheared bentonitic mudstone samples which show a large portion of the failure surfaces passing through a light grey layer that is mainly made up of a relatively moist and plastic clay matrix in the samples (Appendix H, Figure H.1).
2. The presence of peds and lumps at the mesoscopic and microscopic scales and the densely compacted aggregations at the submicroscopic scale in the ice-thrust sediments studied should have caused dilation during shear failure, which is the common deformation behavior of most of the heavily overconsolidated clays. Indeed, the ice-thrust sediments resemble a granular material both at the mesoscopic and the microscopic scales as observed by Barden (1972b) on many natural

clayey deposits. However, the author's shear tests show that the material tended to contract instead of dilating during shear (Figures 7.9 and 7.10). The reason for this is believed to be that the laboratory failure surfaces mainly follow the principal shears, the minor shears, or the remoulded clay matrix, which all are essentially made up of zones of oriented clay platelets. It has been suggested that diagenetic bonds, which probably form primarily at points of interparticle contact and would yield strain energy that would induce dilation when they are broken, are less common in particles in an oriented arrangement (Nelson, 1973). Thus, the development of laboratory-induced failure planes along a horizon of oriented clay platelets should have minimized dilation during shear.

3. Ice thrusting has produced various deformed fabrics in different parts of the shear zone. The principal displacement shears in the area which are completely sheared probably have attained a residual strength; while the strength for the other parts of the shear zone should vary from peak (for the undisturbed or only slightly weathered intact material between discontinuities), to the fully softened strength (for the weathered and partially sheared material), to residual strength (for the sheared material such as along displacement shears). Thus, if the laboratory-induced shear planes are forced to develop in

the materials (such as in a direct shear box test) that are intact, slightly jointed and/or weathered, or along minor shears, the maximum strength obtained would depend on the proportion of the failure surface that developed through the minor shears, the jointed surfaces, and the intact peds. This seems to be the reason that the fissured and crumbly samples tested by the author show a maximum strength that varied from less than that of the fully softened state to residual (Figures 7.6 and 7.12). This is analogous to the average effective strength of the fissured Barton clay which was in general in between peak and residual; however, the sediment might show a peak or a residual strength if the failure surfaces were developed entirely within hard clay lumps or along very smooth fissure respectively (Marsland and Butler, 1967, figs. 3 and 9).

4. The scattering of the residual strength observed in the mudstone and the bentonite in the mine (Figures 7.11 and 7.12) probably is due to the following reasons.
    a. The variation in clay fraction and mineralogy within the sediments investigated. These are shown by the differences in liquid limit and lithology between the samples tested (Appendix H, Tables H.1, H.8 and H.9). The dependence of residual strength on clay content and mineralogy has been indicated by Kenney (1967), Townsend and Gilbert (1974), Skempton (1985), and Mesri and Cepeda-Diaz (1986).

b. The development of the laboratory-induced failure plane along pre-existed discontinuities such as bedding planes, fissures and principal displacement shears (Figures 5.3 and 6.6; Appendix H, Figure H.1) or within intact portion of the sample. This is because these macrofabric features may consist of distinctly different particle gradation and mineralogy and their associated residual strength may be different from the rest of the soil mass (McGown, 1982).

c. Extrusion of remoulded material from the gap between the two halves of the shear box during direct shear test. It has been suggested that the residual strength measured would be influenced by this process (Heley and Maclver, 1971).

5. According to the geologic evidence, the sediments in Highvale mine have been heavily overconsolidated (Nurkowski 1984) and the OCR of the bentonitic mudstone sampled should be in the range of 68 - 89. However, the samples tested behave as a apparently normally consolidated to a lightly overconsolidated soil in the laboratory tests and show a low maximum shear strength and OCR (Figure 7.3). This is believed to be due to the following processes.

   a. Unloading - It has been tentatively concluded that during K_0 unloading of the remoulded shale, passive pressure failure would occur in the range of OCR of

10 - 15 and the sediment should soften to the water content of a normally consolidated soil at that normal stress and attain a fully softened strength (Singh et al., 1973). In view of the removal of thick overburden due to erosion in the study area, it is inferred that the samples tested have undergone the path of passive failure during unloading in the geological past, and many of the structures and strength properties of the soil due to overconsolidation should have been destroyed.

b. Weathering and Permafrost - Laboratory consolidation tests showed that weathering could remove overconsolidation and a weathered overconsolidated soil might be similar to a sediment remoulded at a water content below its liquid limit (Chandler, 1969). The preglacial erosion and glaciation that occurred at the Wabamun Lake area must have allowed weathering and permafrost to extend tens of metres deep as evident from the petrographical and SEM studies (Chapter 6), causing brecciation to develop and strength reduction in this overconsolidated sediments in the study area.

c. Ice Thrusting - The flat-lying overconsolidated bentonitic mudstone in the study area, which had been weathered, jointed, and brecciated due to unloading, weathering, and permafrost, was crumbled and deformed into a horizontal shear zone by ice thrusting. As a result, most of the brecciated sediments in the shear zone were further deformed, remoulded, and sheared. Thus, the structure in the sediments due to overconsolidation were further eliminated. Subglacial deformation that obliterated evidence of preceding stress history in basal till has also been found by Boulton and Paul (1976).

6. This study shows that the shear zone in the ice-thrust terrain studied is the weakest layer. Thus, from a geotechnical point of view, when the depth of the shear zone in an ice-thrust terrain is within the range that will affect the earthworks at the surface, the geotechnical properties and the 3-D subsurface geometrical configuration of the shear zone should be of the most concern. For example, the shear zone in Highvale mine, which is located near the base of the excavation, controls the stability of the highwall. This will be shown in Chapter 10.

7.4 Conclusion

Based on the examination of the geotechnical properties of the ice-thrust clayey sediments observed in the Highvale mine, Wabamum Lake area, and other suspected ice-disturbed clayey deposits investigated by other workers (Eigenbrod and Morgenstern, 1972; Wilson, 1974; Sauer, 1978; Insley et al., 1976), the general geotechnical characteristics of ice-thrust sediments within a clayey layer in the region studied that have undergone loading and unloading, weathering, permafrost, and finally deformed into a shear zone by ice thrusting, are suggested below. Table H.10 summarizes the geotechnical properties of the suspected ice-thrust sediments measured by the investigators mentioned above (Appendix H).

1. The clay fraction of the sediments is high, for example, up to 40 % or higher within which platy clay minerals such as montmorillonite dominates, for instance, up to 30 - 85 % of the clay fraction is made up by montmorillonite clay mineral (Table 7.1; Appendix H, Table H.10; Figure 6.6).
2. The glaciotectonic disturbance does not seem to be evenly distributed within the deformed stratum; as a result, the fabric and strength properties usually vary in different parts within the shear zone. Nevertheless, the sediments appear to be granular, brecciated, fissured, sheared, and consist of continuous and horizontal principal displacement shears. The strength of the brecciated portion of deposits probably varies from fully softened to residual, while the strength along the principal displacement shears is at or close to residual.
3. Although geologically heavily consolidated, the sediments may behave as a normally consolidated to lightly overconsolidated clay and show a low OCR.
4. The sediments seem to show a poor RQD (Appendix H,

Figure 7.13).

8. GLACIOTECTONIC FACIES

8.1 Introduction and Definition

This Chapter investigates the characteristics of certain types of regional bedrock topographic configurations in the study areas that are prone to glaciotectonism, and the probable attitudes of ice-thrust features and deformed macrofabric that would be found in that particular regional topographic configuration. These would provide valuable information in identifying ice-thrust features and areas likely to be underlain by glacially-deformed sediments based solely on terrain analysis and regional topographic and geological map studies.

Each of these topographic configurations will be termed as a type of 'glaciotectonic facies' which refers to a glaciated area on a regional scale that (1) consists of a particular topographic configuration such as an escarpment or the vally wall of a preglacial bedrock channel that is susceptible to ice thrusting, and (2) consists of certain fabric elements such as glaciotectonic-induced shears and surficial features such as meltwater channels with orientations related to the direction of ice movement and/or the strike of the slope of that particular topographic configuration.

8.2 Method of Study

The ice-thrust features found in the areas studied are located in their associated regional bedrock topographic cross-sections. Based on the available surficial maps of the areas, the types of regional surficial deposits in the areas are also shown in the cross-sections. Fabric diagrams in the form of stereographic plots are constructed for the particular type of glaciotectonic facies. These fabric diagrams include the trend of the bedrock topographic configuration such as the strike of the bedrock surface of a preglacial valley, the strike of a (proglacial?) meltwater channel, the trend of the ice-thrust ridges, the direction of the glacial movement, the dip direction of faults, and attitudes of the fold axes and deformed beds due to ice thrusting found in or near the study areas. The movement of the faults and shear planes in the form of slip linears (Bielenstein and Eisbacher, 1969) may be plotted on the fabric diagram in order to indicate the relative movement of the shears and trends or orientations of the macrofabric in an ice-thrust terrain with respect to the direction of the ice movement in the region. Figure 8.1 shows the symbols used in these fabric diagrams. The resulting cross-sections and their associated fabric diagrams contribute to certain types of glaciotectonic facies. Examples of the glaciotectonic facies and the associated bedrock topographic cross-sections and fabric diagrams are delineated in Appendix I. The characteristics of these facies observed in

•	Pole of Bedding
⊙	Fold Axis
△	Pole of Minor Shear Plane
▲	Pole of Thrust Fault
□	Pole of Reverse Fault
■	Pole of Normal Fault
—△→	Slip Linear, arrow indicates sense of movement
--△-->	Slip Linear (approximate), arrow indicates sense of movement
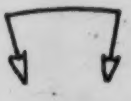	Range of Ice-Flow Direction, arrows indicate sense of movement
———	Strike of Preglacial Bedrock Surface such as Escarpment or Valley Slope
- - - - - -	Trend of Ice-Thrust Ridges and/or Source Depressions
— — —	Strike of Meltwater Channel or Glacial Valley

Figure 8.1 Symbols Used in Fabric Diagrams

the study areas are summarized below.

8.3 Glaciotectonic Facies

The types of glaciotectonic facies found in the study areas in central and southern Alberta are: (a) Escarpment Type, (b) Valley Type, and (c) Plains Type.

Types (a) and (b) have been mentioned by Banham (1975) and Eyles and Menzies (1983, fig. 2.19), Type (c) is suggested by the author for the first time. These Types of glaciotectonic facies are defined as follows.

8.3.1 Escarpment Type

Escarpment facies occurs on an inland cliff or steep to gentle slope such as the scarp-face of an erosional remnant or the slope of a broad river valley that is opposite or inclined to the flowing direction of a glacier. Marine cliffs should also belong to this category although they are not present in the regions studied. In general, the upper portion of the scarp face of the Escarpment Type glaciotectonic facies found in the study areas consists of a slope gradient of about 16 - 53 m/km and the lower portion of the scarp and the plain in front of the scarp has a slope gradient of about 2 - 12 m/km.

For escarpments formed by erosion, very broad river valleys may exist parallel to the scarps. In this case, the escarpment can be treated as the slope of a river valley. Field studies indicate that these valleys have a width from about 10 to 65 km between crests and 1 - 10 km wide at their bottoms. Examples are the Joffre Hills near Lowden Lake and the preglacial Medicine Hat Valley near the Cypress Hills (Appendix I, Figures I.4, I.5 and I.6).

Escarpment Type glaciotectonic facies tend to be located along the slope of a preglacial hill or valley with its strike perpendicular to and its dip against the ice direction. The attitudes of the fabric elements associated with this facies such as the trends of ice-thrust ridges and elongated source depressions, and the trends of the fold axes and the strikes of the ice-deformed beds tend to lie perpendicular to the glacial direction, while the dip directions of the thrusts and shears in these features are often oriented parallel to each other and against the ice direction. Within the Eascarpment Type glaciotectonic facies found in the study area, the ice-thrust features tend to be in the slope of the escarpment, away from the thalwegs of preglacial valleys in front of the escarpment (Appendix I, Figures I.2 and I.3). Figures 8.2 and 8.3 show the fabric model of the typical Escarpment Type glaciotectonic facies observed in Wabamun Lake area and Lowden Lake area.

Figure 8.2 indicates that the direction of displacement of the thrust faults and shear planes, and most of the dip directions of the deformed beds in Wabamun Lake area are parallel to the direction of ice movement in the region. The strike of the north-facing slope of the interglacial North Saskatchewan Valley where the facies is located and the fold

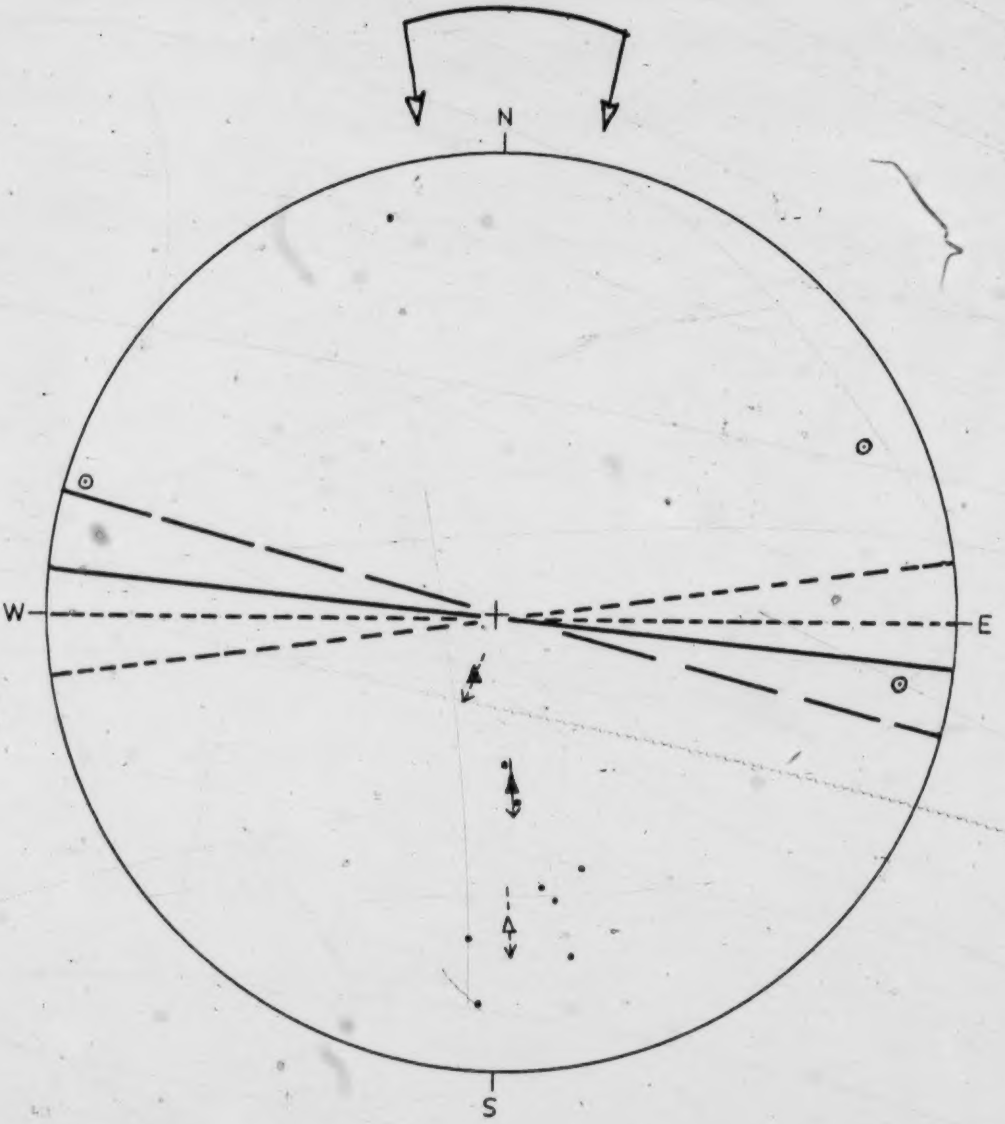

Figure 8.2 Fabric Diagram of Escarpment Type Glaciotectonic Facies, Wabamun Lake Area

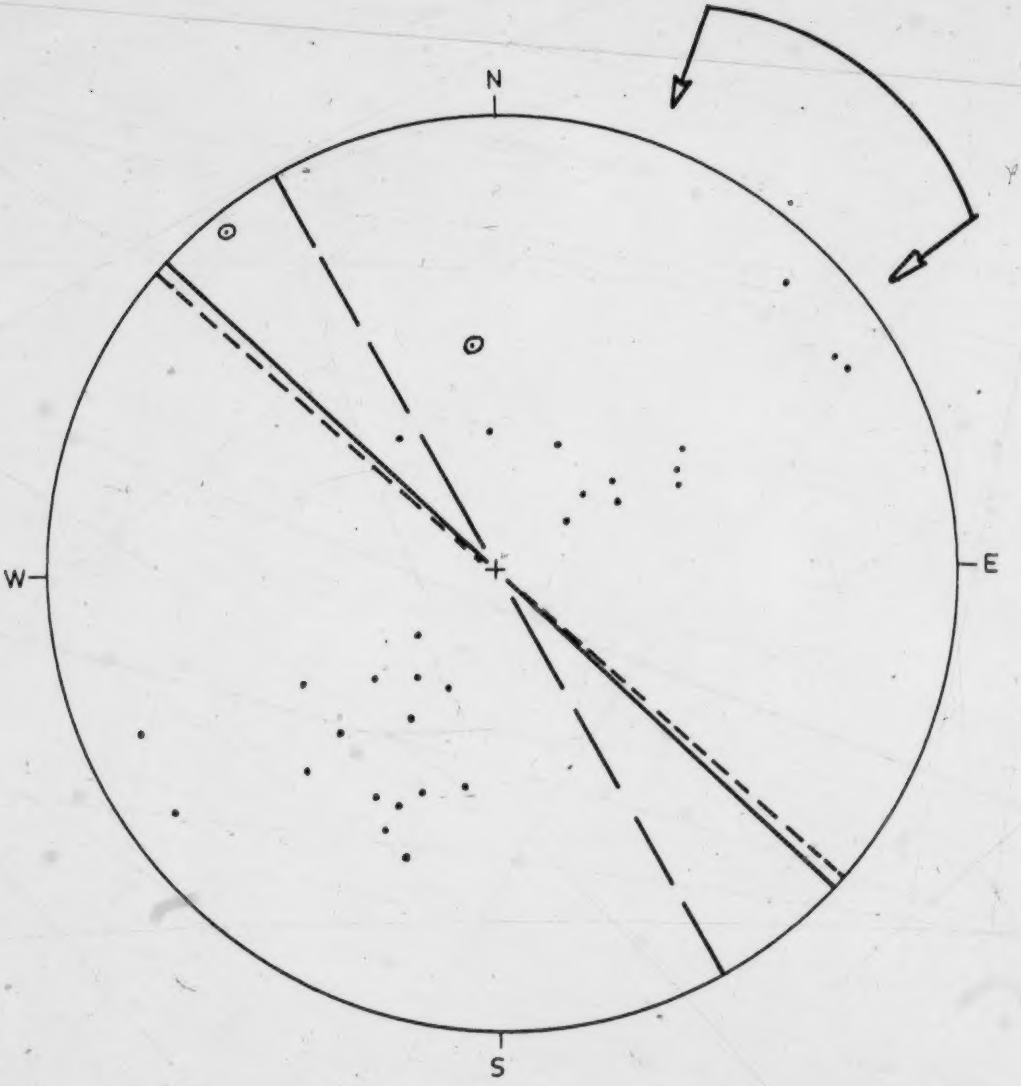

Figure 8.3 Fabric Diagram of Escarpment Type Glaciotectonic Facies, Lowden Lake Area

axes of the deformations found in the area are in general perpendicular to the ice direction. The glacial advances in the area range from 170° to 191° azimuth and are deduced from field observations in Highvale mine and other ice-thrust features found in the adjacent area (Babcock et al., 1978). Figure 8.3 shows that the dip directions of most of the deformed beds found in Lowden Lake area are parallel to the ice flow direction. The ice flow directions range from 201° to 234° azimuth and are inferred from the ice-flow markings found near Lowden Lake (Stalker, 1960a, map 1081A). It is also shown that the trend of the ice-thrust ridges and their associated source depressions (Appendix C, Figure C.12), the fold axes of the ice-thrust features (Appendix C, Figures C.13 and C.14), the strike of the preglacial bedrock slope at the rise of Joffre Hills (Farvolden, 1963a, fig. 14), and the trends of many ridges of undetermined origin found near the area (Stalker, 1960a) are apparently perpendicular to the range of the glacial direction of motion (Figure 8.3).

8.3.2 Valley Type

When an ice lobe enters and flows parallel to the thalweg of a river valley, the flow of the glacier creates compression on both sides of the valley slopes causing thrusting into the slopes away from the thalweg of the valley. The slope of the valley sides found in the study areas range from 11 to 32 m/km, with a width of 4 - 9 km between crests and 0.3 - 4 km at their bottoms. Examples are the Beverly Valley and Namao Valley in the vicinity of the city of Edmonton (Appendix I, Figure I.7 and I.8). Within the Valley Type glaciotectonic facies found in the study area, the ice-thrust features tend to be located in the walls of preglacial valleys, which may have a horizontal distance about 0.8 - 5 km away and a vertical distance about 15 - 69 m above the thalwegs of these valleys (Figures I.7 and I.8).

No fabric model of Valley Type glaciotectonic facies is available at present due to the lack of exposures of ice-thrust features along the two opposite sides of the preglacial valleys studied.

8.3.3 Plains Type

The Plains glaciotectonic facies occurs on a relatively featureless, flat to gently rolling plain which a glacier overrode. The slope gradient of the plains observed in the study areas is very gentle and is about 2 - 5 m/km. Examples are the Castor - Coronation - Brownfield districts (Appendix I, Figure I.10).

Figure 8.4 is a fabric model of the Plains Types glaciotectonic facies observed in Hanna - Sedgewick area and the area northwest of Sullivan Lake. It is shown that some of the deformed beds in this facies have their dip directions within the range of glacial direction which have a range of 201° to 234° azimuth; however, a portion of the

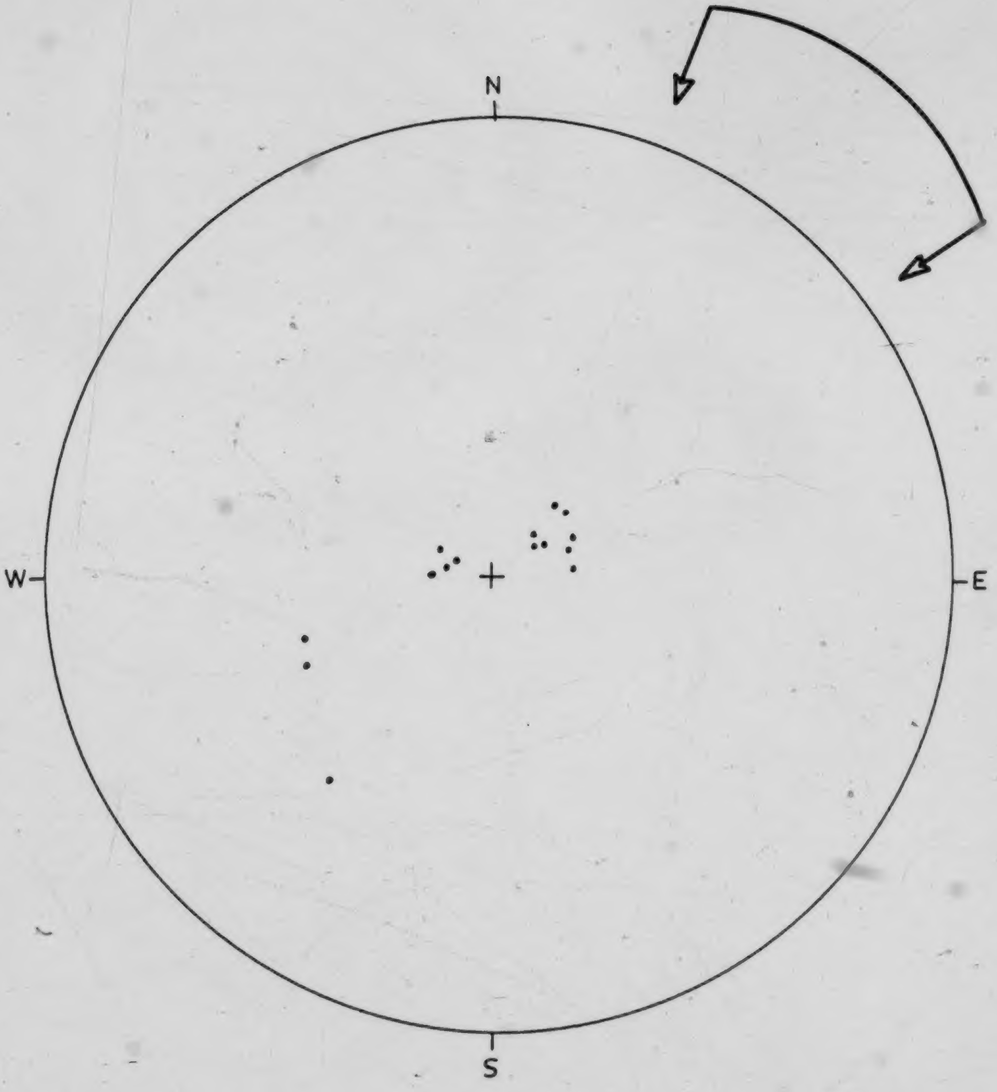

Figure 8.4 Fabric Diagram of Plains Type Glaciotectonic Facies, Hanna - Sedgewick Area

deformed beds observed in the field have their dip directions outside this range. This may be due to (1) insufficient measurements to reveal the range of direction of ice movement and the main attitudes of the ice-deformed beds, (2) the strike error (Ragan, 1985, fig. 5.20) involved in measuring most of the deformed beds in the study area which have a small inclination (9° - 14°) with respect to the horizontal, and (3) the absence of topographic restraint on a plain to confine the movement of ice flow; thus, more ice lobes would appear and flow in different directions along the margin of the ice. As a result, the trend of the ice-thrust features which were formed due to the flow of these ice lobes, should be different from each other.

8.4 Discussion

1. The main difference between the Escarpment Type and the Valley Type glaciotectonic facies is the direction of glacier movement with respect to the orientations of the regional bedrock topographical configuration. When the regional ice flow is perpendicular to an escarpment or when the glacier flows across a river valley, these topographic features are considered as an Escarpment glaciotectonic facies. However, when an ice lobe flows along an escarpment or enters a valley and flows parallel to the thalweg of this trough, these topographic features are treated as a Valley glaciotectonic facies.

2. Some of the ice-thrust features in the Escarpment Type and the Valley Type glaciotectonic facies can be mistaken as slump features or igneous intrusive features. Examples: the deformation of the Whitemud Formation in the Eagle Butte district, Cypress Hills area, was believed to be due to large-scale slumping by Russell and Landes (1940); and the disturbance of the Whitemud and the Eastend Formations near Claybank in southern Saskatchewan had once been attributed to landslides and gravitational gliding (Bell, 1874; Dyer, 1927).

   The macrofabric exposed northwest of the Eagle Butte district investigated by the author and at the Claybank area studied by Byers (1959) indicated that they are ice-thrust features. This is because: (a) the observed structures are composed of folds with low angle thrust faults and absence of inverted limbs which are characteristic of surficial features, (b) the folds seem to die out downwards in the Eagle Butte area (Appendix C, Plate C.1) instead of upwards if they have been produced by igneous intrusives, (c) both areas belong to the Escarpment Type glaciotectonic facies, and (d) aerial photograph studies of the area have not shown any large-scale features such as scarps and slumped debris related to large earth movements.

3. Ice-thrust macrofabric in glaciotectonic facies may show that they have been affected by multiple glaciation.

Examples are the deformed beds and thrust faults measured in the study areas near the Cypress Hills that had been glaciated by ice lobes which flowed mainly toward southwest and southeast (Appendix B; Appendix C, Figure C.30). The glaciotectonized landscape of Holland, North Germany and Poland also show that younger thrust slices commonly overlie ridges and indicate that successive glaciations might cause multiple phases of deformation in the same glaciotectonic facies (Eyles and Menzies, 1983, p. 63; Maarleveld, 1981).

4. Field evidence shows that distinct ice-thrust features tend to form on local topographic barriers such as proglacial channels and regional slope surfaces such as Escarpment and Valley Type glaciotectonic facies (Chapters 4 and 8). The effects of topography on ice thrusting are described as follows.

When an ice sheet flows toward a topographic high, such as escarpment or valley slope, the toe of the glacier and the inclined ground surface would form a drainage basin that traps river water from the highlands and glacial meltwater from the ice (Rutten, 1960). Evidence of the presence of water bodies in front of the margin of the ice sheet that covered the study areas include proglacial meltwater channels and glaciolacustrine deposits, as observed in the Lowden Lake area, the Nisku area, and the Isle Lake area (Appendix C, Figures C.10, C.11 and C.12). It is known that water bodies can cause the permafrost in the underlying sediments to decay. This has been shown by the existence of a deep thawed zone below a water body (lake or river) in an area underlain by continuous permafrost (Johnston and Brown, 1966; Brown et al., 1964; Smith and Hwang, 1973).

Thus, the presence of proglacial lakes and channels suggests the decay or absence of permafrost in the sediments close to or below these water bodies that lie in front of the margin of the ice sheet. The transformation of the permafrost in front of the stagnant frozen snout into unfrozen sediments would decrease the resistance (passive earth pressure) of the subglacial strata against ice thrusting. This is shown by the requirement that a lesser amount of water pressure is needed to act against the potential failure surface under the stagnant frozen toe of a subpolar ice sheet without proglacial permafrost in order to allow glaciotectonic failure to occur (Chapter 9, Tables 9.2 and 9.3). As a result, all things being equal, ice thrusting would occur more often when the marginal area of an ice sheet rests on a slope inclined upglacier toward the glacier margin where proglacial water bodies could be impounded, for example, the Escarpment and Valley Types glaciotectonic facies, than on a plain such as the Plains Type glaciotectonic facies or on a slope inclined downglacier away from the glacier margin

(Appendix I).

9. MODELS OF ICE THRUSTING

9.1 Introduction

In this Chapter, the thermal conditions and the surface profile of the late Pleistocene ice sheet that glaciated the study region will be reviewed. Based on this glaciological description of the ice sheet which was responsible for ice thrusting, and the geological and geotechnical characteristics of the ice-thrust terrains as shown in the previous Chapters, models of the mechanics and the processes of glaciotectonism that occurred in the study areas will be proposed.

9.2 Thermal Conditions of the Late Pleistocene Ice Sheet in the Study Region

The snout of a subpolar ice sheet is thin and frozen to its underlying strata and can only move by internal deformaton, while behind the marginal area the glacier is relatively thick and thus warm-based, and the ice mainly moves by internal deformation and basal sliding (Hooke, 1977; Weertman, 1957, 1961). However, when the toe of a subpolar ice sheet has moved far away from its sources onto broad lowland, it may also become stagnant due to: (1) overloading of the glacier with englacial debris which would reduce the plasticity of the ice (Flint, 1942), and/or (2) critically thinned to the thickness that internal creep is negligible because of the decrease in ice supply from the accumulation area and/or an increase in ablation rate due to ameliorating climatic conditions (Embleton and King, 1975). Indeed, field studies indicate that some subpolar glaciers (ice caps and valley glaciers) consist of an outer marginal stagnant zone with basal temperature below melting point and an inner internal active zone with basal temperature at melting point (Weertman, 1961; Schytt, 1969).

The stagnant snout of a subpolar glacier would become a barrier and be compressed by the ice moving from the internal active zone. This would cause shear planes to form, inclined upglacier, near the boundary between the stagnant and active zones, and subglacial debris in the latter would be transported along these shear planes to the surface of the former (Bishop, 1957, fig. 33; Nye, 1952a; Swinzow, 1962; Souchez, 1967). Because of this, supraglacial and englacial debris should be abundant in the marginal area of a subpolar glacier, and it has been suggested that the retreat of the ice would chiefly deposit flow till, meltout till, and supraglacial outwash, forming kame moraines and other dead-ice disintegration features such as moraine plateaux and hummocky moraines on the ground (Boulton and Paul, 1976, fig. 5; Embleton and King, 1975).

It is noted that the ice-thrust terrains studied are mainly covered by dead-ice disintegration features such as hummocky disintegration moraines and/or outwash (Chapter 4; Appendixes C and I) and the marginal profile of the ice sheet that covered the study region seems to be so low and thin that movement near the toe of the glacier was probably small or negligible (Mathews, 1974). Thus, it is inferred that the late ice sheet that retreated to the study areas is a subpolar type glacier and its margin that was located at or near the areas studied was probably cold-based and stagnant.

9.3 Mechanics of Glaciotectonism

9.3.1 Introduction

The thermal conditions of the late ice sheet that glaciated the study areas suggest that the marginal area of the glacier, which was frozen and stagnant, acted as an ice-dam and resisted the ice that flowed from the active and warm-based portion of the glacier, causing the latter to thicken gradually as it accumulated ice from further upstream. The magnitude of the compression within the stagnant snout and its underlying sediments would have continued to increase as the ice thickened upstream. When the subglacial shear stress due to this compression exceeded the shear strength of the subglacial strata that underlaid the marginal stagnant area, ice thrusting occurred.

The proposed mechanics of glaciotectonism is analogous to the failure mechanism of a retaining wall. In this case, the stagnant frozen toe of a subpolar glacier would be treated as a gravity structure. Accordingly, stability analysis can be performed on the stagnant frozen snout under particular geological, hydrogeological, and glaciological conditions. By examining the factors in these conditions such as the magnitude of water pressure and accumulated ice thickness behind the stagnant snout that will lead to the failure of the toe in the analysis, the relative importance of these conditions and their contributions to the instability of the toe and thus the mechanics of ice thrusting will become obvious.

To do this, the ice surface profile and the thermal conditions of the ground near the snout of the subpolar glacier, the configuration of the failure surface due to ice thrusting, the strength properties of the subglacial sediments and the types and magnitude of the forces on the stagnant toe that cause failure need to be known and these will be shown in the following sections.

9.3.2 Ice Surface Profile and Permafrost

Theoretical and field evidence indicate that the marginal axial profile of a continental ice sheet that flowed onto a gently sloped, broad surface (for example, the topographic surface in central and southern Alberta) can be expressed approximately by a parabola (Mathews, 1974; Paterson, 1981):

$$H = P \cdot x^{1/2} \quad \ldots\ldots\ldots\ldots\ldots\ldots\ldots\ldots\ldots \quad (9.1)$$ where

H = height of ice surface above its terminus,

P = coefficient of glacier profile,

x = distance upglacier from the terminus.

It needs to be noted that the slope of the suface profile is not vertical at the edge so equation 9.1 cannot be applied there.

Field investigations suggest that the marginal profile of the Pleistocene Laurentide ice sheet in central and southern Alberta had a P value of about 0.3 to 1.0 (Mathews, 1974).

Assuming the ice sheet is in a thermal steady state condition, the glacier basal temperature can be estimated by the heat transfer equation (Harlan and Nixon, 1978):

$$Q = k \, . \, \Delta T / \Delta h \, . \, A \quad \text{..............} \quad (9.2)$$ where

Q = heat flow per unit time,

k = thermal conductivity of a material,

T = temperature,

h = thickness or distance,

A = area.

$\Delta T / \Delta h$ = temperature gradient

The geothermal heat flow in central Alberta is about 0.0016 mcal cm^{-2} sec^{-1} , and the thermal conductivity of the ice sheet and the surficial sediments is about 5.2 mcal cm^{-1} sec^{-1} °C^{-1} and 4.8 mcal cm^{-1} sec^{-1} °C^{-1} respectively (Judge, 1973; Garland and Lennox, 1962; Paterson, 1981; Harlan and Nixon, 1978, table 3.3). Substituting these values into equation 9.2, the resulting thermal gradient of the ice sheet is about 0.031 °C/ m and for the sediments in the region is about 0.033 °C/ m.

Assuming the retreating late ice sheet in the region had a P value of 1.0 and rested on a ground surface that can be approximated as a horizontal plane as observed in the Plains Type glaciotectonic facies (Appendix I, Figures I.9 and I.10) and under an annual air temperature of -1 °C, the marginal surface profile of the glacier and the proglacial and subglacial permafrost distribution can be calculated based on equation 9.1 and the estimated thermal gradient. The estimated profile of the glacier before failure or ice thrusting and the thermal conditions of the underlying subglacial sediments are shown in Figure 9.1. The boundary between the cold-based ice and warm-based ice is located at the point where the bottom of the permafrost reaches the ground surface. In the following analyses, this boundary will be approximated as a vertical plane in order to simplify calculations. This simplification is justifiable because field observation on the shear moraines in northwest Greenland suggests that the contact between the outer stagnant zone and the inner mobile zone of the ice inclines upglacier between 45° - 90° with a mean dip of approximately

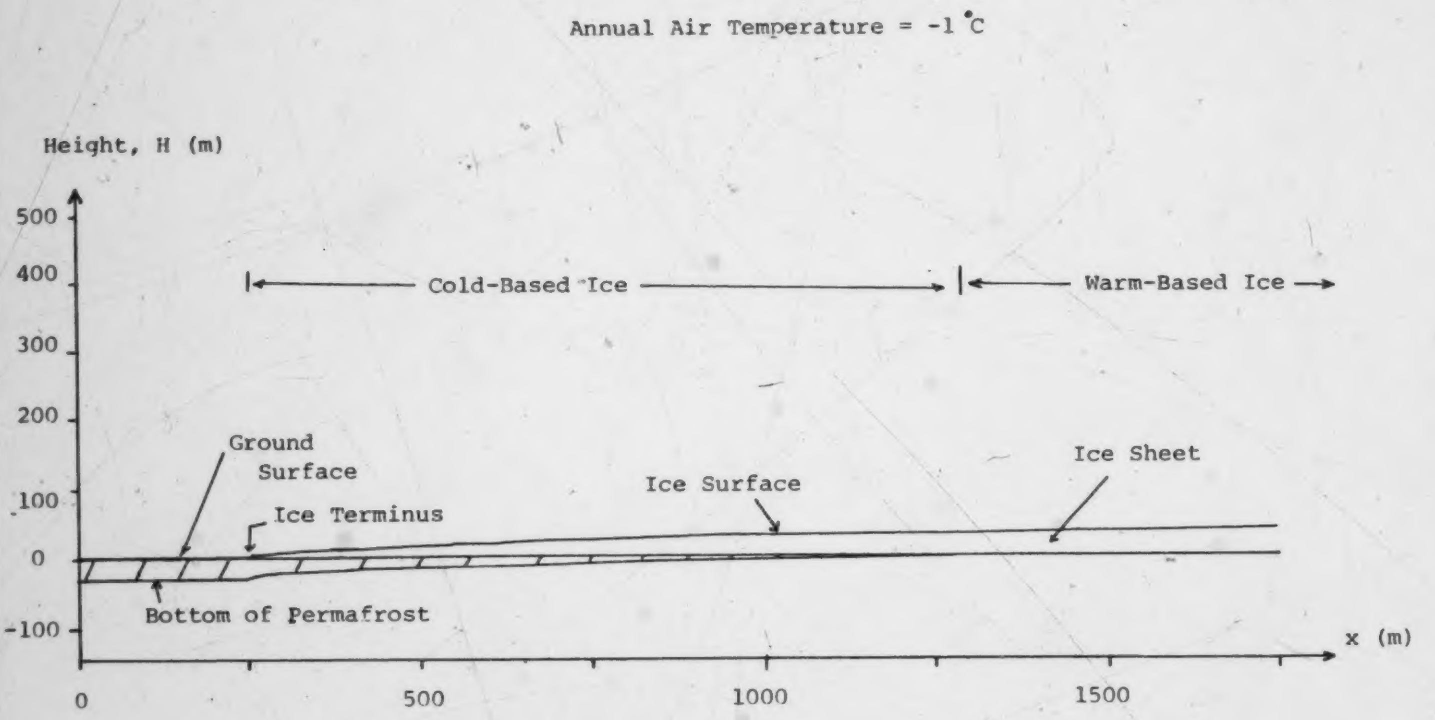

Figure 9.1 : Surface Profile of the Glacier and Thermal Conditions of the Subglacial Sediments

80° with respect to the horizontal (Bishop, 1957).

9.3.3 Geometry of a Glaciotectonic Rupture Surface

The major portion of a glaciotectonic rupture surface should be essentially flat-lying and located within a weak and fine-grained stratum. This inference is based on the observed horizontal shear zone in an ice-thrust terrain studied which was composed of bentonitic mudstone and bentonite layers (Figures 5.2 and 5.3; Chapter 6). It is also believed that that portion of the glaciotectonic rupture surface is probably where the bottom of the permafrost was located during ice thrusting. This is because although the shear strength along frozen/thawed interfaces seem to be higher than unfrozen sediments (Thomson and Lobacz, 1973; Tong, 1983), the shear strength at the failure plane can be significiantly decreased when it coincides with a frozen/thawed interface due to the following processes:

1. Decay of permafrost due to ameliorated climatic conditions and/or increase in the thickness of ice cover due to a glacier advanced over an area with pre-existing permafrost would cause thaw consolidation along the frozen/thawed interface. As a result, high pore water pressure will develop along the bottom of the permafrost if the adjacent strata have a relatively low permeability.
2. The development of permafrost in the marginal area of the ice sheet may block the drainage of the aquifer that

underlies the snout and cause the water table to rise into the temperate portion of the ice sheet behind the marginal area of the glacier. Thus, the hydrostatic pressure at the base of the permafrost will be increased.

The above processes could increase the water pressure at the bottom of the permafrost and thus reduce the shear strength along this frozen/thawed interface.

Subsurface investigations on the glaciotectonic deformations by the author (Figure 5.2) and other workers in other ice-thrust terrains (Kupsch, 1962; Wateren, 1981; Slater, 1927a) indicate that the downglacier ends of glaciotectonic rupture planes tend to join the ground surface by thrust faults with an inclination (θ) of about 20° - 40° with respect to the horizontal, which seem to agree with the inclination of fracture planes ($\theta = 45 - \phi / 2$) formed due to passive earth pressure failure. The upglacier ends of glaciotectonic rupture planes are probably vertical to steeply inclined with respect to the horizontal. This is inferred from the scar structures observed in Lowden Lake area (Figure 5.5) and in other ice-thrust terrains (Lessig and Rice, 1962).

To summarize, the major portion of a glaciotectonic failure surface is flat-lying and located within a weak, fine-grained and horizontal stratum and probably coincides with the base of permafrost during ice thrusting. The downglacier end of the rupture surface joins with the ground surface by a thrust fault with an inclination of about 30° with respect to the horizontal. The upglacier end of the rupture surface is assumed to be a vertical fracture plane that extends upward to the ground surface and joins with the vertical boundary of the warm-based and cold-based portion of the ice sheet.

9.3.4 Strength Properties

The materials that are involved in glaciotectonism can be broadly classified into three main types according to their properties and thermal conditions: (1) ice, (2) frozen sediments, and (3) thawed or unfrozen sediments. The strength properties of these materials are briefly described as follows.

1. Ice

   The ice sheet is mainly made up of polycrystalline ice with randomly oriented and equiaxial ice crystals (Michel, 1978) which will creep or flow under load. Field observations, laboratory work, and theoretical considerations show that it is a reasonable approximation to regard glacier ice under the rates of deformation (< 0.1 year^{-1}) observed in modern ice sheets and glaciers as a perfectly plastic material with a yield stress in shear of about 100 kPa (Nye, 1952a, 1952b; Orvig, 1953; Paterson, 1981; Glen, 1952).

2. Frozen Sediments

The strength of frozen sediments are influenced by the presence and amount of unfrozen water, ice content and its distribution, grain size and shape, strain rate, temperature, and density (Anderson and Morgenstern, 1973). However, laboratory work seem to suggest that the long term ultimate creep strength of a dense frozen sand is a function of the effective frictional strength of the sediments in an unfrozen state (Sayles, 1973). Moreover, laboratory investigations have shown that the shear strength for ice-poor, frozen, fine-grained sediments tested under low strain rate (1×10^{-4} cm/min) was essentially identical to the effective shear strength of the same sediments in a thawed or unfrozen state (Roggensack and Morgenstern, 1978). Thus, if the frozen sediments (such as sandstone and mudstone) deformed by ice thrusting were ice-poor, it seems to be reasonable to suggest that they would have an unfrozen shear strength during ice thrusting. This is because glaciotectonism is thought to be caused by deformation of the subglacial sediments due to ice flow which is a slow process.

3. Unfrozen and Thawed Sediments

The surficial bedrock in central and southern Alberta, which have undergone cycles of loading and unloading, permafrost, and weathering, are believed to have a strength below peak. The properties of some of the unfrozen sediments in the study region are shown in

Chapter 7.

In the following stability analysis, the frozen materials along the glaciotectonic rupture surface are assumed to be ice-poor and have a shear strength as they are in an unfrozen state during glaciotectonic deformation.

9.3.5 Stability Analysis

To simplify the analysis, let the permafrost below the stagnant toe of the subpolar ice sheet, instead of decreasing in thickness gradually upglacier (Figure 9.1), have a constant thickness and end at the boundary between the cold-based and warm-based portions of the glacier. As a result, the geometry of the glacier toe that acts as a retaining structure, which failed during ice thrusting, is outlined by the portion of the ice profile above the frozen sediments, the boundary between the cold-based and warm-based ice, and the configuration of the glaciotectonic rupture surface (the downglacier inclined portion of the rupture surface is replaced by a vertical plane at the terminus instead) described in Section 9.3.3 (Figures 9.2, 9.3 and 9.4).

This glacier toe, which is composed of two halves with glacier ice occupying the upper half and frozen sediments occupying the lower half, is considered to be stagnant and to behave as a rigid retaining structure during ice thrusting. This is because:

1. The stagnant snout of an ice sheet, which is probably

overloaded with englacial and supraglacial debris as discussed in the previous paragraphs, can be regarded as a very dirty ice or ice-rich frozen soil. The classification of frozen soils follows Weaver (1979). Laboratory work on very dirty ice (ice containing dispersed fine sand) and ice-rich fine-grained sediments suggest that the materials have a steady-state creep rate lower than that of polycrystalline ice at comparable temperature and stresses (Savigny and Morgenstern, 1986; Hooke et al., 1972). Since the compression applies to the glacier toe due to ice which flowed from upstream is presumed to be at or below the yield stress of ice; as a result, the creep of the stagnant toe due to this external compression is regarded as very small.

2. The ice and its underlying frozen sediments are bonded together. This is because an ice/rock interface tends to have an adhesion strength stronger than the friction of ice (Tabor and Walker, 1970).

This glacier toe which failed due to ice thrusting will be called the stagnant frozen block in the following paragraphs.

In the following sections, stability analyses are performed on the stagnant frozen toe of a subpolar ice sheet that retreated to a Plains Type glaciotectonic facies and an Escarpment/Valley Type glaciotectonic facies. Although the

Plains Type glaciotectonic facies is less common in the region studied (Chapter 8), it is analyzed first here because the mechanics that causes ice thrusting in this facies is more generalized than the one that initiates glaciotectonic deformation in other facies. Thus, as shown below, the study of the former would be easier to describe and interpret than the latter.

9.3.5.1 Plains Type Glaciotectonic Facies

Figure 9.2 indicates the configuration of the stagnant frozen block, the groundwater conditions, the glaciotectonic rupture surface, and the profile of the warm-based portion of a subpolar ice sheet with proglacial permafrost in a Plains Type glaciotectonic facies during ice thrusting. Figure 9.3a is a free-body diagram which shows the resisting and activating forces on the stagnant frozen block. The stagnant frozen block is chosen to be 1 m in width and 400 m in length. The latter dimension is based on the length of the shear zone deduced from a subsurface investigation in an ice-thrust terrain (Chapter 5). The top surface of the block was drawn based on equation 9.1 with a P value equal to 1.0. The properties of the rigid block are shown in Table 9.1.

The ice mass at the upglacier face of the stagnant frozen block is compressed by the ice flowing from the warm-based portion of the glacier (Figure 9.2). The compression due to this glacier flow (Fi) is estimated

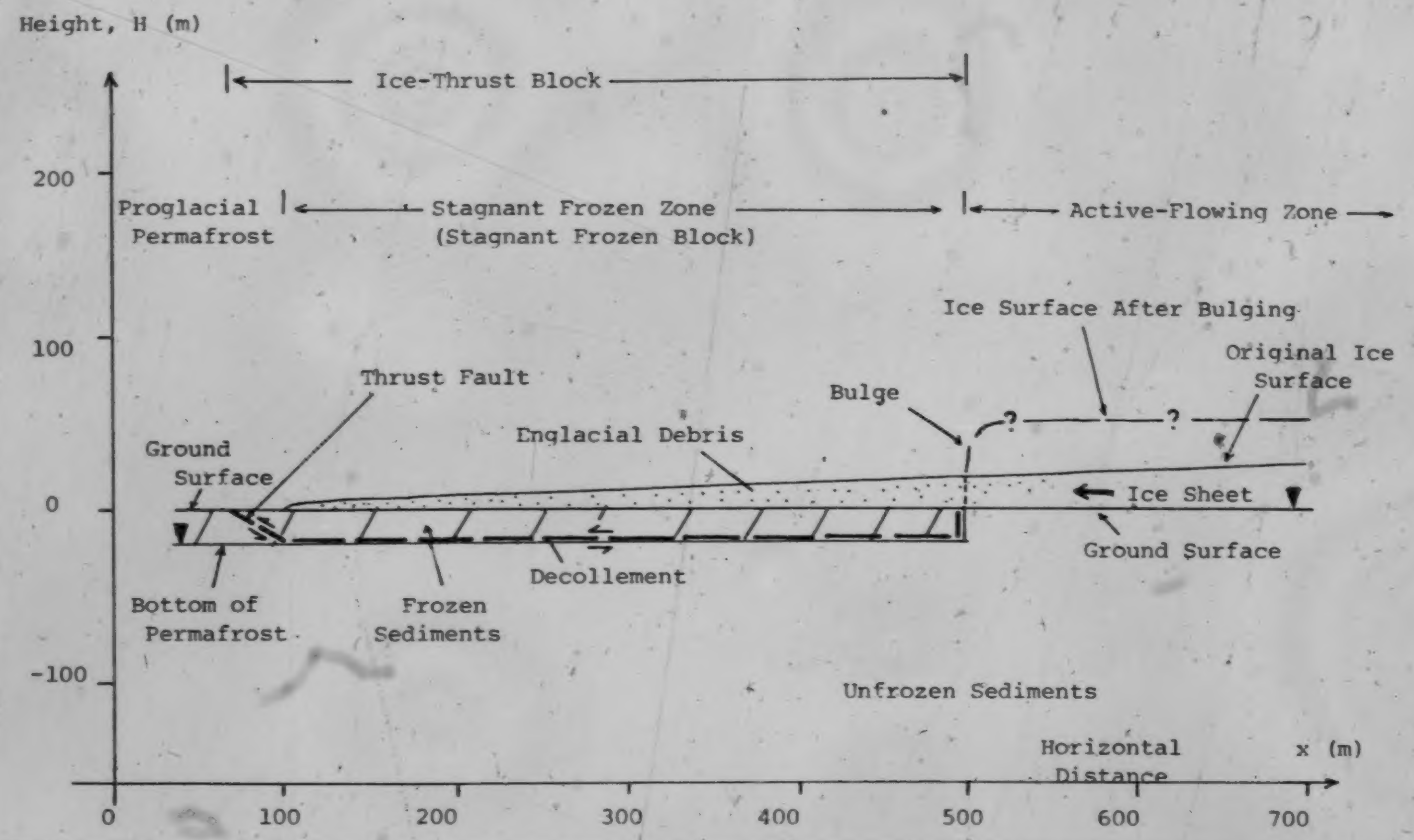
Height, H (m)
Ice-Thrust Block
200
100
0
-100
Proglacial Permafrost
Stagnant Frozen Zone (Stagnant Frozen Block)
Active-Flowing Zone
Ice Surface After Bulging
Original Ice Surface
Thrust Fault
Bulge
?
?
Englacial Debris
Ground Surface
Ice Sheet
Ground Surface
Decollement
Bottom of Permafrost
Frozen Sediments
Unfrozen Sediments
Horizontal Distance
x (m)
0
100
200
300
400
500
600
700

Figure 9.2 : Glaciotectonic Conditions of the Marginal Stagnant Area of a Subpolar Ice Sheet, Plains Type Glaciotectonic Facies

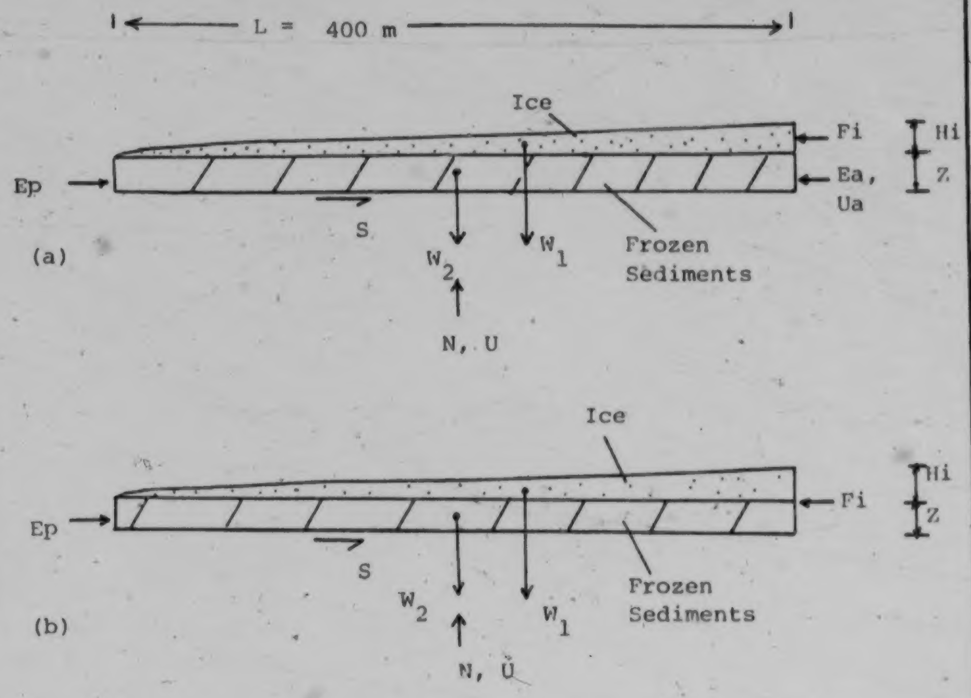
L = 400 m
Ice
Fi
Hi
Z
Ep
Ea,
Ua
S
(a)
W2
W1
Frozen Sediments
N, U
Ice
Hi
Fi
Z
Ep
S
W2
W1
(b)
Frozen Sediments
N, U

W_1= Weight of Stagnant Glacier Toe
W_2= Weight of Frozen Sediments
Ea= Compressive Force due to Active Earth Pressure
Ep= Resisting Force due to Passive Earth Pressure
Fi= Compressive Force due to Glacier Flow
Ua= Hydrostatic Force
N = Normal Force
U = Hydrostatic Force
S = Shear Resistance Force

L = Length of the Stagnant Frozen Block
Hi= Maximum Height of the Block Above the Ground Surface
Z = Depth of Permafrost or the Base of the Block Below Ground Surface

Figure 9.3 Free-Body Diagram: a - Plains Type Glaciotectonic Facies, b - Escarpment/Valley Type Glaciotectonic Facies

Table 9.1 Material Properties of the Frozen Toe Area of a Glacier

Material	γ_t KN/m³	c' (KPa)	ϕ' degree
Ice	8.9	100	0
Sandstone	21.0	0.0	30
Mudstone	20.0	0.0	11.5

to be about 200 kPa which would produce a maximum shear stress equal to the yield stress of glacier ice.

The frozen sediments at the upglacier face of the block are under hydrostatic pressure and active earth pressure during ice thrusting. The latter is a function of the thickness of the overlying active-flowing ice and the subglacial sediments behind the block and above the failure surface. The thickness of the active-flowing ice behind the block may increase or bulge because the block has acted as an ice dam that obstructs ice flow from upstream.

The maximum vertical height to which a bulge can grow behind the stagnant frozen block is about 30 m above the original ice surface of the warm-based portion of the glacier. A wave-like bulge developed near the boundary between warm-based (upglacier) ice and cold-based (downglacier) ice which has a height of about 25 m above the pre-swelling ice surface has been observed in a subpolar glacier in Yukon (Clarke et al., 1984).

The frozen sediments at the downglacier face of the block are under passive earth pressure during ice thrusting which is a function of the thickness of the sediments above the failure surface.

The total active earth pressure (Ea) and passive earth pressure (Ep) on the subglacial frozen strata of the block are calculated according to the following equations based on Rankine earth pressure theory (Terzaghi, 1943, p. 48):

$Ea = 1/2\ \gamma\ Z^2 \tan^2(45° - \phi/2) - 2\ C\ Z \tan(45° - \phi/2)$ .... (9.3)

$Ep = 1/2\ \gamma\ Z^2 \tan^2(45° + \phi/2) + 2\ C\ Z \tan(45° + \phi/2)$ .... (9.4) where

γ = unit weight of soil mass,

Z = depth between the ground surface and the potential rupture surface (in this case, the depth of permafrost),

ϕ = angle of internal friction,

C = cohesion.

During ice thrusting, the effective shear resistance along the base of the stagnant frozen block can be estimated by the following equation:

$\tau' = c' + (\sigma_n - u) \tan \phi'$ ....(9.5) where

c' = effective cohesion,

σ_n = total normal stress,

u = pore water pressure,

ϕ' = effective angle of internal friction.

By varying the height of the bulge (Hb) between 0 and 30 m, and the constant thickness of the permafrost (Z), that is, the depth of the glaciotectonic rupture surface, between 0 - 20 m, the water pressure needed to cause failure of the stagnant frozen block under the corresponding activating and resisting forces (Figure 9.3) is calculated by a limit equilibrium method. Both the factor of safety against sliding and overturning are shown. The results of the analyses are summarized in Table 9.2. Table 9.3 indicates the results of the stability analyses on a stagnant frozen toe without proglacial permafrost.

The stability analyses indicate that the failure of the stagnant frozen toe of a subpolar ice sheet in a Plains Type glaciotectonic facies is mainly governed by (Table 9.2):

1. The magnitude of the water pressure that acts against the potential failure plane, which has been expressed as the height of pressure head (hp) above the failure surface in the analyses (Table 9.2). The results indicate that failure of the stagnant frozen block always occurs when high water pressure has developed at the failure plane. This is shown by the analytical requirement that the water pressure head at the bottom of the stagnant frozen block during failure be above the ground surface.

Table 9.2 Results of Stability Analysis on Glacier Stagnant Toe with Proglacial Permafrost, Plains Glaciotectonic Facies

Z (m)	Hi (m)	Hb (m)	hp (m)	hg (m)	F.S.S	F.S.O
10	20	0	30.9	20.9	1.00	1.00
10	20	10	30.5	20.5	1.00	1.02
10	20	20	30.2	20.2	1.00	1.03
10	20	30	29.8	19.8	1.00	1.05
5	20	0	18.2	13.2	1.00	1.12
5	20	10	18.1	13.1	1.00	1.13
5	20	20	17.9	12.9	1.00	1.15
5	20	30	17.7	12.7	1.00	1.16
15	20	30	43.4	28.4	1.00	0.97
20	20	30	54.9	34.9	1.31	0.96

Z = depth of permafrost below ground surface

Hi = height of ice surface above ground surface

Hb = height of bulge

hp= pressure head above bottom of permafrost

hg = pressure head above ground surface

F.S.S = factor of safety against sliding

F.S.O = factor of safety against overturning

Table 9.3 Results of Stability Analysis on Glacier Stagnant Toe without Proglacial Permafrost, Plains Glaciotectonic Facies

Z (m)	Hi (m)	Hb (m)	hp (m)	hg (m)	F.S.S	F.S.O
10	20	0	29.6	19.6	1.00	1.00
10	20	10	29.3	19.3	1.00	1.02
10	20	20	28.9	18.9	1.00	1.03
10	20	30	28.5	18.5	1.00	1.05

Z = depth of permafrost below ground surface

Hi = height of ice surface above ground surface

Hb = height of bulge

hp= pressure head above bottom of permafrost

hg = pressure head above ground surface

F.S.S = factor of safety against sliding

F.S.O = factor of safety against overturning

2. The depth of the potential failure plane which is believed to coincide with the bottom of the permafrost and/or the depth of a weak impermeable layer. For example, when the depth of the potential failure plane (without bulging behind the block) increased from 5 m to 10 m, the height of water pressure head above the failure plane must rise from 18.2 m to 30.9 m in order for sliding failure to occur. Thus, when the depth of the potential failure surface increases, an abnormally high water pressure acting against the failure plane is needed for instability to occur. Moreover, failure of the stagnant frozen block due to overturning is more likely to occur than sliding as the depth of the failure plane increases.
3. The thickness of the bulge that grows at the boundary of the stagnant frozen block and the warm-based ice. For example, when the depth of the potential failure failure is 10 m below the ground surface, the water pressure at the plane required to cause failure is reduced (as shown by the pressure head which dropped from 30.9 m to 29.8 m with respect to the failure surface) when a bulge behind the stagnant frozen block has grown from 0 to 30 m high above the original ice surface.
4. The decay of proglacial permafrost (due to the presence of proglacial water bodies) would

facilitate glaciotectonic deformation as noted by the lesser amount of water pressure needed to act against the potential rupture surface to cause failure of the stagnant frozen block (compare Tables 9.2 and 9.3).

9.3.5.2 Escarpment/Valley Type Glaciotectonic Facies

The configuration of the stagnant frozen block, the groundwater conditions, the glaciotectonic rupture surface, and the profile of a subpolar ice sheet with proglacial permafrost in an Escarpment/Valley Type glaciotectonic facies during ice thrusting is shown in Figure 9.4. In this analysis, the inclined slopes or valley walls observed in these facies (Chapter 8; Appendix I) are modelled as a vertical face joined by a horizontal plane at its ends (Figure 9.4). Figure 9.3b is a free-body diagram which indicates the resisting and activating forces on the stagnant frozen block. The profile, material properties, and the dimensions of the block are similar to the one described in previous section.

The entire upglacier face of the stagnant frozen block is compressed by the ice flowing from the warm-based portion of the ice. As discussed in earlier sections, the compression due to this glacier flow (Fi) is about 200 kPa. The frozen sediments at the downglacier face of the block are under passive earth pressure during ice thrusting, which is dependent on the

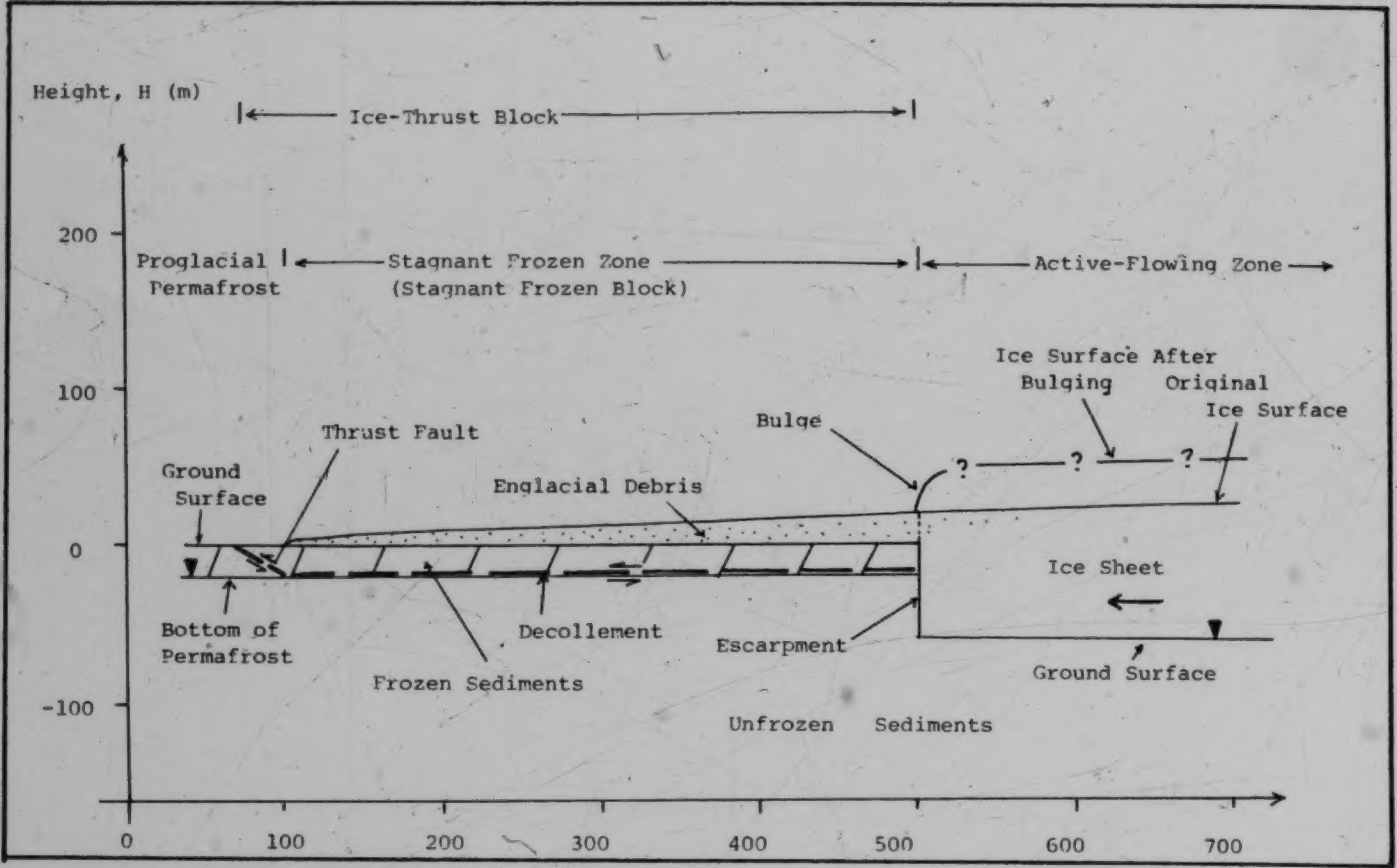
Height, H (m)
Ice-Thrust Block
200
100
0
-100
Proglacial Permafrost
Stagnant Frozen Zone (Stagnant Frozen Block)
Active-Flowing Zone
Ice Surface After Bulging
Original Ice Surface
Bulge
?
?
?
Thrust Fault
Ground Surface
Englacial Debris
Ice Sheet
Bottom of Permafrost
Decollement
Escarpment
Frozen Sediments
Ground Surface
Unfrozen Sediments
0
100
200
300
400
500
600
700

Figure 9.4 : Glaciotectonic Conditions of the Marginal Stagnant Area of a Subpolar Ice Sheet, Escarpment/Valley Type Glaciotectonic Facies

thickness of the sediments above the potential rupture surface. The total passive earth pressure in the frozen sediments and the effective shear resistance along the bottom of the stagnant block during ice thrusting are estimated according to equations 9.4 and 9.5.

By varying the depth of the glaciotectonic rupture surface between 0 - 20 m, the water pressure needed to cause failure of the stagnant frozen block under the corresponding activating and resisting forces (Figure 9.4) are calculated by a limit equilibrium method.

The results of the stability analyses show that (Table 9.4):

1. Sliding failure of the stagnant block would occur when the depth of the potential rupture surface is 10 m or less below the ground surface and is acted on by water pressure with a pressure head reaching from about the middle to the maximum height of the block.
2. When the depth of the potential rupture surface exceeds about 10 m, it is unlikely that the block will fail. This is because a water pressure with a magnitude close to the normal stress of the block is required to act against the rupture plane to cause failure.
3. Because the stagnant frozen block acts as an ice dam, the thickness of the active-flowing ice behind the block may increase or bulge. Due to the Poisson

Table 9.4 Results of Stability Analysis on Glacier Stagnant Toe with Proglacial Permafrost, Escarpment/Valley Glaciotectonic Facies

Z (m)	Hi (m)	Hb (m)	hp (m)	hg (m)	F.S.S	F.S.O
10	20	0	30.0	20.0	1.00	1.04
5	20	0	17.6	12.6	1.00	1.17
15	20	0	44.2	29.2	1.01	0.95

Z = depth of permafrost below ground surface

Hi = height of ice surface above ground surface

Hb = height of bulge

hp= pressure head above bottom of permafrost

hg = pressure head above ground surface

F.S.S = factor of safety against sliding

F.S.O = factor of safety against overturning

effect, the compression on the upglacier face of the block with a bulging ice surface behind should exceed the compressive stress due solely to the glacier flow. Although this effect has not been included in the analysis, it is obvious that relatively less water pressure is required to act along the rupture surface to cause failure when a bulge has developed behind the stagnant block.

To conclude, the most critical forces that trigger foundation instability of the marginal stagnant zone of a subpolar ice sheet and subsequently lead to ice thrusting probably are: (1) the increase of water pressure at the bottom of a potential failure surface, which is probably within a weak and impermeable layer and coincides with the bottom of the permafrost, brought about a significant reduction of the shear strength along the potential failure plane, (2) the decrease in the depth of the potential shear surface which causes a decrease of: (i) the passive earth pressure that resists the forward movement of the stagnant frozen block, and (ii) the normal load on the failure plane which results in a decreased shear strength, and (3) the growth in height of the ice surface (bulging) behind the stagnant zone that causes the increase in active earth pressure and/or ice compression (due to the Poisson effect) which pushes against the stagnant frozen toe.

9.4 Discussion

1. The field observations of the geological and glacial features in the ice-thrust terrains studied, the glaciological descriptions of the late ice sheet that glaciated the region, and the stability analyses performed above indicate that subglacial failure of the stagnant frozen toe of a retreating subpolar ice sheet is the most plausible cause of glaciotectonic deformation found in central and southern Alberta. Because of the scope of this thesis and the analyses presented above which show that the study areas were probably glaciated by a subpolar ice sheet; no investigation is performed on glaciotectonism due to ice sheets with different thermal regime such as temperate glaciers which also seem to be able to cause ice thrusting (Wateren, 1985).
2. In the stability analyses, because the upglacier and downglacier vertical faces of the stagnant frozen block where the earth pressures act are located within soil mass, shearing stresses or wall friction are expected to develop along these vertical planes during ice thrusting and the mobilized angle of wall friction (δ) is probably equal to the angle of shear resistance (ϕ) of the soil mass. It is known that when $\delta = \phi$, the use of Rankine earth pressure theory would overestimate the active

earth pressure (Ea) and underestimate the passive earth pressure (Ep); moreover, the use of Coulomb's earth pressure theory is also inappropriate because it would overestimate the latter (Morgenstern and Eisenstein, 1970; Terzaghi, 1943). As a result, other methods such as the logarithmic spiral method which involve relatively complicated mathematics should be used in the analyses if it is desired to compute the earth pressure accurately.

However, because of certain factors involved in glaciotectonic deformation, such as the depth of permafrost, material properties, and ice thickness, are either unknowns or beyond our present knowledge, it does not seem necessary at this stage of research to use more complicated analytical techniques other than Rankine earth pressure theory to calculate the earth pressure that occurred in the sediments during ice thrusting.

3. At present, there is no universally accepted theory of the mechanics of a surge-type glacier (Paterson, 1981; Boulton and Jones, 1979) which usually alternates periodically between brief periods (usually 1 - 4 years) of very rapid flow or surge and longer period (usually 10 to 100 years) of near stagnation (Meier and Post, 1969; Post, 1969). However, the ice-thrust model presented in this thesis indicates that the compression of the stagnant frozen toe of a subpolar ice sheet by ice flowing from the warm-based portion of the glacier

may lead to shear failure in the subglacial strata near the snout of the glacier. The result is ice thrusting and probable collapse of the overlying ice and short-term rapid flow of the stagnant glacier front. This model seems to explain the cause of glacier surge in subpolar glaciers. A similar cause of glacier surge has been suggested by Flint (1971) and Wright (1971). Indeed, some surge-type subpolar valley glaciers are composed of a cold-based marginal area and a warm-based interior (Schytt, 1969; Clarke and Goodman, 1975; Goodman et al., 1975), and it has been observed that between surges, a bulge up to 25 m high had formed and thickened progressively at the boundary between the warm-based active-flowing ice and the cold-based stagnant ice of a subpolar glacier (Clarke et al., 1984, fig. 2).

9.5 Models of Ice Thrusting

Based on the field observations in the study areas and the mechanics of ice thrusting inferred from the investigation shown above, a model of glaciotectonism for Escarpment/Valley Type glaciotectonic facies is suggested below.

1. A subpolar ice sheet retreated to the slope of a preglacial valley or an escarpment underlain by permafrost. The snout of the glacier, which rested on the plain above the valley, was either far away from the

source or the ablation rate was high so that the frozen toe of the ice had thinned and finally became stagnant. Behind the marginal area, the ice, which remained within the valley, was thick and warm-based and moved forward by creep and basal sliding (Figure 9.5a). Thus, three thermal zones were developed at the base of the the retreating ice sheet as suggested by Clayton and Moran (1974), (a) a proglacial permafrost zone in front of the ice margin, (b) a frozen bed zone at the snout area, and (c) a thawed-bed zone behind the frozen toe.

2. The toe area, which was stagnant and frozen to its bed, had become an ice-dam which obstructed ice that flowed from the warm-based, active-flowing interior. As a result, ice accumulated and bulged up near the boundary between the warm-based and cold-based ice (Figure 9.5b). The ice-dam was compressed by the glacial flow from behind.

The compression of the stagnant snout might cause shear failure along a horizontal stratum with low shear strength that underlay the marginal stagnant zone. The shear strength of the weak layer might further be reduced significantly if it were located along the bottom of the permafrost where high water pressure had developed due to thaw consolidation in stratigraphic layers with low permeability or the presence of impermeable boundaries such as unconformities, stratigraphic pinch-outs, and confined aquifers under

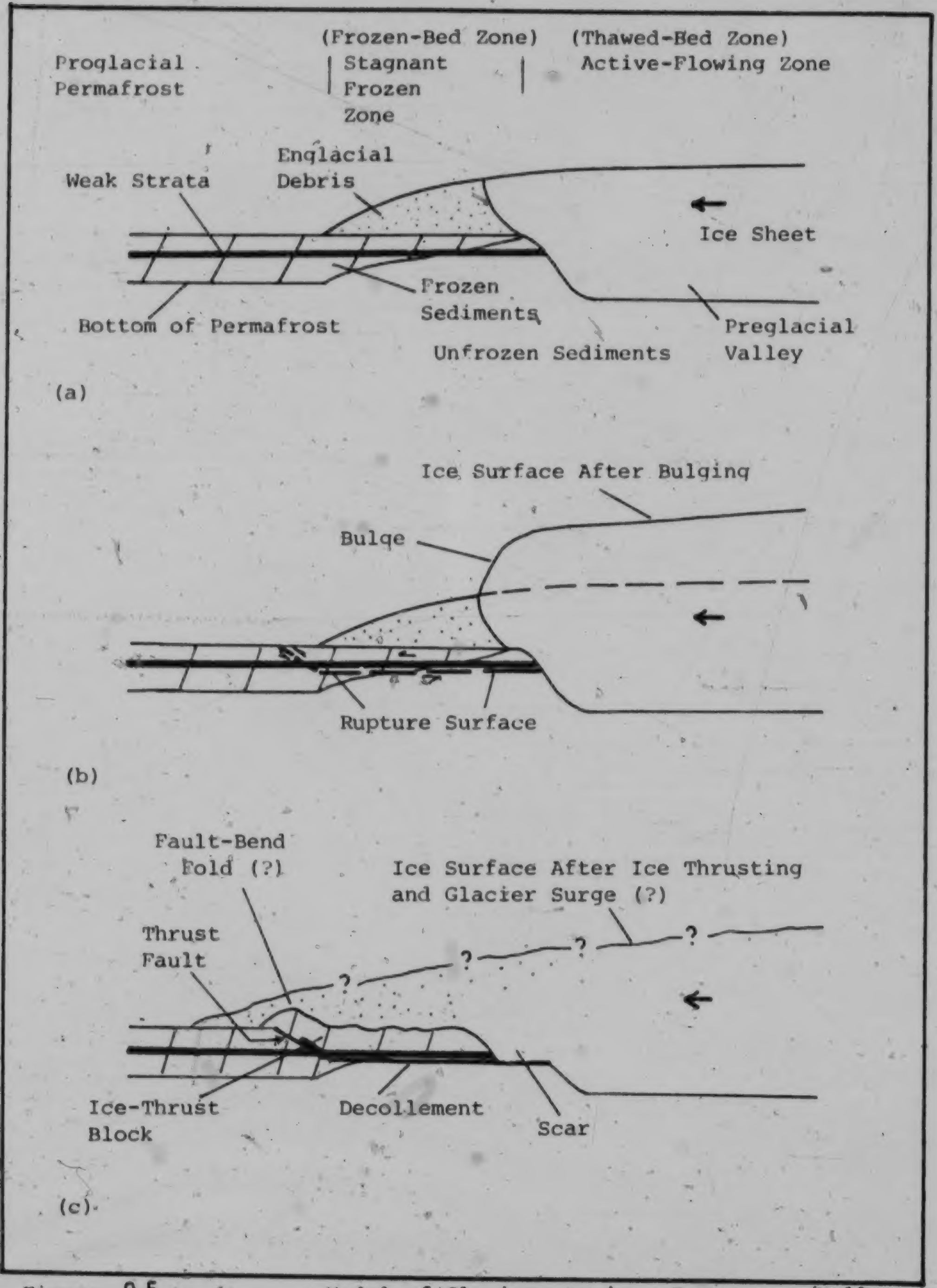
(Frozen-Bed Zone)
Stagnant
Frozen
Zone
(Thawed-Bed Zone)
Active-Flowing Zone
Proglacial
Permafrost
Englacial
Debris
Weak Strata
Ice Sheet
Frozen
Sediments
Bottom of Permafrost
Unfrozen Sediments
Preglacial
Valley
(a)
Ice Surface After Bulging
Bulge
Rupture Surface
(b)
Fault-Bend
Fold (?)
Ice Surface After Ice Thrusting
and Glacier Surge (?)
?
?
?
?
Thrust
Fault
Ice-Thrust
Block
Decollement
Scar
(c)

Figure 9.5 : Model of Glaciotectonism, Escarpment/Valley Glaciotectonic Facies
(The rupture surface is probably located within the weak strata.Due to drawing difficulty, it is drawn slightly below the strata)

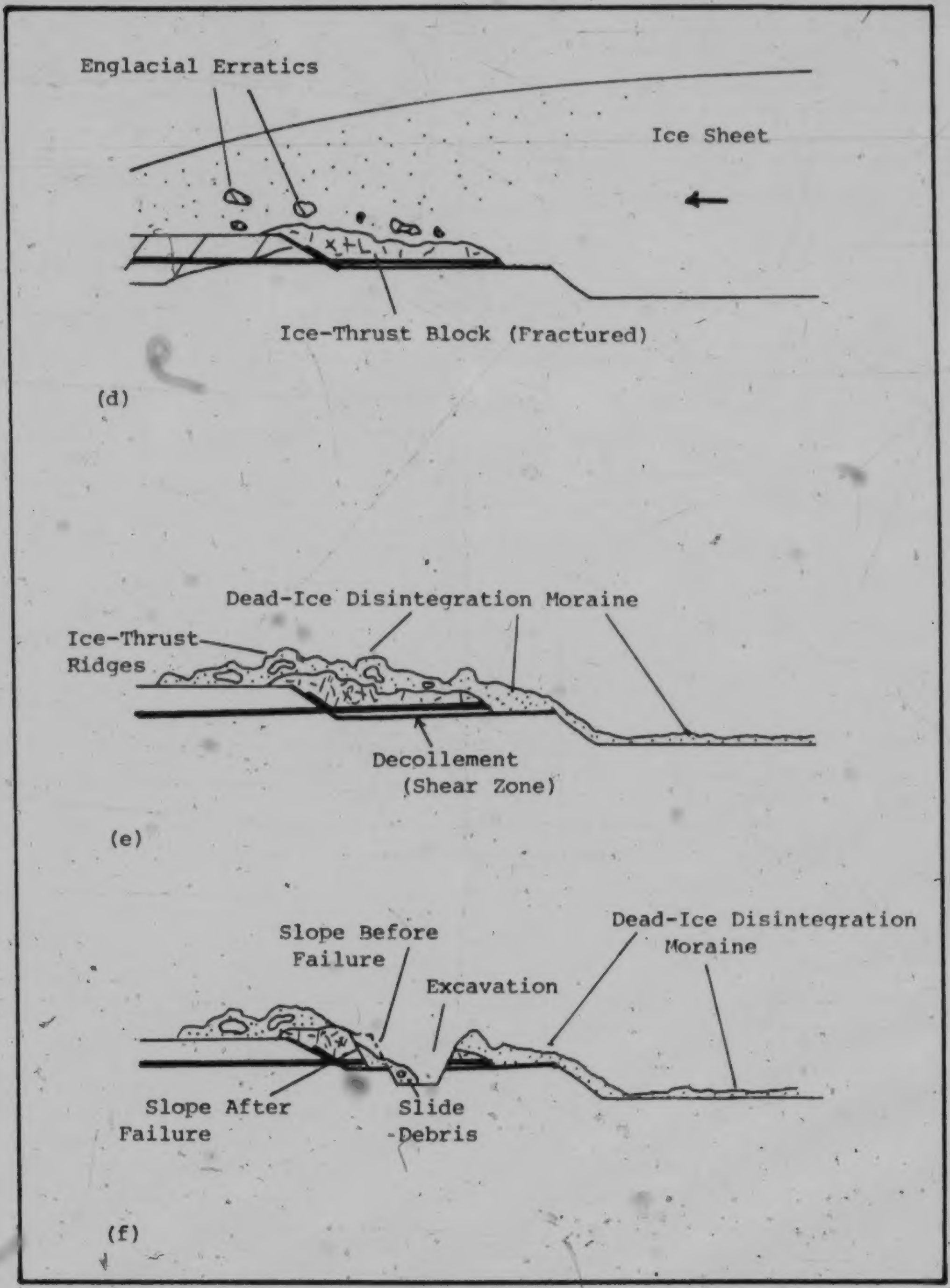
Englacial Erratics
Ice Sheet
Ice-Thrust Block (Fractured)
(d)
Dead-Ice Disintegration Moraine
Ice-Thrust Ridges
Decollement (Shear Zone)
(e)
Slope Before Failure
Excavation
Dead-Ice Disintegration Moraine
Slope After Failure
Slide Debris
(f)

Figure 9.5 (continued): Model of Glaciotectonism artesian conditions.

3. Subglacial failure might thrust the subglacial strata below the stagnant snout forward and/or upward into the foreland of the glacier along the weak layer that had been deformed into a shear zone or decollement and a thrust fault that joined the decollement and the ground surface. As a result, the thrust strata might be deformed into fault-bend folds and/or concentric folds which might express themselves as ice-thrust ridges or hills on the ground surface (Figure 9.5c). For example, the shear zone and concentric folds observed in Highvale mine (Chapter 5) and the ice-thrust ridges found in Lowden Lake area (Appendix C, Figures C.12 and C.18).

   The failure of the subglacial strata that underlay the marginal stagnant area might also cause the accumulated or bulged ice in the active-flowing area behind to collapse and flow rapidly forward. This might initiate a glacier surge.

4. If the climatic conditions remained unchanged, the failed toe of the ice would become stagnant shortly after ice thrusting and subsequently compressed by the active-flowing ice behind. This may lead to another episode of ice thrusting when both the ice thickness upglacier of the stagnant toe and the water pressure at the bottom of the potential failure surface had increased to a critical value. Successive cycles of ice thrusting in the terrain might be able to deform the

subglacial strata into horses or stacks of thrust blocks (Figure 5.7). (It is to be noted that glaciotectonism would not occur if the stagnant frozen area was underlain by strata that are strong and/or under low water pressure. Compression on the stagnant snout area due to increase in ice thickness caused by bulging and ice flow would eventually exceed the yield strength of the ice in the toe and cause the stagnant ice mass to rejuvenate and creep forward.)

5. If the glacier continued to advance after glaciotectonism, the thrust blocks would be overridden by the active-flowing portion of the ice sheet, and thus would be subjected to further subglacial deformation (Figure 9.5d). For instance, some of the fractured and deformed blocks might be plucked by the ice, and incorporated within the ice mass and transported englacially as erratics (Boulton, 1972, 1979; Broster et al., 1979).
6. Uneven distribution of compression of the stagnant snout during ice thrusting might also cause differential shear movement within the ice-thrust block. For example, the strike-slip fault observed in Lowden Lake area (Appendix C, Figure C.12).
7. Melting of the stagnant zone shortly after ice thrusting would deposit supraglacial and englacial sediments onto or near the ice-thrust features, forming dead-ice disintegration moraines (Figure 9.5e). For example, the

hummocky disintegration moraine terrain found in Isle Lake area (Appendix C, Figure C.10).

8. After the retreat of the glacier, the ice-thrust blocks that were lifted to the ground surface would become relaxation structures due to the release of confining pressure and the rotation of the direction of principal stresses (Rotnicki, 1976). As a result, ice-thrust hills and ridges, which were composed of brecciated and sheared sediments were further jointed and fractured, and normal faults and slope failures were likely to occur when these features are excavated (Figure 9.5f). For example, the highwall failure in Highvale mine, Wabamun Lake area (Appendix C, Figure C.6).

The model of glaciotectonism for Plains Type glaciotectonic facies is similar as the one discussed above. The main differences between the glaciotectonic models for Escarpment/Valley Type glaciotectonic facies and for Plains Type glaciotectonic facies are that for the latter, the ice sheet that caused ice thrusting rests on a relatively featureless plain and the stagnant glacier toe, which acts as an ice dam, is compressed by the glacier flow from behind, and the earth pressure in the subglacial sediments (Figure 9.2).

10. APPLICATIONS OF GLACIOTECTONICS

10.1 Geological Applications of Glaciotectonics

The ice-thrust features and ice-thrust terrains observed in the study areas indicate that ice thrusting is a common phenomenon in central and southern Alberta and probably in all recently glaciated sedimentary basins underlain by weakly cemented sediments in other parts of the world. The presence of these features and their associated deformation in an ice-thrust terrain have provided particular problems in geologic and geomorphic studies in a region.

In the following sections, the geologic applications of glaciotectonics will be described and examples will be given.

10.1.1 Ice Direction Indicator. Case Study: Lowden Lake and Beltz Lake Areas

10.1.1.1 Introduction

Many workers (Dellwig and Baldwin, 1965; Banham and Ranson, 1965; Konigsson and Linde, 1977; Hicock and Dreimanis, 1985) have shown that glaciotectonic structures are useful directional indicators of ice movement because axis of folds and strike of fractures and thrusts induced by the overriding ice usually trend perpendicular to the direction of the ice advance. It has been found that the ice movement direction derived from glaciotectonic structures is consistent with the till clast orientation, provenance evidence, and striae on boulders and thus the measurements of just a few ice directional indicators can provide an accurate measurement of ice-movement direction at a site. It has also been reported that, occasionally, the glaciotectonic structures may show a different sense of orientation in successive layers of sediments. This is an indication that the area has been recently glaciated either by different ice lobes coming from different directions or by a single ice lobe that has shifted its flow direction with time (Hicock and Dreimanis, 1985; Catto, 1984).

In the following sections, the author infers that the movement directions of the glacial ice in the study areas of Lowden Lake and Beltz Lake based mainly on the trends of the glaciotectonic structures such as ice-thrust ridges and giant grooves. The glacial features in these areas formed due to an earlier southeast-flowing glacier have been destroyed or severly modified by the most recent southwest-flowing glacial action.

10.1.1.2 Field Descriptions

Two sets of lineations or giant grooves are found in the Beltz Lake area (Appendix C, Figure C.19). Set II was observed at the northeastern shore of Beltz Lake, while Set I was located about 2 to 3.5 km east to southeast of the eastern shore of the Lake.

Set I is in general rectilinear; however, sometimes lineations curve and intersect at acute angles. Thiry-one measurements taken on the grooves of Set I appearing on the aerial photographs show an orientation ranging from 352° - 042° azimuth and having a traceable length of 0.03 - 3.7 km. Some of the grooves of Set I show a change of orientation from 005° azimuth to 010° azimuth and finally change back to 005° azimuth; and from 352° azimuth to 020° azimuth (Appendix C, Figure C.19). Set II has a length of 0.2 - 0.5 km and a range of orientation of 112° - 129° azimuth. The trend of Set I is nearly perpendicular to Set II. Figure 10.1 shows the frequency of giant grooves with respect to their orientation observed in the Beltz Lake area. A ground check was performed on the lineations or giant grooves observed on the aerial photos.

Although giant groove Set I was found over a large area, most of the land is farmed, leaving a small portion of the ~~area gr~~own with grass for grazing. Detailed examination indicated a gently rolling topography on that portion of the area covered with grass, and the presence of subtle NE-SW trending ridges with rounded crests and very gentle slopes (Plate 10.1). Measurement of two of these ridges show that they have a basal width in the order of 28 - 36 m, a trough width of about 54 m, an amplitude of 0.3 - 1.0 m and a wavelength

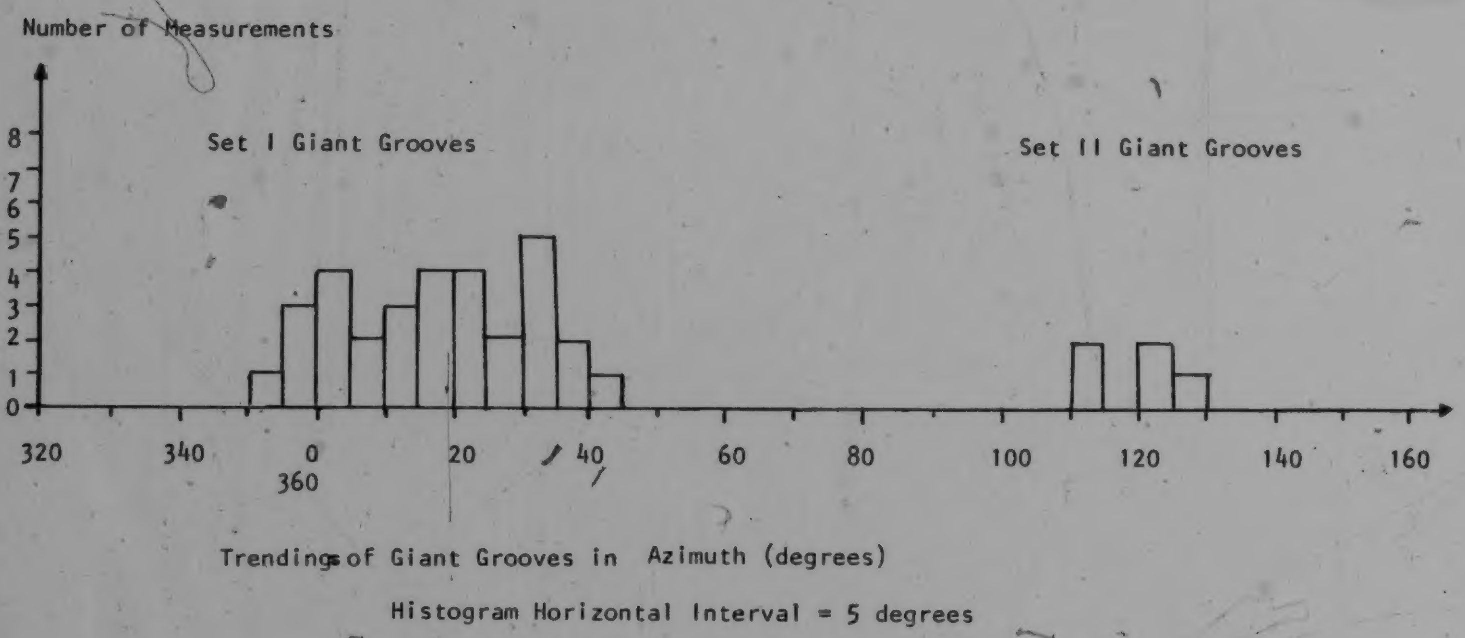

Figure 10.1 : Histogram that shows the Trending of Giant Grooves, Beltz Lake Area

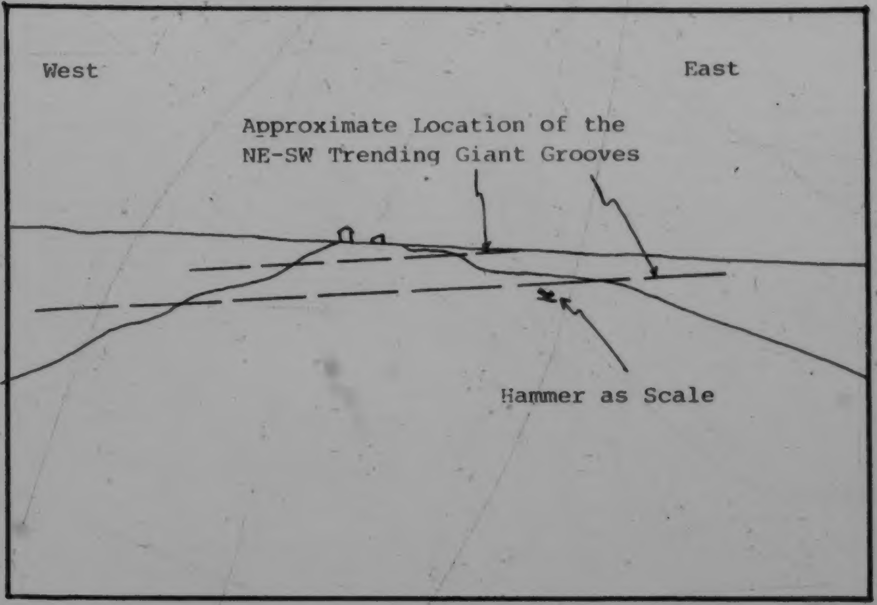
West
East
Approximate Location of the
NE-SW Trending Giant Grooves
Hammer as Scale

Plate 10.1 Set I NE-SW Trending Giant Grooves, Beltz Lake

of 82 - 90 m. These two ridges show a trend of about 018° and 022° azimuth on the ground; and on the aerial photograph, the giant grooves that appeared at approximately the same location as these two ridges also show a trend of about 020° azimuth (Appendix C, Figure C.19). However, at the northeastern shore of Beltz Lake, there are no features on the ground which indicate the presence of Set II giant grooves; the area where Set II giant grooves were observed on the aerial photos taken in 1962, has been ploughed and is covered with well-grown crops. The ploughing must have destroyed the subtle features in the soil which express the giant grooves on the ground surface.

10.1.1.3 Discussion

1. Field observation shows that the thickness of surficial deposits in the ice-thrust terrain in Beltz Lake area is up to 0.3 m (Stalker, 1960a, fig. 20) which indicates that most of the giant grooves found in the area are structures in the underlying bedrock reflecting through the thin surficial deposits. The author believes that they are subglacial erosional features incised in the bedrock mainly by glacial scouring rather than the joint sets of the weakly cemented argillaceous bedrock in the region. This is because the orientation of most of these giant grooves observed in the area studied do not agree with the trend of the regional joint

system, which consists of sets strike approximately 55° - 65°, 140° - 155°, 5°, and 95°, found in the late Cretaceous to Paleocene rocks in central and southern Alberta (Babcock, 1973, 1974).

2. The curving and intersecting of giant grooves in the study area is analogous to the phenomenon observed on glacial striae and is believed to be due to local shifts in the basal currents of the ice which formed striations that deviate up to 10° - 30° from the general trend and intersect other striae (Alden, 1918, p. 205). A change in the flow direction of the basal ice is not uncommon, for instance, layers of deformed preglacial and glacial sediments that show local ice-flow direction shifted more than 90° during one glacial advance has been noted by Catto (1984). A similar process is probably responsible for the formation of some of the giant grooves in the study area in which the trend of the grooves has deviations up to 50°. The reason for the shift of the ice direction may be either due to the change in the overall regional glacial movement pattern, or, as Alden (1918) suggested, that an earlier ice that invaded an area may be thicker and not as strongly influenced by local topography. Indeed, both the Beltz Lake and Lowden Lake are located in a depression that opened to the northeast (Farvolden, 1963a, fig. 14). Thus, if the later glacial ice was

thinner, its direction of movement would be more restricted by the local topography causing flow toward southwest.

3. Compared to other glacial grooves found on the Prairies which are glacial erosional features with conspicuous morphology (Mollard and Janes, 1984, plate 3.4), the giant grooves at the Beltz Lake area are faint and indistinct features appearing on aerial photographs and in the field. This is believed to be due to:
    a. the grooves in the study area were located in a gentle depression, which probably was once a glacial spillway (Appendix C, Figure C.19), and had been under intense glaciofluvial erosion.
    b. the weakly cemented bedrock is relatively less resistant to fluvial erosion in the area.
    c. the glacier that scoured the giant grooves was relatively thinner and its capacity for subglacial erosion was relatively weaker.
4. The giant grooves observed in the study area are comparable to the giant grooves and ridges found in the Interlake area of Manitoba which are believed to be due to glacial gouging of bedrock (Wardlaw et al., 1969). The giant grooves have a length which can be traced a km or more, a width of 15 - 152 m and are most conspicuous on aerial photos although they may vary from less than a metre to several km

wide, an amplitude of 0.3 - 2.4 m, and a wavelength of a few hundred metres which is common on aerial photos. In particular, Wardlaw et al (1969) noticed that these giant grooves and ridges which are distinct on aerial photographs are approximately parallel to the striations and small grooves found on the ground and nearly perpendicular to the trend of the axial planes of folds observed in the ice-thrust ridges which are composed mainly of gypsum and carbonates.

10.1.1.4 Analysis of the Direction of Ice Movement

Ice-flow markings (flutings, furrows, gouges, drumlinoidal forms) with trends of 201° to 234° are observed about 30 km northeast of Lowden Lake; however, ridges (rim ridges of ice block depressions and moraine plateaux, eskers; and ridges of undetermined origin) with a trend of 123° - 173° appear about 10 km southwest of the Lowden Lake area. Moreover, about 60 km northwest of the study areas, drumlins and ice-flow markings show trends of about 125° - 150° azimuth and ridges with a trend of 050° - 068° appear at about 28 km northwest of Lowden Lake (Stalker, 1960a, map 1081A). The glacial map of Canada also indicates northeast-trending and northwest-trending glacial lineations (including glacial flutings, drumlinoid ridges, drumlins, crag and tail hills) are present northeast and northwest of the Stettler region (Prest et al., 1968). Although the regional direction of the last ice movement in southwestern and central Alberta is southward or south-southeastward (Stalker, 1960a, p. 72); the glacial features found in the study area adjacent to the Lowden Lake and Beltz Lake areas show that the directions of the last glacial advance varied from northeast to northwest. The area probably has been recently glaciated by two ice lobes coming from the northeast and northwest.

The morphologic expressions and structural analysis of the ice-thrust features of the Lowden Lake and Beltz Lake areas have shown NW-SE and NE-SW trends respectively (Appendix C, Figures C.12, C.13, C.14, C.19, C.20, and C.21). However, at the eastern shore of Beltz Lake, the set of giant grooves (Set II) with 112° - 129° azimuth is found cutting perpendicularly through the NE-SW trending ice-thrust ridges; while another set of giant grooves (Set I) with 352° - 042° azimuth is also found about 2 - 3.5 km east to southeast of Set II (Appendix C, Figure C.19). Since these two sets of giant grooves are oriented nearly perpendicular to each other and are so close and with their orientation in a convergent sense, they are believed to be formed by a southwest-flowing and a southeast-flowing ice lobes that entered the area separately during the last glaciation. The sense of direction of these glacial features as based on the fact that the last ice that invaded

Alberta, the Keewatin Sector of the Laurentide Ice Sheet of the Late Wisconsinan, originated from the northeast with respect to the Stettler region (Prest, 1984, map 1584A; Fenton, 1984, p. 64). An earlier southeast-flowing ice lobe probably formed the NE-SW trending ice-thrust ridges and the NW-SE trending giant grooves near Beltz Lake; this was probably followed by a subsequent southwest-flowing ice lobe which formed the NW-SE trending ice-thrust ridges south of Lowden Lake and the NE-SW trending giant grooves east of Beltz Lake. The fact that the southeast-flowing ice lobe entered the study area prior to the southwest-flowing ice lobe is based on the following observations.

Giant grooves of Set I found east of Beltz Lake, which is inferred to be formed by the later southwest-flowing ice lobe, are relatively abundant, continuous (up to one km long), and distinct on aerial photographs (Appendix C. Figure C.19). However, Set II grooves, which are inferred to be formed by the earlier southeast-flowing ice lobe, are relatively fewer, shorter (less than half a km long) and diffuse on aerial photograph. Thus, Set I probably occurred later than Set II because the set of grooves that were formed by an earlier ice lobe must have been severely eroded by the later ice lobe or/and covered by its corresponding deposits. This is analogous to the two sets of glacial grooves with distinct and subdued topography respectively, which are believed to be formed by an earlier and a later ice lobe that flowed from two different directions, found in the flat-lying sedimentary strata of Lower Cretaceous age exposed along the escarpment slopes of the Cameron Hills (Mollard and Janes, 1984, plate 3.4).

The NW-SE trending ice-thrust ridges (which are inferred to be formed by the southwest-flowing ice lobe) found at Lowden Lake area (Appendix C, Figure C.12) are much steeper, ridged and curvilinear than those NE-SW trending ice-thrust ridges (which are inferred to be formed by the southeast-flowing ice lobe) found at Beltz Lake area which have a subdued and gentle relief (Appendix C, Figure C.19) suggesting that the former were formed later and have undergone a shorter period of subaerial and glacial erosion than the latter. An example of the NE-SW trending ice-thrust ridges with subdued relief and covered by subsequent glacial deposits is found at a roadcut along the Fritz Hill road, which is about 4.8 km southeast of the southern tip of Lowden Lake and 11 km southwest of the eastern shore of Beltz Lake. The exposures show an anticlinal structure with a fold axis which has a trend/plunge of 025°/ 6° NE. Aerial photograph interpretation indicates that this structure is located within an area covered by non-oriented knobs and kettles.

10.1.1.5 Glacial History

The presence of distinct and steeply-ridged NW-SE trending ice-thrust ridges south of Lowden Lake, the presence of NE-SW trending ice-thrust ridges covered by hummocky moraine or with a very subdued topography and two sets of giant grooves trending NE-SW and SW-NE at Beltz Lake area suggest the following glacial processes in these study areas:

1. A southeast-flowing ice lobe glaciated the region of the Beltz Lake area and the Lowden Lake area. NE-SW trending ice-thrust ridges were formed near the margin of this ice lobe when it was located near Beltz Lake and Lowden Lake. After the formation of these ridges, the ice lobe continued to move southeast due to rejuvenation and overrode and grooved some of these ridges (Appendix C, Figure C.19).
2. Later, this southeast-flowing ice lobe either deviated to the southwest or retreated from the area and a southwest-flowing ice lobe entered the study area later. The final advance of this ice lobe overrode the ice-thrust features and significiantly subdued the ice-thrust features formed by the earlier glacier in the study areas.
3. Finally, the margin of the ice lobe was located near Lowden Lake where ice thrusting occurred and formed ice-thrust features on the surface. Ice thrusting

occurred at or near the margin of this ice lobe, while further behind the snout the ice continued to flow and NE-SW trending giant grooves were formed, for example, near the Beltz Lake area (Appendix C, Figure C.19).

4. Subsequent stagnation and disintegration of this southwest-flowing ice lobe has deposited dead-ice features on top or between the ice-thrust ridges formed by this southwest-flowing ice lobe and the southeast-flowing ice lobe. The topography of the distinct and steeply-ridged NW-SE trending ice-thrust ridges have been masked by these disintegration features but still appear as characteristic linear to curvilinear ridges on aerial photographs (Appendix C, Figure C.12). The older and gentler NE-SW trending ice-thrust ridges, which have undergone a relatively longer period of subglacial and subaerial erosion, are further covered by the disintegration moraines deposited by this southwest-flowing glacier. At present, these gentle ridges are hardly recognizable on aerial photographs unless the surficial cover has been stripped away, for example, where meltwater has removed the glacial sediments east of Beltz Lake; and thus, the subdued NE-SW trending ridges can be detected on aerial photographs (Appendix C, Figure C.19).

The possibility that the NW-SE trending ice-thrust ridges and the corresponding NE-SW trending giant grooves were formed by ice lobes with a similar southwest flowing direction which entered the study area at different times still exists and more evidence is needed before stating that they are exclusively contemporaneous features.

10.1.2 Applications to Surficial Deformation

The recognition of three main types of glaciotectonic facies (Chapter 8) in central and southern Alberta indicates that ice thrusting is likely to occur in glaciated areas with particular bedrock topographic configurations (such as escarpments and valleys) underlain by weakly cemented sediments. Moreover, ice-thrust features and their associated deformation with particular attitudes with respect to the direction of ice movement may be found in these facies (Figures 8.2, 8.3, and 8.4). As a result, the identification of a region as belonging to a certain type of glaciotectonic facies indicates that (1) aerial photograph study, field mapping and subsurface investigation of the area should pay particular attention to ridges oriented perpendicular to the direction of ice motion and prevent the misinterpretation of ice-thrust features as other morainal features, and (2) surficial deformation such as concentric folds, disharmonic folds, thrusts, decollement, scars, and shear zones may be present.

10.1.3 Applications to Log Interpretation

Ice thrusting can produce drag folds and overthrust faults which cause a reversed stratigraphic sequence (Sauer, 1978). This would complicate the stratigraphic correlation which is important in aquifer investigation and the tracing of coal seams. Thus, due to the possibility of reverse stratigraphy, a correlation from one test boring to another in an ice-thrust terrain should be related more to an established sequence of sediments and physical properties than to the elevation of sedimentary changes (Sauer, 1974).

Moreover, ice thrusting may produce thin to thick sheared and brecciated zones and slip planes. Studies of the borehole logs through these materials in Highvale mine (Chapter 5) indicate that ice-thrust brecciated sediments and deformed surfaces are difficult to identify in weakly cemented bedrock. Log interpreters in an ice-thrust terrain should try to observe exposed ice-thrust sediments in the field in order to recognize the characteristic appearance of these deformed sediments in the logs. Furthermore, logs obtained in ice-thrust terrains should be searched for possible correlations of a brecciated layer which may be the indication of the existence of a decollement or sole thrust in the area. For example, the distribution of the shear zone or sole thrust found in Pit 3, Highvale mine (Figures 5.2 and 5.3), is essentially based on borehole correlation.

10.2 Geotechnical Applications of Glaciotectonics

From the geotechnical engineering point of view, ice thrusting influences the fabric and thus the strength properties of the sediments that underlay an ice-thrust terrain. The major geotechical applications of these effects would be the stability of slopes and earth structures built upon ice-thrust sediments, the proper site investigation scheme required in an ice-thrust terrain, and the interpretation of laboratory shear test results of ice-disturbed sediments. These applications are illustrated below.

10.2.1 Applications to Slope Stability Problems. Case Study: Analysis of Two Landslides in Highvale Mine, Wabamun Lake Area

In the past 15 years, several slope instability problems in the Interior Plains of North America have been related to brecciation in thin flat-lying strata of clay, bentonitic clay to clayshale with a strength at or close to residual (Appendix H, Table H.10) due to ice thrusting (Eigenbrod and Morgenstern, 1972; Sauer, 1978; Insley et al., 1976; Wilson, 1974; Morgenstern, 1977). In the following sections, case studies of two landslides occurring in Highvale mine, Wabamun Lake area, which have been studied by the author, will be presented in order to demonstrate the relationship between ice-thrust sediments and slope stability problems in an ice-thrust terrain.

10.2.1.1 Introduction

Two slides occurred along the highwall at the east end of cut #9, Pit 3, Highvale mine. Slide 1, which is located along the north-facing highwall, occurred overnight in early July, 1984. Tension cracks were seen behind the crest of the highwall just before the slide started. Slide 2, which is located along the west-facing highwall, began in April, 1984 and failure was completed about the middle of July, 1984 (C. Jones and J. Pawlowicz, personal communication). The location of these two landslides are shown in Figure C.5 and C.6 in Appendix C.

No instruments were installed in the slide masses before or after the instability occurred. Fortunately, a site investigation had been performed adjacent to the slide area by Monenco Ltd. and Alberta Research Council before the excavation started.

On July 27, 1984, the author examined the slides in the pit. Detailed mapping and sampling were performed in early August. Field observations indicate that Slide 1 was continuing to retrogress into the highwall while Slide 2 seemed to be stable at the time of investigation. The available drillhole data, post-slide mapping, piezometric records and insitu sampling provide enough information for a comprehensive backanalysis of the slides which occurred shortly after an excavation in this ice-thrust terrain.

10.2.1.2 Geology of the Slide Area

The profiles of the highwall before the slides occurred are simple and can be obtained easily by measuring the adjacent portion of the highwall that has not failed; and the width of the slide mass is obtained by measuring the distance with survey tapes between the face of the stable highwall to the back scarp of the slumped blocks. The plan view and profiles of the two slides are shown in Figures 10.2 and 10.3, and Figures C.7 and C.8 indicate the stratigraphic sections of the two landslides.

Nine boreholes were drilled near the slide area before the excavation began in the summer of 1983 (Monenco Ltd., 1984). Geophysical, geotechnical and geological logs together with core sampling were carried out in these boreholes and provide important subsurface information about the slide area. Figure 5.1 shows the location of some of these boreholes.

10.2.1.3 Geometry of Rupture Surface

Tension cracks were observed on the bench behind the scarps of both slides. Most were freshly formed since their surfaces were irregular with matching asperities. In Slide 1 these cracks were more or less parallel to the edge of the scarp (Figure 10.2) with a narrow to moderately wide separation ranging from 6 mm to 102 mm; and a very to extremely wide spacing ranging 0.5 m to 3.35 m. These cracks may persist up to 50 m.

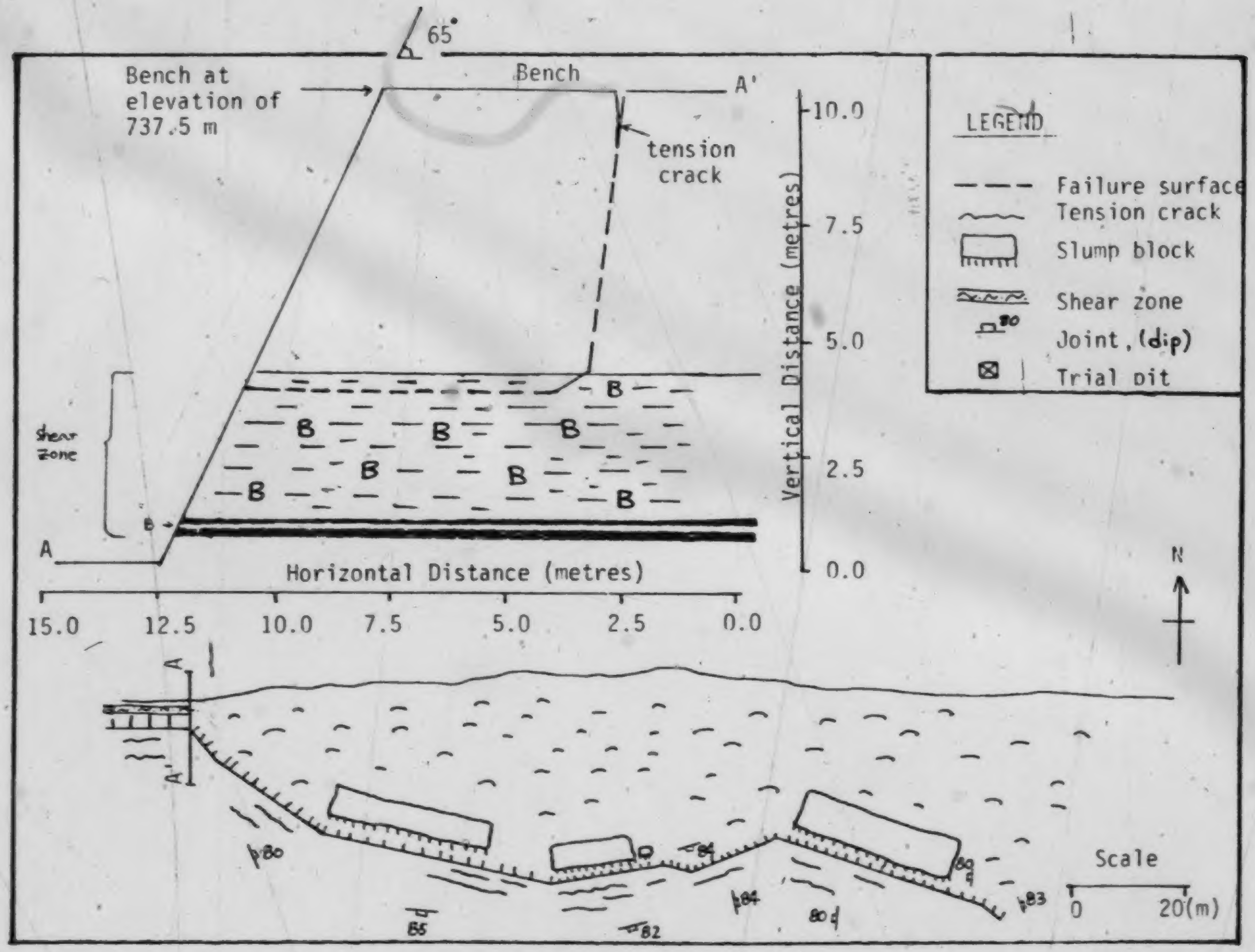
65°
Bench at
elevation of
737.5 m
Bench
A'
tension
crack
A
B
shear
zone
Horizontal Distance (metres)
15.0
12.5
10.0
7.5
5.0
2.5
0.0
Vertical Distance (metres)
10.0
7.5
5.0
2.5
0.0
LEGEND
Failure surface
Tension crack
Slump block
Shear zone
Joint, (dip)
Trial pit
80
N
A
A'
80
85
82
84
84
80
89
83
Scale
0
20(m)

Figure 10.2 Plan View and Profile of Slide 1, Pit 3,
Highvale Mine

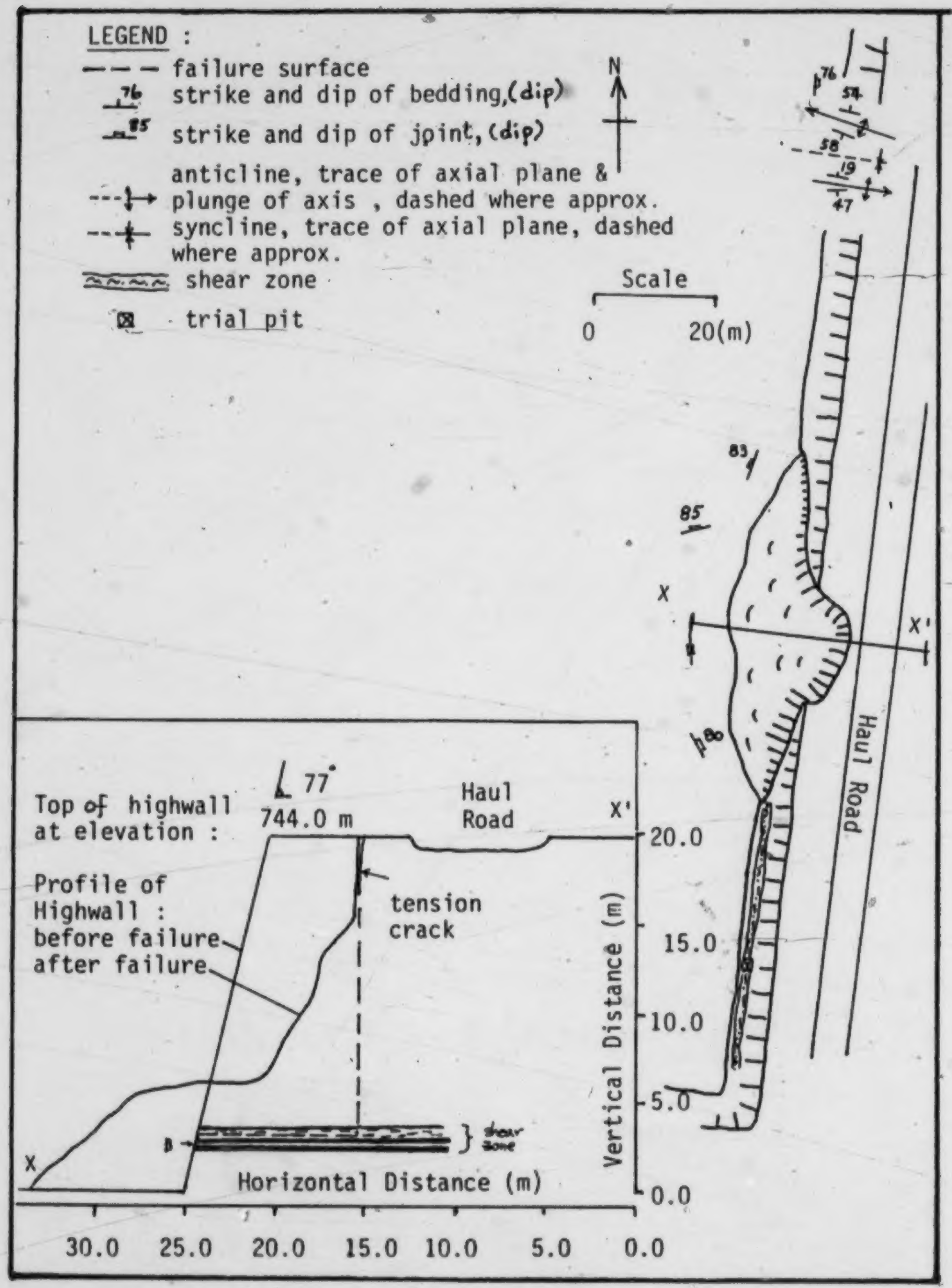
LEGEND :
failure surface
76 strike and dip of bedding,(dip)
85 strike and dip of joint,(dip)
anticline, trace of axial plane & plunge of axis , dashed where approx.
syncline, trace of axial plane, dashed where approx.
shear zone
trial pit
N
Scale
0
20(m)
76
54
58
19
47
83
85
X
X'
80
Haul Road
Top of highwall at elevation :
77°
744.0 m
Haul Road
X'
tension crack
Profile of Highwall :
before failure
after failure
Vertical Distance (m)
20.0
15.0
10.0
5.0
0.0
B
shear zone
X
Horizontal Distance (m)
30.0
25.0
20.0
15.0
10.0
5.0
0.0

Figure 10.3 : Plane view and profile of Slide 2, Pit 3, Wabamun

The measurement of the depth of tension cracks was not possible because of their narrowness and the presence of debris in these cracks; however, field observations seem to indicate that they extended steeply to vertically down into the flat-lying bentonitic mudstone layer. The bentonitic mudstone is the shear zone or sole thrust due to ice thrusting. The composition, lithology, and fabric of this stratum have been described in detail in Chapters 5 and 6. Size of the slumped blocks were measured as lengths x widths of: 7 m x 27 m, 1.2 m x 1.8 m, 4.8 m x 12.6 m. In Slide 2, tension cracks were seen though they are not as distinct as in Slide 1. The exposed till in Slide 2 is highly jointed and these joints connect with joints in the underlying bentonitic sandstone.

Based on the configuration of the joint sets and tension cracks observed in the area, the rupture surface is considered to comprise a horizontal portion, which mainly lies on the bentonitic mudstone or the shear zone of the area, and connects with the inclined portion which tends to follow the steeply inclined to vertical joint sets up through the bentonitic sandstone and the till layers to the scarp of the slide (Figures 10.2 and 10.3). Many workers have reported that this type of rupture surface forms in the Upper Cretaceous weakly cemented bedrock in the western Canadian Plains (Scott and Brooker, 1968; Thomson, 1970, 1971; Thomson and

Matheson, 1970a, 1970b; Eigenbrod and Morgenstern, 1972; Thomson and Hayley, 1975; Insley et al., 1976; Thomson and Tweedie, 1978). All the reported areas have been glaciated by the Wisconsinan-Laurentide ice sheet during the Pleistocene Epoch, and ice-thrust features have been observed in some of them (Thomson and Tweedie, 1978; Thomson and Matheson, 1970a).

In the study area, the intersection of the discontinuities (joint sets within the sandstone and brecciated zone within the mudstone) has produced a 3-dimensional planar surface on which downslope movement of the rock/soil masses can occur.

10.2.1.4 Water table

The piezometric surface in the slide mass at failure was unknown. However, it is possible to determine the approximate configuration of the groundwater table based on field observation of the seepage conditions of the highwall, examining the limited piezometric data collected in the study area prior to the excavation of cut #9, and the laboratory studies on the undisturbed samples collected near the slide area.

Twenty piezometers had been installed in the main coal seams and in the overburden sandstone to investigate the groundwater conditions in Pit 3 (Fenton et al., 1983, p. 31); unfortunately, no piezometers had been placed in the critical bentonitic mudstone layer in the study area. Water level measurements taken in these piezometers during the period from September to November of 1983 when the excavation was near cut #8 (Appendix C, Figure C.6) were used to construct the cross-section of the piezometric surfaces in the bentonitic sandstone and the main coal seams near the slide area (Figure 10.4). The location of the cross-section is indicated in Figure 5.1. Figure 10.4 shows that the bottom thick coal seam has a piezometric surface about 12 - 20 m above the top of the coal at a distance of about 350 m back from the highwall; while the water level in the overburden sandstone was at or near the top of the layer at a distance of about 100 - 150 m back from the highwall (Fenton et al., 1983). Piezometer readings taken at borehole #HV-83-005 (installed in the overburden sandstone about 300 m west and 25 m south of Slide 1) between Sept 1, 1983 and April 11, 1984 also indicate that the groundwater table was only about 2.2 m below the top of the highwall (Figure 10.5).

Laboratory tests performed by the author on the undisturbed samples collected from the bentonitic mudstone exposed near Slide 1 (Figure 10.2) indicate that the sediments where the horizontal portion of the rupture plane lies were unsaturated (Appendix H, Table H.2). However, water was found seeping out of the highwall locally from the bentonitic sandstone, the bentonitic mudstone, and the coal beds above and below

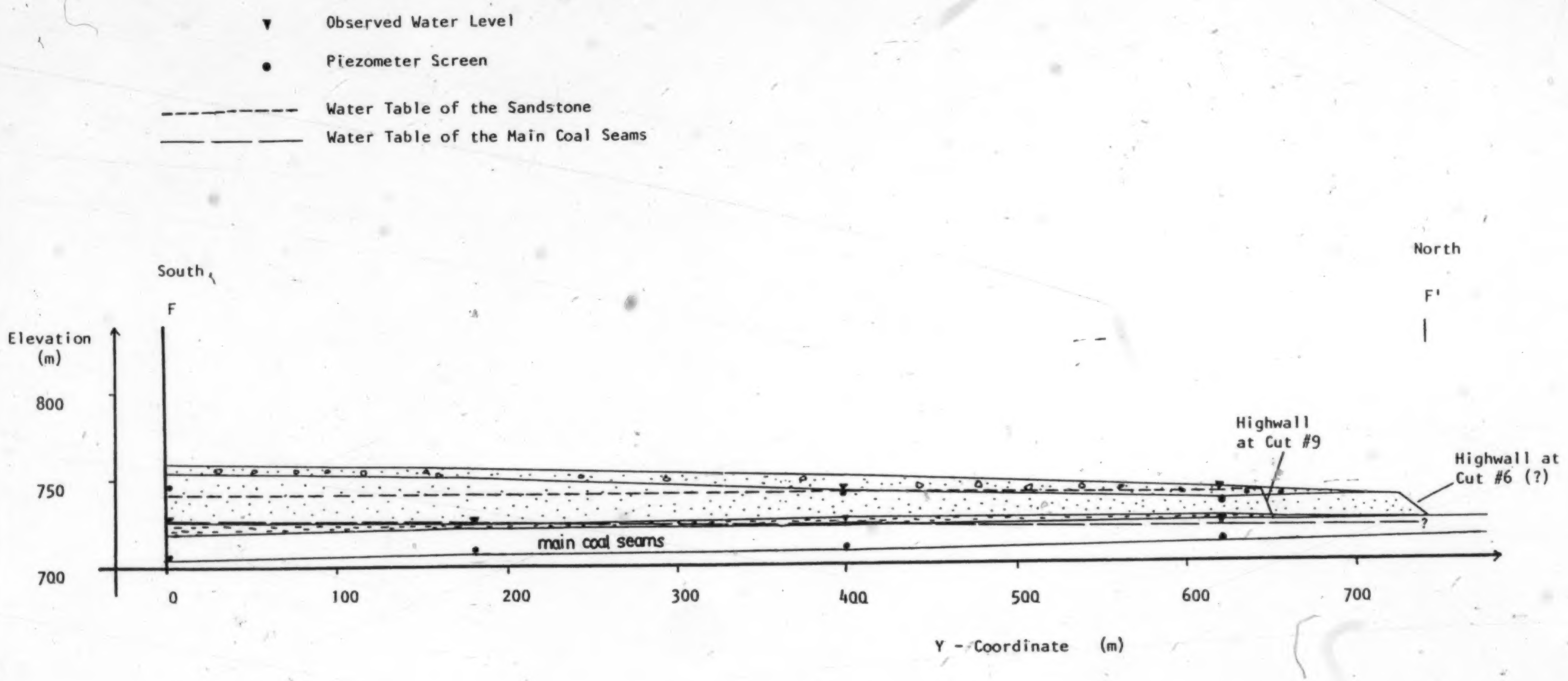
▼ Observed Water Level
● Piezometer Screen
Water Table of the Sandstone
Water Table of the Main Coal Seams
South
F
North
F'
Elevation (m)
800
750
700
Highwall at Cut #9
Highwall at Cut #6 (?)
?
main coal seams
0
100
200
300
400
500
600
700
Y - Coordinate (m)

(Location of Section F - F', see Figure 5.1)

Figure 10.4 Piezometric Surfaces in the Bentonitic Sandstone and Coal Layers, Pit 3, Highvale Mine

(Modified after Fenton et al., 1983, fig. 11)

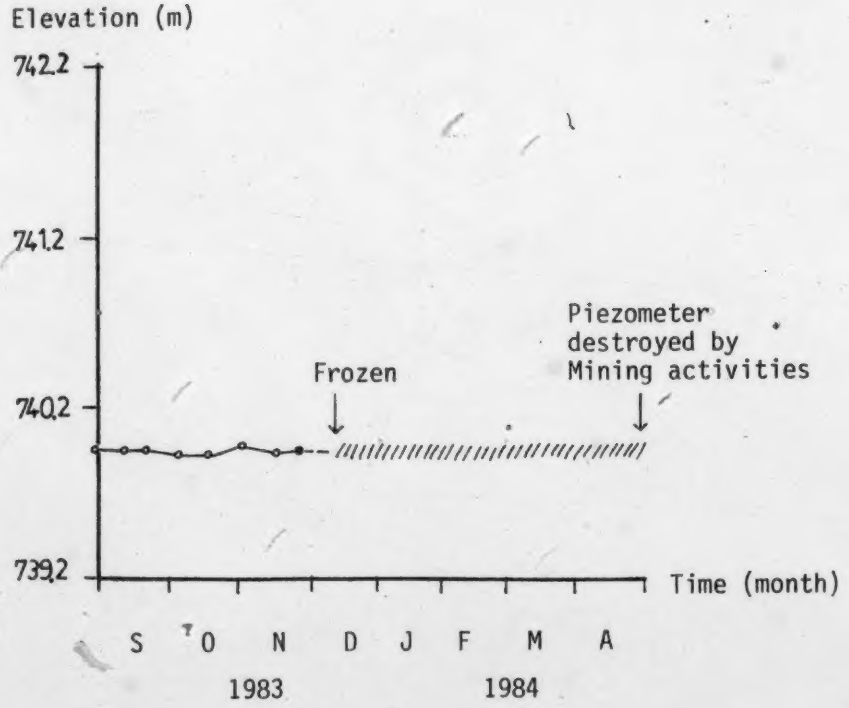

Figure 10.5 Piezometric Readings taken at Borehole #HV-83-005 near Slide 1, Pit 3, Highvale Mine

the bentonite near the slide area. This seems to indicate that the bentonitic mudstone in the slide area acts as an unconfined or confined aquifer. The unsaturated sediments found in the bentonitic mudstone sampled might be due to the drawdown of the piezometric surface when it approached the face of the highwall and/or the water table in the stratum was below the horizontal portion of the rupture surface. The presence of an unconfined or confined aquifer (bentonitic mudstone) between two saturated strata (the overlying sandstone and the underlying coal seams) which consist of different piezometric surfaces suggest that a perched water table has developed in the overlying stratum (Figure 10.4). It must be noted that slug tests performed in standpipe piezometers in the mine indicate that the bentonitic sandstone and the disturbed bentonitic shale/mudstone above the main coal seams have hydraulic conductivities of 0.024 cm/s and 0.0064 cm/s respectively (Monenco Ltd., 1984, vol. 1, table 3-5), which are typical values for jointed rocks (Hoek and Bray, 1977, p. 132). That the bentonitic mudstone, which is a fissured, sheared and shattered shear zone with a hydraulic conductivity typical of jointed rocks and overlain by saturated strata, would behave as an unconfined or confined aquifer may be explained by the seepage properties of a composite fault. Patton and Deere (1971, fig. 8) noted that a composite fault may be composed of a relatively permeable central zone of crushed and shear rock (fault breccia) flanked by fine-grained fault gouge with low permeability on either side. The bentonite (Plate 5.5) and the relatively dense weathered layer (Figure 6.6; Plate 6.5) that bounded the bottom and the top of the deformed fissured bentonitic mudstone (Plate 5.2) respectively probably act as fault gouge or groundwater barriers and restrict water migration into the shear zone.

Thus, the stratigraphy and the piezometric data suggest that there are three piezometric surfaces and two perched water tables in the slide area. The probable configurations of these water tables are shown in Figure 10.6.

10.2.1.5 Strength Properties

The strength properties of the sediments in these landslides used in the stability analysis are shown in Table 10.1. The laboratory tests on the bentonitic mudstone and the bentonite have been described and interpreted in detail in Chapter 7.

10.2.1.6 Stability Analysis

Slide 1

The failure surface in the slide masses was probably horizontal in the bentonitic mudstone and inclined at about 30° near the end before it connected with the steeply inclined joints in the bentonitic

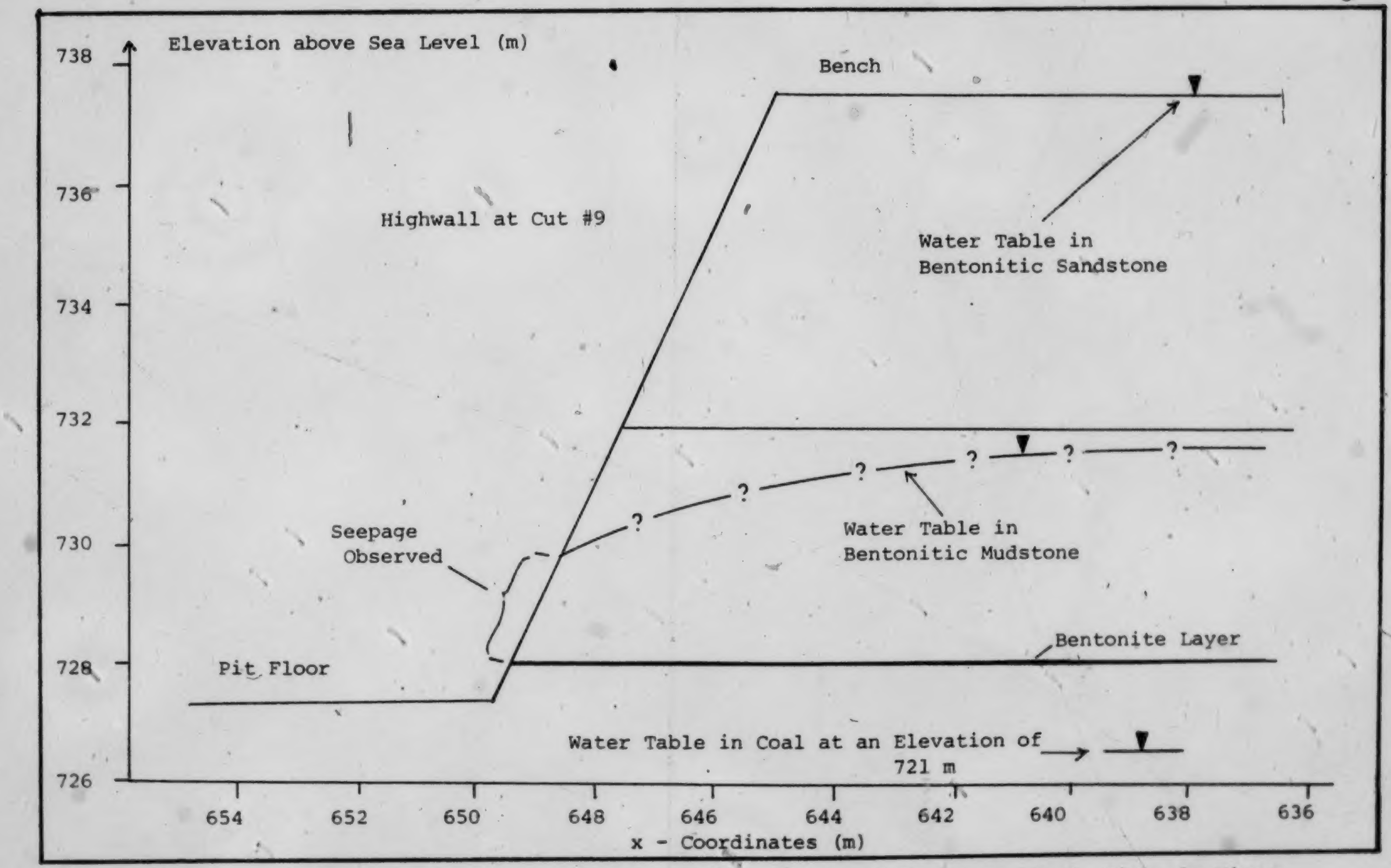
Elevation above Sea Level (m)
738
736
734
732
730
728
726
Bench
Highwall at Cut #9
Water Table in Bentonitic Sandstone
Water Table in Bentonitic Mudstone
Seepage Observed
Bentonite Layer
Pit Floor
?
Water Table in Coal at an Elevation of 721 m
654
652
650
648
646
644
642
640
638
636
x - Coordinates (m)

Figure 10.6 : Probable Configurations of Water Tables in the Slide Area, Pit 3, Highvale Mine

Table 10.1 Soil Strength along the Highwall Adjacent to Slides 1 and 2, Pit 3, Highvale Mine

Material	γ_t KN/m³	Strength Parameters			
		c'_p (kPa)	ϕ'_p (deg)	c'_r (kPa)	ϕ'_r (deg)
Till#	20.0	10	31	...	...
Bentonitic Sandstone##	21.4	0	40	...	...
Bentonitic Mudstone##	20.3	135	37.5	0* 0** 0***	22.5* 11.5** 6.5***
Bentonite##	17.3	...	...	0	11.5
Carbonaceous Shale with Hard Lumps##	19.4	140	37.2	0	13.0
Coal#	13.8	200	31.0	...	...

# Tested by Monenco Ltd. (1984)

## Tested by the Author and the interpretation of borehole data (HV-83-406)

* Upper bound of residual strength

** Average residual strength

***Lower bound of residual strength

sandstone which extend upward to the scarp of the slide. The horizontal and the gently inclined portion of the failure surface within the mudstone are inferred from the horizontal principal slip surface and the inclined minor shears observed in the shear zone (Plates 5.2 and 5.3). The water table in the bentonitic sandstone was perched and the water pressure mainly acted on the inclined portion of the rupture. Figure 10.7 shows the pore pressure distribution along the failure surface of Slide 1. The slope analysis of Slide 1 was performed by using the general method of Morgenstern and Price (1965) and the results are indicated in Table 10.2.

The results of the analyses show that within the possible range of the groundwater table observed in the field, the use of the maximum and the minimum residual strength of the bentonitic mudstone measured in the laboratory would result either a too high or a too low Factor of Safety when failure occurred in Slide 1 (Table 10.2). When the average residual strength of this bentonitic mudstone is used in the analysis, the Factor of Safety for Slide 1 is equal to 1.42 and 1.03 when the water table was about 2.2 m and 0.5 m below the top of the slide mass respectively. It is concluded that when failure began in Slide 1, the shear strength mobilized along the shear zone was equal to the average residual strength of the bentonitic mudstone, that is, $c_r' = 0$ kPa and $\phi_r' = 11.5°$; with a water table in the

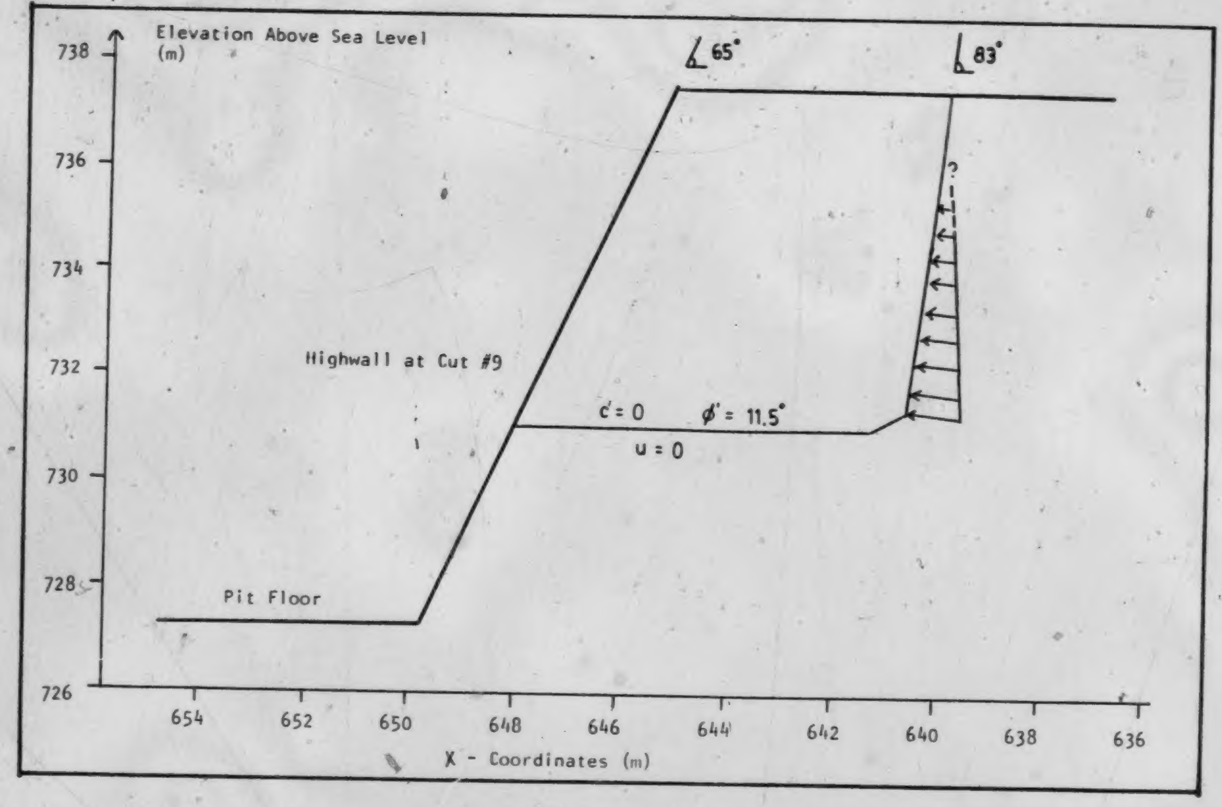
Elevation Above Sea Level (m)
738
736
734
732
730
728
726
65°
83°
?
Highwall at Cut #9
c' = 0
φ' = 11.5°
u = 0
Pit Floor
654
652
650
648
646
644
642
640
638
636
X - Coordinates (m)

Figure 10.7 Pore Water Pressure Distribution along the Rupture Surface of Slide 1, Pit 3, Highvale Mine

Table 10.2 Results of the Stability Analysis, Slides 1 and 2, Pit 3, Highvale Mine

Slide	Depth of Water Table	Bentonitic Mudstone				Factor of Safety
		c'_p (kPa)	ϕ'_p (deg)	c'_r (kPa)	ϕ'_r (deg)	
Slide 1 (non-circular Limit Equilibrium Analysis)	2.2 m			0	22.5	2.73
				0	11.5	1.42
				0	6.5	0.85
	1.0 m			0	22.5	2.16
				0	11.5	1.12
				0	6.5	0.67
	0.5 m			0	22.5	1.98
				0	11.5	1.03
				0	6.5	0.61
Slide 2 (Plane Failure Analysis)	2.2 m	135	37.5			2.97
				0	22.5	0.94
				0	11.5	0.47
		0	37.5			1.76
				0#	23.6#	1.00
	0.0 m	135	37.5			2.19
				0	22.5	0.72
		0	37.5			1.32
				0#	30.0#	1.00

# Back calculated

bentonitic sandstone very close to the ground surface. This seems to be the case since Fenton et al. (1983) have reported that the observed groundwater table in the overburden sandstone is stable, rather than declining as might be expected due to the close proximity of the highwall.

Slide 2

Field studies indicate that the horizontal portion of the failure surface of Slide 2 is also located in the bentonitic mudstone. The scarp portion of Slide 2 is very steep and can be approximated as vertical (Figure 10.3). It was probably formed by opening a roughly vertical joint when the slope was under stress relief following the excavation. As a result, the groundwater in Slide 2 has only created a hydraulic driving force against the vertical tension crack. The backanalysis of Slide 2 was performed by using the plane failure mechanism described by Hoek and Bray (1977) and the results are indicated in Table 10.2.

The use of the peak or the residual strengths for the bentonitic mudstone in Slide 2 in the backanalysis resulted in a Factor of Safety either greater or less than unity. Back calculation shows that the mobilized shear strength on the bentonitic mudstone in Slide 2 during failure was equal to $c' = 0$ kPa and $\phi' = 23.6°$; when the water table was about 2.2 m below the top of the highwall. This is reasonable because: (1) the piezometer, which was installed adjacent to Slide 2, also indicated a constant piezometric surface about 2 m below the top of the slide mass (Figure 10.5), and (2) the bentonitic mudstone and the bentonite in the shear zone observed in Slide 2 are composed of many coal chips and rock fragments and thin coal beds were observed intruded into the strata (Plates 5.4 and 5.5). The coal in the mine has a residual strength of $c_r' = 0$ to 28 kPa, and a $\phi_r' = 13.5°$ to 29.5° (Monenco Ltd., 1983a, vol. 1, fig. E-13). As a result, the mobilized shear strength of the coal and clay mixture which formed the shear zone in Slide 2 is expected to be higher than the shear zone in Slide 1 which is essentially composed of sheared bentonitic mudstone.

The higher shear strength in the shear zone of Slide 2 area than in the zone of Slide 1 area seems to be the reason that the highwall at the former became stable shortly after the slide while slope failure continued to occur into the highwall of the latter.

10.2.1.7 Discussion

1. In the study area, the horizontal portion of the rupture surfaces of Slides 1 and 2 are located in the bentonitic mudstone instead of the bentonite probably because of the following reasons:
    a. The bentonite has a limited lateral extent in the slide area.

   b. The steeply inclined joints in the bentonitic sandstone had not reached the underlying bentonite.

   c. The bentonitic mudstone has a residual strength similar to the bentonite; and at the same time, the principal slip surfaces formed due to ice thrusting are well-developed in the former. These surfaces tend to connect with the joints sets in the immediate overlying bentonitic sandstone to form the failure surface on which the slides could take place.

2. Stress release due to excavation and (frost) weathering should have caused of softening (Terzaghi, 1936; Skempton, 1948) and progressive failure (Bjerrum, 1967) which caused in fissures and joints forming and/or enlarging, and softening with time of the bentonitic sandstone and mudstone along the highwall in Highvale mine. It is believed that these are the processes responsible for the formation of the inclined and vertical portion of the rupture surface which connected with the horizontal shear zone in the study area and allowed failure to occur.

3. Spring thaw and the rise of the water table back to the ground surface probably was the triggering force for Slide 2 which occurred in late April. For Slide 1, a few months more was probably required for the

joint sets in the bentonitic sandstone to grow and extend down into the mudstone to form a continuous rupture surface which allowed failure to occur.

4. Barron, Stimpson and Kosar (1985a, 1985b) developed a theory and a computer program on Multiple Block Plane Shear Slope Failure (MBPSSF) and applied them to the analysis of Slide 1 in Pit 3 of the Highvale Mine. However, field observation indicates that their theory cannot be applied without modification to the landslides in Pit 3 that occurred in the summer of 1984. The reasons are as follows:
    a. MBPSSF assumes a perched water table on the horizontal impervious failure plane in the analysis (Barron et al., 1985a, Part I, p. 6). Based on the lithologic log from borehole #HV-83-406, Barron et al. (1985b) treated the bentonite as the failure surface. Field investigation indicates that the slide mass is seated on a shear plane within the bentonitic mudstone instead of the bentonite. This view is supported by a continuous, horizontal shear plane about 300 m long in the bentonitic mudstone overlying the bentonite which was exposed on the highwall adjacent to Slide 1 (Plate 5.2). Moreover, field and laboratory investigations suggest that the base of the slide mass of Slide 1 was free of water pressure

when the failure occurred.

b. Barron et al. (1985a, Part III, p. 75; appendix 2, p. 103) assigned 'peak' strength ($c_p' = 9.3$ kPa, $\phi_p' = 24.6°$) to the failure plane in the analysis. However, field observation indicates that both the bentonite and the overlying bentonitic mudstone had been sheared and slickensides were found in these beds. Studies on more than 80 lithologic logs obtained from the boreholes at Pit 3 by the author show that zones of weakness due to ice thrusting were present in the pit before excavation and prior to the occurrence of Slide 1 (Figures 5.2 and 5.3). Moreover, backanalysis of Slide 1 by the author has shown that the horizontal portion of the failure surface which lies within the bentonitic mudstone has a strength of $c_r' = 0$ kPa, and $\phi_r = 11.5°$ (Table 10.2). Thus, the use of peak strength in analyzing the slide which seated on this zone of weakness is inappropriate.

c. MBPSSF analysis assumes that a vertical tension crack will form when the factor of safety is equal to unity in the general equilibrium equation (Barron and Stimpson, 1985, p. 5). The tension crack then descends from the surface to the horizontal clay band below which completes the geometry for the block failure (Barron et al., 1985a, Part I, p. 1). As seen by the author, this assumption does not apply to Slide 1 in the study area. First, joint measurements in Pit 3 suggest that the major portion of the scarp of Slide 1 follows the major joint sets which are inclined. Secondly, MBPSSF only considers the formation of a vertical tension crack in the scarp area but does not pay attention to lateral separation of the slide mass from the surrounding rock mass. However, as ice thrusting has definitely occurred in the slide area (see Chapter 5) and produced sets of discontinuities, the slide geometry follows these pre-existing planes of weakness rather than vertical tension cracks and the horizontal bentonite layer.

d. Since the geometry of Slide 2 is consistent with the geometrical assumptions in the MBPSSF analysis described by Barron et al. (1985a), the author performed a deterministic analysis by using MBPSSF. The analysis indicates that a water table at a depth of about 4.7 m below the top of the highwall, 2.7 m lower than observed in the field, is required to initiate the slide. Alternatively, a larger slide will occur (that is, the horizontal distance between the scarp and the toe of the slide needs to be increased from the observed 9.6 m to about 14.2 m) if the water table observed in the field is input into the analysis.

The analysis based on MBPSSF does not agree with field observations mainly because the MBPSSF assumes hydrostatic pressure acts both on the horizontal and vertical portions of the failure surface once the water table has risen above this surface. It does not deal with the fact that the horizontal portion of the rupture plane could be free of water pressure, resulting in hydrostatic pressure acting on the vertical portion of the failure surface only.

To conclude, a slope stability analysis that can account for an inclined tension crack and non-uniform water table should be used in the study of Slide 1.

5. The rupture surface in the study area is essentially a pre-existing geological feature that is composed of a flat-lying portion due to glaciotectonic deformation and an inclined to vertical portion due to regional and local jointing. Progessive failure, commonly responsible for the development of a continuous failure surface in overconsolidated clays resulting from the removal of the lateral support described by Bjerrum (1967), has played only a small

role in the slope stability problem in this investigation.

10.2.1.8 Conclusions

For the safety of the draglines operating on the crest of highwall in Highvale mine, Wabamun Lake area, the following activities should be part of the design of the highwall or any large excavation in an ice-thrust terrain.

1. Identify the presence and extent of brecciated layers or shear zones in the area by field mapping and examining the available geological, geophysical and geotechnical logs, and core samples. The layer which is described as brecciated, crushed, and slickensided and with a poor RQD may be an indication of the location of a shear zone.
2. A joint or fissure pattern survey should be undertaken over the excavated area to : (1) predict any possible failure surfaces formed by the intersection of the local and regional joint systems (due to glaciotectonics or orogenic tectonics) and the shear zone with the slope, (2) evaluate the proportion of slip surface that passes different through the kinds of fissures (such as open or closed) and the strength that the failure plane may consist of (Skempton and LaRochelle, 1965).
3. Piezometers and slope indicators should be installed in the disturbed regions of the excavation site

where ice-disturbed sediments and shear zones are observed or expected to exist. The groundwater table should be closely monitored especially during spring runoff, heavy storms, seasonal rainfall, and ice freezing on the face of the slope all of which may cause large increases in the elevation of the phreatic surface (Terzaghi, 1936; Piteau, 1970). The corresponding piezometric readings should be correlated with the amount of slope movement shown by the slope indicators.

4. Residual strength parameters should be used as the mobilized strength for the continuous horizontal slip surface within the crumbly shear zone in a stability analysis of the slope with a shear zone observed near its base.

10.2.2 Applications to Site Investigation and Laboratory Testing

The study of the shear zone exposed in Highvale mine has shown that ice thrusting may produce a crumbly shear zone which is composed of a few continuous and planar principal slip surfaces with a strength at close to residual, and many discontinuous minor shears with strengths varying from peak to residual, depending on the amount of movement or shearing that the material has undergone. Thus, the recognition of the location of the shear zone and its major slip surfaces should be the primary target in site investigation in an ice-thrust terrain since these features often control the stability of engineering structures built on them.

In detecting the location of a shear zone in an ice-thrust terrain, field mapping should be performed whenever is possible since case histories indicated that core sampling and geophysical logs may not be able to detect the thin plane of weakness (Plate 5.2; Insley et al., 1976, p. x-24; Wilson, 1974).

Moreover, a reasonable interpretation of the geotechnical strength parameters of ice-thrust sediments measured in laboratory can only be obtained if they are coupled with accurately described geologic fabric observed in the test samples and the shear zone in the field. This has been shown by the laboratory studies presented in Chapters 6 and 7. The integration of the above information can be used in planning the number and location of drillholes needed in a certain area within a construction site in an ice-thrust terrain to understand the variation of strength and the distribution of ice-deformed sediments within the area. Then economical and safe design of the sites for engineering works can be obtained in any ice-thrust terrain. The importance of soil fabric and profile mapping in site investigation for engineering works in ice-thrust terrain or in other terrains cannot be overemphasized (Rowe, 1972; Marsland et al. 1980).

10.3 Glaciological Applications of Glaciotectonics

10.3.1 Ice-Rock Avalanches

The proposed mechanics of glaciotectonic deformation, which essentially describe the factors (such as the flow and thermal conditions of a glacier, the strength of subglacial sediments, depth of permafrost at the snout) that caused subglacial failure at the stagnant snout of a subpolar glacier, probably also explain the cause of ice-rock avalanches that occur in some alpine valley glaciers. This is because ice-rock avalanches in mountainous areas, which have been suggested as triggered by the failure of bedrock and superincumbent glacier ice near the snout of hanging glaciers or cirque glaciers (Eisbacher and Clague, 1984, fig. 33), also seem to be caused by foundation instability near the margin of the ice and result in the collapse of the overlying ice and the corresponding subglacial strata. This is shown by a devastating ice-rock slide (which consisted of about 2.5 x 10^6 m^3 of glacier ice and 26 x 10^6 m^3 of debris and had claimed four human lives) which appears to be related to the development of high pore water pressure in the 'poorly consolidated' strata that underlay the margin (frozen and stagnant?) of a retreating but active cirque glacier (Mokievsky-Zubok, 1977, 1978).

Thus, according to the ice-thrust model, the favourable conditions or factors for the development of ice-rock avalanches probably are an active hanging glacier with a stagnant margin underlain by weak and frozen subglacial strata under high water pressure. The appearance of a bulge on the ice surface near the boundary of the stagnant and active zone of a valley glacier and high runoff during spring melting should be critical for the stability of the glacier margin and may be a warning that indicates ice-rock avalanches may soon occur. This also indicates that when resort areas or settlements are planned to be built close to the margin of an Alpine glacier where ice-rock avalanches are common, the stratigraphy and permafrost condition of the area, the strength properties and hydrogeological conditions of the subglacial strata that underlay the margin of the ice, and the thermal and flow conditions of the glacier should be investigated. Based on this information, a preliminary stability analysis of the glacier and its foundation should be performed. The understanding of the mechanics and the factors that contribute to the development of ice-rock avalanches are important because glacier-related mass movement always causes hazards to human safety and property in high mountain areas such as the Canadian Cordillera which are under rapid economic development (such as transportation routes, settlements, and recreational areas) in the recent years, and the Alps where reservoirs and dams have been constructed close to the snouts of hanging glaciers (Eisbacher and Clague, 1984).

11. CONCLUSIONS

11.1 Conclusions

Aerial photograph interpretation and field studies of the ice-thrust terrains in central and southern Alberta indicate that, unlike well-known ice-thrust features, which are quite distinct on aerial photographs, many ice-thrust features are expressed as linear forms on the ground and may be easily misinterpreted as other oriented morainic features such as end moraines and corrugated ground moraines. A classification method has been proposed, which involves ground checks and subsurface investigation, to distinguish ice-thrust features which are mainly composed of deformed bedrock from end moraines and corrugated ground moraines which are chiefly composed of till. Investigation of the surficial geology, glacial features, and glacial history of the region studied show that glaciotectonic deformation in central and southern Alberta probably occurred at the margin of a stagnant and downwasting ice sheet and was associated with readvances of the snout of the glacier.

Field mapping and subsurface investigation indicate that glaciotectonic macrofabric consists chiefly of: (a) decollements or sole thrusts, (b) concentric folds and fault-bend folds, (c) strike-slip faults and normal faults, (d) imbricate thrusts, (e) piggy-back thrust sequences, (f) scars, and (g) local joint systems.

In the Highvale coal mine, it is shown that the minimum distances of travel of thrust blocks due to glacial deformation in that area ranged from 280 to 860 m, depths of sole thrusts ranged from 8.7 to 27 m, and the average thickness of sole thrusts was about 2.3 m with a range of 0.5 to 4.2 m, lengths of about 395 m or greater, and widths of at least 1200 m. In the Lowden Lake area, it was found that ice thrusting has caused about 16 m of shortening due to horizontal internal deformation and 512 m of translation due to horizontal external deformation leading to the formation of ice-thrust ridges and depressions or scars behind the ridges. Local and regional joint studies seem to suggest that the joint system in the Highvale mine had been subjected to a regional stress field due to the past tectonic events and also to a local stress field due to the recent glacial ice thrusting. However, this is only a tentative inference and more joint studies must be performed in other ice-thrust terrains before a definite conclusion can be reached.

The types and geometry of the macrofabric in the glaciotectonic thrust system closely resemble the thrust system observed in orogenic tectonic terrains; thus, it seems reasonable that the kinematic analysis of glaciotectonic macrofabric can be performed based on the available understanding of orogenic tectonics.

The microfabric and submicrofabric of the ice-thrust fine-grained sediments found in a glaciotectonic shear zone or sole thrust indicate that the submicrofabric of the sediments were composed mainly of aggregations which have dense cores of randomly oriented groups of clay platelets wrapped by an external layer of oriented clay particles in a turbostratic arrangement. It is believed that glaciotectonic deformation and high overburden pressure have caused the collapse of the original sediment structure, resulting secondary aggregations embedded in a sea of oriented clay platelets. The presence of shear structures such as principal displacement shears and Riedel shears indicate that large shear strains have occurred in the ice-thrust sediments studied.

The sediments in the study areas have been heavily overconsolidated. However, the geological processes such as cycles of unloading and loading due to erosion and glaciation, weathering, permafrost, and glaciotectonic deformation, have further brecciated, jointed, sheared, and remoulded the sediments. This caused the sediments within the glaciotectonic shear zone found in the areas studied to behave as a normally consolidated to lightly overconsolidated sediments in laboratory tests and to show a non-brittle, plastic mode of deformation, a low OCR, and a maximum shear strength below peak and, in general, close to residual. To conclude, the general geotechnical characteristics of ice-thrust sediments within a clayey layer in the region studied are:

1. High clay fraction, for example, up to 40 % or higher

within which platy clay minerals such as montmorillonite dominate.

2. Glaciotectonic deformation probably is not evenly distributed within the layer; as a result, the fabric and strength properties in general vary in different parts within the glaciotectonic stratum. The strength of the brecciated sediments in the layer probably varies between the fully softened state and residual, while the strength along principal displacement shears is at or close to residual.
3. Poor RQD.

Based on the relationship between the direction of ice movement, the regional bedrock topographic configurations in central and southern Alberta and the attitudes of their corresponding fabric elements such as ice-thrust features and meltwater channels, three types of glaciotectonic facies are proposed, namely, (a) Escarpment, (b) Valley, and (c) Plains. The Escarpment glaciotectonic facies tends to be located along the slope of a preglacial hill or valley with its strike perpendicular to the ice direction. The Valley glaciotectonic facies occurs in a valley when an ice lobe enters and flows parallel to the thalweg of the valley. Both of these facies have the slope of their bedrock surface approximately perpendicular to the axes of folds, the trends of ice-thrust ridges, the strike of deformed beds and thrust faults, and approximately parallel to the direction of the ice movement. The Plains glaciotectonic facies occur on relatively featureless plain where ice-deformed beds might have their dip directions parallel to the glacial direction. The identification of certain types of glaciotectonic facies in a region, which is solely based on terrain analysis and regional topographic and geological map studies, would indicate that: (i) glacial-deformed sediments and glaciotectonic structures are likely to exist in the area, and (ii) the probable attitudes of ice-thrust features and their associated deformations with respect to the orientations of other glacial and surficial features, and the direction of ice movement in the region.

It is proposed that glaciotectonism in the study areas is caused by foundation failure at the snout of a subpolar ice sheet when its marginal stagnant and frozen area is compressed by the active-flowing upglacier ice and the corresponding earth pressure in the strata. The failure caused the deformation of subglacial strata near the snout and probably resulted in the collapse of the overlying ice which may lead to a glacier surge.

The main forces that cause ice thrusting are: (a) the forces due to the ice flow behind the stagnant zone, (b) the earth pressure in the subglacial strata, and (c) the hydrostatic uplifting force that acted on the potential failure surface. Among these, the increase in the active earth pressure and/or ice compression due to the bulge at the boundary of the stagnant and active-flowing zones, and the increase in water pressure at the potential failure surface (which is probably located at a weak and impermeable stratum and coincides with the bottom of permafrost which is underlain by aquifers) are believed to be the critical factors that trigger glaciotectonism.

Geological applications of glaciotectonics include:

1. Ice direction indicator - the axis of folds and strike of fractures and thrusts in glaciotectonic structures usually trend perpendicular to the direction of the ice advance; thus, the latter can be derived from the attitudes of ice-thrust structures.
2. Log interpretation - ice thrusting can produce deformations such as drag folds and thrust faults. As a result, stratigraphic correlation based on borehole logs in ice-thrust terrain should consider complicated stratigraphic sequences in the area due to glaciotectonic deformation.

Geotechnical applications of glaciotectonics include:

1. Slope stability problems - glaciotectonic shear zones are weak layers and are composed of continuous horizontal planes having a residual strength. Thus, slope stability analysis of a slope with glaciotectonic shear zones observed at its base should consider the intersection of these zones with local joint systems forming potential rupture surfaces where slope movement is most likely to occur. It is recommended that residual strength parameters should be used as the mobilized strength for the horizontal portion of these surfaces.

2. Site investigation and laboratory testing - the recognition of the location of glaciotectonic shear zones and their major slip surfaces should be the primary target in site investigation undertaken in ice-thrust terrains since these features often control the stability of engineering structures built on them. The amount and distribution of principal displacement shears, Riedel shears, remoulded clay matrices, and clay peds in samples obtained from glaciotectonic shear zones could significantly influence their strength properties as measured in a laboratory. As a result, a reasonable interpretation of the geotechnical strength parameters of ice-thrust sediments cannot be attained unless the geologic fabric observed in the samples and the shear zones have been accurately described.

Glaciological applications of glaciotectonics include the use of the mechanical models of glaciotectonism developed in this study to understand the cause of glacier surge and ice-rock avalanches.

11.2 Recommendations for Future Research

11.2.1 Strength of Ice-Thrust Sediments

More geotechnical laboratory and insitu tests should be performed on the brecciated sediments sampled across an ice-thrust shear zone in order to increase the understanding of the distribution and range of strength of these troublesome deposits, and their effects on the slope and foundation stability of the area.

In addition to the conventional geotechnical tests, work needs to be done on correlations between the geological, geophysical and geotechnical logs. The success of this research would help to:

1. Interpret geological features (such as heavily fractured zones) and geotechnical parameters (such as elastic constants) from geophysical logs (Hoffman et al., 1982). As a result, these logs may indicate the locations of fractured zones, glacial thrust blocks and the configuration of the major potential rupture surfaces in an ice-thrust terrain with estimates of the geotechnical properties of the ice-thrust sediments.
2. Obtain a continuous geotechnical borehole log from the geophysical logs which can provide more subsurface geotechnical information than the conventional coring methods. This is particularly useful in detecting the many horizons of slip surfaces in the ice-thrust sediments and the properties of these materials.
3. Minimize the cost for most site investigation since geophysical logging methods permit deeper drilling up to 100 m or more without greatly increasing the cost, while coring costs beyond 30 m deep are usually prohibitive (Sauer, 1980, p. 551). This is economically very important because the depth of glacial deformation in ice-thrust terrains may exceed 30 m (Mathews and Mackay,

1960; Moran et al., 1980).

4. Provide insitu undisturbed physical properties of the sediments when the geophysical logs are run in a well-controlled borehole. This would eliminate the disturbances due to in-situ sampling and transportation of the samples to the laboratory.

Thus, it is suggested that more drillholes with well-controlled geophysical logs should be cored, and correlations between the logs and properties of the sediments measured by laboratory tests on the cored samples and by insitu tests.

11.2.2 Field Mapping and Classifying an Ice-Thrust Terrain

The bentonitic mudstone in the Highvale mine, Wabamun Lake area, has a wide range of strength properties (Chapter 7), fabric, and lithology (Plates 5.3 and 5.5). This has created difficulties in deciding the most critical area in this brecciated layer for detailed investigation while, at the same time, obtaining a general view of the distribution of the deformation in the area.

It has been suggested that the geotechnical complexity of a site can be analyzed by applying the concept of facies and the associated process model (Morgenstern and Cruden, 1979). Field mapping and classifying an ice-thrust terrain into fabric domains (Cruden, 1978) or glacial-deformed units (Fenton et al., 1983) seems to be the initial step in recognizing the general distribution and variation of the fabric and strength properties in the geotechnically and structurally complicated ice-thrust terrain and deciding on suitable locations for subsequent detailed sampling and testing in the area.

11.2.3 Local Joint System due to Ice Thrusting

The joint set studies performed in the Highvale mine, Wabamun Lake area (Chapter 5) seem to show that ice thrusting may produce a local joint system that deviates from the regional joint system. The recognition of these two systems may help: (1) to point out the orientations of the principal stresses imposed on the area due to the recent glaciation, and (2) to indicate the direction of ice movement in the area.

However, the joint data used in differentiating the ice-induced local joint system from the regional joint system in Highvale mine are limited to one rock type, the bentonitic sandstone, and are also restricted to a small area of the mine. In order to fully understand the relationship between the joint systems and glaciotectonism, more measurements and investigation on the joint systems in different types of sediments in other ice-thrust terrains in central and southern Alberta are definitely needed.

11.2.4 Thrust System of Ice-Thrust Terrain

Log data from other ice-thrust terrains (if available) should be compiled to construct subsurface structural cross-sections of the regions. This would help to generate a better understanding of the structural geology of ice-thrust areas and also to show whether the macrosocpic fabric elements such as duplex structure, horses, shear zones or sole thrusts, concentric folds and fault-bend folds, pointed out in this thesis (Chapter 5) are common features in other glaciotectonic areas.

11.2.5 Regional Studies of the Occurrence of Ice Thrusting

The recognition of the types of glaciotectonic facies in central and southern Alberta indicates that ice thrusting should be a widespread phenomenon in the region. The fact that ice-thrust features are relative rarely observed in the field is probably because some ice-thrust features have indistinct topographic expressions or resemble morainal features (Chapter 4). Thus, more field work and aerial photograph interpretation to search for ice-thrust features should be performed in areas that have been identified as certain types of glaciotectonic facies based on geologic and topographic studies.

11.2.6 Models of Ice Thrusting

The thermal and flow conditions of the ablation area of modern surge-type subpolar glaciers, the strength properties and pore water conditions of the subglacial strata that underlay the marginal area of the ice should be investigated. The information should be used to perform stability analyses of the foundation near the snout of the glacier and be related to the movement of the glacier toe and the deformation in its underlying strata. A similar study should also be performed near the marginal area of valley glaciers in mountainous areas where ice-rock avalanches have occurred. The results would test the validity of the ice-thrust model proposed in this thesis and its application in the mechanics of glacier surge and ice-rock avalanches.

REFERENCES

Aber, J.S. 1982. Model for glaciotectonism. Bulletin of the Geological Society of Denmark, 30, pp. 79-90.

Alberta Research Council. 1983. Highvale Mine - lithologs of field program July, 1983. Alberta Geological Survey, Edmonton, Alberta.

Alden, W.C. 1918. The Quaternary geology of southern Wisconsin with a chapter on the older rock formations. U.S. Geological Survey Professional Papers, v. 106, pp. 1 - 356.

Anderson, D.M., and N.R. Morgenstern. 1973. Physics, chemistry, and mechanics of frozen ground: a review. Proceedings of the 2nd International Conference on Permafrost, North American Contribution, Yakutsk, U.S.S.R., pp. 257 - 288.

Andrews, D.E. 1980. Glacially thrust bedrock - An indication of late Wisconsin climate in Western New York State. Geology, 8, pp. 97-101.

Andriashek, L.D., M.M. Fenton, and J.D. Root. 1979. Surficial geology of the Wabamun Lake area, Alberta, NTS 83 G. Alberta Research Council, Map, Scale 1: 250,000.

ASTM Standards. 1986. Soil and Rock; Building Stones. Volume 04.08, Section 4, 1078 pages.

Aylmore, L.A.G., and J.P. Quirk. 1960. Domain or turbostratic structure in clay. Nature, 187, p. 1046.

Babcock, E.A. 1973. Regional jointing in southern Alberta. Canadian Journal of Earth Sciences, 10, pp. 1769 - 1781.

Babcock, E.A. 1974. Jointing in central Alberta. Canadian Journal of Earth Sciences, 11, pp. 1[illegible]81 - 1186.

Babcock, E.A., M.M. Fenton, and L.D. Andriashek. 1978. Shear phenomena in ice-thrust gravels, central Alberta. Canadian Journal of Earth Sciences, 15, pp. 277 - 283.

Banham, P.H. 1975. Glacitectonic structures: a general discussion with particular reference to the contorted drift of Norfolk. In: Ice Ages: Ancient and Mordern. Edited by A.E. Wright and F. Moseley. Seel House Press, Liverpool, pp. 69 - 94.

Banham, P.H., and C.E. Ranson. 1965. Structural study of the contorted drift and disturbed chalk at Weybourne, North

Norfolk. Geological Magazine, 102, pp. 164 - 174.

Bannatyne, B.B. 1971. Industrial minerals of the sedimentary area of southern Manitoba. Geological Association of Canada, Special Paper 9, pp. 243 - 251.

Barden, L. 1972a. The relation of soil structure to the engineering geology of clay soil. Quarterly Journal of Engineering Geology, 5, pp. 85 - 102.

Barden, L. 1972b. The influence of structure on deformation and failure in clay soil. Geotechnique, 22, pp. 159 - 163.

Barden, L. 1973. Macro- and microstructure of soils. Appendix to the Proceedings of the International Symposium on Soils Structure, Gothenburg 1973, Sweden, pp. 20 - 26.

Barden, L., and A. McGown. 1973. Microstructural disturbance in soft clays resulting from site investigation sampling. Proceedings of the International Symposium on Soil Structure, Gothenburg 1973, Sweden, pp. 205 - 215.

Barden, L., and G. Sides. 1971a. Sample disturbance in the investigation of clay structure. Geotechnique, 21, pp. 211 - 222.

Barden, L., and G. Sides. 1971b. The influence of weathering on the microstructure of Keuper Marl. Quarterly Journal of Engineering Geology, 3, pp. 259 - 260.

Barron, K., and B. Stimpson. 1985. Multiple block plane shear slope failure. Canmet seminar - May 17, 1985, Report #8542-F1, Canada Centre for Mineral and Energy Technology, Energy, Mines and Resources, Canada.

Barron, K., B. Stimpson, and K. Kosar. 1985a. Multiple block plane shear slope failure. Part I: Theoretical analysis. Part II: Computer program. Part III: Sensitivity analyses, case histories and conclusions. Coal Mining Research Centre Report 84/31-C, March, 1985, Canada Centre for Mineral and Energy Technology, Energy, Mines and Resources, Canada.

Barron, K., B. Stimpson, and K. Kosar. 1985b. A regressive mode of highwall failure in coal strip mines. In preparation.

Bates, R.J., and J.A. Jackson. 1980. Glossary of Geology. American Geological Institute, Virginia, 751 pages.

Bayrock, L.A. 1958a. Glacial geology Alliance - Brownfield district, Alberta. Research Council of Alberta, Preliminary Report 57-2, 56 pages.

Bayrock, L.A. 1958b. Glacial geology Galahad - Hardisty district, Alberta. Research Council of Alberta, Preliminary Report 57-3, 35 pages.

Bayrock, L.A. 1972. Surficial Geology of Edmonton, NTS 83H. Alberta Research Council, Map, Scale 1: 250,000.

Berthelsen, A. 1979. Recumbent folds and boudinage structures formed by subglacial shear: an example of gravity tectonics. Geologie en Mijnbouw, 58, pp. 253 - 260.

Bell, R. 1874. Report on the country between Red River and the South Saskatchewan, with notes on the geology of the region between Lake Superior and Red River. Geological Survey of Canada, Report of Progress 1873-1874, pp. 66 - 93.

Bielenstein, H.U., and G.H. Eisbacher. 1969. Tectonic interpretation of elastic-strain-recovery measurements at Elliot Lake, Ontario. Department of Energy, Mines and Resources, Ottawa, Mines Branch Research Report R 210, 64 pages.

Bishop, A.W., and D.J. Henkel. 1962. The Measurement of Soil Properties in the Triaxial Test. Second Edition. Edward Arnold, London, 227 pages.

Bishop, B.C. 1957. Shear moraines in the Thule area, northwest Greenland. U.S. Army Corps of Engineers, Snow, Ice and Permafrost Research Establishment, Research Report 17, 46 pages.

Bjerrum, L. 1967. Progessive failure in slopes of overconsolidated plastic clay and clay shales. Proceedings of the American Society of Civil Engineers, SM 5, 93, pp. 3 - 49.

Bloss, F.D. 1961. An Introduction to the Methods of Optical Crystallography. Holt, Rinehart and Winston, New York, 294 pages.

Bluemle, J.P. 1966. Ice-thrust bedrock in northwest Cavalier County, North Dakota. Proceedings of North Dakota Academy of Science, 20, pp. 112 - 118.

Bluemle, J.P. 1970. Anomalous hills and associated depressions in central north Dakota. Geological Society of America. Abstracts with Programs, 2, pp. 325 - 326.

Bluemle, J.P., and L. Clayton. 1984. Large-scale glacial thrusting and related processes in North Dakota. Boreas, 13, pp. 279 - 299.

Boulton, G.S. 1972. The role of thermal regime in glacial sedimentation. In: Polar Geomorphology. Edited by R.J. Price, and D.E. Sugden. Institute of British Geographers Special Publication #4, pp. 1 - 19.

Boulton, G.S. 1979. Processes of glacier erosion on different substrata. Journal of Glaciology, 23, pp. 15 - 38.

Boulton, G.S., and A.S. Jones. 1979. Stability of temperate ice caps and ice sheets resting on beds of deformable sediment. Journal of Glaciology, 24, pp. 29 - 43.

Boulton, G.S., E.M. Morris, A.A. Armstrong, and A. Thomas. 1979. Direct measurement of stress at the base of a glacier. Journal of Glaciology, 22, pp. 3 - 34.

Boulton, G.S., and M.A. Paul. 1976. The influence of genetic processes on some geotechnical properties of glacial tills. Quarterly Journal of Engineering Geology, 9, pp. 159 - 194.

Boyer, S.E., and D. Elliott. 1982. Thrust systems. Bulletin of the American Association of Petroleum Geologists, 66, pp. 1196 - 1230.

Brewer, R. 1964. Fabric and Mineral Analysis of Soils. John Wiley & Sons, New York, 470 pages.

Brinkmann, R. 1953. Uber die diluvialen Storungen auf Rugen. Geologische Rundschau, 41, Sonderband, pp. 231 - 241.

Broster, B.E., A. Dreimanis, and J.C. White. 1979. A sequence of glacial deformation, erosion, and deposition at the ice-rock interface during the last glaciation: Cranbrook, British Columbia, Canada. Journal of Glaciology, 23, pp. 283 - 295.

Brown, W.G., G.H. Johnston, and R.J.E. Brown. 1964. Comparison of observed and calculated ground temperatures with permafrost distribution under a northern lake. Canadian Geotechnical Journal, 1, pp. 147 - 154.

Brumund, W.F., E. Jonas, and C.C. Ladd. 1976. Estimating in situ maximum past (preconsolidation) pressure of saturated clays from results of laboratory consolidometer tests. Special Report 163, Transportation Research Board, Washington, D.C., pp. 4 - 12.

Bucher, W.H. 1956. Role of gravity in orogenesis. Bulletin of the Geological Society of America, 67, pp. 1295 -

1318.

Byers, A.R. 1959. Deformation of the Whitemud and Eastend Formations near Claybank, Saskatchewan. Transactions of Royal Society of Canada, 53, series 3, section 4, pp. 1 - 11.

Canadian Foundation Engineering Manual. 1985. 2nd Edition. Canadian Geotechnical Society, Technical Committee on Foundations. BiTech Publishers, Vancouver, 456 pages.

Carey, S.W. 1962. Folding. Journal of the Alberta Society of Petroleum Geologists, 10, pp. 95 - 144.

Carlson, V.A. 1967. Bedrock topography and surficial aquifers of the Edmonton district, Alberta. Research Council of Alberta, Report 66-3, 21 pages.

Carlson, V.A. 1970. Bedrock topography of the Oyen map-area, NTS 72M, Alberta. Research Council of Alberta, Map, Scale 1 : 250,000.

Carlson, V.A. 1971. Bedrock topography at the Wabamun Lake map-area, NTS 83 G, Alberta. Alberta Research Council, Map, Scale 1: 250,000.

Carlson, V.A., and L.M. Topp. 1972. Bedrock topography of the Wainwright map-area, NTS 73D, Alberta. Research Council of Alberta, Map, Scale 1 : 250,000.

Carrigy, M.A. 1971. Lithostratigraphy of the Uppermost Cretaceous (Lance) and Paleocene strata of the Alberta Plains. Research Council of Alberta, Bulletin 27, 161 pages.

Catto, N.R. 1984. Glacigenic deposits at the Edmonton Convention Centre, Edmonton, Alberta. Canadian Journal of Earth Sciences, 21, pp. 1473 - 1482.

Chan, A.C.Y. 1986. Geotechnical characteristics of Genesee clay. Unpublished Ph. D. Thesis. Department of Civil Engineering, University of Alberta, Edmonton, 374 pages.

Chandler, R.J. 1969. The effect of weathering on the shear strength properties of Keuper Marl. Geotechnique, 19, pp. 321 - 334.

Chandler, R.J. 1972. Lias clay: weathering processes and their effect on shear strength. Geotechnique, 22, pp. 403 - 431.

Chandler, R.J. 1973. A study of structural discontinuities in stiff clays using a polarizing microscope. Proceedings of the International Symposium on Soil

Structure, Gothenburg 1973, Sweden, pp. 78 - 86.

Charlesworth, J.K. 1957. The Quaternary Era. Edward Arnold, London, Volume 1, 591 pages.

Christiansen, E.A. 1971. Tills in southern Saskatchewan, Canada. In: Till - a Symposium. Edited by R.P. Goldthwait. Ohio State University Press, Columbus, pp. 167 - 183.

Christiansen, E.A., and S.H. Whitaker. 1976. Glacial thrusting of drift and bedrock. In: Glacial Till - An Interdisciplinary Study. Edited by R.F. Legget. Royal Society of Canada Special Publications, no. 12, pp. 121 - 130.

Clarke, G.K.C., S.G. Collins, and D.E. Thompson. 1984. Flow, thermal structure, and subglacial conditions of a surge-type glacier. Canadian Journal of Earth Sciences, 21, pp. 232 - 240.

Clarke, G.K.C., and R.H. Goodman. 1975. Radio echo soundings and ice-temperature measurements in a surge-type glacier. Journal of Glaciology, 14, pp. 71 - 78.

Clayton, L., and S.R. Moran. 1974. A glacial process-form model. In: Glacial Geomorphology. Edited by D.R. Coates. Binghamton Symposia in Geomorphology, International Series no. 5, State University of New York, Binghamton, pp. 89 - 119.

Collins, K., and A. McGown. 1974. The form and function of microfabric features in a variety of natural soils. Geotechnique, 24, pp. 223 - 254.

Cruden, D.M. 1978. Analyzing geological field data for rock slope design. Bulletin of the Canadian Institute of Mining and Metallurgy, 71, no. 793, pp. 117 - 120.

Cruden, D.M., and H.A.K. Charlesworth. 1976. Errors in strike and dip measurements. Bulletin of the Geological Society of America, 87, pp. 977 - 980.

Dahlstrom, C.D.A. 1969a. Balanced cross sections. Canadian Journal of Earth Sciences, 6, pp. 743 - 757.

Dahlstrom, C.D.A. 1969b. The upper detachment in concentric folding. Bulletin of Canadian Petroleum Geology, 17, pp. 326 - 346.

Dahlstrom, C.D.A. 1970. Structural geology in the eastern margin of the Canadian Rocky Mountains. Bulletin of Canadian Petroleum Geology, 18, pp. 332 - 406.

Davis, G.H. 1984. Structural Geology of Rocks and Regions. Wiley, New York, 492 pages.

Deer, W.A., R.A. Howie, and J. Zussman. 1966. An Introduction to the Rock-Forming Minerals. Longman, London, 528 pages.

DeJong, J., and N.R. Morgenstern. 1973. Heave and settlement of two tall building foundations in Edmonton, Alberta. Canadian Geotechnical Journal, 10, pp. 261 - 281.

Dellwig, L.F., and A.D. Baldwin. 1965. Ice-push deformation in northeastern Kansas. Kansas Geologial Survey, Bulletin 175, part 2, 16 pages.

Douglas, R.J.W. 1950. Callum Creek, Langford Creek, and Gap map-area, Alberta. Geological Survey of Canada, Memoir 255.

Douglas, R.J.W. (editor). 1970. Geology and Economic Minerals of Canada. Geological Survey of Canada, Economic Geology Report no. 1, 838 pages.

Dyer, W.S. 1927. Oil and gas prospects in southern Saskatchewan. Geological Survey of Canada, Summary Report 1926, Part B, pp. 30 - 38.

Eigenbrod, K.D., and N.R. Morgenstern. 1972. A slide in Cretaceous bedrock, Devon, Alberta. In: Geotechnical Practice for Stability in Open Pit Mining. Edited by C.O. Brawner and V. Milligan. AIME, pp. 223 - 238.

Eisbacher, G.H., and J.J. Clague. 1984. Destructive mass movements in high mountains: hazard and management. Geological Survey of Canada, Paper 84-16, 230 pages.

Eisenstein, Z., and N.A. Morrison. 1973. Prediction of foundation deformations in Edmonton using in situ pressure probe. Canadian Geotechnical Journal, 10, pp. 193 - 210.

Elliott, D. 1976. The energy balance and deformation mechanisms of thrust sheets. Royal Society of London Philosophical Transactions, Series A, 283, pp. 289 - 312.

Elliott, D. 1983. The construction of balanced cross-sections. Journal of Structural Geology, 5, p. 101.

Elliott, D., and M.R.W. Johnson. 1980. Structural evolution in the northern part of the Moine thrust belt, NW Scotland. Transactions of the Royal Society of Edinburgh: Earth Sciences, 71, pp. 69 - 96.

Embleton, C., and C.A.M. King. 1975. Glacial Geomorphology. Edward Arnold, London, 573 pages.

Environment and Land Use Committee Secretariat. 1978. Terrain Classification System. British Columbia Department of the Environment, Victoria, 56 pages.

Eyles, N., and J. Menzies. 1983. The subglacial landsystem. In: Glacial Geology. An Introduction for Engineers and Earth Scientists. Edited by N. Eyles. Pergamon Press, Toronto, pp. 19 - 70.

Farvolden, N.R. 1963a. Bedrock topography, Edmonton - Red Deer map-area, Alberta. In: Early contributions to the groundwater hydrology of Alberta. Research Council of Alberta, Bulletin 12, pp. 57 - 62.

Farvolden, N.R. 1963b. Bedrock channels of southern Alberta. In: Early contributions to the groundwater hydrology of Alberta. Research Council of Alberta, Bulletin 12, pp. 63 - 75.

Fenton, M.M. 1984. Quaternary stratigraphy of the Canadian Prairies. In: Quaternary Stratigraphy of Canada - A Canadian Contribution to IGCP Project 24. Edited by R.J. Fulton. Geological Survey of Canada, Paper 84-10, pp. 57 - 68.

Fenton, M.M., and L.D. Andriashek. 1983. Surficial geology of Sand River area, Alberta, NTS 73L, 1 : 250,000. Allberta Research Council, Edmonton, Alberta.

Fenton, M.M., C.E. Moell, J.G. Pawlowicz, G. Sterenberg, M.R. Trudell, and S.R. Moran. 1983. Highwall stability project - Highvale Mine study. Alberta Research Council, Internal Report, 70 pages.

Fleuty, M.J. 1964. The description of folds. Proceedings of Geologists' Association, 75, pp. 461 - 492.

Flint, R.F. 1942. Glacier thinning during deglaciation. Part II. Glacier thinning inferred from geologic data. American Journal of Science, 240, pp. 113 - 136.

Flint, R.F. 1971. Glacial and Quaternary Geology. John Wiley & Sons, New York, 892 pages.

Fookes, P.G. 1965. Orientation of fissures in stiff overconsolidated clay of the Siwalik system. Geotechnique, 15, pp. 195 - 206.

Fookes, P.G., and B. Denness. 1969. Observational studies on fissure patterns in Cretaceous sediments of south-east England. Geotechnique, 19, pp. 453 - 477.

Fordjor, C.K., J.S. Bell, and D.I. Gough. 1983. Breakouts in Alberta and stress in the North American plate. Canadian Journal of Earth Sciences, 20, pp. 1445 - 1455.

Foster, R.H., and P.K. De. 1971. Optical and electron microscopic investigation of shear induced structures in lightly consolidated (soft) and heavily consolidated (hard) kaolinite. Clays and Clay Minerals, 19, pp. 31 - 47.

Fulton, R.J. 1984. Summary: Quaternary stratigraphy of Canada. In: Quaternary Stratigraphy of Canada - A Canadian Contribution to IGCP Project 24. Edited by R.J. Fulton. Geological Survey of Canada, Paper 84-10, pp. 1 - 5.

Funder, S., and K.S. Petersen. 1980. Glacitectonic deformations in East Greenland. Bulletin of the Geological Society of Denmark, 28, pp. 115 - 122.

Garga, V.K. 1973. Some observations on microstructure of clays at large strains. Proceedings of the International Symposium on Soils Structure, Gothenburg 1973, Sweden, pp. 217 - 225.

Garland, G.D., and D.H. Lennox. 1962. Heat flow in western Canada. Journal of the Royal Astronomical Society, 6, pp. 245 - 262.

Geikie, J. 1889. Address to the Geological Section of British Association; Newcastle-Upon-Tyne. Edinburgh University Press, Edinburgh, Scotland, 27 pages.

Geikie, J. 1894. The Great Ice Age. 3rd Edition. Edward Stanford, London, 850 pages.

Gillott, J.E. 1969. Study of the fabric of fine-grained sediments with the scanning electron microscope. Journal of Sedimentary Petrology, 39, pp. 90 - 105.

Glen, J.W. 1952. Experiments on the deformation of ice. Journal of Glaciology, 2, pp. 111 - 114.

Goguel, J. 1962. Tectonics. Freeman, San Francisco, 384 pages.

Goodman, R.H., G.K.C. Clarke, and G.T. Jarvis. 1975. Radio soundings on Trapridge glacier, Yukon Territory, Canada. Journal of Glaciology, 14, pp. 79 - 84.

Gough, D.I. and J.S. Bell. 1981. Stress orientations from oil-well fractures in Alberta and Texas. Canadian Journal of Earth Sciences, 18, pp. 638 - 645.

Gough, D.I. and J.S. Bell. 1982. Stress orientations from borehole wall fractures with examples from Colorado, east Texas, and northern Canada. Canadian Journal of Earth Sciences, 19, pp. 1358 - 1370.

Grainger, P. 1984. The classification of mudrocks for engineering purposes. Quarterly Journal of Engineering Geology, 17, pp. 381 - 387.

Grant, K. 1975a. The PUCE program for terrain evaluation for engineering purposes, I. Principles CSIRO Division of Applied Geomechanics, Technical Paper, 15, 2nd edition, 32 pages.

Grant, K. 1975b. The PUCE program for terrain evaluation for engineering purposes, II. Procedures for Terrain Evaluation, CSIRO Division of Applied Geomechanics, Technical Paper, 19, 2nd edition, 68 pages.

Gravenor, C.P. 1956. Glacial geology of Castor District, Alberta. Research Council of Alberta, Preliminary Report 56-2, 23 pages.

Gravenor, C.P., and L.A. Bayrock. 1955. Glacial geology of Coronation district, Alberta. Research Council of Alberta, Preliminary Report 55-1, 38 pages.

Gravenor, C.P., and L.A. Bayrock. 1956. Stream-trench systems in east-central Alberta. Research Council of Alberta, Preliminary Report 56-4, 11 pages.

Gravenor, C.P., and R.B. Ellwood. 1957. Glacial geology of Sedgewick District, Alberta. Research Council of Alberta, Preliminary Report 57-1, 43 pages.

Gravenor, C.P., R. Green, and J.D. Godfrey. 1960. Airphotographs of Alberta. Research Council of Alberta. Bulletin 5, 79 pages.

Gravenor, C.P., and W.O. Kupsch. 1959. Ice-disintegration features in western Canada. Journal of Geology, 67, pp. 48 - 64.

Green, R. 1982. Geological map of Alberta. Alberta Research Council, Map, Scale 1: 1,267,000.

Hansen, E., S.C. Porter, B.A. Hall, and A. Hills. 1961. Decollement structures in glacial-lake sediments. Bulletin of the Geological Society of America, 72, pp. 1415 - 1418.

Harlan, R.L., and J.F. Nixon. 1978. Ground thermal regime. In: Geotechnical Engineering for Cold Regions. Edited by O.B. Andersland and D.M. Anderson. McGraw-Hill, New

York, Chapter 3, pp. 103 - 163.

Heley, W., and B.N. Maclver. 1971. Engineering properties of clay shales. Report 1. Development of classification indexes for clay shales. U.S. Army Engineer Waterways Experiment Station, Technical Report S-71-6.

Hicock, S.R., and A. Dreimanis. 1985. Glaciotectonic structures as useful ice-movement indicators in glacial deposits: four Canadian case studies. Canadian Journal of Earth Sciences, 22, pp, 339 - 346.

Hobbs, B.E., W.D. Means, and P.F. Williams. 1976. An Outline of Structural Geology. John Wiley & Sons, New York, 571 pages.

Hoek, E., and J. Bray. 1977. Rock Slope Engineering. Institution of Mining and Metallurgy, London, 527 pages.

Hoffman, G.L., G.R. Jordan, and G.R. Wallis. 1982. Geophysical Borehole Logging Handbook for Coal Exporation. Coal Mining Research Centre, Edmonton, Alberta, 207 pages.

Hollingworth, S.E., J.H. Taylor, and G.A. Kellaway. 1944. Large scale superficial structures in the Northampton Ironstone field. Quarterly Journal Geological Society, London, 100, pp. 1 - 44.

Holtz, R.D., and W.D. Kovacs. 1981. An Introduction to Geotechnical Engineering. Prentice-Hall, New Jersey, 733 pages.

Hooke, R. LeB. 1977. Basal temperature in polar ice sheets: a qualitative review. Quaternary Research, 7, pp. 1 - 13.

Hooke, R. LeB, B.B. Dahlin, and M.T. Kauper. 1972. Creep of ice containing dispersed fine sand. Journal of Glaciology, 11, pp. 327 - 336.

Hopkins, O.B. 1923. Some structural features of the Plains Area of Alberta caused by Pleistocene Glaciation. Bulletin of the Geological Society of America, 34, pp. 419 - 430.

Hossack, J.R. 1983. A cross-section through the Scandinavian Caledonides constructed with the aid of branch-line maps. Journal of Structural Geology, 5, pp. 103 - 111.

Hurlbut, Jr. C.S., and C. Klein. 1977. Manual of Mineralogy (after J.D. Dana). John Wiley & Sons, New York, 532 pages.

Insley, A.E., P.K. Chatterji, and L.B. Smith. 1976. Embankment foundation stability using residual strength. 29th Canadian Geotechnical Conference, Vancouver, British Columbia, 32 paes.

Irish, E.J.W. 1967. Geology of Foremost. Geological Survey of Canada, Map 22-1967, Scale 1: 253,440.

Jahn, A. 1973. Pleistocene glacitectonic structures in the light of observations in the recently glaciated areas. English summary. Geo Abstracts, A Landforms and the Quaternary, 73A/1330, pp. 401 - 402.

Jaroszewski, W. 1984. Fault and Fold Tectonics. Translated by W.L. Kirk. Halsted Press, New York, 565 pages.

Johnston, G.H., and R.J.E. Brown. 1966. Occurrence of permafrost at an Arctic lake. Nature, 211, pp. 952 - 953.

Johnstrup, F. 1869. Om Brunkuldannelserne i Danmark, samt om de deri forekommende forstyrrede Leiringsforhold. Forhandlinger ved De Skandinaviske Naturforskeres tiende Mode i Christiania 1868.

Judge, A. 1973. The prediction of permafrost thickness. Canadian Geotechnical Journal, 10, pp. 1 - 11.

Kathol, C.P., and R.A. McPherson. 1975. Urban Geology of Edmonton. Albera Research Council, Bulletin 32, 61 pages.

Kenney, T.C. 1967. The influence of mineral composition on the residual strength of natural soils. Proceedings of the Geotechnical Conference, Oslo, 1, pp. 123 - 129.

Konigsson, L.-K., and L.A. Linde. 1977. Glaciotectonically disturbed sediments at Ronnerum on the island of Oland. Geologiska Foreningens i Stockholm Forhandlingar, 99, pp. 68 - 72.

Koster, R. 1957. Schuppung und faltung im glazialtektonischen experiment. Geologische Rundschau, 46, pp. 564 - 571.

Kupsch, W.O. 1962. Ice-thrust ridges in western Canada. Journal of Geology, 70, pp. 582 - 594.

Lamerson, P.R., and L.F. Dellwig. 1957. Deformation by ice push of lithified sediments in south-central Iowa. Journal of Geology, 65, pp. 546 - 550.

Langenberg, W. 1985. Jointing and glaciotectonism in Pit 02 of the Highvale mine. Prepared for TransAlta. Alberta

Geological Survey, Alberta Research Council, 19 pages.

Le Breton, E.G. 1963. Groundwater geology and hydrology of east-central Alberta. Research Council of Alberta, Bulletin 13, 64 pages.

Lessig, H.D., and W.A. Rice. 1962. Kansan drift of the Elkton, Ohio, rift. American Journal of Science, 260, pp. 439 - 454.

Locker, J.G. 1973. Petrographic and engineering properties of fine-grained rocks of Central Alberta. Research Council of Alberta, Bulletin 30, 144 pages.

Lupini, J.F., A.E. Skinner, and P.R. Vaughan. 1981. The drained residual strength of cohesive soils. Geotechnique, 31, pp. 181 - 213.

Maarleveld, G.C. 1981. The sequence of ice-pushing in the central Netherlands. Mededelingen Rijks Geologische Dienst, 34-1, pp. 2 - 6.

Mackay, J.R. 1959. Glacier ice-thrust features of the Yukon coast. Geographical Bulletin, 13, pp. 5 - 21.

Mackay, J.R. 1971. The origin of massive icy beds in permafrost, western arctic coast, Canada. Canadian Journal of Earth Sciences, 8, pp. 397 - 422.

Marsland, A., and M.E. Butler. 1967. Strength measurements on stiff fissured Barton clay from Fawley (Hampshire). Proceedings of the Geotechnical Conference, Oslo, 1, pp. 139 - 145.

Marsland, A., A. McGown, and E. Derbyshire. 1980. Soil profile mapping in relation to site investigation for foundations and earthworks. Bulletin of the International Association of Engineering Geology, 21, pp. 139 - 155.

Marsland, A., A. Prince, and M.A. Love. 1983. The role of soil fabric studies in the evaluation of the engineering parameters of offshore deposits. Proceedings of the 3rd International Conference on the Behavior of Off-shore Structures, August 2-5, 1982, MIT, Cambridge, Massachusetts, 1, pp. 181 - 200.

Matheson, D.S. 1972. Geotechnical implications of valley rebound. Ph. D. Thesis, University of Alberta, Edmonton, Alberta, 424 pages.

Matheson, D.S., and S. Thomson. 1973. Geological implications of valley rebound. Canadian Journal of Earth Sciences, 10, pp. 961 - 978.

Mathews, W.H. 1964. Water pressure under a glacier. Journal of Glaciology, 5, pp. 235 - 240.

Mathews, W.H. 1974. Surface profiles of the Laurentide ice sheet in its marginal areas. Journal of Glaciology, 13, pp. 37 - 43.

Mathews, W.H., and J.R. Mackay. 1960. Deformation of soils by glacial ice and the influence of pore pressures and permafrost. Transactions of Royal Society of Canada, Series 3, Section 4, pp. 27-36.

McClay, K.R. 1981. What is a thrust? What is a Nappe? In: Thrust and Nappe Tectonics. Edited by K.R. McClay and N.J. Price. Geological Society of London Special Publication no. 9, pp. 7 - 9.

McGown, A. 1982. Discussion on the drained residual strength of cohesive soils. Geotechnique, 32, pp. 76.

McGown, A., A. Marsland, A.M. Radwan, and A.W.A. Gabr. 1980. Recording and interpreting soil macrofabric data. Geotechnique, 30, pp. 417 - 447.

McPherson, R.A., and C.P. Kathol. 1972. Stratigraphic sections and drill hole logs, Edmonton area, Alberta. Research Council of Alberta, Report 72-6, 78 pages.

Meier, M.F., and A. Post. 1969. What are glacier surges? Canadian Journal of Earth Sciences, 6, pp. 807 - 817.

Mellor, M. 1973. Mechanical properties of rocks at low temperature. North American Contribution 2nd International Permafrost Conference, Yakutsk, pp. 334 - 344.

Mesri, G., and A.F. Cepeda-Diaz. 1986. Residual shear strength of clays and shales. Geotechnique, 36, pp. 269 - 274.

Michel, B. 1978. Ice Mechanics. Les Presses de l'Universite Lavel, Quebec, 499 pages.

Mills, H.C., and P.D. Wells. 1974. Ice-shove deformation and glacial stratigraphy of Port Washington, Long Island, New York. Bulletin of the Geological Society of America, 85, pp. 357 - 364.

Mitchell, J.M. 1956. The fabric of natural clays and its relation to engineering practice. Highway Research Board, 35, pp. 693 - 713.

Mokievsky-Zubok, O. 1977. Glacier-caused slide near Pylon Peak, British Columbia. Canadian Journal of Earth

Sciences, 14, pp. 2657 - 2662.

Mokievsky-Zubok, O. 1978. A slide of glacier ice and rocks in western Canada. Journal of Glaciology, 20, pp. 215 - 217.

Mollard, J.D. 1982. Landforms and Surface Materials of Canada. Seventh Edition. J.D. Mollard & Associates, Regina, Saskatchewan.

Mollard, J.D., and J.R. Janes. 1984. Airphoto Interpretation and the Canadian Landscape. Energy, Mines and Resources Canada, 415 pages.

Monenco Limited. 1979. Coal subcrop study for the Highvale Mine prepared for Calgary Power Ltd.

Monenco Limited. 1983a. Highvale Mine 1982 drilling program data report prepared for TransAlta Utilities Co. Volumes 1, 2, 3, 4.

Monenco Limited. 1983b. Glaciotectonic evaluation map prepared for TransAlta Utilities Corporation, Map, Scale 1 : 1,000.

Monenco Limited. 1983c. Laboratory testing on geotechnical samles from the 1983 summer drilling program at the Highvale mine.

Monenco Limited. 1984. Highvale (1983) fall drilling program data report. Volumes 1, 2 and 3.

Moran, S.R. 1971. Glaciotectonic structures in drift. In: Till: A Symposium. Edited by R.P. Goldthwait. Ohio State University Press, Columbus, pp. 127 - 148.

Moran, S.R., L. Clayton, R.L. Hooke, M.M. Fenton, and L.D. Andriashek. 1980. Glacier-bed landforms of the Prairie Region of North America. Journal of Glaciology, 25, pp. 457 - 476.

Morgenstern, N.R. 1967. Shear strength of stiff clay. Proceedings of Geotechnical Conference, Oslo, 2, pp. 59 - 71.

Morgenstern, N.R. 1977. Slopes and excavations in heavily over-consolidated clay. State-of-the-Art Reports, Proceedings of the 9th International Conference on Soil Mechanics and Foundation Engineering, Tokyo, Japan, 2, pp. 567 - 581.

Morgenstern, N.R., and D. Cruden. 1979. Description and classification of geotechnical complexities. Proceedings of International Symposium on the Geotechnics of

Structurally Complex Formations, Capri, Associazione Geotechnica Italiana, 2, pp. 195 - 203.

Morgenstern, N.R., and K.D. Eigenbrod. 1974. Classification of argillaceous soils and rocks. ASCE, GT10, 100, pp. 1137 - 1156.

Morgenstern, N.R., and Z. Eisenstein. 1970. Methods of estimating lateral loads and deformation. Proceedings of the ASCE Specialty Conference on Lateral Stresses in the Ground and the Design of Earth-Retaining Structures, Cornell University, Ithaca, New York, pp. 51 - 102.

Morgerstern, N.R., and V.E. Price. 1965. The analysis of the stability of general slip surfaces. Geotechnique, 15, pp. 79 - 93.

Morgenstern, N.R., and J.S. Tchalenko. 1967a. Microstructural observations on shear zones from slips in natural clays. Proceedings of the Geotechnical Conference, Oslo, 1, pp. 147 - 152.

Morgenstern, N.R., and J.S. Tchalenko. 1967b. Microscopic structures in kaolin subjected to direct shear. Geotechnique, 17, pp. 309 - 328.

Morgenstern, N.R., and J.S. Tchalenko. 1967c. The optical determination of preferred orientation in clays and its application to the study of microstructure in consolidated kaolin. I. Proceedings of the Royal Society of London, Series A, 300, pp. 218 - 234.

Morgenstern, N.R., and J.S. Tchalenko. 1967d. The optical determination of preferred orientation in clays and its application to the study of microstructure in consolidated kaolin. II. Proceedings of the Royal Society of London, Series A, 300, pp. 235 - 250.

Nelson, J.D. 1973. Influence of clay fabric on bonds and dilatation. Proceedings of the International Symposium on Soil Structure, Gothenburg 1973, Sweden, pp. 153 - 159.

Norris, D.K. 1967. Structural analysis of the Queensway folds, Ottawa, Canada. Canadian Journal of Earth Sciences, 4, pp. 299 - 321.

Nurkowski, J.R. 1984. Coal quality, coal rank variation and its relation to reconstructed overburden, Upper Cretaceous and Tertiary Plains coals, Alberta, Canada. American Association of Petroleum Geologists Bulletin, 68, pp. 285 - 295.

Nye, J.F. 1952a. The mechanics of glacier flow. Journal of

Glaciology, 2, pp. 82 - 93.

Nye, J.F. 1952b. A method of calculation the thickness of the ice-sheets. Nature, 169, pp. 529 - 530.

O'Brien, N.R. 1970. The fabric of shale - an electron-microscope study. Sedimentology, 15, pp. 229 - 246.

Odom, I.E. 1967. Clay fabric and its relation to structural properties in mid-continent Pennsylavian sediments. Journal of Sedimentary Petrology, 37, pp. 610 - 623.

Oldale, R.N., and C.J. O'Hara. 1984. Glaciotectonic origin of the Masachusetts coastal end moraines and a fluctuating late Wisconsinan ice margin. Bulletin of the Geological Society of America, 95, pp. 61 - 74.

Orvig, S. 1953. The glaciological studies of the Baffin Island expedition, 1950. Part V: on the variation of the shear stress on the bed of an ice cap. Journal of Glaciology, 2, pp. 242 - 247.

Otsuki, K. 1978. On the relationship between the width of shear zone and the displacement along fault. Journal of the Geological Society of Japan, 84, pp. 661 - 669.

Park, R.G. 1983. Foundations of Structural Geology. Blackie, New York, 135 pages.

Paterson, W.S.B. 1981. The physics of Glaciers. 2nd Edition. Pergamon, Oxford, 380 pages.

Patton, F.D., and D.U. Deere. 1971. Geologic factors controlling slope stability in open pit mines. In: Stability in Open Pit Mining, edited by C.O. Brawner, and V. Milligan. Society of Mining Engineers, American Institute of Mining, Metallurgical and Petroleum Engineers, pp. 23 - 48.

Pawlowicz, J.G., C.E. Jones, and M.M. Fenton. 1985. Highwall Stability Project. Highvale Mine - Pits 03/04 core lithologs of field program June/July, 1984, prepared for TransAlta Utilities Co. Alberta Research Council, Terrain Sciences, Edmonton, Alberta.

Paul, M.A. 1983. The supraglacial landsystem. In: Glacial Geology. An Introduction for Engineers and Earth Scientists. Edited by N. Eyles. Pergamon Press, Toronto, pp. 71 - 90.

Pearson, G.R. 1959. Coal reserves for strip-mining, Wabamun Lake district, Alberta. Research Council of Alberta, Geological Division, Preliminary Report 59-1, 55 pages.

Petersen, K.S. 1977. Applications of glaciotectonic analysis in the geological mapping of Denmark. Geological Survey of Denmark, Yearbook 1977, pp. 53 - 61.

Phillips, D.W. 1939. Microscopical evidence of shearing in argillaceous rocks. Proceedings of the Yorkshire Geological Society, 24, pp. 67 - 69.

Piteau, D.R. 1970. Geological factors significant to the stability of slopes cut in rock. Proceedings of the Open Pit Mining Symposium, Johannesburg, Republic of South Africa, pp. 33 - 53.

Post, A. 1969. Distribution of surging glaciers in western North America. Journal of Glaciology, 8, pp. 229 - 240.

Prest, V.K. 1968. Nomenclature of moraines and ice-flow features as applied to the glacial map of Canada. Geological Survey of Canada Paper 67-57, 32 pages.

Prest, V.K. 1984. The Late Wisconsinan Glacier Complex. In: Quaternary Stratigraphy of Canada - A Canadian Contribution to IGCP Project. Edited by R.J. Fulton. Geological Survey of Canada, Paper 84-10, pp. 21 - 36.

Prest, V.K., D.R. Grant, and V.N. Rampton. 1968. Glacial map of Canada. Geological Survey of Canada, Map 1253A, Scale 1: 5,000,000.

Price, N.J. 1966. Fault and joint development in brittle and semi-brittle rock. Pergamon Press, Toronto, 176 pages.

Price, R.A. 1973. Large-scale gravitational flow of supracrustal rocks, southern Canadian Rockies. In: Gravity and Tectonics. Edited by K.A. DeJong and R. Scholten. John Wiley and Sons, New York, pp. 491 - 502.

Price, R.A., E.W. Mountjoy, and G.G. Cook. 1978. Geologic map of Mount Goodsir (west half), British Columbia. Geological Survey of Canada, Map 1477A, Scale 1 : 50,000.

Pusch, R. 1973a. Structural variations in boulder clay. Proceedings of the International Symposium on Soil Structure, Gothenburg 1973, Sweden, pp. 113 - 122.

Pusch, R. 1973b. Physico-chemical processes which affect soil structure and vice versa. Appendix to the Proceedings of the International Symposium on Soil Structure, Gothenburg 1973, Sweden, pp. 27 - 35.

Pusch, R. 1973c. Influence of salinity and organic matter on the formation of clay microstructure. Proceedings of the International Symposium on Soil Structure, Gothenburg

1973, Sweden, pp. 161 - 173.

Ragan, D.M. 1985. Structural Geology - An Introduction to Geometrical Techniques. Third Edition. John Wiley & Sons, Toronto, 393 pages.

Rawlings, G.E. 1977. The description of rock masses for engineering purposes. Quarterly Journal of Engineering Geology, 10, pp. 355 - 388.

Rich, J.L. 1934. Mechanics of low-angle overthrust faulting as illustrated by Cumberland thrust block, Virginia, Kentucky, and Tennessee. Bulletin of the American Association of Petroleum Geologists, 18, pp. 1584 - 1596.

Roggensack, W.D., and N.R. Morgenstern. 1978. Direct shear tests on natural fine-grained permafrost soils. Proceedings of the 3rd International Conference on Permafrost, Edmonton, Canada, 1, pp. 729 - 735.

Rotnicki, K. 1976. The theoretical basis for a model of the origin of glaciotectonic deformation. Quaestiones Geographicae, 3, pp. 103 - 139.

Rowe, P.W. 1972. The relevance of soil fabric to site investigation practice. Geotechnique, 22, pp. 195 - 300.

Ruegg, G.H.J. 1981. Ice-pushed Lower and Middle Pleistocene deposits near Rhenen (Kwintelooijen): Sedimentary-structural and lithological/granulometrical investigations. Mededelingen Rijks Geologische Dienst, 35-2/7, pp. 165-177.

Russell, L.S., and R.W. Landes. 1940. Geology of the southern Alberta Plains. Geological Survey of Canada, Memoir 221, 223 pages.

Rutherford, R.L. 1939. Edmonton, Alberta. Department of Mines and Resources, Canada, Map 506A, Scale 1: 253,440.

Rutten, M.G. 1960. Ice-pushed ridges, permafrost and drainage. American Journal of Science, 258, pp. 293 - 297.

Sardeson, F.W. 1898. The so-called Cretaceous deposits in southeastern Minnesota. Journal of Geology, 6, pp. 679 - 691.

Sardeson, F.W. 1905. A particular case of glacial erosion. Journal of Geology, 13, pp. 351 - 357.

Sardeson, F.W. 1906. The folding of subjacent strata by glacial action. Journal of Geology, 14, pp. 226 - 232.

Sauer, E.K. 1974. Geotechnical implications of Pleistocene deposits in southern Saskatchewan. Canadian Geotechnical Journal, 11, pp. 359 - 373.

Sauer, E.K. 1978. The engineering significance of glacier ice-thrusting. Canadian Geotechnical Journal, 15, pp. 457 - 472.

Sauer, E.K. 1980. Geotechnical applications of electrical borehole logging in southern Saskatchewan. Canadian Geotechnical Journal, v. 17, pp. 545 - 558.

Savigny, K.W. 1980. In situ analysis of naturally occurring creep in ice-rich permafrost soil. Unpublished Ph. D. Thesis. Department of Civil Engineering, University of Alberta, Edmonton, 439 pages.

Savigny, K.W., and N.R. Morgenstern. 1986. Creep behaviour of undisturbed clay permafrost. Canadian Geotechnical Journal, 23, pp. 515 - 527.

Sayles, F.H. 1973. Triaxial and creep tests on frozen Ottawa sand. Proceedings of the 2nd Internatinal Conference on Permafrost, North American Contribution, Yakutsk, U.S.S.R., pp. 384 - 391.

Schroeder, J., M. Beaupre, and M. Cloutier. 1986. Ice-push caves in platform limestones of the Montreal area. Canadian Journal of Earth Sciences, 23, pp. 1842 - 1851.

Schytt, V. 1969. Some comments on glacier surges in eastern Svalbard. Canadian Journal of Earth Sciences, 6, pp. 867 - 873.

Scott, J.S., and E.W. Brooker. 1968. Geological and engineering aspects of Upper Cretaceous shales in western Canada. Geological Survey of Canada, paper 66-37, 75 pages.

Sergeyev, Y.M., B. Grabowska-Olszewska, V.I. Osipov, V.N. Sokolov, and Y.N. Kolomenski. 1980. The classification of microstructures of clay soils. Journal of Microscopy, 120, pp. 237 - 260.

Shaw, J. 1982. Melt-out till in the Edmonton area, Alberta, Canada. Canadian Journal of Earth Sciences, 19, pp. 1548 - 1569.

Shetsen, I. 1984. Application of till pebble lithology to the differentiation of glacial lobes in southern Alberta. Canadian Journal of Earth Sciences, 21, pp. 920 - 933.

Sinclair, S.R., and E.W. Brooker. 1967. The shear strength of Edmonton shale. Proceedings of Geotechnical Conference, Oslo, 1, pp. 295 - 299.

Singh, R., D.J. Henkel, and D.A. Sangrey. 1973. Shear and K_0 swelling of overconsolidated clay. Proceedings of the 8th International Conference on Soil Mechanics and Foundation Engineering, Moscow, 1.2, pp. 367 - 376.

Skempton, A.W. 1948. The rate of softening in stiff fissured clays with special reference to London clay. Proceedings of the 2nd International Conference on Soil Mechanics and Foundation Engineering, Rotterdam, 2, pp. 50 - 53.

Skempton, A.W. 1954. The pore-pressure coefficients A and B. Geotechnique, 4, pp. 143 - 147.

Skempton, A.W. 1966. Some observations on tectonic shear zones. Proceedings of the 1st Congress of International Society of Rock Mechanics, Lisbon, 1, pp. 329 - 335.

Skempton, A.W. 1985. Residual strength of clays in landslides, folded strata, and the laboratory. Geotechnique, 35, pp. 3 - 18.

Skempton, A.W., and P. LaRochelle. 1965. The Bradwell slip: a short-term failure in London Clay. Geotechnique, 15, pp. 221 - 242.

Skempton, A.W., and D.P. Petley. 1967. The strength along structural discontinuities in stiff clays. Proceedings of the Geotechnical Conference on shear strength properties of natural soils and rocks, 2, pp. 29 - 46.

Slater, G. 1926. Glacial tectonics as reflected in disturbed drift deposits. Proceedings of the Geologists' Association, 37, pp. 392 - 400.

Slater, G. 1927a. Structure of the Mud Buttes and Tit Hills in Alberta. Bulletin of the Geological Society of America, 38, pp. 721 - 730.

Slater, G. 1927b. Studies in the drift deposits of the south-western part of Suffolk. Proceedings of the Geologists' Association, 38, pp. 157 - 216.

Sloane, R.L., and T.F. Kell. 1966. The fabric of mechanically compacted kaolin. Proc. 14th Nat. Conf. Clays and Clay Minerals, pp. 289 - 296.

Smalley, I.J., and J.A. Cabrera. 1969. Particle association in compacted kaolin. Nature, 222, pp. 80 - 81.

Smart, P., and N.K. Tovey. 1981. Electron Microscopy of Soils and Sediments: Examples. Clarendon Press, Oxford, 177 pages.

Smith, M.W., and C.T. Hwang. 1973. Thermal distribution due to channel shifting, Mackenzie delta, N.W.T., Canada. Proceedings of the 2nd International Conference on Permafrost, North American Contribution, Yakutsk, U.S.S.R., pp. 51 - 60.

Sonstegaard, E. 1979. Glaciotectonic deformation structures in unconsolidated sediments at Os, south of Bergen. Norsk Geologisk Tidsskrift, 59, pp. 223 - 228.

Souchez, R.A. 1967. The formation of shear moraines: an example from south Victoria land, Antarctica. Journal of Glaciology, 6, pp. 837 - 843.

Stalker, A. MacS. 1960a. Surficial geology of the Red Deer-Stettler Map-area, Alberta. Geological Survey of Canada, memoir 306, 140 pages.

Stalker, A. MacS. 1960b. Ice-pressed drift forms and associated deposits in Alberta. Geological Survey of Canada, Bulletin 57, 38 pages.

Stalker, A. MacS. 1961. Buried valleys in central and southern Alberta. Geological Survey of Canada, Paper 60-32, 13 pages.

Stalker, A. MacS. 1973. Surficial geology of the Drumheller area, Alberta. Geological Survey of Canada, memoir 370, 122 pages.

Stimpson, B., and G. Walton. 1970. Clay mylonites in English coal measures - their signifiance in opencast slope stability. Proceedings of the 1st International Congress of International Association of Engineering Geology, Paris, Section 9, pp. 1388 - 1393.

Sugden, D.E., and B.S. John. 1976. Glaciers and Landscape. Arnold, London, 376 pages.

Swinzow, G.K. 1962. Investigation of shear zones in the ice sheet margin, Thule Area, Greenland. Journal of Glaciology, 4, pp. 215 - 229.

Tabor, D., and J.C.F. Walker. 1970. Creep and friction of ice. Nature, 228, pp. 137 - 139.

Tchalenko, J.S. 1968a. The microstructure of London clay. Quarterly Journal of Engineering Geology, 1, pp. 155 - 168.

Tchalenko, J.S. 1968b. The evolution of kink-band and the development of compression textures in sheared clays.

Tectonophysics, 6, pp. 159 - 174.

Tchalenko, J.S. 1970. Similarities between shear zones of different magnitudes. Bulletin of the Geological Society of America, 81, pp. 1625 - 1640.

Tchalenko, J.S., and N.N. Ambraseys. 1970. Structural analysis of the Dasht-e Bayaz (Iran) earthquake fractures. Bulletin of the Geological Society of America, 81, pp. 41 - 60.

Terzaghi, K. 1936. Stability of slopes in natural clay. Proceedings of the 1st International Conference in Soil Mechanics, Harvard, 1, pp. 161 - 165.

Terzaghi, K. 1943. Theoretical Soil Mechanics. John Wiley & Sons, New York, 510 pages.

Terzaghi, R.D. 1965. Sources of error in joint surveys. Geotechnique, 15, pp. 287 - 304.

Thomson, S. 1970. Riverbank stability study at the University of Alberta, Edmonton. Canadian Geotechnical Journal, 7, pp. 157 - 168.

Thomson, S. 1971. Analysis of a failed slope. Canadian Geotechnical Journal, 8, pp. 596 - 599.

Thomson, S., and D.W. Hayley. 1975. The Little Smoky Landslide. Canadian Geotechnical Journal, 12, pp. 379 - 392.

Thomson, S., and E.F. Lobacz. 1973. Shear strength at a thaw interface. North American Contribution 2nd International Permafrost Conference, Yakutsk, pp. 419 - 426.

Thomson, S., and D.S. Matheson. 1970a. Clay pits in south-eastern Alberta. Department of Civil Engineering, University of Alberta, Edmonton, Alberta, Unpublished Internal Note SM 7, 19 pages.

Thomson, S., and D.S. Matheson. 1970b. The Dunphy Landslide. Department of Civil Engineering, University of Alberta, Unpublished Internal Note SM 8, 7 pages.

Thomson, S., and R.W. Tweedie. 1978. The Edgerton Landslide. Canadian Geotechnical Journal, 15, pp. 510 - 521.

Tong, Z.Q. 1983. In-situ direct shear tests at the freeze/thaw interface and in thawed soils. Proceedings of the 4th International Conference on Permafrost, Fairbanks, Alaska, pp. 1278 - 1282.

Tovey, N.K., and K.Y. Wong. 1977. Preparation, selection and interpretation problems in scanning electron microscope studies of sediments. In: Scanning Electron Microscopy in the Study of Sediments. Edited by W. Brain Whalley. GeoAbstracts Limited, England, pp. 181 - 199.

Tovey, N.K., and K.Y. Wong. 1980. The microfabric of deformed kaolin. Journal of Microscopy, 120, pp. 329 - 342.

Townsend, F.C., and P.A. Gilbert. 1974. Engineering properties of clay shales. Report 2. Residual shear strength and classification indexes of clay shales. U.S. Army Engineer Waterways Experiment Station, Technical Report S-71-6.

Townsend, F.C., and P.A. Gilbert. 1976. Effects of specimen type on the residual strength of clays and clay shales. Soil Specimen Preparation for Laboratory Testing, ASTM STP 599, American Society for Testing and Materials, pp. 43 - 65.

Trainer, F.W. 1973. Formation of joints in bedrock by moving glacial ice. Journal of Research of the United States Geological Survey, 1, pp. 229 - 235.

Ussing, N.V. 1907. Om Floddale og Randmoraener i Jylland-Kgl. Danske Vidensk. Selsk. Forh., 4, pp. 161 - 213.

Van Olphen, H. 1963. An Introduction to Clay Colloid Chemistry. John Wiley & Sons, New York.

Verrall, P. 1968. Observations on geological structures between the Bow and North Saskatchewan Rivers. Alberta Society of Petroleum Geologists, 16th Annual Field Conference Guide Book, pp. 107 - 118.

Wardlaw, N.C., M.R. Stauffer, and M. Hoque. 1969. Striations, giant grooves, and superposed drag folds, Interlake area, Manitoba. Canadian Journal of Earth Sciences, 6, pp. 577 - 593.

Wateren, F.M. van der. 1981. Glacial tectonics at the Kwintelooijen sandpit, Rhenen, the Netherlands. Mededelingen Rijks Geologische Dienst, 35-2/7, pp. 252 - 268.

Wateren, F.M. van der. 1985. A model of glacial tectonics, applied to the ice-pushed ridges in the central Netherlands. Bulletin of the Geological Society of Denmark, 34, pp. 55 - 74.

Weaver, J.S. 1979. Pile foundations in Permafrost. Unpublished Ph. D. thesis. Department of Civil

Engineering, University of Alberta, Edmonton, 225 pages.

Webb, J.B. 1951. Geological history of Plains of western Canada. Bulletin of the American Association of Petroleum Geologists, 35, pp. 2291 - 2315.

Weertman, J. 1957. On the sliding of glaciers. Journal of Glaciology, 3, pp. 33 - 38.

Weertman, J. 1961. Mechanism for the formation of inner moraines found near the edge of cold ice caps and ice sheets. Journal of Glaciology, 3, pp. 965 - 978.

Welton, J.E. 1984. SEM Petrology Atlas. American Association of Petroleum Geologists, Tulsa, 237 pages.

Westgate, J.A. 1968. Surficial geology of the Foremost-Cypress Hills area, Alberta. Research Council of Alberta, Bulletin 22, 122 pages.

Williams, G.D. 1984. The calculation of horizontal thrust transport using excess area in cross-section. Tectonophysics, 104, pp. 177 - 182.

Williams, M.Y., and W.S. Dyer. 1930. Geology of southern Alberta and southwestern Saskatchewan. Geological Survey of Canada, Memoir 163, 160 pages.

Wilson, S.D. 1974. Landslide instrumentation for the Minneapolis Freeway. Transportation Research Board, Transportation Research Record, no. 482, pp. 31 - 42.

Wright, H.E.Jr. 1971. Retreat of the Laurentide Ice Sheet from 14,000 to 9,000 years ago. Quaternary Research, 1, pp. 316 - 330.

Yong, R.N., and D.E. Sheeran. 1973. Fabric unit interaction and soil behaviour. Proceedings of the International Symposium on Soil Structure, Gothenburg 1973, Sweden, pp. 176 - 183.

Zandstra, J.G. 1981. Petrology and Lithostratigraphy of ice-pushed Lower and Middle Pleistocene deposits at Rhenen (Kwintelooijen). Mededelingen Rijks Geologische Dienst, 35-2/7, pp. 178 - 191.

Appendix A - Location and Accessibility of the Outcrops and Ice-Thrust Features in the Study Areas

A.1 Wabamun Lake Area

South of Wabamun Lake, sections are exposed on the highwalls in Pits 2 and 3, Highvale Coal Mine, which is about 1 to 3.3 km west of the village of Sundance (Appendix C, Figure C.5). The sections were cut into terraces which have a flat to slightly rolling topography.

A section is also found at a roadcut about 800 m south of the southwestern shore of Isle Lake along Highway 16, which is about 1.2 km west of the village of Gainford and 13 km east of the village of Entwistle (Appendix C, Figure C.10). The section is about 18 m high, 350 m long and consists of two ridges trending approximately east-west, that is, roughly parallel to the southwestern shore of Isle Lake.

Figure 3.1 shows the regional location of the sections in the area.

A.2 Edmonton Area

Two sites were investigated in the Edmonton area. These are (Figure 3.1):

1. Nisku - about 22 km south of city of Edmonton. The outcrops are located along the ditches of Highway 625 and are about 2.5 km east of the turnoff from Highway 2 at the town of Nisku (Sec. 30, Tp. 50, R. 24, W. 4th

Mer.).

2. Gibbons - about 30 km north of city of Edmonton and can be reached by travelling along Highway 37. The exposed section is located near the bridge abutment that crosses the Sturgeon River north of the town of Gibbons (Sec. 15, Tp. 56, R. 23, W. 4th Mer.).

No field visits were performed in the city of Edmonton. The ice-thrust features of this city mentioned in this study are mainly based on the examination of the published surficial geology reports and drill hole logs (McPherson and Kathol, 1972; Kathol and McPherson, 1975).

A.3 Red Deer - Stettler Area

Four sites were investigated in the Red Deer - Stettler area (Figure 3.1). They are:

1. Lowden Lake area - the exposures are located at roadcuts and ditches along Highway 56 and are approximately 22 km south of town of Stettler (Tp. 36, R. 19, W. 4th Mer.).
2. Beltz Lake area - exposures are found along the eastern shore of Beltz Lake northeast of the Lowden Lake area (Sec. 30, Tp. 37, R. 18, W. 4th Mer.).
3. Nevis Area - the outcrops are found along roadcuts of Highway 21A and are about 0.5 km and 0.9 km east of its intersection with Highway 21 (Sec. 34, Tp. 38, R. 22, W. 4th Mer.). The exposures are situated in a north-south

trending ridge.

4. Northwest of Sullivan Lake Area - the section is exposed in a ditch along Highway 12 northwest of Sullivan Lake, about 18 km west of the town of Castor and about 31 km east of town of Stettler. The section is about 32.6 m long and 2.4 m high.

A.4 Hanna - Sedgewick Area

In the Hanna - Sedgewick area, the outcrops are chiefly exposed in roadcuts, ditches and river valleys along Highway 36 between the towns of Hanna and Alliance (Figure 3.1). In order to understand the glaciotectonic distribution in east-central Alberta, other districts adjacent to the exposures were also investigated by studying the published surficial and glacial geology reports of these districts. As a result, the total study area in Hanna - Sedgewick area is about 11,086 km² that extends from latitude 51°35' N and longitude 111°00' W - 112°00' W to latitude 53°00' N and longitude 111°00' W - 112°00' W. It includes the districts of Sedgewick, Galahad-Hardisty, Alliance-Brownfield, Castor and Coronation (Figure 3.1).

Four exposures in these districts had been examined by the author (Sec. 13, Tp. 33, R. 14; Sec. 24 and 36, Tp. 34, R. 14; Sec. 20, Tp. 39, R. 13, W. 4th Mer.).

A.5 Cypress Hills Area

In the Cypress Hills area, the sections studied, which are exposed within two clay pits, Pit 39 (Sec. 21, Tp. 8, R. 4, W. 4th Mer.) and Pit 45 (Sec. 9, Tp. 8, R. 4, W. 4th Mer.), are located on the northwestern flank of Eagle Butte at the western margin of the Cypress Hills Plateau (Figure 3.1). The Pits are about 35 and 37.5 km south of the town of Dunmore.

Pit 39 is about 135 m wide and 180 m in length, and the section studied is exposed on a south-facing wall inside this Pit. Pit 45 has a length and width of about 450 m and 300 m respectively and the section studied is located on its southwest-facing wall. Pits 39 and 45 are at topographic elevations of about 1097 m (3600 ft) and 1234 m (4050 ft) respectively. At present, these clay pits are mined by the Medicine Hat Brick and Tile Co. Ltd. for manufacturing brick, tile and clay pipes.

Appendix B - Physiography, Surficial Geology, and Glacial History of the Study Areas

B.1 Wabamun Lake Area

B.1.1 Physiography

Physiographically, the area lies within the Alberta Plain where the land slopes from an elevation of 1200 m in the southwest to 700 m in the northeast (Andriashek et al., 1979). Isle Lake lies in the preglacial Onoway Valley while Wabamun Lake seems to be located in the interglacial North Saskatchewan Valley (Stalker, 1961, map 47). The former is equivalent to the Onoway Valley of Carlson (1971). The preglacial valleys are broad and gently sloped, and usually have a width ranging from 3.2 to 16 km; while the interglacial valleys are generally 0.4 to 4.8 km wide. Two meltwater channels exist in the area and both flow from the southern shore of Isle Lake southward to enter the western tip of Wabamun Lake.

B.1.2 Surficial Geology

The surficial geology of the area has been studied by Andriashek et al. (1979) and Fenton et al. (1983). The terrain north of Isle and Wabamun Lakes is covered by more than 2 m of hummocky moraine and with a relief more than 3 m. Ice-deformed bedrock with a relief ranging from less than 3 to 30 m and occasional depressions filled with bog and marsh are noted south of Wabamun Lake. This relief extends to the modern North Saskatchewan River. Between the southern shore of Isle Lake and the northwestern shore of Wabamun Lake, the area is overlain by flat to gently rolling outwash and glaciolacustrine deposits with local areas of hummocky moraine.

The surficial bedrock is the Lower Tertiary Paskapoo Formation which is mainly composed of bentonitic sandstone, coal, and thin shaly layers. It is underlain by the Upper Cretaceous Battle Formation which chiefly consists of bentonitic sandstone, shales, coal and bentonite layers.

It has been suggested that Wabamun Lake might have been formed and/or enlarged by glacial thrusting (Andriashek et al., 1979). About 35 km northeast of this lake, ice-deformed bedrock of Tertiary age and preglacial Saskatchewan Gravels are observed (Babcock et al., 1978); moreover, in Genesee which is about 26 km southeast of Wabamun Lake, sand and till were found underlying about 1 m of the Lower Tertiary Paskapoo Formation due to the rejuvenation of a local ice lobe (Chan, 1986, plates 2.1 and 2.4).

B.1.3 Glacial History

Stalker (1961) suggested that the Laurentide glacier, which advanced into and retreated out of the preglacial valleys several times during the Pleistocene Epoch, had blocked and diverted the course of some major preglacial rivers in central and southern Alberta, causing new channels to form during glacial and/or interglacial periods. The proglacial meltwater channels or spillways probably had produced new river valleys which might be entered by the ice sheet during a later advance.

B.2 Edmonton Area

B.2.1 Physiography

The Edmonton area is located on the Alberta Plains with the near surface Upper Cretaceous bedrock dipping gently southwest (Bayrock, 1972). According to Farvolden (1963a, p. 58; fig. 14), the area is bounded by the Joffre Hills bedrock physiographic unit and the Kingman bedrock physiographic divide in the south and in the east by the Cooking Lake bedrock physiographic divide.

The Beverly Valley, or the North Saskatchewan Bedrock Channel of Farvolden (1963a), is the largest preglacial valley in the Edmonton area. It is a broad valley, up to 8 km wide and 60 m deep, with gently sloping valley walls having a gradient of approximately one metre per kilometre (Kathol and McPherson, 1975, p. 23; fig. 22). North of this valley, the plain is relatively flat and rises gradually from about 610 m to 732 m in elevation; while south of the valley the surface rises toward the Kingman and Cooking Lake bedrock physiographic divides with a gradient generally less than 9.5 m/km. Other tributaries of the Beverly Valley in the Edmonton area include the Stony, the Namao, and the New

Sarepta Valleys. These Valleys have a width varying from 2 - 3 km, a depth of 8 - 30 m, and a gradient of 1.3 m per km to 4 m per km. A north-south trending tributary of the preglacial Beverly Valley, which is occupied by Blackmud Creek at present, is located at about 1 km east of the town of Nisku (Farvolden, 1963a, fig 14). Another tributary of the Beverly Valley, which is occupied by the Sturgeon River, is located close to the town of Gibbons.

B.2.2 Surficial Geology

In the Edmonton area, glaciolacustrine sediments form a NE-SW trending belt with a width of about 37 km (Bayrock, 1972). Essentially this belt is surrounded by ground moraine and locally by aeolian deposits and glaciofluvial deposits. A region of hummocky disintegration moraine is located just behind the ground moraine on the southeastern side of the belt.

The study area located east of the town of Nisku is on an eroded lacustrine plain with glaciofluvial deposits overlying lacustrine deposits, till and bedrock (Bayrock, 1972). These surficial deposits are underlain by the Upper Cretaceous Horseshoe Canyon Formation. The study area located at Gibbons is covered mainly by ground moraine and outwash which is underlain by the Upper Cretaceous Wapiti Formation. The surficial geology of the Edmonton area (including Nisku and Gibbons) has been studied by Kathol and McPherson (1975), Green (1982), and Rutherford (1939).

According to Kathol and McPherson (1975), ice-disturbed bedrock had been observed in the Edmonton area and in some places large pieces of bedrock were excavated and carried away by the glacier while in other places the bedrock was squeezed and folded but not significantly transported. An east-west trending ridge of deformed bedrock, 2.5 km wide and 3 km long and covered by less than 7 m of overburden, was observed approximately 2 km northwest of Sherwood Park, and a section of contorted bedrock was exposed on Highway 14 in the vicinity of the city of Edmonton (sec. 27, Tp. 52, R. 23, W. 4th Mer.) (Kathol and McPherson, 1975, p. 30; figs. 25, 26). Moreover, ice-disturbed preglacial and glacial sediments were found in an excavation in downtown Edmonton (Catto, 1984). Indeed, stratigraphic sections and drillhole logs prepared by McPherson and Kathol (1972) in the Edmonton area indicated that suspected ice-shoved bedrock was found along the broad valley slopes of the preglacial Beverly Valley and its tributaries, the Stony Valley and the Namao Valley. Most of the ice-shoved bedrock was observed away from the thalwegs of the preglacial valleys although [illegible] drillhole shows ice-deformed bedrock is present directly below the thalweg of the Beverly Valley (McPherson and Kathol, 1972, drillhole #190, p. 67).

B.2.3 Glacial History

It is believed that the last ice advanced into the area about 25,000 to 30,000 years ago in late Wisconsinan time and deglaciation was probably completed about 9,000 years ago (Bayrock, 1972).

Generally, the till is thickest along the buried valleys, for example, the till thickness along the entire length of the Beverly valley often exceeds 15 m (Kathol and McPherson, 1975). The presence of thick layers of till in these preglacial valleys indicates that they were occuppied by the glacier during the last glaciation. Farvolden (1963a) and Bayrock (1972) showed that the Sturgeon River Valley was a meltwater channel which trended approximately northeast except close to the town of Gibbons, where it turned toward the southeast.

B.3 Red Deer - Stettler Area

B.3.1 Physiography

Physiographically, the Red Deer - Stettler area can be divided into the Central Highland, the Red Deer Lowland, the Torlea Flats Lowland and the Western Highland (Stalker, 1960a). As far as this study is concerned, interest is focussed on the Central Highland and the Torlea Flats Lowland where the sections are exposed and have been examined.

The Central Highland is located in the central and south-central parts of the Red Deer - Stettler map-area and is underlain by the relatively resistant Lower Tertiary Paskapoo Formation. It is bordered by the Torlea Flats

Lowland on the east and is about 60 - 90 m higher in elevation than the adjoining areas. The Torlea Flats Lowland occupies a broad area in southeastern Alberta and includes all the area east of the Central Highland. It is underlain mainly by the less-resistant Upper Cretaceous bedrock.

Two major preglacial channels are present in the area. They are the Red Deer Bedrock Channel and the Buffalo Lake Bedrock Channel (Farvolden, 1963a, fig. 14; Stalker, 1961, map 47-1960). At present, Big Valley Creek follows a former meltwater channel and flows southeastwards about 2.5 km southwest of the study area near Lowden Lake. The study area near Nevis is drained both by Tail Creek and the modern Red Deer River which follows an interglacial valley.

The study areas in the Red Deer - Stettler area are located immediately beside the bedrock physiographic boundary of the Joffre Hills and the Battle Plain (Farvolden, 1963a, fig. 14). The Joffre Hills are expressed on the surface by an escarpment which rises westward from an elevation of 792 m at its foot or the boundary with the Battle Plain to about 1036 m in Tp. 37, R. 25 - 26, W. 4th Mer. (Farvolden, 1963a, p. 58). It is noted that the southeastern boundary of the Joffre Hills and the Battle Plain approximately coincides with the southeastern edge of the Central Highland physiographic unit of Stalker (1960a). The study areas at Nevis lie at the southeastern corner of the Central Highland near the boundary with the Torlea Flats Lowland, or according to Farvolden (1963a), they are situated at the foot of the Joffre Hills bedrock physiographic unit with the Battle Plain physiographic unit lying east of it. Bedrock topographic and geology maps (Farvolden, 1963a, fig 14; Green, 1982) indicate that the relatively resistant sandstone of the Paskapoo Formation has formed a 30 m high NW-SE trending escarpment 4.2 km west of the Lowden Lake area. The Neutral Hills, Mud Buttes and Tit hills, where ice-thrust features were found by other workers (Slater, 1927a; Kupsch, 1962), are located 150 km east of the Lowden Lake area.

B.3.2 Surficial Geology

The study area is mainly covered by the Buffalo Lakes moraine and the Torlea Flats ground moraine.

The Buffalo Lake moraine overlies the eastern part of the Central Highland physiographic unit and extends beyond its northern and eastern boundaries into the Torlea Flats Lowland (Stalker, 1960a, p. 8). This moraine is chiefly composed of hummocky dead-ice moraine which formed belts surrounding Buffalo Lake. The Torlea Flats ground moraine lies east of the Buffalo Lake moraine and corresponds roughly to the Torlea Flats physiographic unit. It is composed mainly of ground moraine and locally consists of hummocky moraine.

The near surface bedrock in the Red Deer - Stettler area is the Lower Tertiary Paskapoo Formation and the Upper Cretaceous Whitemud and Battle Formations which are exposed to the west, the Upper Cretaceous Horseshoe Canyon Formation which outcrops to the east, and the Upper Cretaceous Bearpaw Formation which is exposed in the northeastern and southeastern corners of the area.

B.3.3 Glacial History

During the glacial periods, several major glacier advances and retreats occurred in the region. The late glacial stage in southern Alberta, the Late Wisconsinan Substage, took place about 23,000 years ago when the ice sheet had extended southward into Montana (Fulton, 1984, p. 4). Deglaciation was completed at about 9,000 years ago (Bayrock, 1972). Stalker (1960a, p. 67) observed the presence of two or more tills in individual exposures in the Red Deer - Stettler area which are evidence of multiple local glaciation in this region.

Stalker (1960a, p. 74) has estimated that the last glacier rose to an altitude of about 1370 m in southwestern and central Alberta, and the maximum ice thickness in the Torlea Flats region and the Central Highland was approximately 610 m and 400 m respectively.

The regional direction of the last ice movement in southwestern and central Alberta is southward or south-southeastward (Stalker, 1960a, p. 72); as evident from the orientation of drumlins and ice-flow markings, which show trends of about 125° - 150° azimuth, found about 8.9 km to 17.8 km northwest of the town of Bashaw. However, the local direction of movement varies as much as 70° to the east or west of the general direction. Indeed, ice-flow markings (flutings, gouges, drumlinoidal forms) with trends of 201° to 234° are observed 30 km northeast of Lowden Lake. Furthermore, ridges of undetermined origin with a trend of 123° - 173° appear about 9.7 km southwest of the study area near Lowden Lake (Stalker, 1960a, map 1081A). The orientation of these linear features seem to suggest that the ice direction in Red Deer-Stettler area varied from southeast to west.

Initial deglaciation occurred in the Central Highland and ice stagnation started to spread northward and eastward as the ice-sheet thinned. The following processes were inferred (Stalker, 1960a):

1. While the ice had stagnated on the Central Highland which caused the formation of the Buffalo Lake moraine system with extensive pitted outwash, moraine plateaus, kames, ice-block ridges and hummocky moraine; the ice in the adjoining areas (Torlea Flats Lowland) was still active and continued flowing against the Central Highland (Stalker, 1960a, figures 11, 12).
2. When the ice had retreated and stagnated in the study area for some time, a rejuvenation probably occurred which caused the ice to cover the entire Torlea Flats Lowland (Stalker, 1960a, p. 92). This might be due to a prolonged decrease in regional temperature and a rapid thickening of the glacier. Various ice-flow markings

with a trend of 213° near the southeastern shore of Gough Lake (about 18 km southeast of the Lowden Lake) are evidence of this rejuvenation (Stalker, 1960a, Map 1081A).

B.4 Hanna - Sedgewick Area

B.4.1 Physiography

In general, the area mainly lies in the Torlea flats which is a north-south trending belt of relatively featureless ground moraine (about 322 km in length and about 40 - 80 km in width) in east-central Alberta (Gravenor and Bayrock, 1955; Gravenor, 1956; Gravenor and Ellwood, 1957; Bayrock, 1958a). The flats are bounded by the Viking moraine in the east and by the Buffalo Lake moraine in the west. The northern and eastern portions of Sedgewick district, the Hardisty district and the eastern portion of Alliance-Brownfield district lie in the hummocky dead-ice Viking moraine; while the western portion of Sedgewick district, the western portion of Alliance-Brownfield district, the Castor and the Coronation districts lie in the Torlea flats.

Erosional remnants of the Bearpaw Formation such as the Neutral Hills, which are a series of SE-NW trending ridges and valleys formed due to glacial action, are found at about 70 km east of the town of Castor (Figure 3.1). Moreover, a small mesa (about 70 m high) which is believed to be glacially contorted Upper Cretaceous sediments (Bayrock, 1958a, p. 27) is found at the southeast corner of the Brownfield district.

Although no buried valleys or preglacial gravels have been found in the Alliance-Brownfield district (Bayrock, 1958a, p. 27), many debris filled stream-trenches are found in the Galahad-Hardisty district, the central and eastern Sedgewick district (Gravenor and Ellwood, 1957), the northwestern portion of the Brownfield district and the northeastern portion of the Alliance district. The valleys of these trenches may follow preglacial troughs and vary from 0.32 - 8.24 km (Battle River) wide although generally they have a width of about 0.9 km (Bayrock, 1958a, 1958b). They were completely to partially filled by hummocky dead-ice moraine to coarse-grained glaciofluvial deposits (Bayrock, 1958b, p. 7), and in most cases, the morphology of the till surface at the base of the stream-trenches is similar to the till surface outside the stream-trenches. It is thought that stream-trenches were glacial in origin and were formed when a cold glacier became stagnant and downwasted about 11,000 years ago. Supraglacial meltwater channels flowed along crevasses of the glacier and incised through both the ice and the underlying bedrock, producing stream-trenches. The position of these trenches was partly controlled by fractures which developed in the cold ice. Some of the stream-trench ice banks collapsed during this process and forced water to seek new channels thus forming an anastomosing or interconnected pattern of stream-trenches. Later the ice wasted away from the trenches; however, subsequent climatic change probably caused a minor readvance of the ice into the meltwater channels. The ice spreaded out as a viscous fluid conforming to topography, and in this manner the stream trenches were partly to totally filled with till (Bayrock, 1958b, p. 20; Gravenor and Ellwood, 1957).

The Sullivan Lake basin is considered as part of a glacial spillway (Gravenor, 1956, p. 8), and the Battle River is believed to be a glacial spillway (Gwynne outlet in part) and the overflow of this spillway northwest of the Alliance district had formed an outlet which is occupied by the Paintearth Creek at present.

B.4.2 Surficial Geology

The surficial bedrock in Torlea flats is mainly the Upper Cretaceous Horseshoe Canyon, the Bearpaw and the Belly River Formations (Green, 1982), and the strata slope gently to the southwest with a dip of 0.076° to 0.15° (Le Breton, 1963).

The thickness of till in Torlea flats varies from 7.6 to 15.2 m (Gravenor, 1956). Outwash deposits are usually found in the north, northwest and northeast of the town of Sedgewick and east of Sullivan Lake. In general, there is only one till layer in the area and this is probably due to the last glacier which had removed all the evidence of previous glaciations in the region (Gravenor and Bayrock, 1955, p. 24; Gravenor, 1956, p. 10). The overflows of the Gwynne and Paintearth Creek outlets near the town of Alliance had flooded the surrounding countryside, eroded away most of the till cover and deposited a layer of outwash material or left exposed bedrock behind (Bayrock, 1958a). The meltwaters that collected in the Sullivan Lake basin, were later spilled and moved in an easterly to southeasterly direction. This flow removed much of the ground moraine and either exposed large flat areas of the Horseshoe Canyon Formation (mainly sandstone) or covered the area with a layer of glaciofluvial sediments (mainly gravels and sands) east of Sullivan Lake (Gravenor, 1956, map 56-2).

B.4.3 Glacial History

Field studies indicate that the general regional ice movement of the last Wisconsinan glacier in east-central Alberta is south to southwest (Gravenor, 1956; Gravenor and Bayrock, 1955, p. 25; Gravenor and Ellwood, 1957). However, Gravenor and Ellwood (1957, p. 25; maps 57-1A, 57-1B) suggested that during different periods of the same ice-advance or retreat, local ice movement directions varied considerably over short distances due to local topographic control. Indeed, flutings found at the north and east of the Sedgewick district show that the ice moved in a southeasterly direction following a glacial trough; while a few kilometres south of the town of Jarrow lineations suggest a southwesterly ice movement direction (Gravenor and Ellwood, 1957, p. 3).

The last glacier which advanced into the Galahad-Hardisty and the Alliance-Brownfield districts at about 21,600 ± 900 years ago (Gravenor and Ellwood, 1957) has a maximum thickness of about 1067 m (Bayrock 1958a, p. 27; 1958b, p. 18). Bayrock (1958a, p. 28) believed that deglaciation in Alberta might have taken place at about 11,000 years ago. Surficial deposits and regional glacial landforms in east-central Alberta suggest that the dominant method of the last glacial retreat was by large-scale stagnation and downwasting in a downslope direction to the east and northeast (Gravenor and Bayrock, 1955, 1956; Bayrock, 1958a, 1958b). This is inferred by the north-south trending Buffalo Lake and Viking dead-ice moraines which lie at about 45° to the ice advance direction. Moreover, the lack of eskers and related ice-contact features over much of central Alberta is also a direct result of this downslope retreat. This is because proglacial lakes, which always form in a downslope retreat glacier, would raise the water table above the base of the ice and reduce the hydraulic heads of subglacial meltwater channels and decrease the subglaciofluvial activities. However, the position of the Gwynne outlet near the Edmonton and the Sedgewick districts suggests that the ice retreated to the north or slightly east of north (Gravenor and Ellwood, 1957, p. 28; Gravenor and Bayrock, 1956).

The debris filled stream-trenches, and the Viking and the Buffalo Lake moraines are thought to be contemporaneous with the retreat of the last glacier due to stagnation (Gravenor and Bayrock, 1956).

B.5 Cypress Hills Area

B.5.1 Physiography

The study area is in the well dissected Upland Areas physiographic unit of the Foremost-Cypress Hills area (Westgate, 1968, fig. 14). The Upland Areas surround the Cypress Hills Plateau which, in turn, are surrounded by an undulating till plain. Williams and Dyer (1930) showed that the small mesas and buttes just west of the Cypress Hills Plateau are probably remnants of the Flaxville Plain which is an erosional surface formed during Miocene to early Pliocene time and has an elevation of about 1219 m (4000 ft) in the study area. Eagle Butte probably is one of these remnants.

In the area of concern, the preglacial Medicine Hat Valley which runs along the western flank of Cypress Hills Plateau, is about 40 km to 65 km wide between water divides and is about 3.75 km to 10 km wide at its bottom, and has a depth of 76 m to 366 m. Several tributaries of the Medicine Hat Valley lie on the northern and western slopes of the Cypress Hills and some of the heads of these tributaries have reached the northern, western and southern flanks of Eagle Butte west of the Cypress Hills Plateau (Westgate, 1968, fig. 6).

At present, the area is drained mainly by the Milk River in the south and the south Saskatchewan River in the northwestern corner of the area. The Medicine Lodge Coulee, which is an ice marginal channel (Westgate, 1968, p. 37), flows toward the southeast between the Eagle Butte and the base of the Cypress Hills Plateau.

B.5.2 Surficial Geology

According to Westgate (1968, map 29), the Upland Areas are mainly covered by three belts of surficial deposits which successively surround the Cypress Hills Plateau. The closest belt to the Plateau is a thin layer of drift which veneered the bedrock upland, this is followed by a belt of hummocky disintegration moraine, the farthest is a belt of ground moraine. Hummocky and ridged end moraines are found locally within the Medicine Lodge Coulee (Westgate, 1968, map 29).

The Cypress Hills Plateau is free of drift. The glacial drift in Eagle Butte area (where the exposures of ice-thrust features are found), is 0.0 - 15.2 m thick. The Medicine Lodge Coulee is filled with drift, 15.2 - 30.5 m thick. Four tributaries of the preglacial Medicine Hat Valley which extend from the north and west to the vicinity of the Butte, have a drift thickness of 15.2 - 30.5 m (Westgate, 1968, figs. 6 and 7).

Detailed descriptions of the Upper Cretaceous to Lower Tertiary Formations that occur at or close to the surface in the area have been given by Russell and Landes (1940) and Irish (1967).

The southern Alberta Plains are situated on a broad, northerly plunging anticline known as the Sweet Grass Arch. Since the Foremost-Cypress Hills area lies east of this Arch, the dominant dip direction of the beds is to the east and northeast (Westgate, 1968, p. 13). Many subsidiary folds and deformations are associated with the Sweet Grass Arch and disturbed strata in the vicinity of Eagle Butte have been reported and studied by Russell and Landes (1940), Irish (1967), Westgate (1968) and Thomson and Matheson (1970a).

Russell and Landes (1940, p. 124) observed overturned Whitemud Formation in a coulee at an elevation of 1250 m (4100 ft) at the northwestern flank of Eagle Butte (Sec. 9, Tp. 8, R. 4, W. 4th Mer.) which is the approximate location of Pit 45 where the outcrops of ice-thrust features were observed (Appendix A); moreover, disturbed strata of the Eastend, Whitemud and Ravenscrag Formations were found at an elevation of about 1097 m (3600 ft) (Sec. 21, Tp. 8, R. 4, W. 4th Mer.) which is close to the location of Pit 39 (Appendix A). Furthermore, thrust faults which upthrust toward the south were found near and just north of Eagle Butte (Russell and Landes, 1940, p. 126; Irish, 1967);

however, slumping and thick surficial glacial deposits in the region have obscured the lateral extension of these faults. Irish (1967) noted that a NE-SW trending thrust fault (upthrusting southeast), with a length of 6.1 km, is located at about 2.8 km northwest of Pit 45. Westgate (1968, fig. 4) observed highly disturbed bedrock in the Bullshead Creek district (Tp. 8 and 9, R. 4 and 5, W. 4th Mer.) and showed that a series of NW-SE aligned thrust faults brought the Alberta shale to the surface with a vertical displacement of at least 914 m, and there is also the presence of several NE-SW to N-S trending faults.

While Russell and Landes (1940) believed that the deformation in the Eagle Butte district was mainly due to large-scale slumping, Westgate (1968, p. 13) thought the disturbance northwest of Cypress Hills may be because of the emplacement of an igneous body at depth, probably synchronous with the Sweet Grass intrusions in northern Montana.

B.5.3 Glacial History

Immediately west of the Cypress Hills Plateau, the area has been glaciated by two Laurentide ice sheets, the Elkwater glacier and the Wild Horse glacier, which mainly flowed in a southeasterly direction in Wisconsinan time. This is supported by petrological and geomorphological data which show that the last continental ice developed in southern Alberta as three glacial lobes which advanced in three different directions, and tentative interpreation of till pebble lithological studies indicate that the western flank of the Cypress Hills Plateau had been glaciated by two lobes which flowed mainly to the southwest and southeast (Shetsen, 1984, fig. 19, p. 932). Since the area is located at the boundary of these two lobes, the interaction of these lobes might cause the ice flow direction in the area to deviate from the general trend. Shetsen (1984) suggested that initially, the ice lobe arrived in the region from the east. As this lobe started to waste downslope, the central lobe expanded into the area and partly overrode the glacial features of the eastern lobe. Westgate (1968, p. 62; fig. 28) also proposed that the erratic pebble composition of the tills suggested that the earlier, more extensive glacier did advance into the region to the southeast and later less extensive glacier moved to the southwest. Indeed, the direction of the ice movement is considerably influenced by local topography and the ice flow direction varies considerably near the ice margin. Furthermore, Westgate (1968, p. 81) also stated that the presence of a lobate end moraine near the village of Wild Horse (Tp. 1, R.1, W. 4th Mer.) indicates that during recession of the Wild Horse glacier from Montana and the map-area, minor readvances had occurred.

The distribution of the Wild Horse drift shows that the study area is located inside the outer limit of the Wild Horse glacier (Westgate, 1968, fig. 30, p. 70). The Elkwater drift is thin to discontinuous and is usually found at elevations of 1250 - 1372 m (4100 - 4500 ft); while Wild Horse drift is in general less than 15.2 m thick and lies at an elevation of about 975 - 1250 m (3200 - 4100 ft). It is known that, at the northern slopes of the Cypress Hills, the ice reached an elevation of 1372 m (4500 ft) above sea level at the time of the most extensive Laurentide glaciation (Westgate, 1968, p. 58), and it is believed that at the time of the most extensive Laurentide glaciation the minimum estimates of ice thickness over the Foremost-Cypress Hills area are about 701 m (2300 ft) at the city of Medicine Hat and 457 m (1500 ft) at the villages of Foremost, Manyberries, Aden and Wild Horse. Although the regional slope of the ice surface south of the Cypress Hills is less than 0.57 m per km toward the south, the slope of the ice surface may have been steepened to about 8.52 m per km around Cypress Hills (Westgate, 1968, p. 58).

The presence of glacial lineaments, ice-marginal channels and the semi-circular belts of hummocky disintegration moraine, end moraine and ground moraine around the Cypress Hills Plateau seem to indicate that the ice had flowed upslope against the flanks of the Cypress Hills Plateau in all directions, although the general ice flow direction was southeast away from this Plateau. The ice probably became stagnant there during deglaciation to form belts of drift deposits.

Appendix C - Airphotograph Interpretation, Field Observations, Terrain Units, Terrain Pattern, and Measured Sections of the Study Areas

The symbols used to describe the terrain units within the terrain pattern of the study areas follow the ELUC system developed by the Environment and Land Use Committe Secretariat (1978) and these symbols are delineated in Figure C.1. Figure C.2 indicates the symbols used in terrain analysis and Figure C.3 shows the lithologic symbols used in the geologic sections and stratigraphic columns. The symbols used in the stereographic plots are shown in Figure 8.1. The descriptions of folds observed in the areas mainly follow Fleuty (1964).

C.1 Wabamun Lake Area

C.1.1 Southern Shore of Wabamun Lake

Airphoto interpretation shows that a meltwater channel had once existed along the southern shore of Wabamun Lake which is at present covered by fluvial and/or lake sediments (Photo AS 135-5309-20, 21, 22; scale 1: 40,000). The southern half of the area (Figure C.4) is occupied by hummocky moraine and locally is covered by glaciolacustrine deposits. Undifferentiated isolated hills with gentle morphology are observed near the north-facing valley wall of the meltwater channel. Slope movement has occurred in two of the hills indicating that they might be composed of weak and

Explanation of ELUC Symbols Used in the Thesis (after Environment and Land Use Committee Secretariat, 1978)

Example of ELUC Symbology:

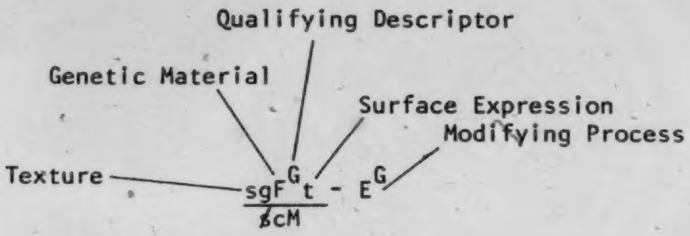
Qualifying Descriptor
Genetic Material
Surface Expression
Modifying Process
Texture
sgF G t - E G
ṡcM

A sandy gravelly fluvioglacial terrace over silty clay moraine whose surface has been eroded by glacial meltwater channels

Explanation of Symbols:

Texture

g - gravelly
s - sandy
ṡ - silty
c - clayey

Genetic Materials:

F - Fluvial
L - Lacustrine
M - Morainal
O - Organic
R - Bedrock
U - Undifferentiated

Qualifying Descriptors:

G - Glacial
A - Active
I - Inactive

Figure C.1 Explanation of ELUC Symbols

Explanation of ELUC Symbols Used in the Thesis (continued):

Surface Expression:

a - apron
b - blanket
f - fan
h - hummocky
l - level
m - subdued
r - ridged
s - steep
t - terraced
v - veneer

Modifying Processes:

E - Channelled
F - Failing
H - Kettled
V - Gullied

Composite Units:

A system of composite units is employed whereby up to three types of terrain may be designated within a common unit boundary. The relative amounts of each terrain type are indicated by the use of the symbols =, /, and //.

= components on either side of this symbol are approximately equal

/ the component in front of the symbol is more abundant than the one that follows

// the component in front of the symbol is considerably more abundant than the component that follows

Example:

Mb//R R considerably less than Mb

Figure C.1 (continued)

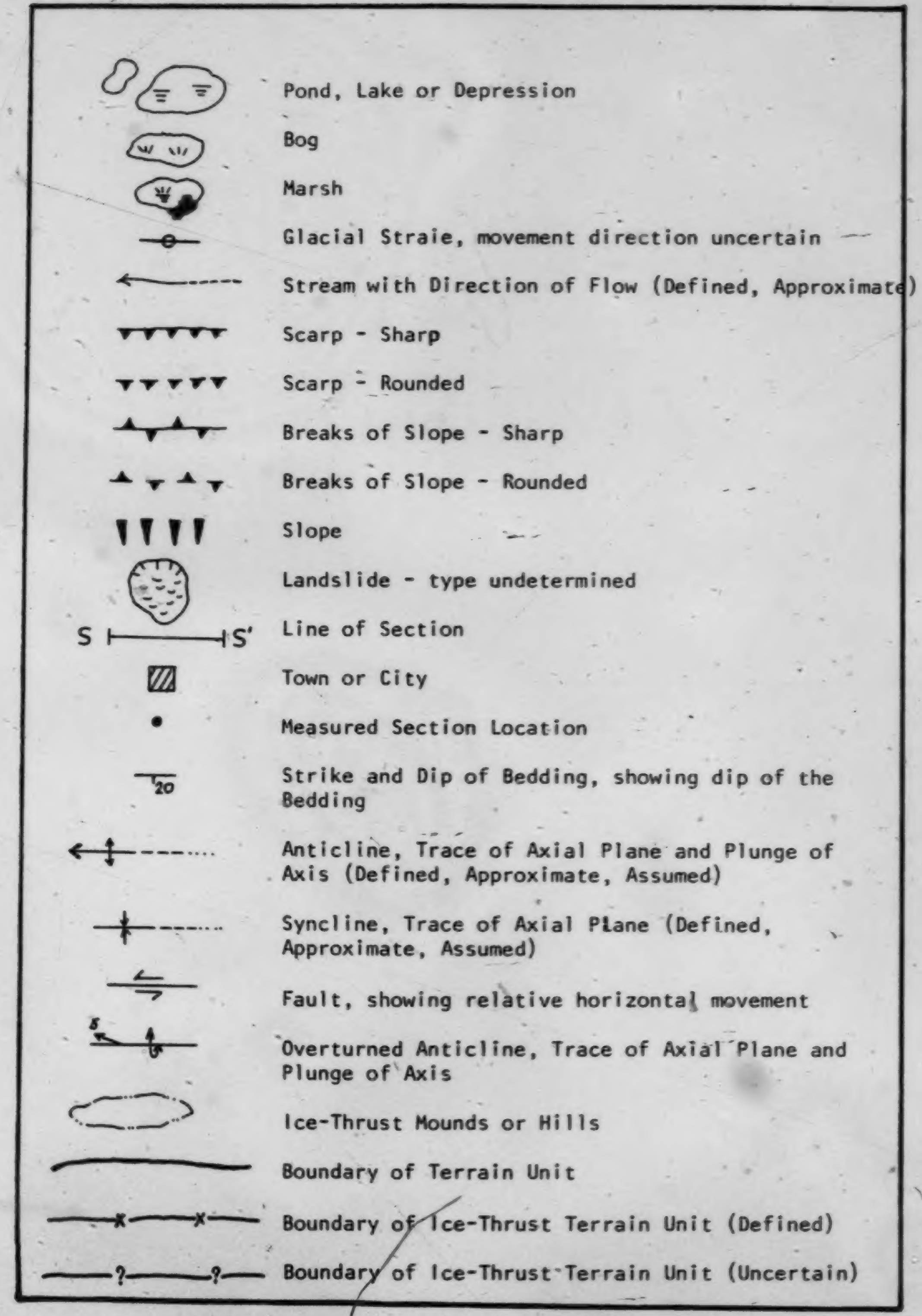
Pond, Lake or Depression
Bog
Marsh
Glacial Straie, movement direction uncertain
Stream with Direction of Flow (Defined, Approximate)
Scarp - Sharp
Scarp - Rounded
Breaks of Slope - Sharp
Breaks of Slope - Rounded
Slope
Landslide - type undetermined
S
S'
Line of Section
Town or City
Measured Section Location
20
Strike and Dip of Bedding, showing dip of the Bedding
Anticline, Trace of Axial Plane and Plunge of Axis (Defined, Approximate, Assumed)
Syncline, Trace of Axial Plane (Defined, Approximate, Assumed)
Fault, showing relative horizontal movement
5
Overturned Anticline, Trace of Axial Plane and Plunge of Axis
Ice-Thrust Mounds or Hills
Boundary of Terrain Unit
Boundary of Ice-Thrust Terrain Unit (Defined)
Boundary of Ice-Thrust Terrain Unit (Uncertain)

Figure C.2 Symbols Used in Terrain Analysis

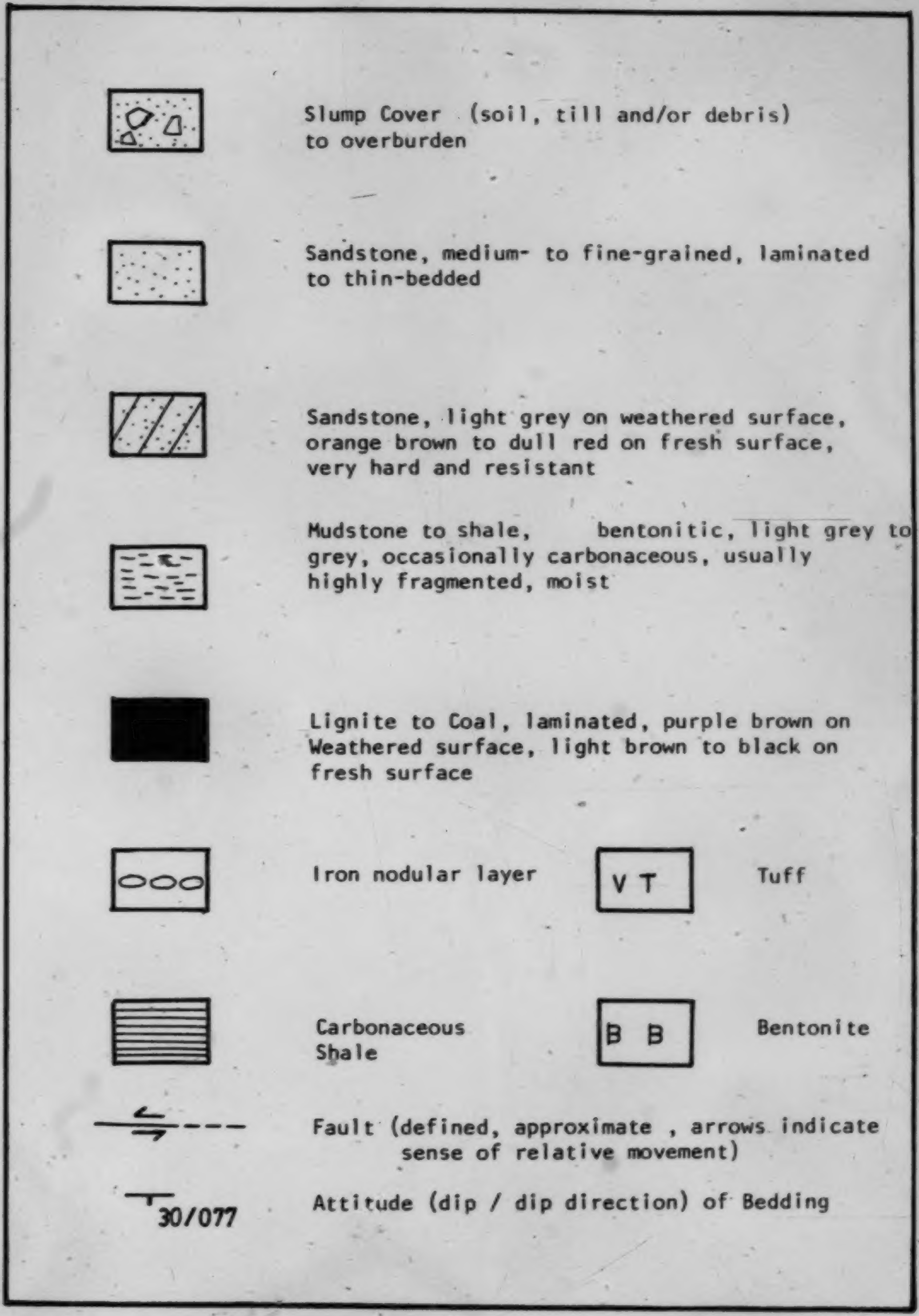

Slump Cover (soil, till and/or debris) to overburden

Sandstone, medium- to fine-grained, laminated to thin-bedded

Sandstone, light grey on weathered surface, orange brown to dull red on fresh surface, very hard and resistant

Mudstone to shale, bentonitic, light grey to grey, occasionally carbonaceous, usually highly fragmented, moist

Lignite to Coal, laminated, purple brown on Weathered surface, light brown to black on fresh surface

Iron nodular layer

Tuff

Carbonaceous Shale

Bentonite

Fault (defined, approximate , arrows indicate sense of relative movement)

Attitude (dip / dip direction) of Bedding

Figure C.3 Symbols Used in Geologic Sections and Stratigraphic Columns

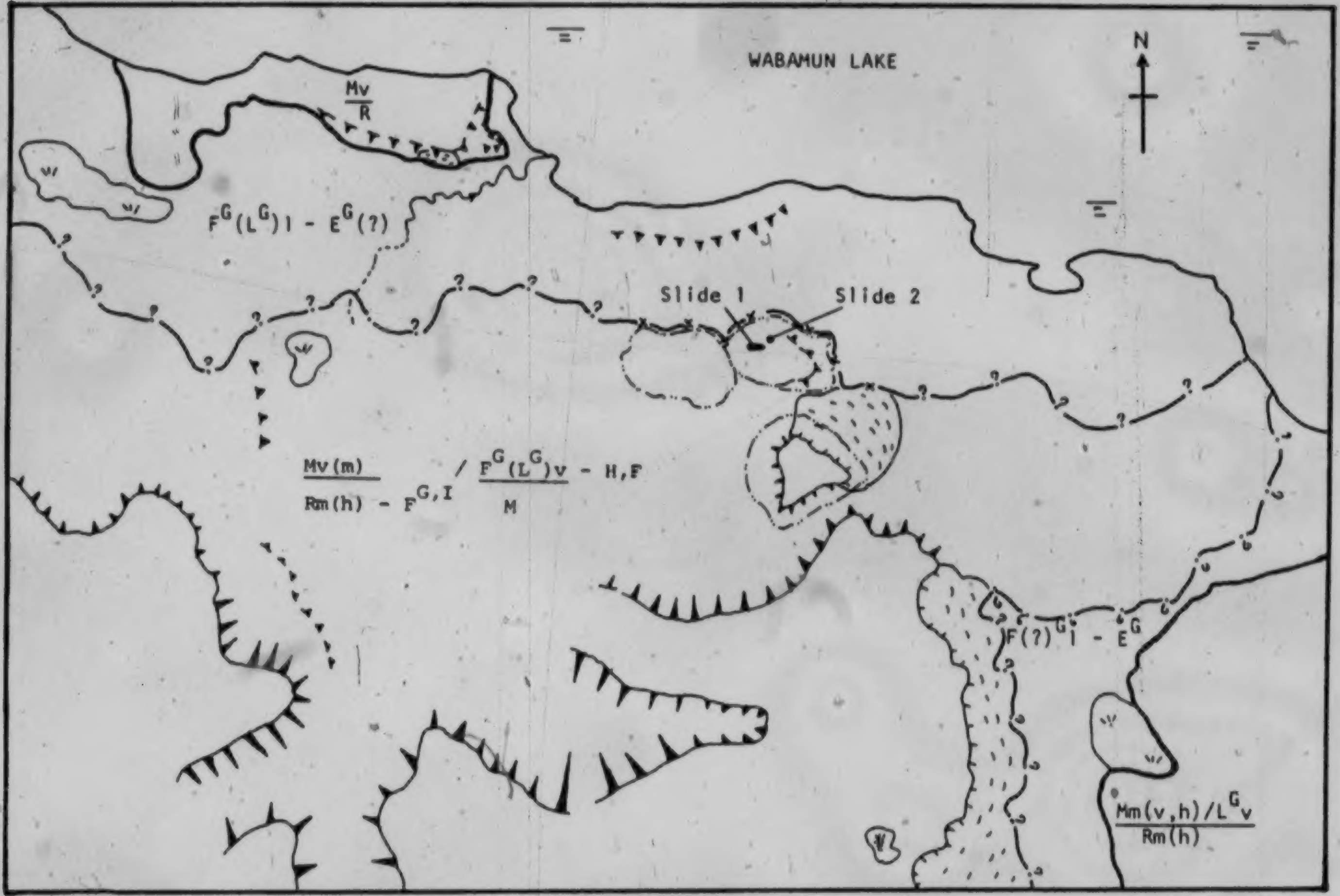
WABAMUN LAKE
N
$\frac{Mv}{R}$
$F^G(L^G)l - E^G(?)$
Slide 1
Slide 2
$\frac{Mv(m)}{Rm(h) - F^{G,I}} / \frac{F^G(L^G)v - H,F}{M}$
$F(?)^G l - E^G$
$\frac{Mm(v,h)/L^G v}{Rm(h)}$

Figure C.4 : Terrain Pattern of the Southern Shore of Wabamun Lake (Interpreted and Traced from Airphoto AS 135-5309-21, Scale 1: 40,000)

unstable materials.

Field studies by Fenton et al. (1983) and the author in the Pits excavated into the hills located on the north-facing valley wall of the meltwater channel indicate that these mounds are composed of gentle to close folds, thrust faults and shear zones up to 3.6 m thick. The location of one of these Pits, Pit 3, and the stratigraphic sections measured in two slides occurred in the Pits are shown in Figures C.5, C.6, C.7, and C.8. A stereographic plot of the poles to the bedding planes and minor shear planes measured in Pit 2 which is about 8 km southeast of Pit 3 is shown in Figure C.9a. Symbols used in the plots are shown in Figure 8.1. Detailed descriptions of these deformed features and the geology of the area are presented in Chapter 5.

The presence of the deformed structure in the hills located in a region which has no recent regional tectonic activities indicates that these mounds are glacial-thrust hills within an ice-thrust terrain unit. Figure C.4 shows the ice-thrust terrain pattern of the area.

C.1.2 Southern Shore of Isle Lake

Airphoto interpretation shows that a meltwater channel runs east-west along the southwestern shore of Isle Lake and has an outlet near the village of Gainford (Photo AS 134-5310-80, 81, 82; scale 1: 40,000). This channel trends southeast and joins the western shore of Wabamun Lake

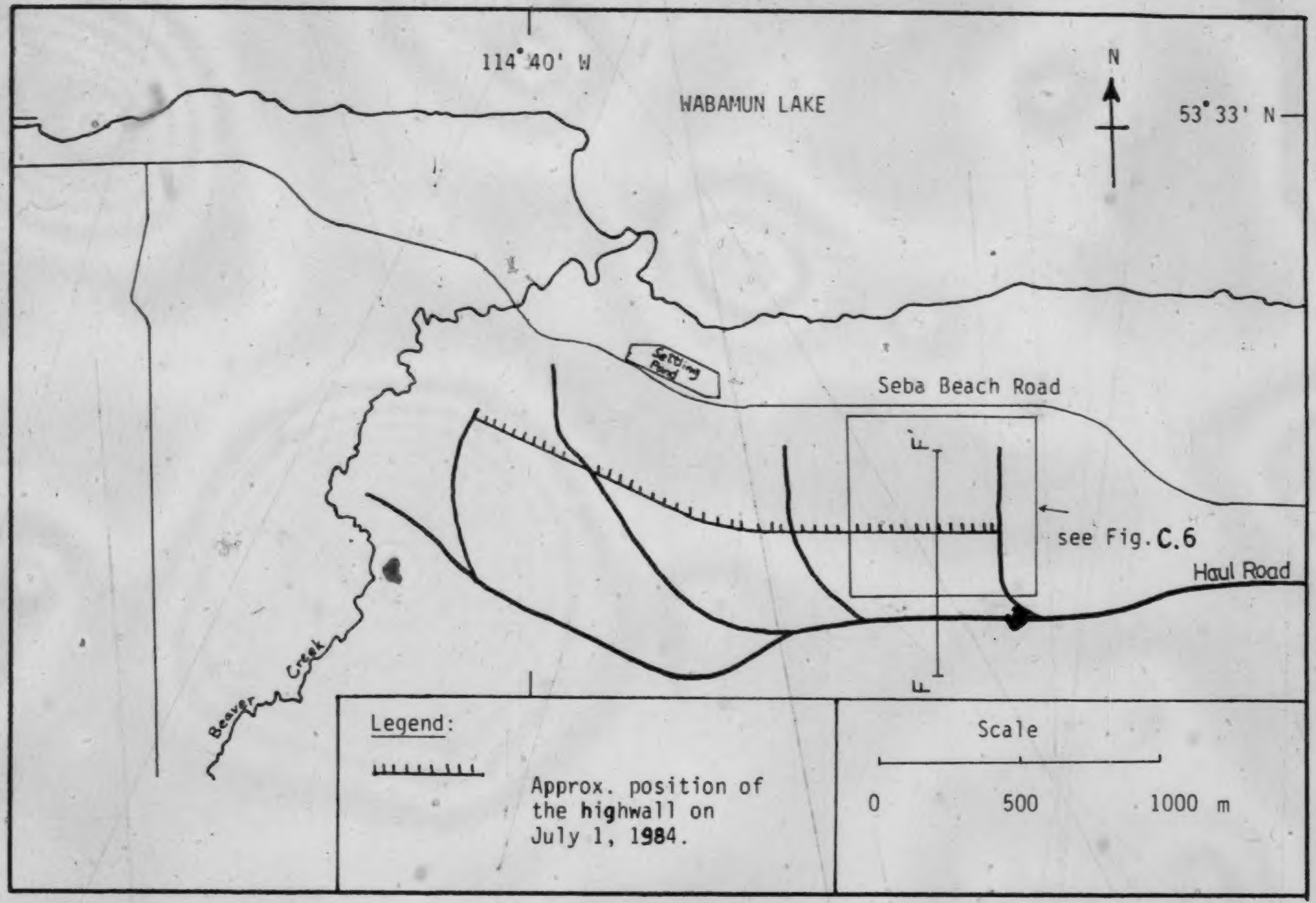
114°40' W
WABAMUN LAKE
N
53°33' N
Settling Pond
Seba Beach Road
F'
F
see Fig. C.6
Haul Road
Beaver Creek
Legend:
Approx. position of the highwall on July 1, 1984.
Scale
0
500
1000 m

Figure C.5 : Plan view of Highvale Mine, Pit 3 and the location of the highwall on July 1, 1984.

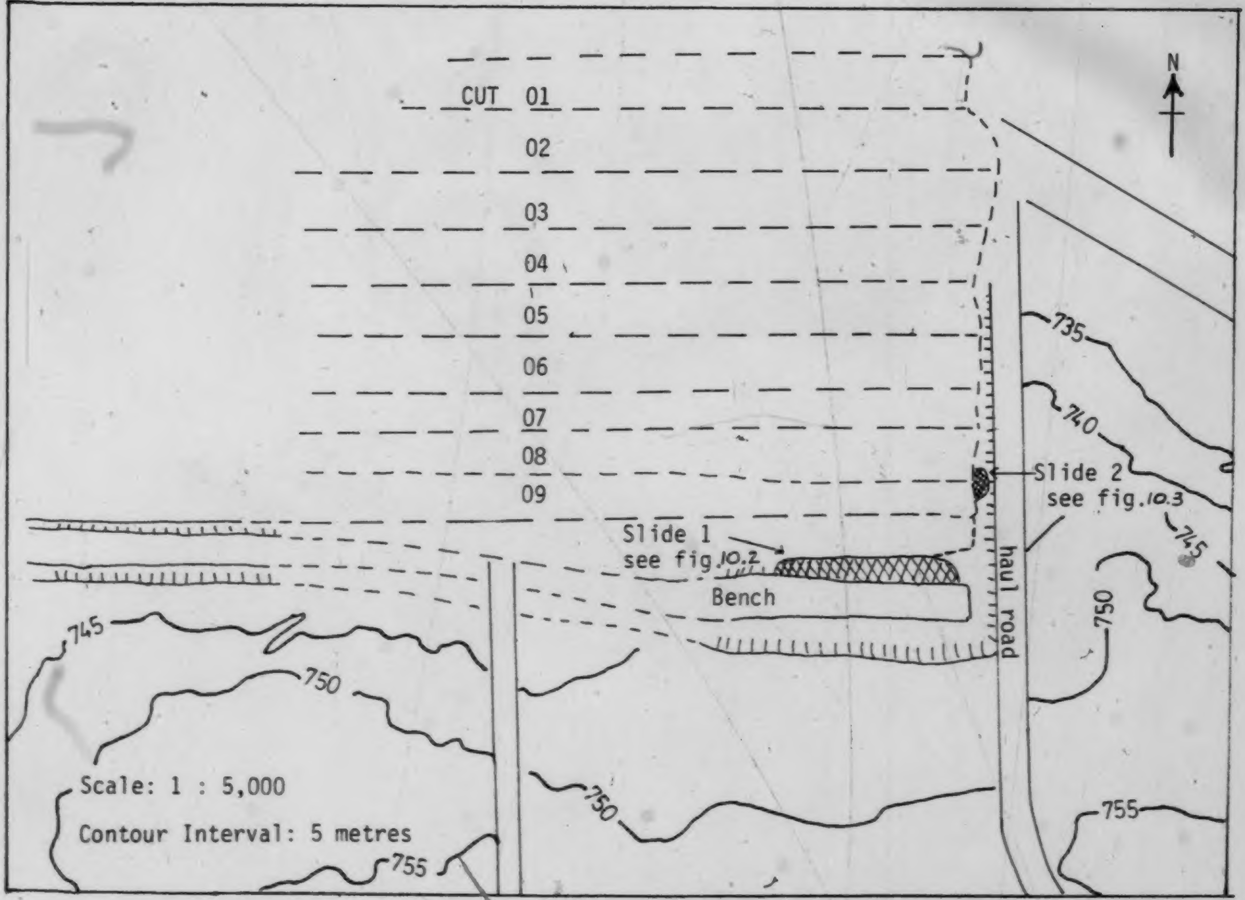
N
CUT 01
02
03
04
05
06
07
08
09
Slide 2
see fig.10.3
Slide 1
see fig.10.2
Bench
haul road
735
740
745
750
755
745
750
750
755
Scale: 1 : 5,000
Contour Interval: 5 metres

Figure C.6 Location Map of the Two Slides in Pit 3, Highvale Mine

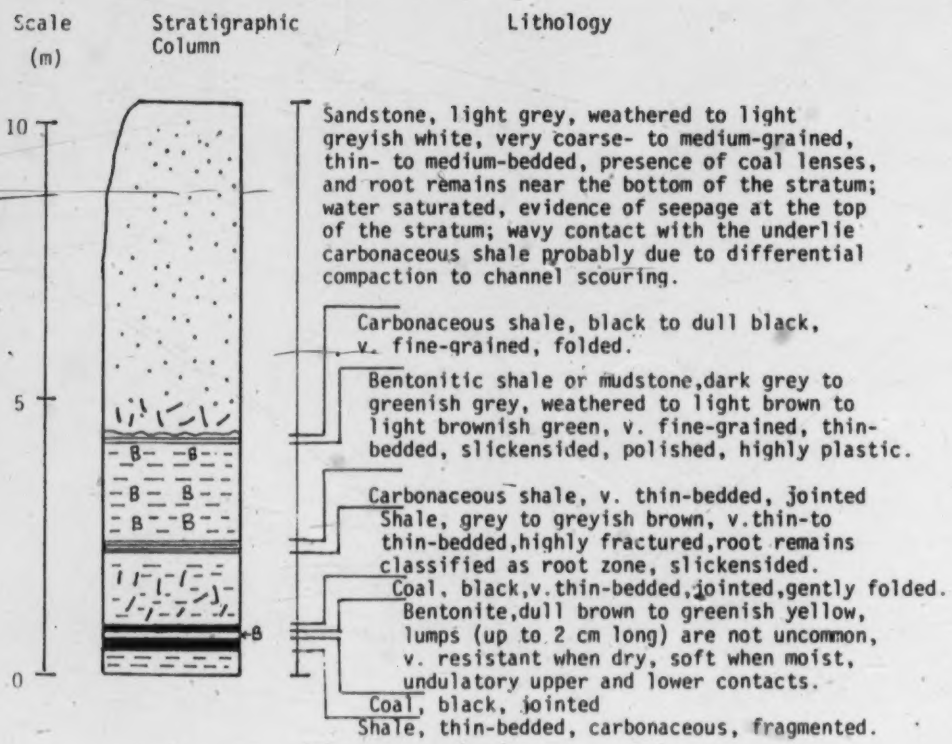

Sandstone, light grey, weathered to light greyish white, very coarse- to medium-grained, thin- to medium-bedded, presence of coal lenses, and root remains near the bottom of the stratum; water saturated, evidence of seepage at the top of the stratum; wavy contact with the underlie carbonaceous shale probably due to differential compaction to channel scouring.

Carbonaceous shale, black to dull black, v. fine-grained, folded.

Bentonitic shale or mudstone, dark grey to greenish grey, weathered to light brown to light brownish green, v. fine-grained, thin-bedded, slickensided, polished, highly plastic.

Carbonaceous shale, v. thin-bedded, jointed

Shale, grey to greyish brown, v. thin-to thin-bedded, highly fractured, root remains classified as root zone, slickensided.

Coal, black, v. thin-bedded, jointed, gently folded.

Bentonite, dull brown to greenish yellow, lumps (up to 2 cm long) are not uncommon, v. resistant when dry, soft when moist, undulatory upper and lower contacts.

Coal, black, jointed

Shale, thin-bedded, carbonaceous, fragmented.

Figure C.7 Stratigraphic Section of Slide 1, Pit 3, Highvale Mine

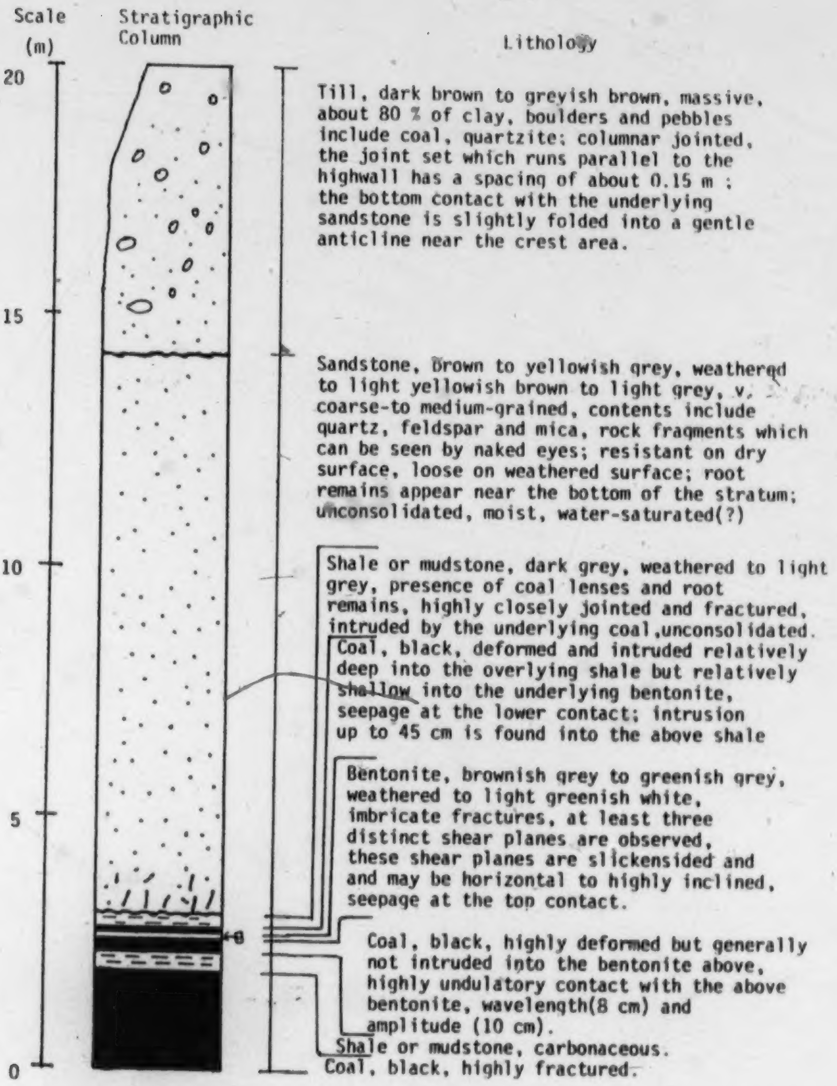

Till, dark brown to greyish brown, massive, about 80 % of clay, boulders and pebbles include coal, quartzite; columnar jointed, the joint set which runs parallel to the highwall has a spacing of about 0.15 m ; the bottom contact with the underlying sandstone is slightly folded into a gentle anticline near the crest area.

Sandstone, brown to yellowish grey, weathered to light yellowish brown to light grey, v. coarse-to medium-grained, contents include quartz, feldspar and mica, rock fragments which can be seen by naked eyes; resistant on dry surface, loose on weathered surface; root remains appear near the bottom of the stratum; unconsolidated, moist, water-saturated(?)

Shale or mudstone, dark grey, weathered to light grey, presence of coal lenses and root remains, highly closely jointed and fractured, intruded by the underlying coal,unconsolidated.

Coal, black, deformed and intruded relatively deep into the overlying shale but relatively shallow into the underlying bentonite, seepage at the lower contact; intrusion up to 45 cm is found into the above shale

Bentonite, brownish grey to greenish grey, weathered to light greenish white, imbricate fractures, at least three distinct shear planes are observed, these shear planes are slickensided and and may be horizontal to highly inclined, seepage at the top contact.

Coal, black, highly deformed but generally not intruded into the bentonite above, highly undulatory contact with the above bentonite, wavelength(8 cm) and amplitude (10 cm).

Shale or mudstone, carbonaceous.

Coal, black, highly fractured.

Figure C.8 Stratigraphic Section of Slide 2, Pit 3, Highvale Mine

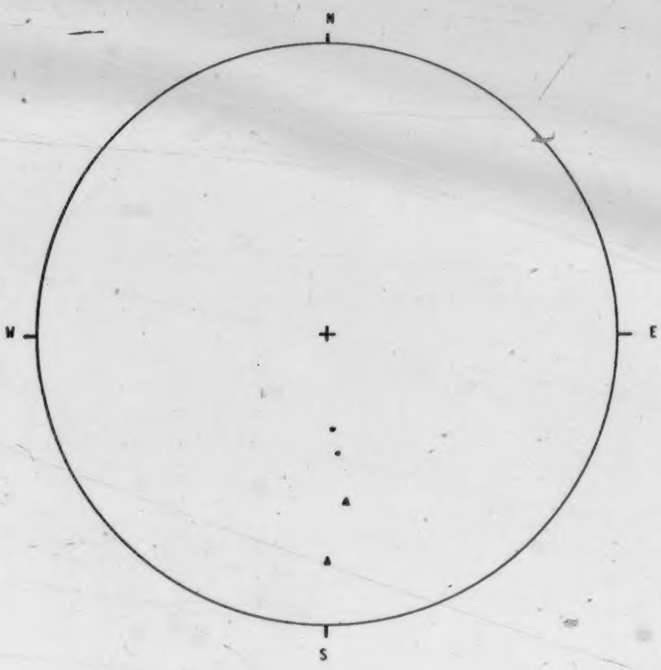

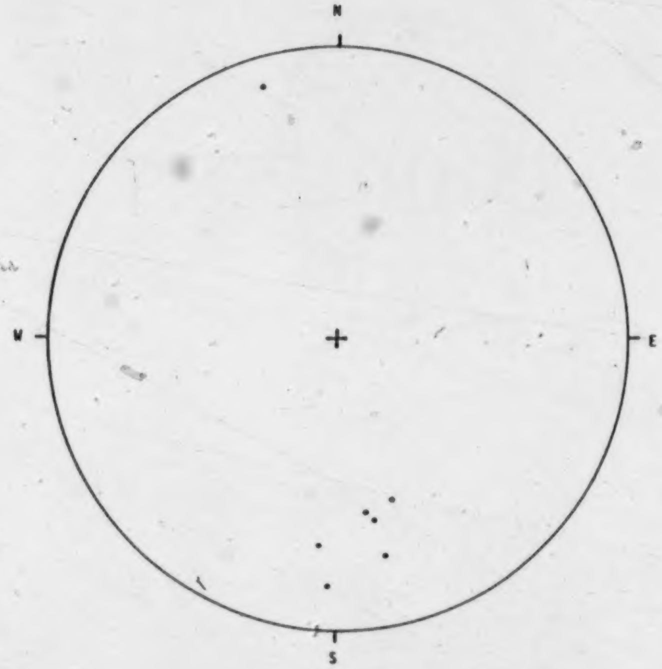

Figure C.9 Stereographic Plots of Deformed Beds: a - Pit 2, Highvale Mine, b - Southern Shore of Isle Lake

(Figure C.10). A hummocky terrain unit, with an area of approximately of 1.92 km^2 and composed of several curvilinear ridges. These arcuate ridges, which are about 0.28 - 0.56 km long with their convex sides facing south, have an east-west trend and are located within the meltwater channel just south of the southwestern shore of Isle Lake. In general, the Lake is surrounded by a rolling and undulating till plain. North of Isle Lake, glaciolacustrine deposits and glaciofluvial deposits are present on the till plain and the lake plain respectively.

Field investigation indicates that the section cut by Highway 16 has exposed the cross-section of one of these ridges. The exposure is mainly composed of alternate layers of coarse-grained bentonitic sandstone, greenish-grey bentonitic shale, lignite/coal, and nodular ironstone beds. Digging into the exposures with a spade has shown that the bentonitic shale and the coal have been highly fractured to angular fragments with a common diameter of less than 1 cm. A layer of till 0.6 m thick was found underlying the fractured shale and coal beds. The contact of these strata in the field is intensely weathered. The exposed strata have been deformed into gentle folds and tilted beds in general with a dip/dip direction of 55°/ 350° (Figure C.9b).

The inverse stratigraphic sequence and deformed structure found in these ridges indicate the hummocky terrain unit is an ice-thrust terrain unit. Figure C.10 indicates the ice-thrust terrain pattern of the area.

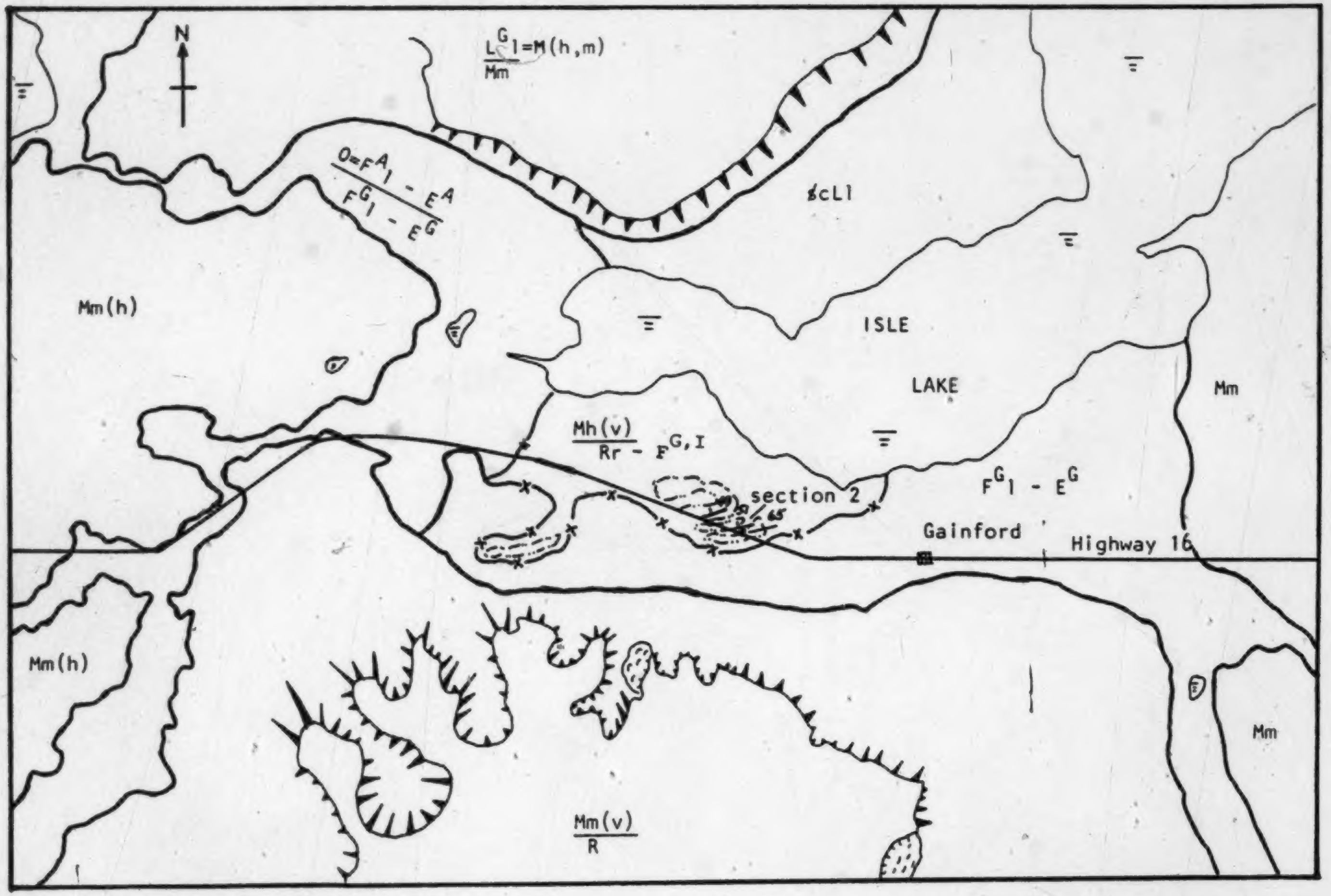
N
$\frac{L^{G}l=M(h,m)}{Mm}$
$\frac{O=F^{A}l - E^{A}}{F^{G}l - E^{G}}$
scLl
Mm(h)
ISLE
LAKE
Mm
$\frac{Mh(v)}{Rr} - F^{G,I}$
section 2
65
$F^{G}l - E^{G}$
Gainford
Highway 16
Mm(h)
Mm
$\frac{Mm(v)}{R}$

Figure C.10 Terrain Pattern at the Southern Shore of Isle Lake (Interpreted and Traced from Airphoto AS 134-5310-81, Scale 1: 40,000)

Other outcrops (230 m long and 6 m high), trending east-west and about 6 km east of the village of Entwistle on a roadcut along Highway 16, have also exposed symmetrical to asymmetrical gently folded anticlines. The attitudes of the strata are impossible to measure because they are intensely weathered. A fault with an apparent dip to the east was observed. Noted that the exposed sections in the area of Isle Lake show only anticlinal folds or tilted beds; but no synclinal folds were observed.

C.2 Edmonton Area

C.2.1 Nisku

Airphoto interpretation indicates that the east half of the study area is located on an eroded lacustrine plain locally overlain by glaciofluvial deposits; while the west half is a flat glaciolacustrine plain (Photo AS 2792-174, 175; scale 1:60,000) (Figure C.11). A meltwater channel, now occupied by Blackmud Creek, flows slightly west of north. Glacial flutings with trends of about 027° to 043° azimuth are found at about 25 - 30 km southwest of the study area (Bayrock, 1972).

Field studies show that smaller folds are observed in the sandstone and siltstone layers in the area. Generally, they have an apparent wavelength and amplitude of about 11 m and 0.46 m respectively. Lignite/coal beds and sideritic nodule layers tend to be highly deformed and have an apparent wavelength and amplitude of 0.46 - 1.8 m and 0.15 - 0.46 m respectively. It is also noticed that although the sideritic nodule layers are highly deformed, the strata above and below them tend to remain as gentle folds. The fold axes of some of these highly deformed layers have a trend of 096° - 130° and a plunge of 12° - 27° E.

The morphology of the ice-thrust features is indistinct both on aerial photos and in the field, and the ice-thrust terrain unit cannot be ascertained except at the location of the exposed sections. Figure C.11 shows the terrain pattern and the locations of the ice-thrust features exposed in the area.

C.2.2 Gibbons

Airphoto interpretation indicates that the exposed section is located on a glaciofluvial outwash plain in the southwestern to southern portion of the area (Photo AS 2793-228, 229, 230; scale 1:60,000). Ground moraine occupies two third of the area with aeolian deposits surrounding Lostpoint Lake. The Sturgeon River flows northeast but when it reaches just north of the town of Gibbons, it turns abruptly toward the southeast and finally joins the modern North Saskatchewan River to the south.

The outcrops consist of a light grey, fine- to medium-grained sandstone; a dark grey to black mudstone; and a brown lignite layer. Due to intense weathering, no attitude measurements on the outcrops are possible. However,

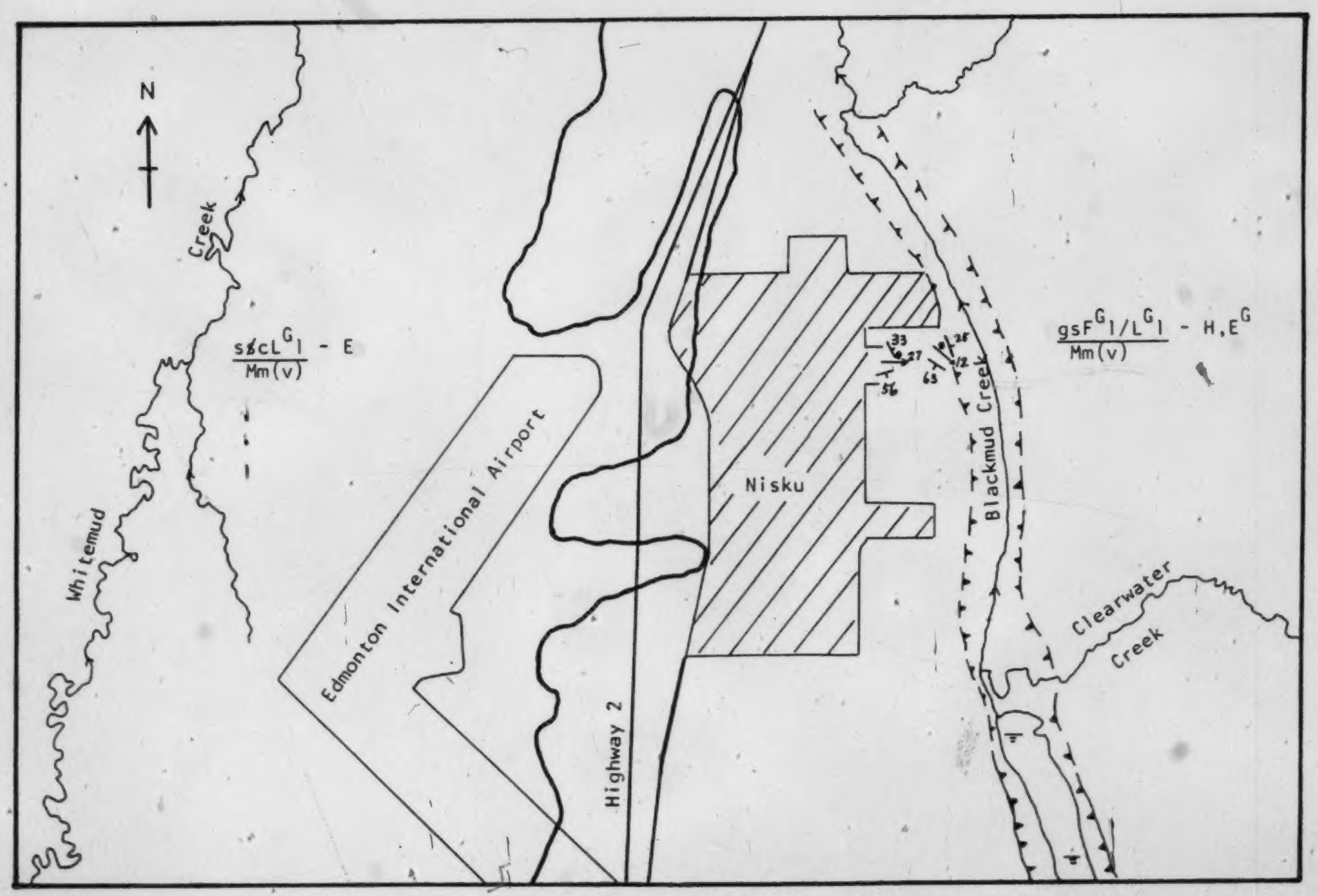
N
Creek
Whitemud
$\frac{s\not{s}cL^{G}{}_{1}}{Mm(v)}$ - E
Edmonton International Airport
Highway 2
Nisku
33
27
56
65
28
12
Blackmud Creek
$\frac{gsF^{G}{}_{1}/L^{G}{}_{1}}{Mm(v)}$ - H,E^{G}
Clearwater
Creek

Figure C.11 Terrain Pattern at Nisku Area (Interpreted and Traced from Airphoto AS 2792-174, Scale 1: 60,000)

a tongue of dark grey mudstone was observed intruded into the overlying light grey sandstone with a shear plane at the bottom of the mudstone which sloped gradually to about 7° from the horizontal at the tongue and subsequently flattened out. The vertical and horizontal displacements of the tongue are about 1.2 m and 6 m respectively.

C.3 Red Deer - Stettler Area

C.3.1 Lowden Lake Area

Airphoto interpretation indicates that south of Lowden Lake, the land surface has a ridged and undulatory topography which resembles hummocky disintegration moraine (Photo AS 1532-133, 134, scale 1 : 31,680; and AS 2156-139, 140, 141, Scale 1 : 60,000). Further south the land surface is inclined downward into a plain which is occupied by Big Valley Creek. Highway 56 cuts through some of the NW-SE trending ridges and exposes deformed anticlinal structures which are overlain by a relatively thin layer of till.

Eight outcrops of these ridges found south of Lowden Lake have been studied in detail. Figure C.12 shows the location of these outcrops. Figures C.13, C.14 and C.15 show the stereographic plots of the attitudes of the deformed structures observed in these exposures and Figure 8.1 shows the symbols used in the plots. Figures C.16, C.17 and C.18 are sections measured from three of these exposures. The fold axes of these deformations measured in two of these

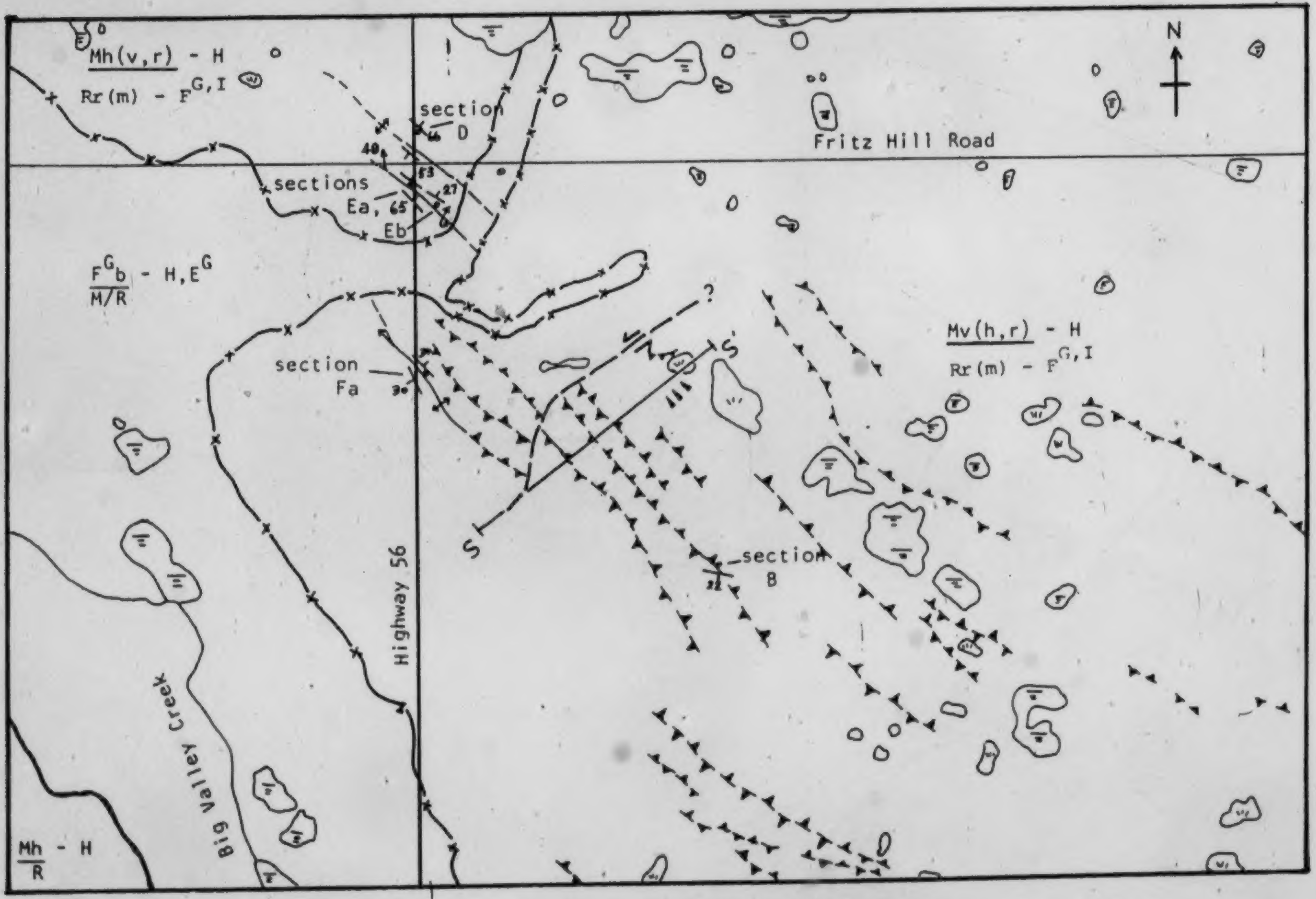
N
Mh(v,r) - H
Rr(m) - F^G,I
section D
40
53
27
sections
Ea, 65
Eb
Fritz Hill Road
F^G b - H,E^G
M/R
section
Fa
30
?
S'
S
Mv(h,r) - H
Rr(m) - F^G,I
section
B
21
Highway 56
Big Valley Creek
Mh - H
R

Figure C.12 Terrain Pattern at Lowden Lake Area
(Interpreted and Traced from Airphoto
AS 1532-133, Scale 1: 31,680)

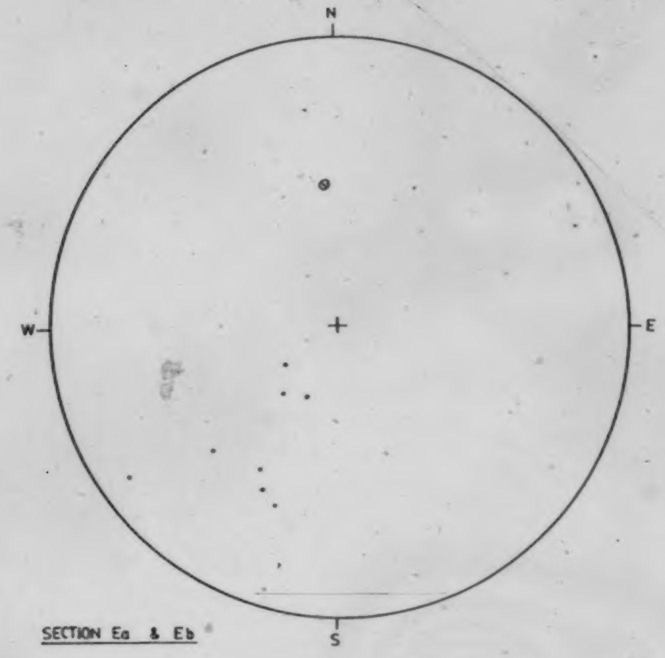
N
W
E
S
SECTION Ea & Eb

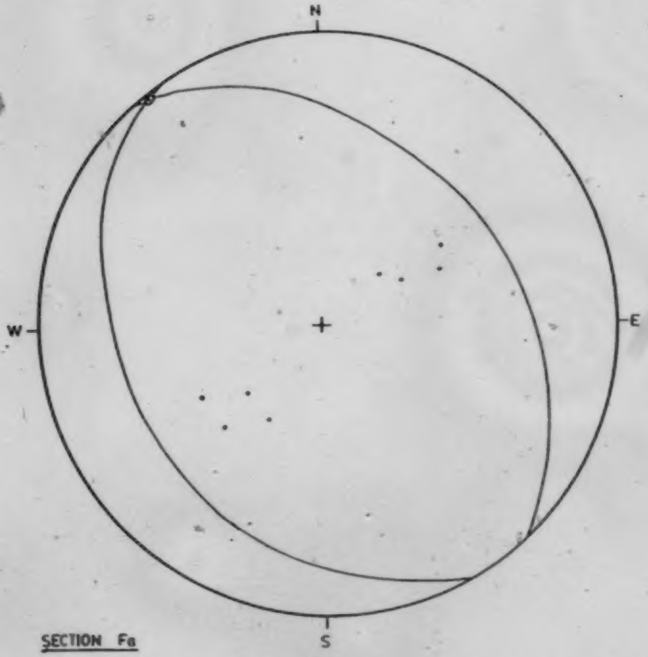
N
W
E
S
SECTION Fa

Figure C.13 Stereographic Plot of Deformed Beds Exposed in Sections Ea, Eb and Fa, Lowden Lake Area

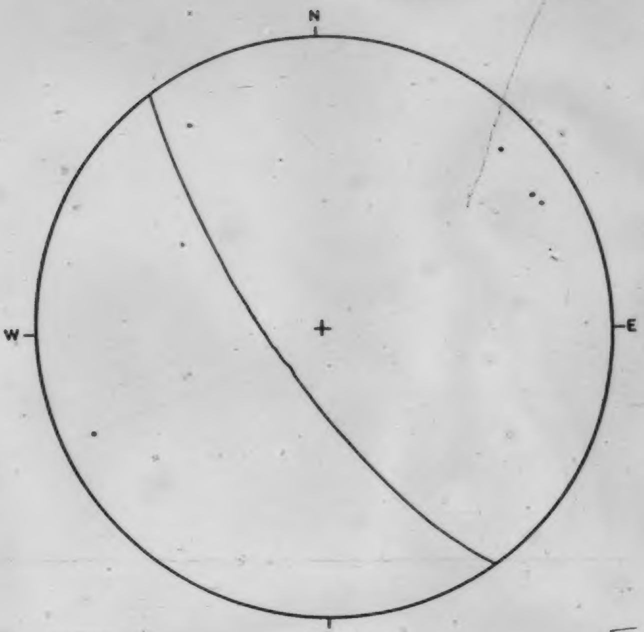

SECTION 1

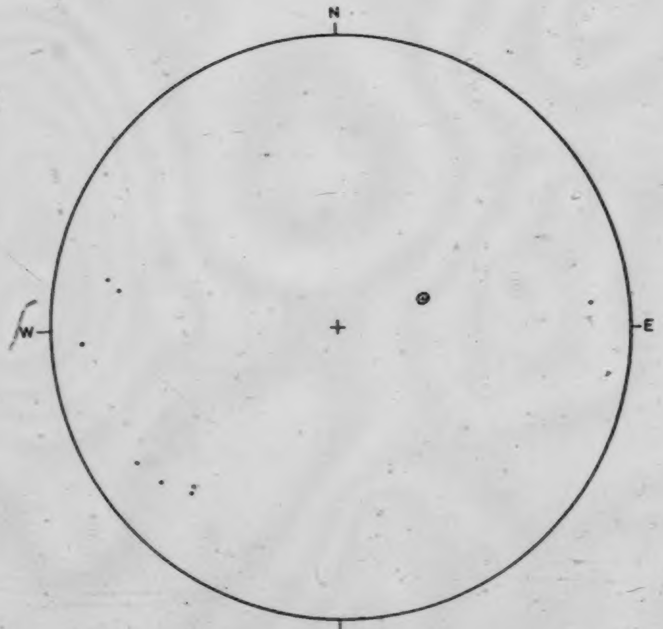

SECTION D

Figure C.14 Stereographic Plot of Deformed Beds Exposed in Sections 1 and D, Lowden Lake Area

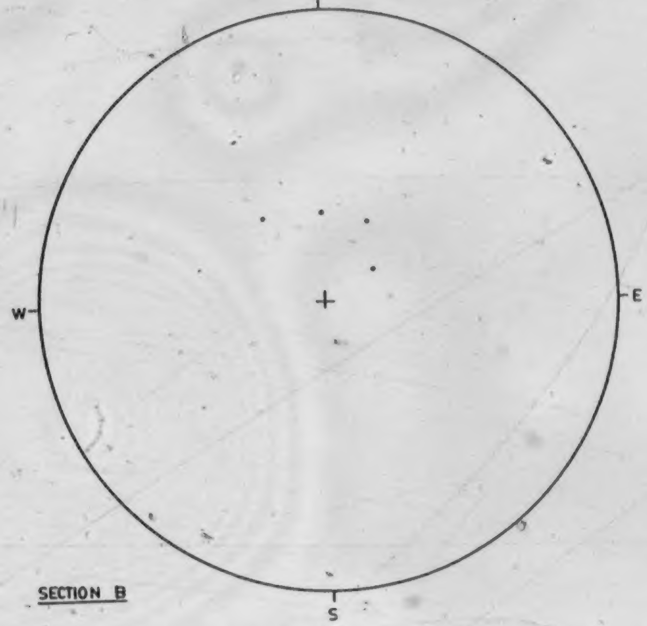
N
E
S
W
SECTION B

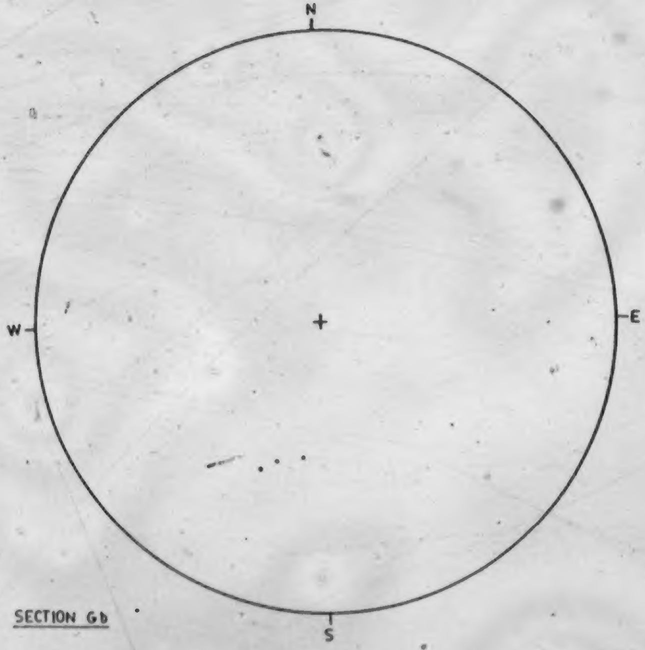
N
E
S
W
SECTION Gb

Figure C.15 Stereographic Plot of Deformed Beds Exposed in Sections B and Gb, Lowden Lake Area

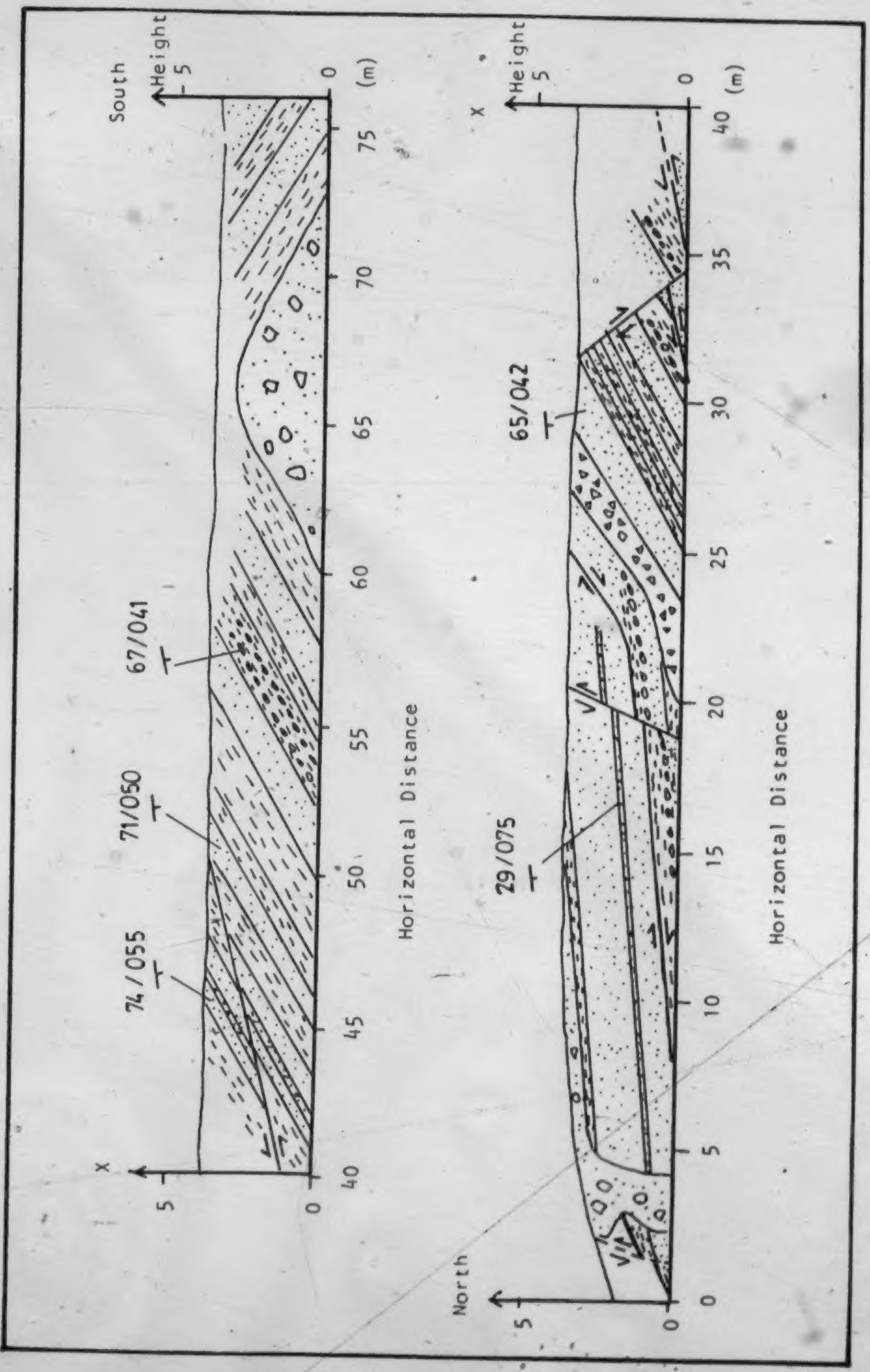
South
North
Height
5
0
(m)
X
74/055
71/050
67/041
65/042
29/075
40
45
50
55
60
65
70
75
0
5
10
15
20
25
30
35
40
Horizontal Distance
Horizontal Distance

Figure C.16 Section D, Lowden Lake Area (exposed in the ditch along Highway 56 about 22 km south of the town of Stettler)

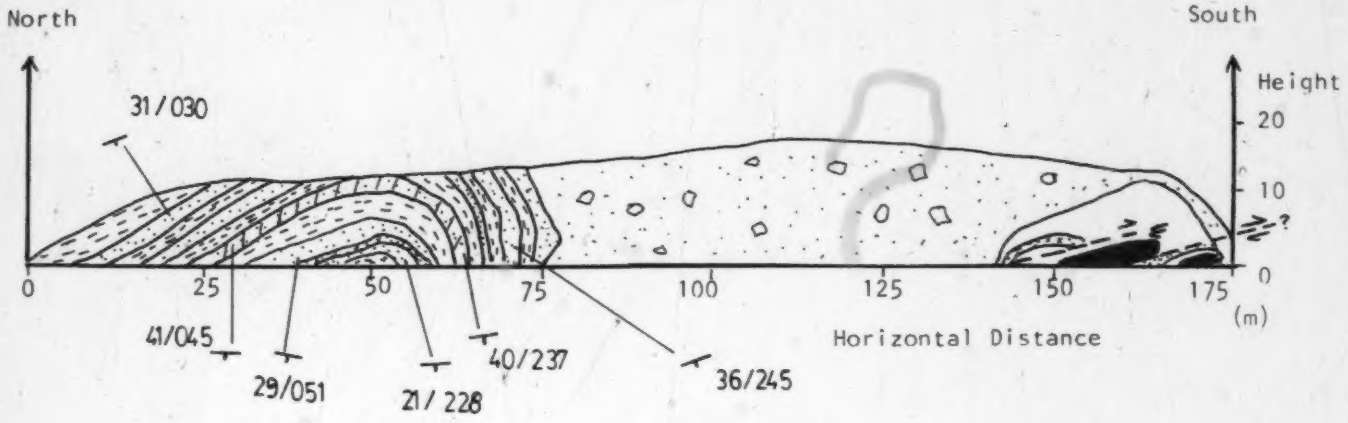
North
South
Height
20
10
0
(m)
31/030
41/045
29/051
21/228
40/237
36/245
0
25
50
75
100
125
150
175
Horizontal Distance
?

Figure C.17 Section Fa, Lowden Lake Area (exposed along Highway 56 about 22 km south of the town of Stettler)

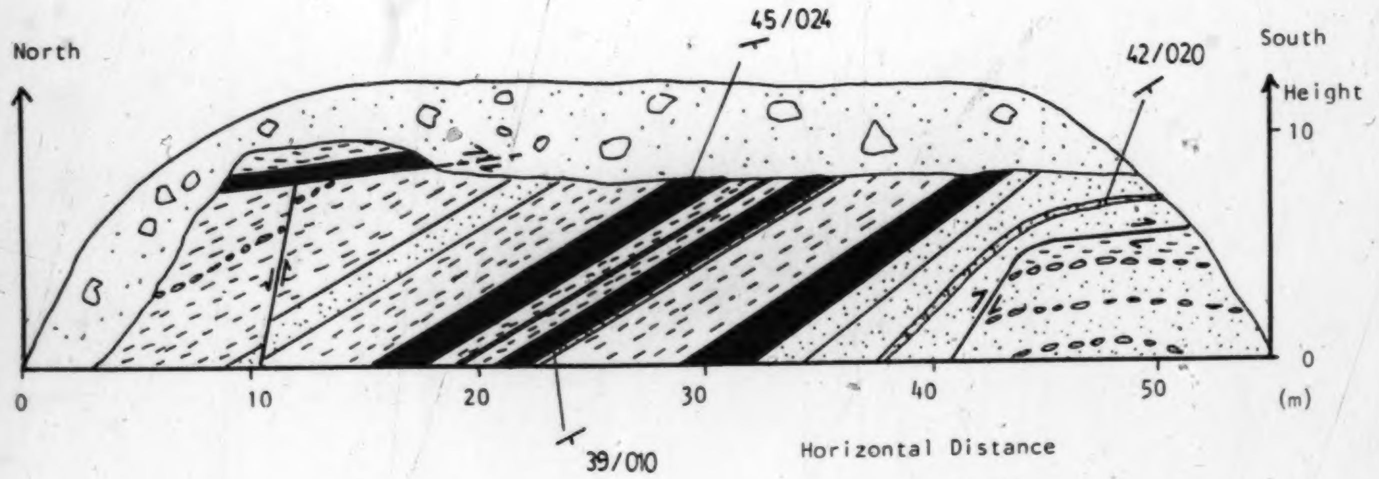
North
South
Height
10
0
(m)
0
10
20
30
40
50
Horizontal Distance
45/024
42/020
39/010

Figure C.18 Section Gb, Lowden Lake Area (exposed on roadcut along Highway 56 about 18.4 km south of the town of Stettler)

outcrops (Figure C.13, Sections Ea and Fa) have trends of 323° - 356° and plunges of 4° - 48° NW; however one section (Section D) indicates an anticlinal structure with a trend and a plunge of 071° and 64° E respectively (Figure C.14). Beddings observed in all outcrops except section D, in general, dip toward the northeast and/or southwest. At section D, the presence of normal faulting that occurred after folding and thrusting probably caused rotation and/or translation of the previously folded beds (Figure C.16). This may be the reason for the structures measured in section D deviating from the general orientation of the structures measured in other outcrops in the study area. As a result, section D should be treated as an anomaly in the study area as far as the orientation of structures is concerned and should not be included in the analysis of the glacial direction in the Lowden Lake area (Chapter 10, Section 10.1.1). Many highly deformed sideritic nodule layers were found in the fine-grained sandstone strata.

Thrust faults and normal faults were observed on outcrops in the Lowden Lake area. Thrust faults found in the study area show apparent dips of 5° - 15° and a separation of about 1.5 m. A reverse, listric fault was observed (Figure C.16) in which the fault initially followed a slightly dipping bedding plane and then becames concave upward and turned into a high-angle reverse fault near the surface. However, another thrust fault had an gentle inclination (with an apparent dip of about 5 degrees) that roughly followed a bedding plane near the surface and turned into a high angle reverse fault (with an apparent dip of about 56 degrees) when it extended further backward into the ground (Figure C.18). All the thrust faults observed south of Lowden Lake have an apparent northward dip. Moreover, they were always found in groups and seem to form an imbricate structure. The thrust faults tend to follow the bedding planes with sandstone above and claystone below (Figures C.16 and C.18), although sometimes they were exclusively found within claystone strata (Figure C.18).

Normal faults with apparent dips of 51° - 80° and apparent displacements of 0.15 - 2.1 m are observed at the outcrops in the area. These faults dip in different directions; however, they cut across the thrust faults which indicate that these normal faults (exposed in the study area) were formed later than the thrust faults (Figure C.16).

In the Lowden Lake area, the NW-SE trending ridges with surficial deformations are interpreted as ice-thrust ridges. The study of these ridges and the adjacent glacial deposits indicate that there are three main terrain units in the study area (Figure C.12). They are:

1. Ice-Thrust Terrain Unit - Many curvilinear, aligned and roughly parallel NW-SE trending ridges with steep sides and with an orientation of about 132° azimuth are found in this terrain. Occasionally, a series of lakes with a similar trend are observed immediately behind some of

these ridges. The morphology of these ridges are similar to the descriptions of the typical ice-thrust ridges reported in literature (Gravenor et al., 1960) although those found in the study area are fewer in number and smaller in dimensions. Near the centre of Figure C.12, the mis-alignment of the ridges seems to suggest that a strike-slip fault with sinistral movement has caused the ridges at the northwestern portion of the unit to be shifted toward southwest with respect to the ridges at the southeastern portion of the unit. The measurement of the relative movement of the mis-aligned ridges on the aerial photographs shows an apparent displacement of about 285 m to the southwest (Figure C.12).

Other ice-disintegration features occupy the area between the ice-thrust ridges. These are mainly hummocky disintegration moraine which consists of non-oriented knobs and kettles, linear disintegration ridges and moraine plateau. Indeed, the ice-thrust ridges have created a rather undulatory and rolling topography which resembles disintegration moraine.

2. Glaciolacustrine Terrain Unit - Glaciolacustrine to recent lake deposits which cover the plain that surrounds Lowden Lake and its adjacent ponds.
3. Meltwater Channnel Unit - Recent fluvial deposits found within a meltwater channel occupied by Big Valley Creek at present. This meltwater channel has a trend of about 150° azimuth in the study area and runs roughly parallel

to the ridges observed in the adjacent ice-thrust terrain unit.

The ice-thrust terrain pattern of the area is shown in Figure C.12.

C.3.2 Beltz Lake Area

Airphoto analysis show that the study area near Beltz Lake is gently rolling with bedrock at or very close to the ground surface. Exposures are found on the scarp along the eastern shore of Beltz Lake and in the ditches along a gravel road near this lake (Photo As 825-78, 79, 80, scale 1 : 31,680). Giant grooves or lineaments are observed east of the eastern shore of the Lake (Figure C.19).

Anticlinal and synclinal structures, which are exposed at the eastern shore of Beltz Lake, have an amplitude and wavelength of 2.5 m and 24 m respectively. Figures C.20 and C.21 are stereographic plots of these deformed structures and show that the fold axis of three of these deformations have a NE-SW trend and a plunge of 0° - 6°. Asymmetrical fold structures are exposed at the northern portion of the eastern shore of Beltz Lake which tend to change to symmetrical fold structures when the southern portion of the shore is approached (Figures C.20 and C.21, Sections 3, 4, and 5). Figure 8.1 shows the symbols used in the stereographic plots (Figures C.20 and C.21). The asymmetrical deformed structures show a gentler northwest dipping limb and a steeper southeast dipping limb (Figure

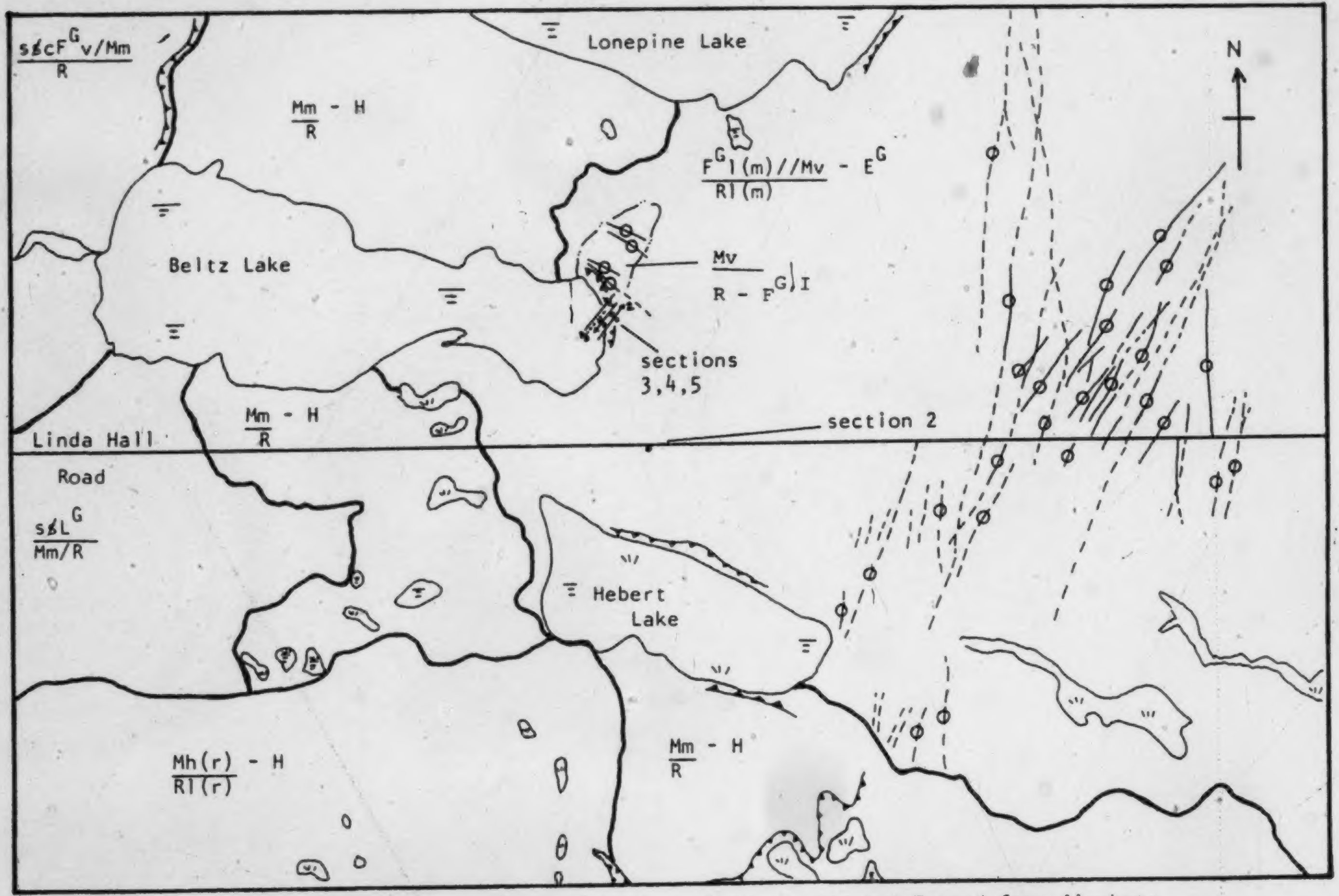
sℓcF^G v/Mm / R
Lonepine Lake
Mm - H / R
F^G l(m)//Mv - E^G / Rl(m)
Beltz Lake
Mv / R - F^G) I
sections 3,4,5
Mm - H / R
section 2
Linda Hall Road
sℓL^G / Mm/R
Hebert Lake
Mh(r) - H / Rl(r)
Mm - H / R
N

Figure C.19 : Terrain Pattern of Beltz Lake Area (Interpreted and Traced from Airphoto AS 825-79 Scale 1: 31,680)

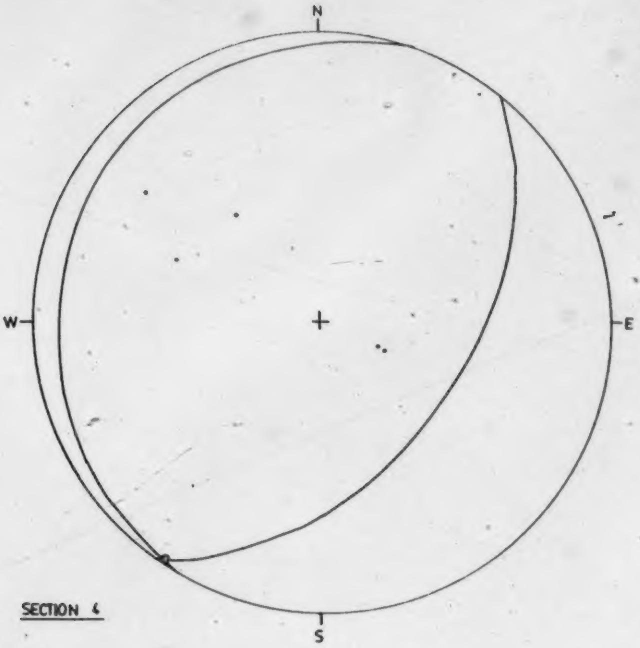
N
W
E
S
SECTION 4

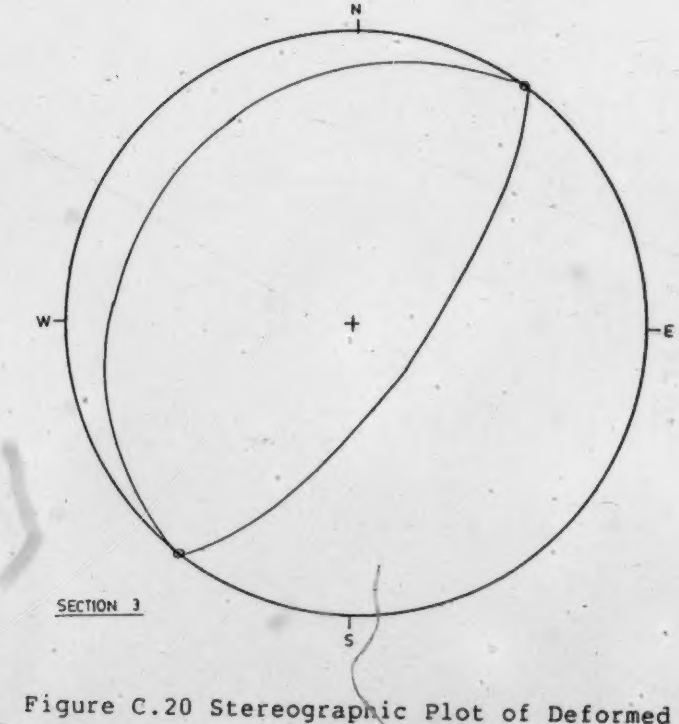
N
W
E
S
SECTION 3

Figure C.20 Stereographic Plot of Deformed Beds Exposed in Sections 3 and 4, Beltz Lake Area

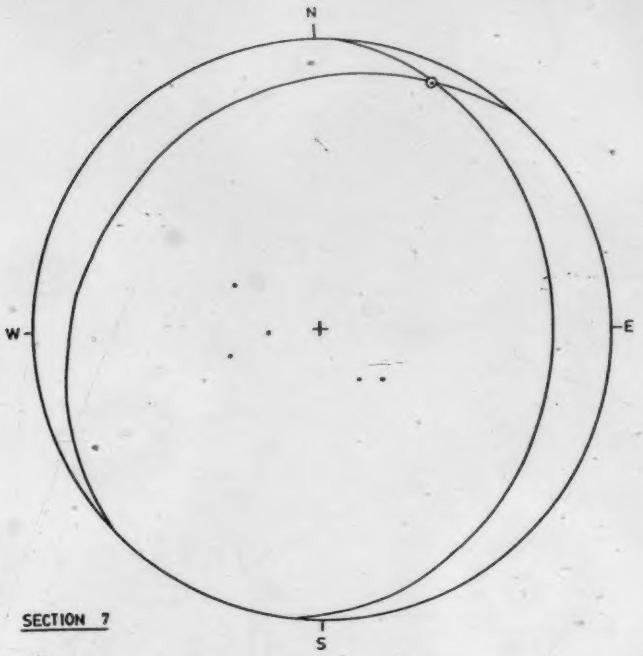
N
W
E
S
SECTION 7

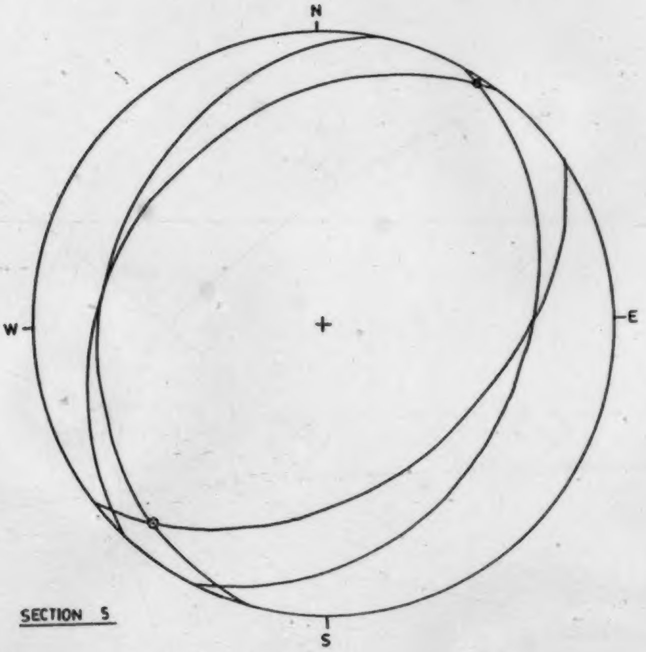
N
W
E
S
SECTION 5

Figure C.21 Stereographic Plot of Deformed Beds Exposed in Sections 5 and 7, Beltz Lake Area

C.20, Section 3). Exposures, which are found in the ditch of a gravel road about 0.63 km south of the southern shore of Beltz Lake, show bedding with a dip/dip direction of 22°/ 163°.

The morphology and distribution of this deformation outlines the ice-thrust terrain units in the area. Figure C.19 shows ~~that~~ the ice-thrust terrain pattern of the study area consist essentially of four terrain units. They are:

1. Ice-Thrust Terrain Unit - This is a belt with uncertain boundary which probably includes the area between the eastern shore of Beltz Lake and the eastern margin of the area. The overall gentle topographic relief and very thin surficial deposits of the area indicate that it has probably acted as a spillway during deglaciation.

   Ice-thrust features with indistinct topographic expressions were exposed on the scarp along the eastern shore of Beltz Lake and have been described in the preceding paragraphs. On the airphotos, two sets of giant grooves were found in this unit.

2. Hummocky Disintegration Moraine Terrain Unit - This unit is found in the southwestern corner of the photograph. Disintegration features such as non-oriented to oriented knobs and kettles together with linear ridges are present. Since no outcrops were found during field investigation in this unit, no conclusions can be drawn as to whether the linear ridges are ice-thrust ridges or other ice-disintegration features.

3. Ground Moraine Terrain Unit - This unit is located just north and south of Beltz Lake and forms a belt trending roughly north-south.
4. Glaciolacustrine to Glaciofluvial Veneer Terrain Unit - This unit is seen at the western edge of the photo and is mainly composed of a thin layer of glaciolacustrine and glaciofluvial sediments overlying the ground moraine and/or bedrock.

C.3.3 Northwest of Sullivan Lake Area

Air photo interpretation indicates that the study area is essentially an undulating to gently-rolling plain of ground moraine (Photo AS 3026 - 201, 202; scale 1 : 30,000). Bigknife Creek, which is probably a meltwater channel, flows in the western margin of the study area. Recent fluvial sediments are found along the sides of the Creek. A ridge with a NW-SE trend is found about 1.65 km northeast of the exposures (Figure C.22).

Field observations indicate that the outcrops are located at the crest of a very gently inclined and roughly north-south trending ridge. The exposures are the Horseshoe Canyon Formation and are composed mainly of fine-grained, cross-bedded, bentonitic sandstone, bentonitic siltstone to mudstone, lignite and iron nodular layers. They are overlain by a thin layer of clayey till about 0.3 m thick. Water well drilling reports show that the till in the ground moraine

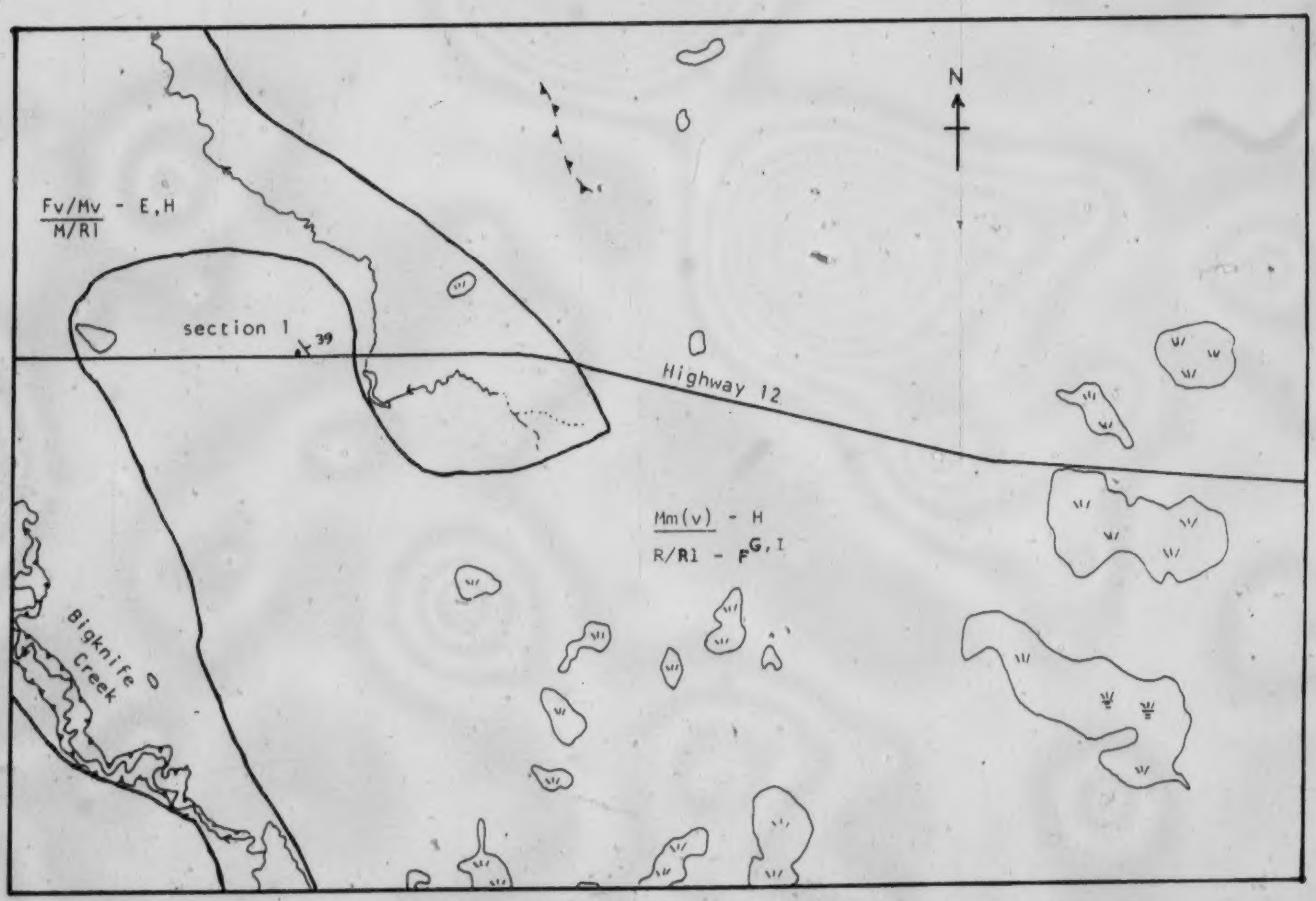
N
Fv/Mv - E,H
M/Rl
section 1
39
Highway 12
Mm(v) - H
R/Rl - F G,I
Bigknife Creek

Figure C.22 : Terrain Pattern of Area Northwest of Sullivan Lake (Interpreted and Traced from Airphoto AS 3026-202, Scale 1: 30,000)

terrain unit in the study area ranges from 0 to 5 m thick; however, the till may be absent locally and up to 6.7 m of clay overlies the bedrock, for example, the bedrock along the Bigknife Creek is covered mainly by 2.7 - 7.6 m of clay.

The beds exposed at the ridge are folded and faulted (Figure C.23). The faulted beds have an average dip/dip direction of 39°/ 061° (Figure C.24a, Section 1). Figure 8.1 shows symbols used in the stereographic plots. A gentle anticlinal fold is observed on the western part of the section while imbricate faults are found in the eastern part of the section. The eastern limb of the anticline is truncated by the thrust fault. The exposed thrusts have a similar dimensions and an apparent dip of about 14° toward east, forming an imbricate thrust system. Within each thrust sheet, drag folds are found overlying the imbricate thrusts with a steeply westward-dipping limb and a gently eastward-dipping limb with lengths of 0.9 m and at least 1.8 m respectively (Figure C.23). These form a series of asymmetrical, anticlinal structures (Figure C.23). The bottom portion of the thrust sheet is composed mainly of bentonitic sandstone which is overlain by bentonitic mudstone and ironstone nodule layers. The lower portion of the thrust is located within the sandstone and tends to incline more gently than the bedding plane while the upper portion is located approximately at the contact of the sandstone and the mudstone layers. The imbricate thrusts are overlain by layers of gently folded sandstone and mudstone.

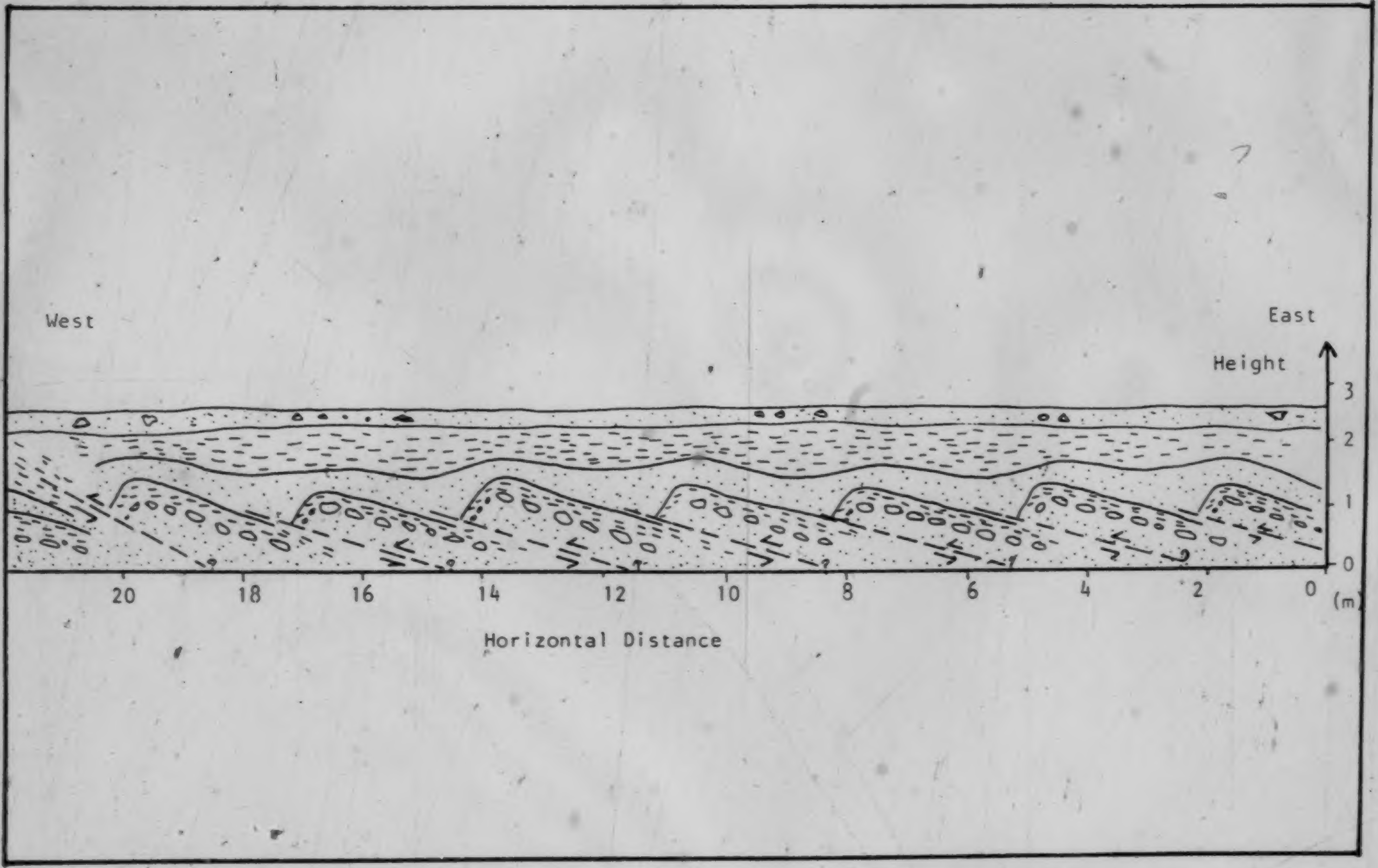
West
East
Height
3
2
1
0
(m)
20
18
16
14
12
10
8
6
4
2
0
Horizontal Distance

Figure C.23 : Section Exposed in Area Northwest of Sullivan Lake
(exposed in a ditch along Highway 12 about 31 km east of the town of Stettler)

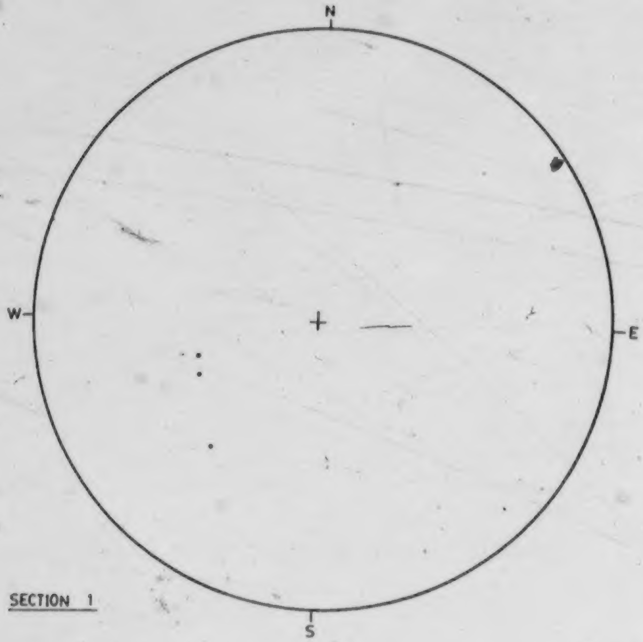

SECTION 1

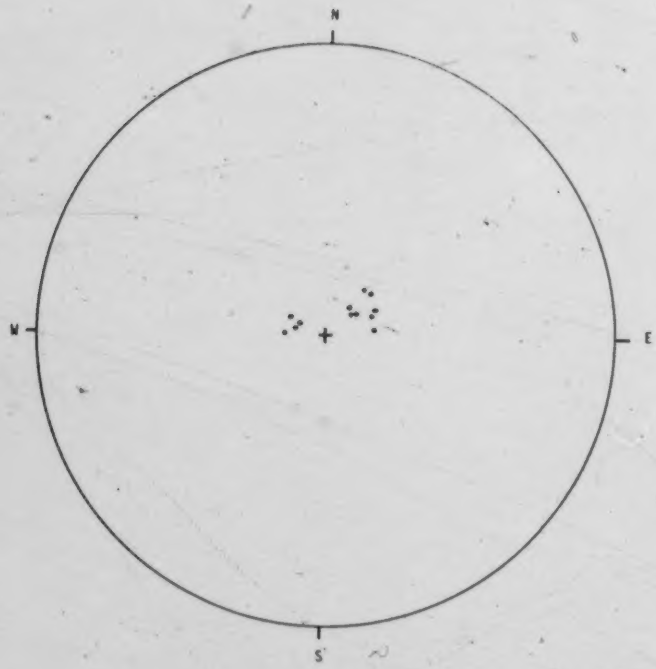

Figure C.24 Stereographic Plots of Deformed Beds: a - Section 1, Area Northwest of Sullivan Lake, b - Sections 3, 4a, 4b and 5, Hanna - Sedgewick Area

The thrusts seem to die upward into the gently folded sandstone. Due to the weathering on the outcrops, the amount of apparent minimum shortening due to folding and thrusting is difficult to measure; nevertheless, the exposed section indicates that there is at least 2.5 m of shortening due to thrusting.

The deformed N-S trending ridge is interpreted as an ice-thrust ridge. Due to insufficient morphology and exposures of the ice-thrust features in the area, the complete boundary of the ice-thrust terrain unit cannot be outlined; nevertheless, the ice-thrust terrain pattern of the area is shown in Figure C.22.

C.3.4 Nevis Area

Airphoto interpretation indicates that sections along Highway 21A are located near the west-facing top edge of a meltwater channel that runs from north to south into the modern Red Deer River (Photo AS 2562-151, 152, 153; scale 1: 30,000) (Figure C.25).

Field studies showed that the exposed bedrock consisted of coarse- to fine-grained sandstone to bentonitic sandstone, coarse-grained, cross-bedded sandstone, greenish grey bentonitic shale, black shale, nodular ironstone, coal and lignite. The sections are overlain by a thin pebbly till of less 0.1 m to 0.6 m thick. The sections exposed consist of folds with an apparent wavelength of 12.5 m, an amplitude of 0.46 m, and fold axes with trend/plunge of 140°/ 16° SE,

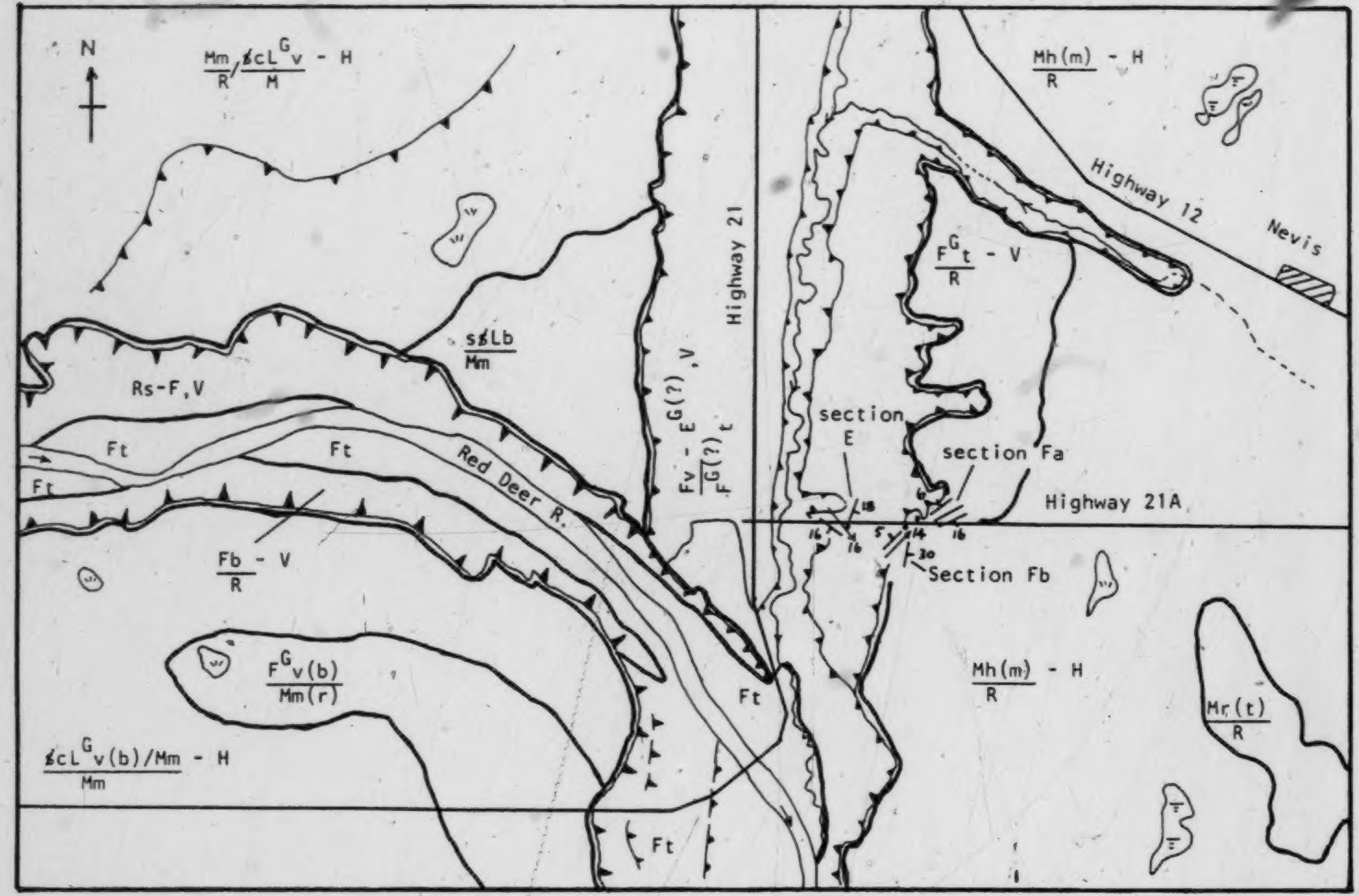
N
Mm/R / ≮cL^G v/M - H
Mh(m)/R - H
Highway 12
Nevis
Highway 21
Fv - E^G(?),V / F^G(?)t
s≮Lb/Mm
Rs-F,V
Ft
Ft
Ft
Red Deer R.
F^G t/R - V
section E
section Fa
Highway 21A
Section Fb
18
16
16
5
14
16
30
6
Fb/R - V
F^G v(b)/Mm(r)
Mh(m)/R - H
Mr(t)/R
Ft
Ft
≮cL^G v(b)/Mm - H / Mm

Figure C.25 : Terrain Pattern of Nevis Area (Interpreted and Traced from Airphoto AS 2562-152, Scale 1: 30,000)

042°/ 14° NE, 027°/ 0°, 241°/ 0. The stereographic plots of the poles to the structures measured in the area are presented in Figure C.26 and Figure 8.1 shows the symbols used in the plots. Near the intersection of Highways 21 and 21A, the beds on the exposed sections are mostly inclined toward northwest or south or gently folded.

The portion of the meltwater channel where the deformed sections are found is thought to be ice-deformed. At present, the available geological information is not enough to outline the complete boundary of the ice-thrust terrain unit in the area. Figure C.25 shows the ice-thrust terrain pattern of the study area.

C.4 Hanna - Sedgewick Area

Four sections (Sections 3, 4a, 4b and 5) which are exposed along Highway 36 east of the southeastern shore of Sullivan Lake have been studied in detail. The exposed bedrock is composed mainly of coarse- to fine-grained bentonitic sandstone, bentonitic siltstone to mudstone, coal/lignite and nodular ironstone which are overlain by sandy to clayey till about 0.3 m to 0.8 m thick. Field observations indicate that the exposed bedrock is tilted and deformed. The measured dip/dip direction of the bedrock exposed are 9°/ 108°, 9°/ 254°, 12°/ 249°, 10°/ 100°, 12°/ 222° and 14°/ 232° (Figures C.24b and 8.1). At one section, the coal/lignite and bentonitic sandstone beds have been intruded by a layer of bentonitic mudstone with an apparent

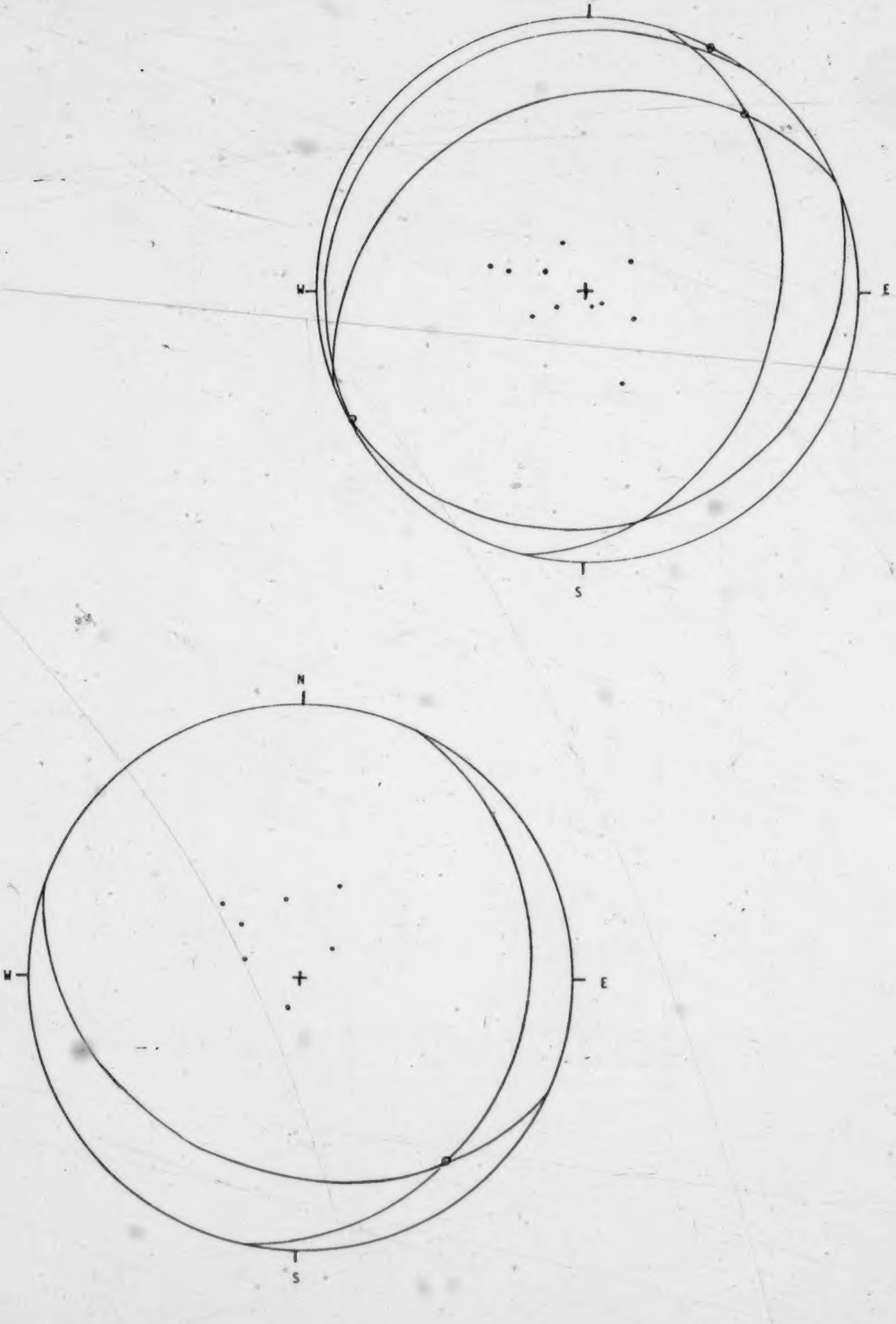

Figure C.26 Stereographic Plot of Deformed Beds, Nevis Area

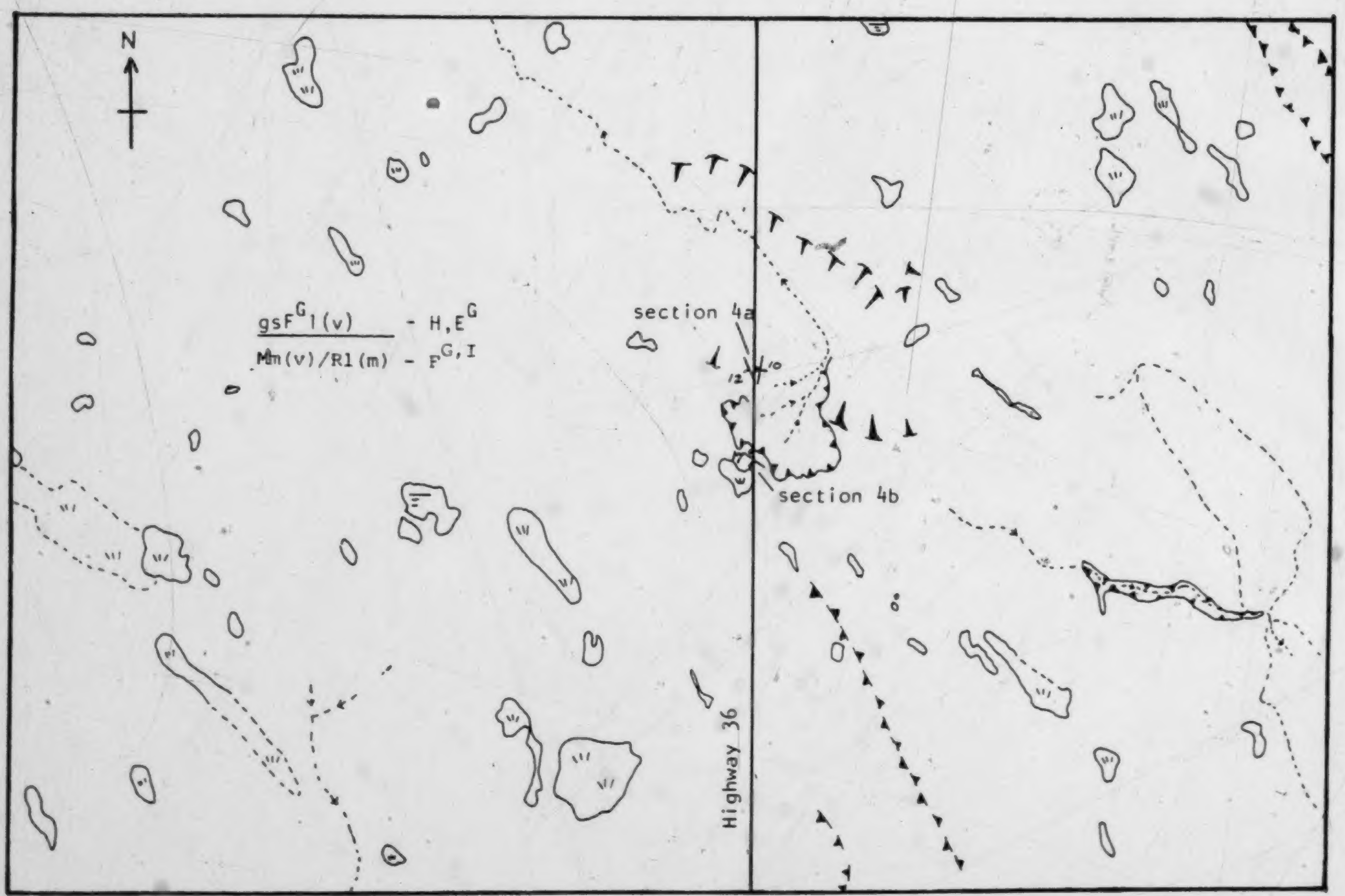
N
gsF^{G}l(v) - H,E^{G}
Mm(v)/Rl(m) - F^{G,I}
section 4a
12
10
section 4b
Highway 36

Figure C.27 : Terrain Pattern at Hanna - Sedgewick Area (Interpreted and Traced from Airphoto AS 1336-225, Scale 1: 31,680)

movement of at least 0.46 m.

Airphoto interpretation indicated that on the whole, the study area is a gently rolling plain (Torlea flats) and is located within or adjacent to a spillway with coarse-grained glaciofluvial deposits overlying bedrock or covered by a thin layer of till which in turn overlies bedrock (Photo AS 1336-224, 225, 226, 278, 279; scale 1: 31,680). Several NW-SE aligned shallow troughs, kettles and marshes are seen on the plain. These depressions probably formed when the spillway overflowed and meltwater flowed over the area east of Sullivan Lake. Two linear ridges, which are roughly parallel to the trend of the aligned depressions, are found at about 317 m and 475 m northeast and southwest of an exposed section respectively (Photo AS 1336-115, 116, 117; scale 1: 31,680).

In this area, the morphology of the ice-thrust features is indistinct on aerial photographs and in the field, and the complete boundary of the ice-thrust terrain unit cannot be delineated based only on the exposures. The ice-thrust terrain pattern of the area where sections 4a and 4b exposed are shown on Figures C.27.

C.5 Cypress Hills Area

Airphoto interpretation indicates that the area is composed mainly of a badland terrain unit veneered by a thin layer of till, a meltwater channel (the Medicine Lodge Coulee) that runs roughly NW-SE, and a kettled hummocky disintegration moraine terrain unit which occupied the northern and southwestern corner of the photograph (Photo AS 2503-171, 172; scale 1: 60,000) (Figure C.28). The wall of the meltwater channel is steep and is usually covered by fluvial deposits. Gully erosion is common along these slopes.

Field studies are performed in two clay pits, Pits 39 and 45, in the area. Pit 39 is located at the boundary of the badland terrain unit and the meltwater channel; while Pit 45 is situated along the walls of a valley within the badland terrain unit (Figure C.28). The stratigraphic section exposed in the Pit 45 was mapped and is shown in Figure C.29.

In Pit 39, the beds are inclined with a general dip toward southeast. A thrust fault (dip/ dip direction: 32°/ 078°) and a normal fault (71°/ 070°) are found with dip toward northeast; while a reverse fault (54°/ 230°) shows a dip toward southwest (Figure C.30). The symbols used in the stereographic plots are shown in Figure 8.1. Small-scale open folds are observed in the shale of the Battle Formation with apparent amplitudes and wavelengths of 0.15 - 0.66 m and 0.9 - 3.9 m respectively, with one fold axis having a trend/plunge of 177°/14° S. The folds found in the area were formed earlier than the faults since the former are observed being displaced by the latter. Some of the dips of the beds decrease from 30° E to about 22° SE.

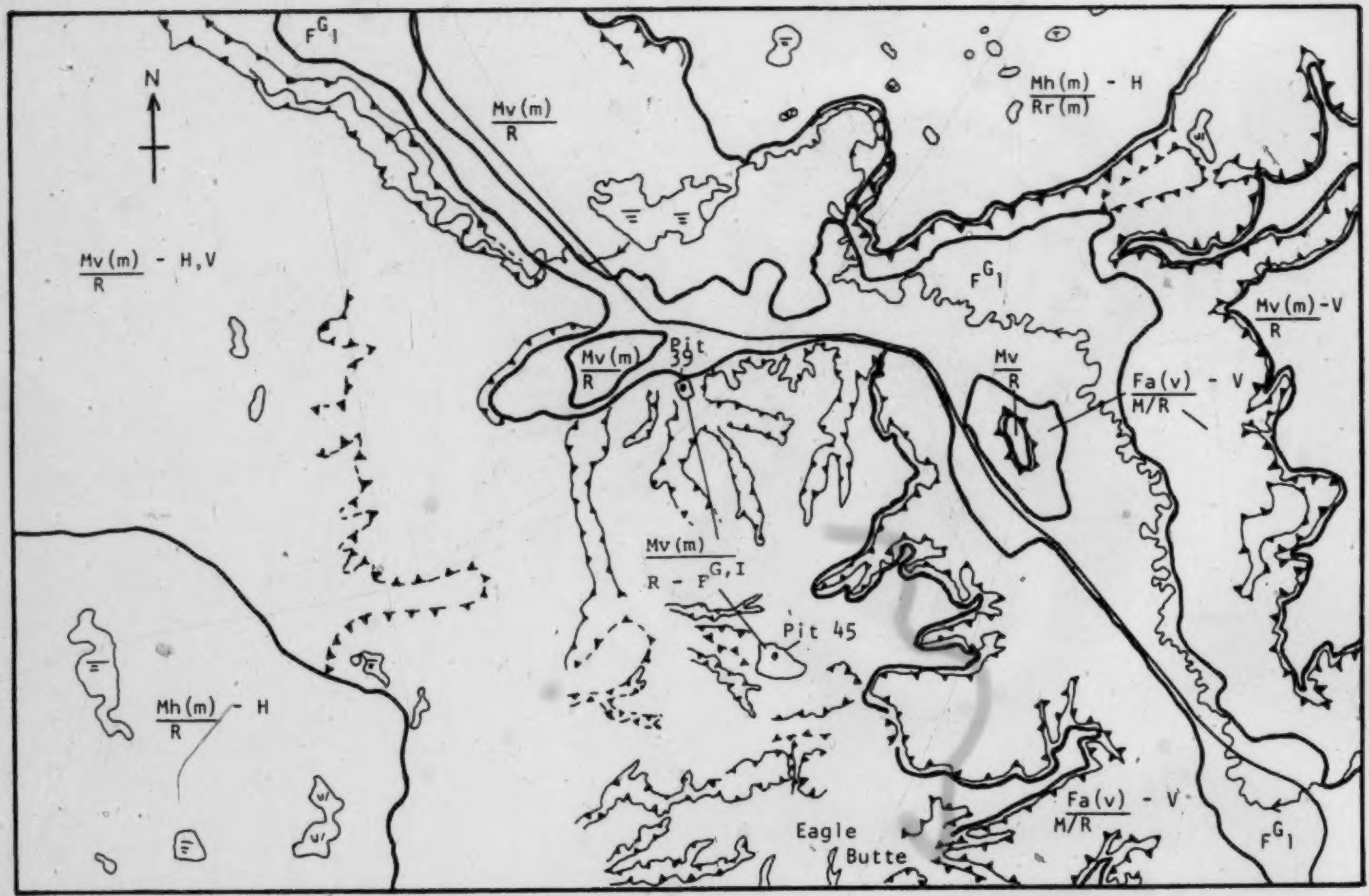
F^{G}_{1}
N
Mv(m)/R
Mh(m)/Rr(m) - H
Mv(m)/R - H,V
F^{G}_{1}
Mv(m)/R - V
Mv(m)/R
Pit 39
Mv/R
Fa(v)/M/R - V
Mv(m)/R - $F^{G,I}$
Pit 45
Mh(m)/R - H
Fa(v)/M/R - V
Eagle Butte
F^{G}_{1}

Figure C.28 : Terrain Pattern of Cypress Hills Area (Interpreted and Traced from Airphoto AS 2503-171, Scale 1: 60,000)

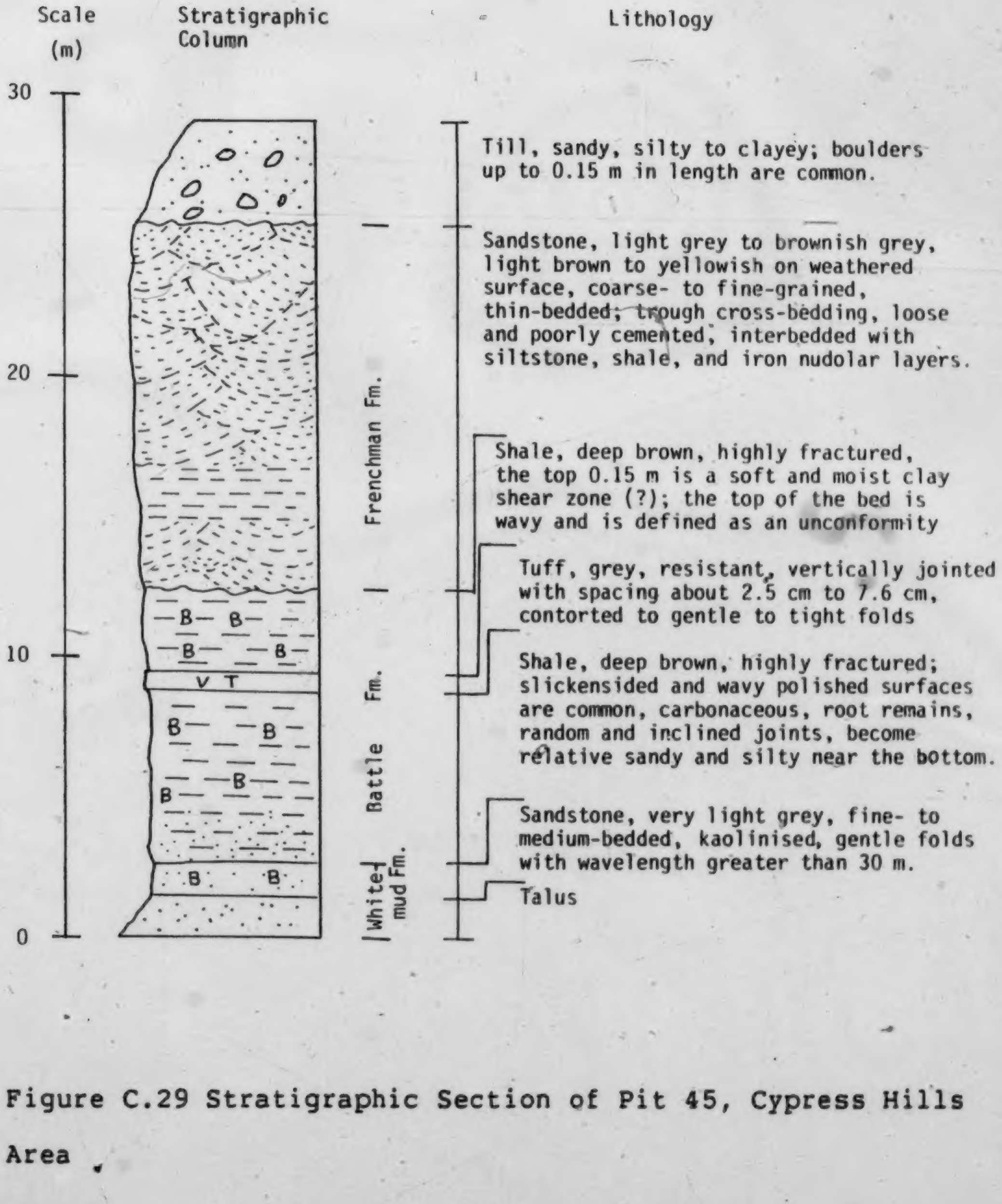

Till, sandy, silty to clayey; boulders up to 0.15 m in length are common.

Sandstone, light grey to brownish grey, light brown to yellowish on weathered surface, coarse- to fine-grained, thin-bedded; trough cross-bedding, loose and poorly cemented, interbedded with siltstone, shale, and iron nudolar layers.

Shale, deep brown, highly fractured, the top 0.15 m is a soft and moist clay shear zone (?); the top of the bed is wavy and is defined as an unconformity

Tuff, grey, resistant, vertically jointed with spacing about 2.5 cm to 7.6 cm, contorted to gentle to tight folds

Shale, deep brown, highly fractured; slickensided and wavy polished surfaces are common, carbonaceous, root remains, random and inclined joints, become relative sandy and silty near the bottom.

Sandstone, very light grey, fine- to medium-bedded, kaolinised, gentle folds with wavelength greater than 30 m.

Talus

Figure C.29 Stratigraphic Section of Pit 45, Cypress Hills Area

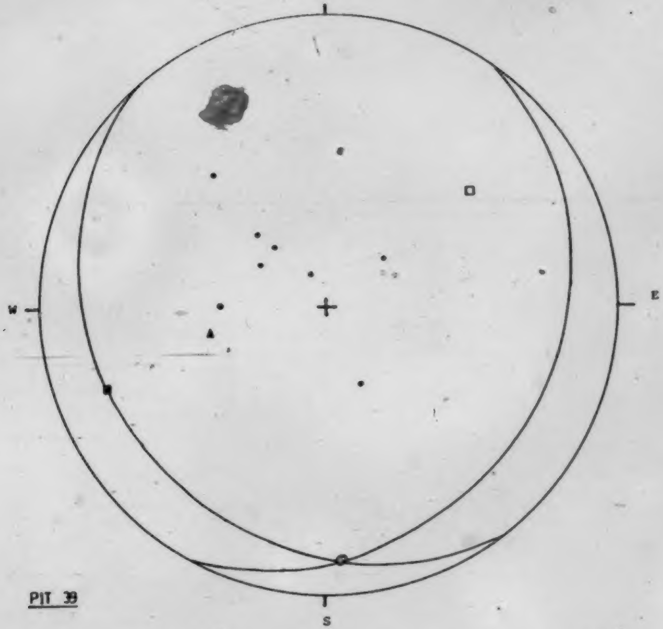

PIT 39

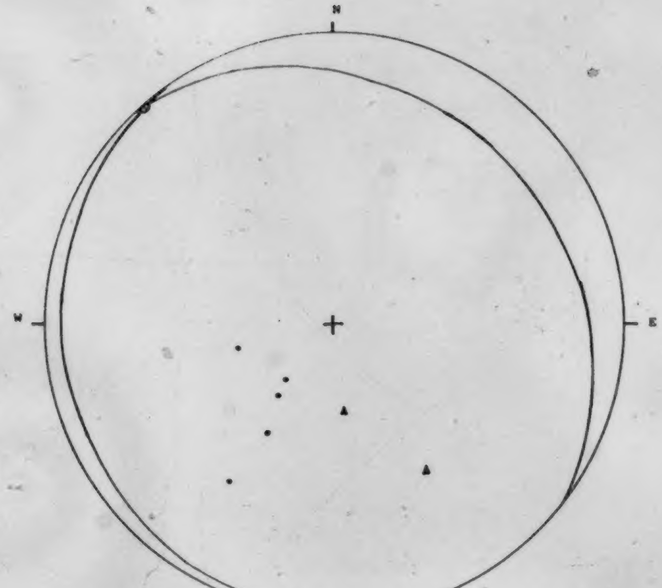

PIT 45

Figure C.30 Stereographic Plot of Deformed Beds, Pits 39 and 45, Cypress Hills Area

In Pit 45, the beds are in general tilted toward the northeast. However, the tuff bed in the Battle Formation has been deformed into a gentle to tight fold with a trend/plunge of 319°/ 2° NW; and a thrust fault is observed near the crest of this fold (Plate C.1). Figure C.30 is a stereographic plot of the poles of bedding and faults measured in Pit 45. Thrust faults are observed in the cross-bedded sandstone of the Frenchman Formation and the bentonitic shale of the underlying Battle Formation which dip northwest to north. These thrust faults seem to be listric. The shale of the Battle Formation appears to be a shear zone because of the brecciated and fractured nature of the material, and the presence of many continuous and discontinuous, planar and wavy thrust faults. A normal fault, with an apparent displacement of at least 2.6 m, is found in the crest of the gently folded anticline in the overlying Frenchman Formation. On the whole, the beds are deformed into a broad gentle anticline with an apparent wavelength and amplitude of 490 m and 13 m respectively. Plate C.1 shows the macrofabric observed in Pit 45. It is noted that only anticlinal features but no synclinal features were observed in Pit 45.

Due to the limited deformed structures exposed in the area, the boundary of the ice-thrust terrain unit has not been drawn. Figure C.28 shows the ice-thrust terrain pattern of the study area.

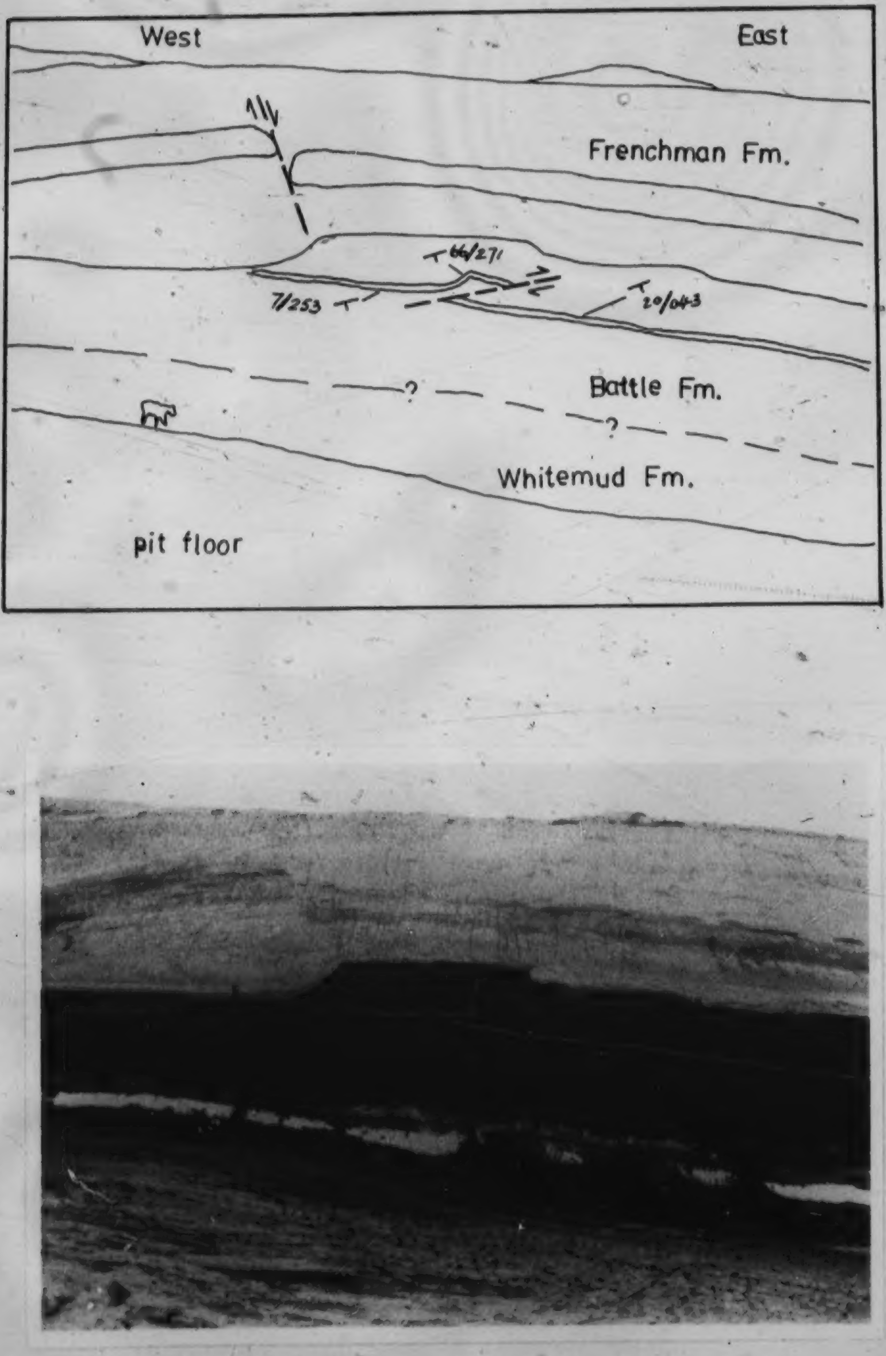
West
East
Frenchman Fm.
66/271
7/253
20/043
Battle Fm.
?
?
Whitemud Fm.
pit floor

Plate C.1 Macrofabric Exposed in Pit 45, Cypress Hills area

Appendix D - Calculation of Interbed Slip along Highwall due to Excavation

Matheson (1972, p. 270) noticed that artificial excavations under undrained conditions in the overconsolidated Tertiary and Upper Cretaceous bedrock have a maximum rebound of less than 1 % of the excavation depth; and the upper bound of vertical displacement of the excavation edge is about 1/3 of the maximum rebound occurring in the centre of the excavation (Matheson and Thomson, 1973, p. 971). Although no measurements have been taken by the author on the elastic rebound movement on the pit wall and floor due to the excavation, the amount of interbed slip that occurred near the highwall in Pit 3, Highvale mine, can still be estimated by examining the recorded rebound in an excavation in similar material.

Eisenstein and Morrison (1973, fig. 16, p. 207) and DeJong and Morgenstern (1973, fig. 10, p. 272) studied the movement in an excavation with a depth of about 11.3 m in downtown Edmonton. The overconsolidated Horseshoe Canyon Formation at the site (where most rebound occurred) is about 6 m below the bottom of the excavation; however, measurements indicate that heaving mainly took place in the bedrock. The recorded heave data measured by DeJong and Morgenstern (1973) show the time delay to reach approximately 80 % of the two year heave is roughly two months; as a result, the total rebound in response to unloading can be treated as instantaneous and elastic. Two months after the excavation had started, there was a heave of about 1.3 cm at the wall which diminished rather linearly to about zero at approximately 6 m behind the wall, and the heave in the centre of the excavation was about 4.5 cm. In this case, the vertical heave at the excavation wall is about 29 % of the maximum rebound at the centre of the excavation, which is rather close to the value of 1/3 as suggested by Matheson (1972).

With the observations mentioned above, the edge of the highwall in Highvale mine is believed to have an instantaneous and elastic heave of about 1/3 of the maximum rebound at the centre of the excavation, which would be equal to about 1 % of the height of the wall. The measured depth of the excavation in Pit 3 and the bedding thickness are about 20 m and 0.3 m respectively; thus, the resulting maximum rebound in the centre of the excavation would be about 0.2 m with a vertical displacement at the edge of about 7 cm. Let the heave diminish to zero at 6 m behind the edge of the highwall; thus, the maximum inclination of the bedding against horizontal on the wall is equal to $\tan^{-1}(7 / 600)$. According to Norris (1967, p. 318) and Matheson (1972, p. 313), interbed slips between two layers at their common interface for a sinusoidal arc can be estimated as follows:

$S = (T \cdot \pi \cdot \theta) / 180$ ....(D.1)

where T = thickness of each layers, θ = deflected inclination (in degrees) of the fold layer with respect to the horizontal, and $\pi = 3.1416$.

Substituting the above infomation into equation (D.1), the amount of interbed slip that might occur on the strata exposed along the highwall due to the excavation in Highvale mine is equal to about 3.5 mm. This value is much smaller than the displacements (30 - 200 mm) required for a shear surface of a normally or overconsolidated clay to reach close to a residual strength (Skempton, 1985).

Appendix E - Location and Procedures for Block Sampling, Pit 3, Highvale Mine

In the summer of 1983, slope instability occurred in the highwall of Pit 3, Highvale mine, Wabamun Lake area, which endangered the draglines operating on the bench of the highwall.

A field program was set up to study the geological and geotechnical properties of ice-thrust sediments in Pit 3 of the mine in the summers of 1983 and 1984. These included field mapping of the slide area and block sampling at the shear zone which was suspected to be formed by ice thrusting.

In the summer of 1984, the author studied the slides that occurred in Pit 3 about one month after they had taken place. Two trial pits were dug in the shear zone exposed along the highwall about 20 m from the two main slide bodies (Slides 1 and 2). Figures 10.2 and 10.3 show the locations for the block sampling. Field observations have shown that these trial pits were located on a stable area. Samples were collected at or close to the flat-lying principal displacement shear that appeared in the shear zone within the bentonitic mudstone and the bentonite layer from trial pits 1 and 2 respectively (Figures 10.2 and 10.3). These trial pits were carefully dug into the highwall about 0.7 m from the face of the wall to eliminate desiccated material due to drying and to expose 'unweathered' material for sampling. Desiccation did not extend more than 0.3 m below the exposed surface of the overconsolidated clays that had been exposed for several years (Fookes and Dennes, 1969, p. 473). Direct shear test moulds were taken to the field and placed directly on the bottom of the trial pits where the samples were desired. The moulds were pushed gradually into the layer while the outer edge of the soil (about 5 mm from the outer faces of the moulds) were continuously carved away. Plate E.1 shows one of the shear test moulds being pushed through the failure surface of the slide. The height of the samples collected was greater than the height of the moulds prior to extraction in order to reduce disturbance. Block samples, 0.3 m x 0.3 m x 0.15 m, were also collected. These block samples and the direct shear test moulds were waxed in the field and were transported to the laboratory within a few hours. In the laboratory, they were further waxed and stored in the moisture room ready for examination and testing.

Plate E.1 Sampling the Bentonitic Mudstone by a Direct Shear Test Mould, Pit 3, Highvale Mine

Appendix F - Microfabric: Laboratory Preparation and Method of Study

F.1 Preparation of Samples for Thin Sectioning

The orientation of the fold axes and slickensided features found in the deformed structure observed in Highvale mine indicate that the sediments were deformed by an ice lobe coming from the north (Appendix C, Figure C.9a). As a result, the configuration of any deformed fabric (such as grain alignments and faulting) due to ice thrusting should be best exposed on north-south oriented cross sections through the deformed layer (Figure 5.2). Thus, in order to study the microfabric of the ice-disturbed sediments, samples for thin sectioning were cut approximately parallel to north-south and vertically down through the block samples collected in the ice-deformed strata in the mine.

Four slices were cut from the bentonitic mudstone block sample and five slices were obtained from the bentonite block sample. Figure F.1 shows the locations in the block sample of bentonitic mudstone taken for thin sectioning. The geologic features appearing on these slices and hand specimens have already been described earlier in the Mesofabric Section of Chapter 6. All samples were cut with a steel wire to a thickness of about 1 cm, a length of 5 cm and a height of 8 cm. They were logged, photographed and immediately sent for thin sectioning.

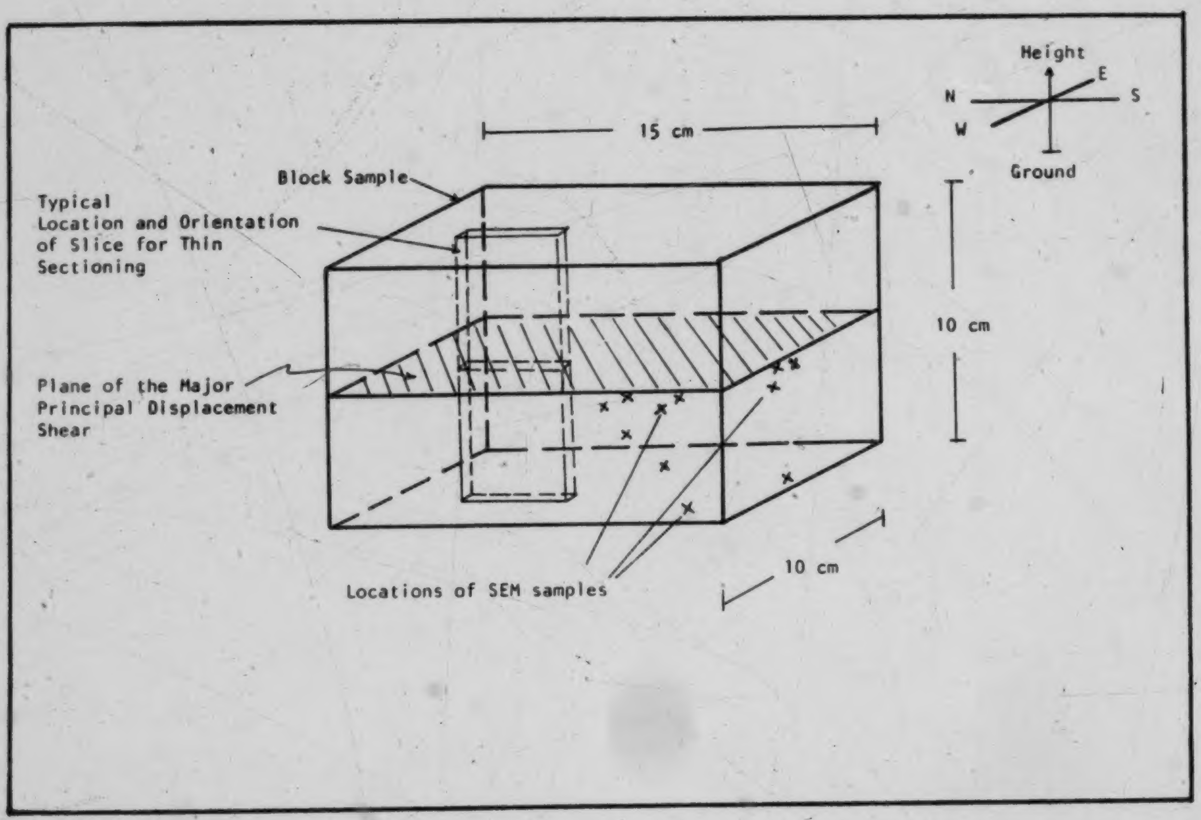
Height
E
N
S
W
Ground
15 cm
Block Sample
Typical
Location and Orientation
of Slice for Thin
Sectioning
10 cm
Plane of the Major
Principal Displacement
Shear
Locations of SEM samples
10 cm

Figure F.1 Locations in Block Samples for Thin Sectioning and SEM Samples

F.2 Preparation of Thin Sections

1. The slices were dried in room temperature for about 12 hours before being put into an oven at a temperature of 35° C for half an hour. This drying process is to ensure most of the pore spaces within the samples are dry so that when the samples are impregnated with the hardening mixture, the pore space of the samples would be entirely filled by the mixture.

   Shrinkage occurring during drying may disturb the microfabric of the samples. To evaluate the amount of shrinkage associated with the drying under room temperature for about 12 hours, the shrinkage limits of the samples, which indicate the amount of shrinkage, were estimated following the procedures outlined by Holtz and Kovacs (1981, p. 182). The resulting shrinkage limits of the bentonitic mudstone and the bentonite are 24.4 and 16.7 % respectively. Since the average natural moisture content of the bentonitic mudstone is about 28 %, the amount of overall shrinkage of the bentonitic mudstone samples associated with drying under room temperature is considered to be small. On the other hand, the bentonite has an average natural moisture content of about 47 %. As a result, shrinkage disturbance of the microscopic features is thought to be significant for the bentonite during preparation of thin sections. Thus, both the mesoscopic and microscopic fabric of the bentonitic mudstone that appear in hand specimens and thin sections was studied by the unaided eye and under microscope respectively; however, only the mesoscopic fabric of the bentonite is described.

2. The dried samples were impregnated with a hardening mixture after removing from the oven. The hardening mixture is made up of 4 parts of resin (EPO-TEC301) and 1 part of dyed hardener (8 grams of blue dye (Orocet Blue) mixed with 350 grams of hardener to produce the dyed hardener). The blue dye would show whether the pore spaces within the samples were saturated with the hardening mixture; and moreover, it differentiates natural fissures from those formed due to thin sectioning.

Carbowax 6000, although the most common impregnating agent used to cement the clay fabric against disturbance during thin sectioning (Mitchell, 1956; Morgenstern and Tchalenko, 1967c), was not used in this study because: (a) EPO-TEC 301 has an index of refraction the same as glass and is thus non-birefringent and would not influence the birefringence of any clay minerals under polarized light, (b) EPO-TEC 301 is harder than Carbowax which has a Moh's hardness number of 1 (Barden and Sides, 1971a), the use of the former as the impregnation agent would further decrease the thickness of the disturbed zone due to grinding, (c) the lineal shrinkage of Carbowax is generally less than 8 % while the shrinkage of EPO-TEK 301 with room temperature/overnight cure is about 1.5 % only.

3. After the samples were saturated with the mixture, they were taken from the mixture and left in the air for about 12 hours to harden.
4. One of the surfaces of the hardened samples was smoothed by hand grinding on silicon carbide paper (220 grit and 400 grit).
5. The smoothed surfaces of the samples were glued to a glass plate with the same hardening mixture described. However, no blue dye was in the mixture this time. Again, the samples were left for 12 hours for the mixture to harden.
6. The other side of the rough surfaces of the samples were hand ground on silicon carbide paper to a thickness of about 32 μm.
7. Finally, a thin glass cover (about 0.17 mm thick) was glued to the smooth surface with a fast hardening liquid (Eukitt). The samples were then ready for examination under microscope.

F.3 Optical Theory Used to Study the Microfabric of Clay

The study of the microfabric of clay based on the optical properties of clay under a polarizing microscope has been performed by Mitchell (1956), Morgenstern and Tchalenko

(1967a, 1967b, 1967c, 1967d), Tchalenko (1968a), and Chandler (1973). The following outlines the basic optical theory used in these studies.

The most common and abundant clay minerals in the ice-thrust sediments found in the study area are montmorillonite, illite and kaolinite (Figure 6.6) which have an essentially plate-like structure. The crystallographic axes of these clay minerals are orthogonal and parallel to nearly parallel to their optical axes; moreover, the refractive indices along the two optical axes lying parallel to the basal planes are equal to each other for all practical purposes (Deer et al., 1966). Thus, although these clay minerals are biaxial crystals, the optical properties shown under crossed-nicols of a polarizing microscope are similar to uniaxial crystals. That is, the clay minerals would show low birefringence (mainly greyness to opacity) when the basal planes are normal to the axis of the microscope or to the incident polarized light. However, when the basal planes are parallel to the axis of the microscope or the incidence of the polarized light, the clay minerals would show minimum illumination or extinction when the trace of basal plane of the crystal is parallel or normal to the vibration of polarized light; and maximum illumination when the trace of the basal plane is 45° from the polarizing direction. As a result, there are four directions of extinction and four directions of maximum illumination when the stage of the polarized microscope is rotated 360° under cross-nicols (Bloss, 1961; Hurlbut and Klein, 1977).

Since clay minerals always occur as submicroscopic crystals in nature, the shape of individual clay mineral is often indiscernable under a standard microscope. Indeed, clay minerals always appear as a matrix or aggregates under SEM (Yong and Sheeran, 1973; Pusch, 1973b; Collins and McGown, 1974). This implies that if the clay minerals within the aggregate are randomly oriented, there will be no obvious change in the intensity of illumination of the aggregate under polarized light when the stage of the polarized microscope is rotated 360°; on the other hand, if there is preferred orientation within the matrix, the rotation of the stage to a certain position would cause the oriented clay minerals within the matrix to display maximum illumination or extinction while the rest of the matrix is under extinction or relative weaker illumination. In this case, the magnitude of illumination of the aggregates would be enhanced by the increase in preferred particle orientation. Using the above technique, the shape, size and the spatial relationship of the oriented and/or randomly oriented groups of clay minerals, and other microfabric can be recognized.

F.4 Method of Study

This is essentially a qualitative approach and mainly follows similar work performed on clays and shale by Phillips (1939), Mitchell (1956), Tchalenko (1968b, 1970), and Locker (1973). In general, the aligned clay particles are identified when a group of clay particles have shown four positions of maximum illumination and four positions of minimum illumination or extinction when the stage of the polarized microscope is rotated 360° in contrast to the relatively constant intensity of illumination shown by the surrounding matrix which is composed of a randomly oriented structure. No attempts were made to measure the birefringence ratio or the degree of orientation of clay particles semi-quantitatively by the photometric method, which essentially deals with monomineralic material, as outlined by Morgenstern and Tchalenko (1967c).

A standard polarized microscope (ZIESS Photomicroscope) with a 35 mm camera mounted to take photomicrographs was used to study the microfabric of the ice-thrust sediments. The objectives of the microscope have powers of 2.5x, 10x, and 40x, and the diameter of the field of view of the first two objectives are 5.4 mm and 1.4 mm respectively.

Appendix G - Submicrofabric: Laboratory Preparation and Method of Study

G.1 Preparation of SEM Samples

The samples used for the SEM study were prepared by freezing, fracturing, drying, mounting, peeling, and gold coating following the methods suggested by Gillott (1969), Barden and Sides (1971a), and Tovey and Wong (1977).

The samples are freeze-dried instead of air-dried because the moisture content of the samples studied varied from above to close to the shrinkage limit. Barden and Sides (1971a) and Tovey and Wong (1977) reported that the amount of shrinkage related to air-dried and freeze-dried samples with a moisture content above the shrinkage limit are 8 % or higher and 0.5 % respectively. Moreover, although the critical point drying method creates less shrinkage than the freeze-drying method, the latter method was employed in this study because the samples studied are relatively fissured and locally unsaturated. It is noted that the impregnation of unsaturated samples required for the critical point drying method may cause disintegration (Tovey and Wong, 1977, p. 187).

The procedures for the sample preparation are briefly described below. Figure F.1 shows the locations in the block sample of the bentonitic mudstone where SEM samples were taken.

1. 1.5 cm x 1.5 cm x 2 cm retangular blocks were cut gently

from the block samples with a razor blade. In order to eliminate edge disturbances on the microfabric of the specimens caused by field sampling as pointed out by Barden and McGown (1973), all the SEM samples were taken at least 2 cm away from the sides of the block samples.

2. Each sample was gently notched at the place where fracture would be made after freezing.
3. These small sample blocks were frozen in liquid nitrogen, and then fractured along the notches into small cubes with sides of about 1 cm by sharp blows on a frozen razor placed against the notch.
4. The cubes were put into the freeze dryer where the frozen water would be sublimed.
5. After about 24 hours, the cubes were taken out of the dryer and each was mounted on a metal stand. The loose particles on the fracture face were peeled away by applying adhesive tape to the face about 50 times.
6. The peeled samples were put into the sputter coater where the fracture face was coated with a thin layer of pure gold about 0.02 μm thick. The samples were then ready for SEM examination.

G.2 Method of Study

The Cambridge Stereoscan 250 equipped with the Kevex 7000 Energy Dispersive Analyzer for mineral identification was used in this study. Twelve SEM samples, which were taken at and below the major principal displacement shear that appeared in the block sample collected from the shear zone exposed in Pit 3, Highvale mine, were examined under the SEM. The fractured faces of these samples for the SEM examination were chosen such that they were either parallel or normal to the plane of the major principal displacement shear and its displacement direction.

The fracture face of each sample was scanned thoroughly under magnifications of 20x to 1,000x in order to obtain a general picture of the microfabric of the sample and the presence of any peculiar features. About 20 sites on each face were then studied in detail under medium to high magnifications of 1,000x to 20,000x. These sites were either areas of interest that were found during the preliminary viewing of the samples under low magnifications or were randomly scanned sites. An attempt was also made to obtain the energy dispersive system spectrum of some of the grains for mineral identification (Welton, 1984). Features of interest were described, hand-sketched and photographed.

Appendix H - Laboratory Tests Results

Table H.1 Atterberg Limits of Bentonitic Mudstone* in Highvale Mine

Borehole/ Sample #HV	Depth (m)	w (%)	P_L (%)	L_L (%)	I_P (%)	I_L	γ_t KN/m^3
83-3/C10	27.3	26.3	37.9	92.9	55.0	-0.21	19.44
83-3/C19	27.3	22.5	31.1	82.0	50.9	-0.17	19.25
83-7/C9	30.2	19.3	26.8	75.1	48.3	-0.16	19.70
83-8/C4	13.0	45.0	26.6	72.5	45.9	0.40	
83-8/C9	24.0	25.6	26.3	88.0	61.7	-0.01	19.94
83-9/C4	16.2	29.4	37.3	110.0	72.7	-0.11	20.17
83-9/C8	29.1	25.2	34.4	127.1	92.7	-0.10	18.89
83-10/C6	19.5	23.6	38.8	90.3	51.5	-0.30	20.13
83-17/C7	23.0	23.7	53.6	74.8	21.2	-1.41	19.14
83-406/7	11.6	26.6	31.0	61.0	30.0	-0.15	19.41
83-406/9	14.3	19.3	23.9	62.6	38.7	-0.12	20.29
83-406/11	14.7	49.3	23.9	67.4	43.5	0.58	17.28
83-408/RC10	36.85	18.0	23.6	87.4	63.8	-0.09	
83-413/RC4A	9.04	46.5	47.0	121.0	74.0	0.0	
83-413/RC4B	9.36	47.5	47.0	121.0	74.0	0.0	
83-415/RC3B	10.5	23.2	27.7	135.5	107.8	-0.04	
83-415/RC3B	10.85	26.3					
83-415/RC5	16.7	15.0					
83-416/RC8	33.16	20.3					
83-417/RC7	31.95	30.0	40.0	235.0	195.0	-0.05	
83-418/RC4	9.70	11.9					

*Tested by Thurber Consultants Ltd., Hardy Associates Ltd., and Monenco Ltd.

Table H.2 Summary of Consolidation Tests on Bentonitic Mudstone

Sample No	Depth (m)	w (%)	γ_t KN/m³	e_o	S_i (%)
1	14	28.2	19.26	1.03	73.9
2	14	17.8	18.81	1.01	47.6

Sample No	OCR	P_o' (KPa)	P_c' (KPa)	C_c'	C_s'	a_v $\times 10^{-4}$
1	1.8	176	320	0.125	0.042	-6.3
2	2.1	176	370	0.097	0.029	-3.7

S_i = initial degree of saturation

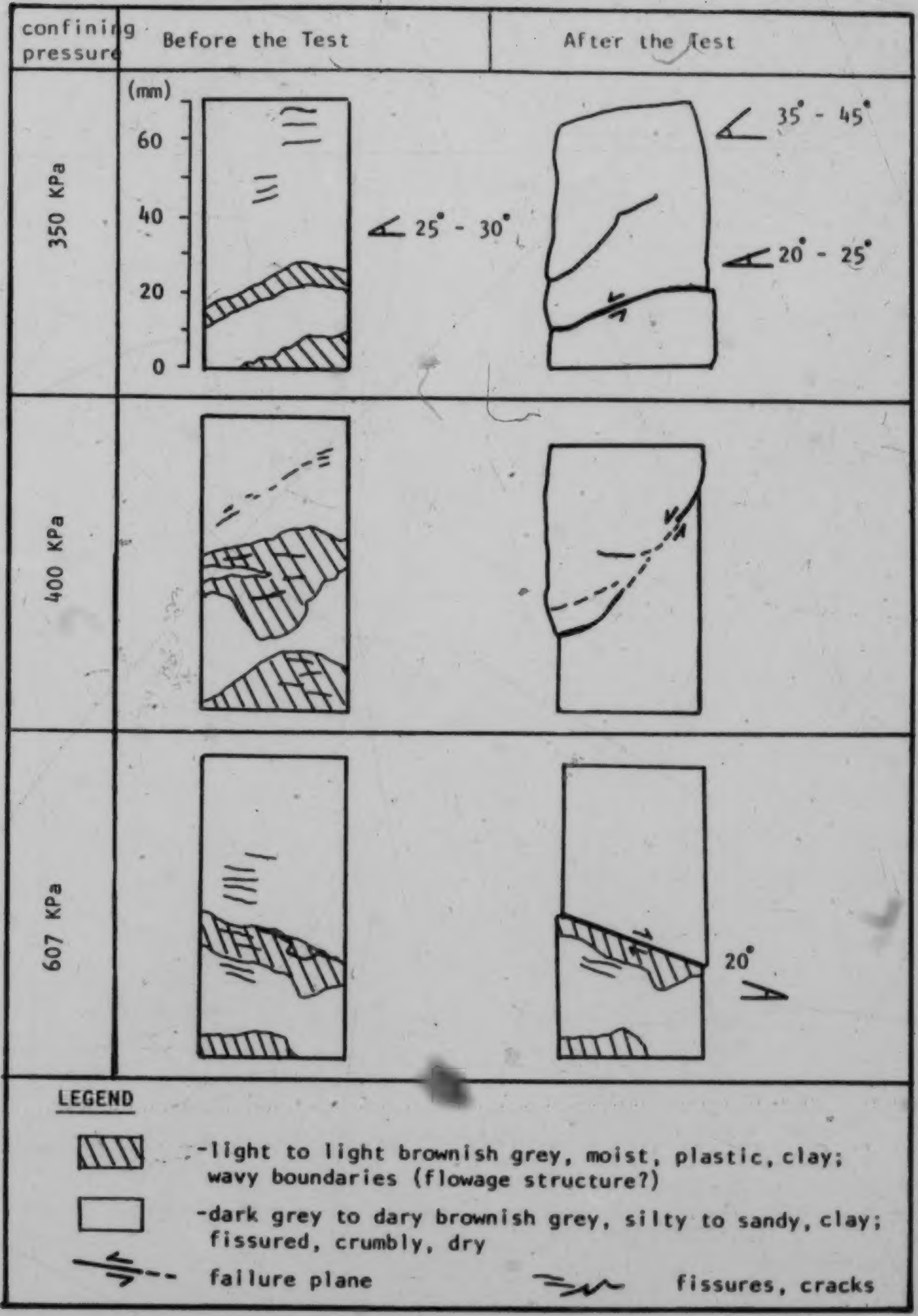
confining pressure
Before the Test
After the Test
350 KPa
400 KPa
607 KPa
(mm)
60
40
20
0
25° - 30°
35° - 45°
20° - 25°
20°
LEGEND
-light to light brownish grey, moist, plastic, clay; wavy boundaries (flowage structure?)
-dark grey to dary brownish grey, silty to sandy, clay; fissured, crumbly, dry
failure plane
fissures, cracks

Figure H.1 Lithological and Structural Descriptions of Triaxial Test Samples, Bentonitic Mudstone

Table H.3 Summary of Consolidated Undrained Triaxial Tests on Bentonitic Mudstone

Sample No	Depth (m)	w (%)	γ_t KN/m³	σ_c' (KPa)
1*	14	35.6	19.2	400
2*	14	36.7	19.12	526
3*	14	28.6	19.44	701
HV-83-406**	12.8	19.1	20.72	150
HV-83-406**	12.8	18.9	20.72	300
HV-83-406**	12.8	17.9	20.72	600

Sample No	At Failure				Failure Angle To Horizontal
	σ_3' (KPa)	$\sigma_1-\sigma_3$ (KPa)	Axial ϵ (%)	A	
1*	260	315	6.0	0.44	
2*	385	368	10.7	0.38	30 to 35°
3*	428	522	3.05	0.52	50°
HV-83-406**	79	396	6.2	0.18	
HV-83-406**	163	598	2.5	0.23	
HV-83-406**	293	977	2.1	0.32	

* Tested by the Author

** Tested by Thurber Consultant Ltd.

A = Pore Pressure Coefficient

Table H.4 Summary of Unconsolidated Undrained Traxial Tests on Bentonitic Mudstone

Sample No	Depth (m)	w (%)	P_L (%)	L_L (%)	γ_t KN/m^3
1*	11.9	30.1	39.8	76.5	19.68
HV-83-3/ C8**	21.7-22.0	16.8	30.1	75.1	21.14
HV-83-10/ C4**	13.4-14.30	21.3	21.4	76.2	20.02

Sample No	At Failure			Failure Angle To Horizontal
	σ_c (KPa)	$\sigma_1 - \sigma_3$ (KPa)	Axial ϵ (%)	
1*	350	264	5.5	25 and 40°
HV-83-3/ C8**	0	130	0.5	
HV-83-10/ C4**	0	151	0.5	

* Tested by the Author

** Tested by Hardy Associates

Table H.5 Summary of Drained Direct Shear Tests on Bentontic Mudstone

Sample No	Depth (m)	w (%)	w_{fa} (%)	w_{fp} (%)	γ_t KN/m³	e_o	S_i (%)
1	14	29.4	37.5	41.3	18.24	1.13	70.5
2	14	34.7	36.9	47.6	17.54	1.16	80.8
3	14	29.8	37.3		18.85	1.16	69.3
4	14						

Sample No	σ'_n (KPa)	τ'_p (KPa)	τ'_r (KPa)
1	286	81	51.5
2	400	150	92
3	525	202.5	155
4	156	43	32

w_{fa} = average water content at failure
w_{fp} = water content at plane of failure
S_i = initial degree of saturation

Table H.6 Summary of Drained Direct Shear Tests on Bentonte

Sample No	Depth (m)	w (%)	w_{fa} (%)	w_{fp} (%)	γ_t KN/m³	σ'_n (KPa)	τ'_p (KPa)	τ'_r (KPa)
1	17.2	53.3	53.2	52.0	16.17	338	176	63
2	17.2	49.8	52.7	54.6	15.75	525	249	180
3	17.2	45.8	45.5	47.1	15.78	625	194	121.5

w_{fa} = average water content at failure

w_{fp} = water content at plane of failure

Table H.7 Summary of Drained Direct Shear Tests on Bentonitic Mudstone Core Samples*, Highvale Mine

Borehole/ Sample #HV	Depth (m)	σ'_n (KPa)	τ'_p (KPa)	τ'_r (KPa)
83-3/C10	27.3	450	124	46
83-3/C19	27.3	1200	490	320
83-7/C9	30.2	400	445	212
83-8/C4	13.0	150	64	44
83-8/C9	24.0	606	143	66
83-9/C4	16.2	300	136	116
83-9/C8	29.1	450	217	94
83-10/C6	19.5	300	275	60
83-17/C7	23.0	450	286	155
83-406/7	11.6	150	113.8	40
		300	365.6	87
		600	456.7	120
83-406/9	14.3	150	317.7	40
		300	340.7	50
		600	729.9	160
83-406/11	14.7	150	88.5	47
		300	170.7	65
		600	298.5	105
83-408/RC10	36.85	400	231.9	75
	36.95	600	597.8	150
83-413/RC4A	9.04	200	160.5	50
83-413/RC4B	9.36	300	235.8	70
	9.56	500	366.7	75
83-415/RC3B	10.5	100	106.8	24
	10.85	200	159.9	63
83-415/RC5	16.7	300	536.8	80
83-416/RC8	33.16	600	459.1	250
83-417/RC7	31.95	350	232.7	100
	32.65	600	237.9	130
83-418/RC4	9.70	150	180.6	85

*Tested by Thurber Consultants Ltd., Hardy Associates Ltd., and Monenco Ltd.

Table H.8 Geological Descriptions of Core Samples, Highvale Mine

Borehole #/ Sample #	Geologic Descriptions*
HV-83-3 / C10	Highly fractured, shear zone? Slickensided, mudstone, a shattered siltstone lies immediately above it.
HV-83-3 / C19	Mudstone,fractured, slickensided.
HV-83-7 / C9	Mudstone, fractured, oriented 60 to 65 degrees, very carbonaceous, bentonitic; it is about 40 cm below a fractured mudstone and 2.4 m above the main coal seam.
HV-83-8 / C4	Mudstone, fractured, slickensided, polished, blocky; a melange zone underlies it, rubbly, decollement? The fractured mudstone together with the melange zone is about 2.64 m thick and is approximately 14.2 m above the main coal seam.
HV-83-8 / C9	Similar as above. It is about 4.2 m thick and is 3 m above the main coal seam.
HV-83-9 / C4	Mudstone, slightly carbonaceous, about 15.8 m above the main coal seam; the layers immediately above and below it does not show any sign of deformation.
HV-83-9 / C8	Mudstone, bentonitic, strongly deformed, folded and fractured mudstone is present immediately above and below it. It is about 1.8 m above the main coal seam.
HV-83-10 / C6	Mudstone, fractured at 15, 20, and 70 degrees, high degree of internal fracture, dark brown, slickensided, rubbly; a mudstone about 20 cm above it also shows fracturing and slickensided features. It is about 1.5 m above the main coal seam.

*Based on cored samples, and geologic and geophysical logs run by the Alberta Research Council and Monenco Ltd.

Table H.8 (continued)

HV-83-17 / C7	Mudstone, fractured, slickensided, dark brown green, high degree of internal fracturing, numerous coal clasts; the mudstone immediately overlies and underlies it shows fracturing and slickensided features; the coal seam is about 0.8 m beolow the layer.
HV-83-406 / 7, 9 11	Shale, weathered, carbonaceous, silty, bentonitic, CH, presence of hard coal chips; jointed and slickensided at certain elevation.
HV-83-408 / RC10	Shale, carbonaceous, silty, bentonitic, CH, jointed, presence of hard coal stringers.
HV-83-413 /RC4A RC4B	Shale, carbonaceous, silty, bentonitic, slickensided, hard; greenish glauconitic nodules?
HV-83-415 / RC3B RC5	Shale or hard clay, silty, CH, jointed, blocky structure, presence of coal stringers.
HV-83-416 / RC8	Shale, weathered, silty, hard, CH, highly jointed and slickensided.
HV-83-417 / RC7	Shale, silty, hard, CH, jointed, polished, numerous slickensides, presence of rock chips in soft matrix.
HV-83-418 / RC4	Shale, bentonitic, hard, CH, silty, minor thrust zone or shear plane.

Table H.9 Summary of Drained Direct Shear Test on Bentonite Core Samples*, Highvale Mine

Sample No	Depth (m)	w (%)	P_L (%)	L_L (%)	I_P (%)	I_L	γ_t KN/m^3
1977-78#4	25		47	238	191		16.48
1982#3		38.3	39	103	64	-0.01	17.95
83-10	20.7	49	46	178	132	0.02	
83-9	29.1	25	34	127	93	-0.10	
83-6	31.9	43	50	233	183	-0.04	

Sample No	Depth (m)	σ'_n (KPa)	τ'_p (KPa)	τ'_r (KPa)
1977-78#4	25	135	100	50
		280	100	30
		410	240	110
		570	260	100
1982#3		350	205	90
		450	235	90
		600	320	110
83-10	20.7	300	115	55
83-9	29.1	450	215	75
83-6	31.9	600	250	135

* Tested by Monenco Ltd. (1983, fig. E-12; 1984, fig. 3-13)

Table H.10 Strength Properties of Suspected Ice-Thrust Sediments

Sample No	Lithology	w (%)	γ_t KN/m³
A*	Sheared Bentonitic Clay	48	
B*	Weathered Mudstone	31.8	
C**	Sheared Bentonitic Clay		
D+	Sheared Interglacial Clay	30.0	18.84
E++	Sheared Clayshale	18.7	20.41
F++	Clayshale with Soft Zone	29.7	20.41
G++	Intact Clayshale		20.41

Sample No	P_L (%)	L_L (%)	I_P (%)	I_L	C.F (%)	Mont. (%)	Ill. (%)	Kaol. (%)
A*	39.8	100.0	60.2	0.14	47			
B*	20.1	84.8	64.7	0.18	52			
C**		60				50	50	
D+	25	72	47	0.11	76	30	35	25
E++	24.1	68.9	44.8	-0.12		45	36	19
F++	23.3	82.3	59.0	0.11				

Sample No	c' (KPa)	ϕ' deg.	c'_r (KPa)	ϕ'_r deg.
A*			0	5
			0	10
			0	9
B*	9.1	33		
D+			0	8 to 15
E++			0	10
F++			0	13
G++			0	15

C.F. = Clay Fraction (< 2 microns)

* Tested by Eigenbrod and Morgenstern (1972)
** Tested by Wilson (1974)
+ Tested by Insley et al. (1976)
++ Tested by Insley et al. (1976)

Appendix I - Examples of Glaciotectonic Facies

I.1 Escarpment Facies

I.1.1 Wabamun Lake Area

Figure I.1 is a north-south bedrock topographic cross-section drawn across the area at the southern shore of Wabamun Lake and is roughly perpendicular to the east-west trending interglacial North Saskatchewan Valley. The north-facing slope of this valley in the area has a gradient of 19 m/km and the valley is about 10.3 km wide between its top edges and about 5 km wide at its bottom. The north-facing bedrock slope gradient in the area probably does not represent the bedrock surface prior to the last glaciation because most of the slope is underlain by deformed bedrock (Figure I.1; Andriashek et al., 1979). Since the last general ice direction in the area near Highvale mine was from the north (Appendix C, Figure C.9a; Figure 10.3), it is inferred that the last glacier flowed across the interglacial North Saskatchewan Valley and compressed against the north-facing slope of the Valley at least in the Highvale mine area, causing subglacial bedrock deformation. The relatively lesser amount of deformed bedrock in the south-facing slope of the interglacial North Saskatchewan Valley and the large extent of ice-thrust features in the north-facing slope of the Valley also suggest this view. The area just south of the southern shore

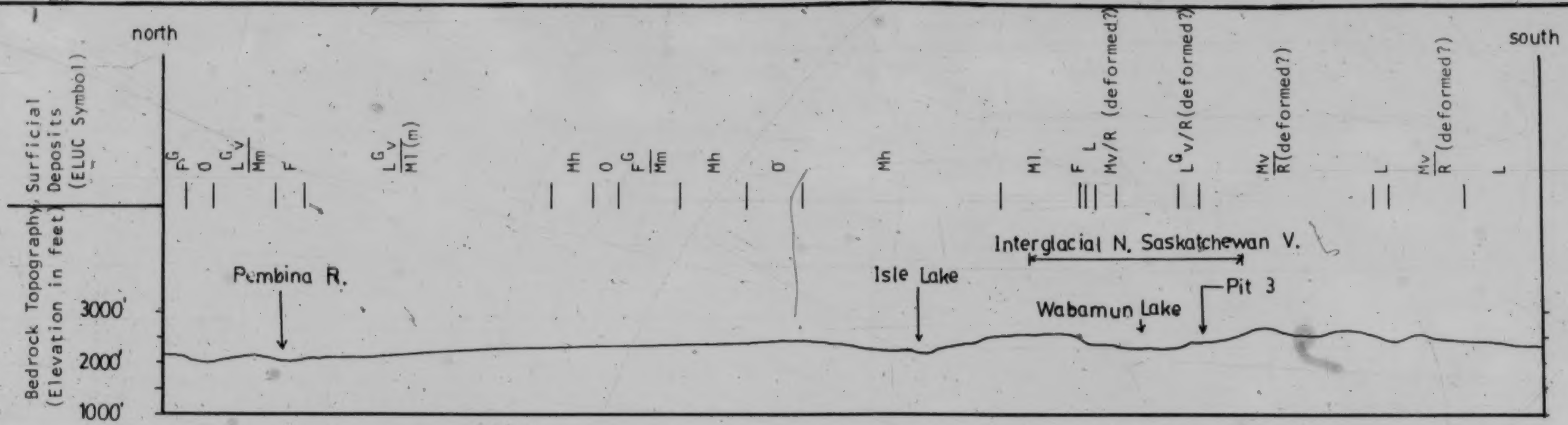
north
south
Surficial Deposits (ELUC Symbol)
Bedrock Topography (Elevation in feet)
3000'
2000'
1000'
Pembina R.
Isle Lake
Interglacial N. Saskatchewan V.
Wabamun Lake
Pit 3
Mh
Ml
Mv/R (deformed?)
Lv/R (deformed?)
Mv/R (deformed?)
Mv/R (deformed?)

Horizontal Scale: 1: 250,000
Vertical Scale: 1: 30,480

(Source: Carlson, 1971; Andriashek et al., 1979)
Vertical Exaggeration: 8.2 x

Figure I.1 : Bedrock Topographic Cross-Section, Wabamun Lake Area (cross-section drawn at 355° azimuth with respect to Section 1 measured in Pit 3, Highvale Mine)

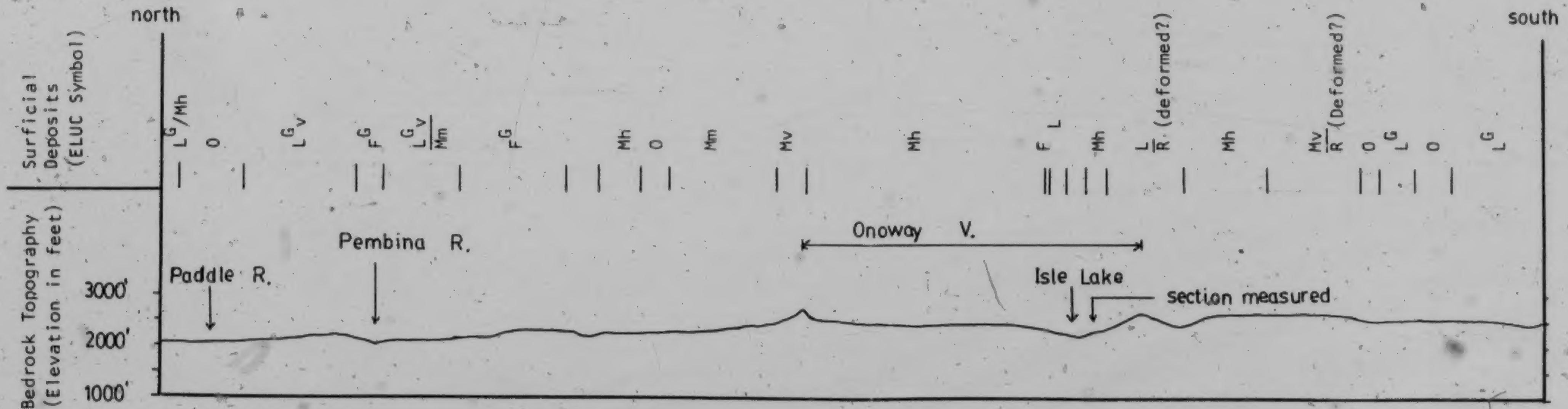
north
south
Surficial Deposits (ELUC Symbol)
Bedrock Topography (Elevation in feet)
3000'
2000'
1000'
Paddle R.
Pembina R.
Onoway V.
Isle Lake
section measured
Mh
Mm
Mv
L/R (deformed?)
Mv/R (Deformed?)

Horizontal Scale: 1: 250,000
Vertical Scale: 1: 30,480

(Source: Carlson, 1971; Andriashek et al., 1979)
Vertical Exaggeration: 8.2 x

Figure I.2 : Bedrock Topographic Cross-Section, Isle Lake Area (cross-section drawn at 355° azimuth with respect to the section measured near the southern shore of Isle Lake)

of Wabamun Lake is interpreted as an Escarpment Type glaciotectonic facies.

Figure I.2 shows that the ice-thrust features found at the southern shore of Isle Lake are located on the north-facing slope of the Onoway Valley which is about 16.6 km wide at its top and about 1.1 km at its bottom. This north-facing slope has a gradient of 39 m/km and rises from the thalweg of the Onoway Valley for a horizontal distance of 3.1 km southward before it slopes down into another meltwater channel. The ice-thrust features are located 0.9 km south and 30 m higher than the thalweg of the Onoway Valley. North of the Onoway Valley, the bedrock surface slopes gently northward with a gradient of about 4.7 m/km. From the adjacent ice direction indicators, the orientations of the ice-thrust ridges located at the southwestern side of the Isle Lake (Appendix C, Figure C.10), and the topography of the bedrock surface, the last ice probably advanced from the north to northeast, which might follow or flow across the Onoway Valley and compress against the north-facing bedrock slope situated just south of the modern Isle Lake. The presence of extensive hummocky moraine and ice-thrust features in the Onoway Valley and its adjacent terrain indicate that the ice margin was stagnant and had remained within the valley for some period of time.

The Isle Lake area is considered as an Escarpment Type or Valley Type glaciotectonic facies. The present information is not enough to distinguish which type the area belongs to.

Figure 8.2 is a fabric diagram of the Escarpment Type glaciotectonic facies found in the Wabamun Lake area.

I.1.2 Nisku Area

Figure I.3 shows that the northeast-facing wall of Blackmud Creek near the town of Nisku where ice-thrust features are observed, has a gradient of 35 m/km. This slope extends for a horizontal distance of about 0.55 km and then flattens gradually toward southwest.

In the Nisku area, if Blackmud Creek was present before the last glacial advance, the ice which probably flowed from a northeast direction into the area would compress the northeast-facing wall of Blackmud Creek, causing ice thrusting to take place. In this case, the Nisku area should be considered as an Escarpment Type glaciotectonic facies. However, if Blackmud Creek formed after the ice had retreated, then the ice-thrust features in the Nisku area were formed when the last glacier had flowed across this relatively featureless plain. Thus, this would be a Plains Type glaciotectonic facies. Recent subsurface information seems to suggest Nisku area has an Escarpment Type glaciotectonic facies. This is because the bedrock topography and preglacial thalwegs map in the Edmonton area (McPherson and Kathol, 1975, fig. 20) shows that the Blackmud Creek roughly follows the path of the Ellerslie preglacial valley southwards, and it is reasonable to

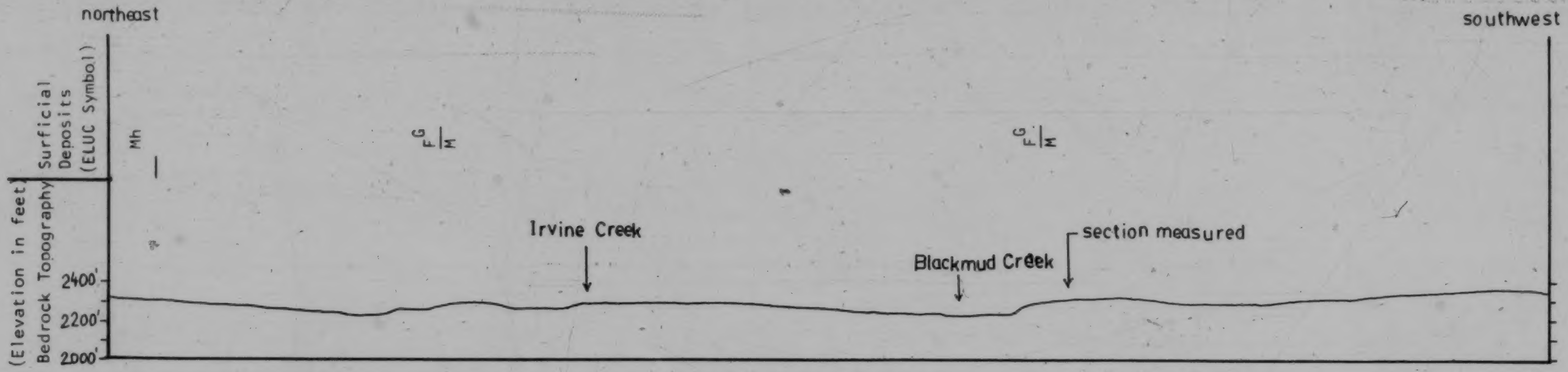
northeast
southwest
Surficial Deposits (ELUC Symbol)
(Elevation in feet) Bedrock Topography
Mh
F G / M
F G / M
Irvine Creek
Blackmud Creek
section measured
2400'
2200'
2000'

Horizontal Scale: 1: 50,000
Vertical Scale: 1: 7,620

(Source: Carlson, 1967, figs. 2c,2d; Bayrock, 1972)
Vertical Exaggeration: 6.6 x

Figure I.3 : Bedrock Topographic Cross-Section, Nisku Area (cross-section drawn at N35° E with respect to the section measured at the Nisku Area)

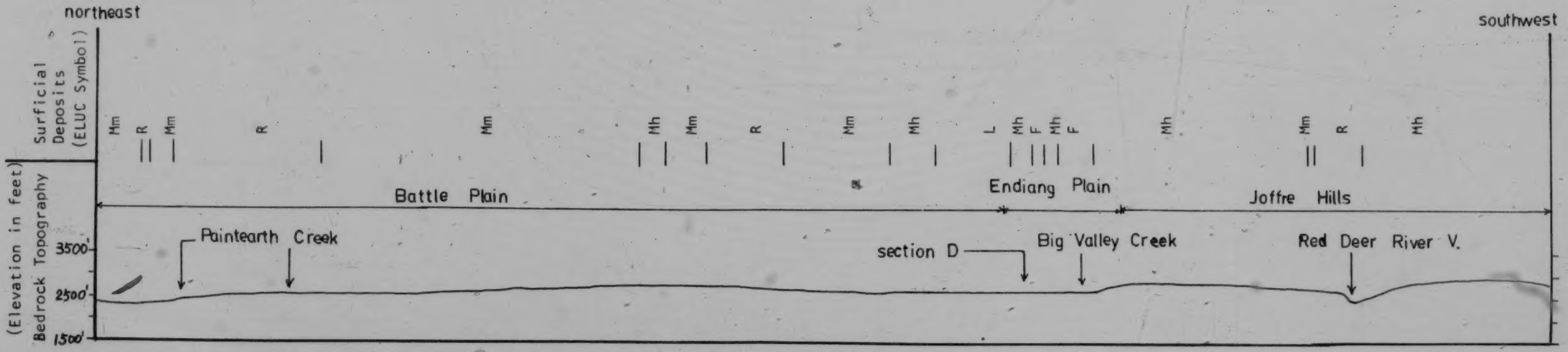
northeast
southwest
Surficial Deposits (ELUC Symbol)
(Elevation in feet) Bedrock Topography
Mm
R
Mm
R
Mm
Mh
Mm
R
Mm
Mh
L
Mh
F
Mh
F
Mh
Mm
R
Mh
Battle Plain
Endiang Plain
Joffre Hills
Paintearth Creek
section D
Big Valley Creek
Red Deer River V.
3500'
2500'
1500'

Horizontal Scale: 1: 250,000
Vertical Scale: 1: 30,480

(Source: Stalker, 1960a, map 1081A; Farvolden, 1963a, fig. 14)
Vertical Exaggeration: 8.2 x

Figure I.4 : Bedrock Topographic Cross-Section, Lowden Lake Area (cross-section drawn at N45° E with respect to section D measured south of Lowden Lake)

believe that both the Creek and the preglacial valley run together for another 20 km in approximately the same direction into the Nisku area.

I.1.3 Lowden Lake Area

Due to insufficient information on the bedrock topography in the Red Deer - Stettler area, only the bedrock topographic cross-section of the Lowden Lake area has been constructed.

Figure I.4 shows that ice-thrust features occur on the Endiang and the Battle Plains. The slope of these Plains dip gently to the northeast and have a gradient of 2.1 m/km. The Joffre Hills, which are located about 4.3 km southwest from the ice-thrust features, forms a topographic high that rises toward southwest with a gradient of 16.6 m/km for a horizontal distance of about 2.75 km before it gradually slopes toward the modern Red Deer River (Figure I.4). Hummocky moraine covers the topographic highs, the Endiang Plain and the southwestern portion of the Battle Plain. The Lowden Lake area has an Escarpment Type glaciotectonic facies. Figure 8.3 is a fabric diagram of the area.

I.1.4 Cypress Hills Area

Bedrock topographic maps (Westgate, 1968, fig 6) shows that both Pits 39 (topo. elev. : 1097 m) and 45 (topo. elev. : 1234 m) in Cypress Hills area (Appendix C, Figure C.28) are located on a spur of a elongated butte which points roughly toward the north and with its sides facing northeast and northwest. The heads of tributaries of the preglacial Medicine Hat Valley extend very close to the spur. Compared with the topographic elevation of glacial sediments deposited by the Elkwater and Wild Horse glaciers in the Cypress Hills area, it is noted that the study area has been glaciated by both glaciers. Glacial lineations, the attitudes of the ice-thrust structures and glacial deposits suggest that the last glacier had advanced into the study area from the northeast and northwest (Appendix C, Figure C.30).

Figure I.5 shows the NW-SE bedrock topographic cross-section which indicates that the study area (Pits 39 and 45) is located near the top edge of the northwest-facing slope of the preglacial Medicine Hat Valley. The study area is located at approximately 36.5 km horizontally and 0.53 km vertically from the thalweg of the Medicine Hat Valley. From the top edge of the valley to about 1 km northwestward of Pit 39, the bedrock surface has a gradient of about 50.8 m/km; and from there northwestward to the thalweg of the valley, the surface becomes much gentler and has a gradient of about 11.6 m/km (Figure I.5).

Figure I.6 is the NE-SW bedrock topographic cross-section and shows that the tributary of the Medicine Hat Valley and meltwater channel have formed relative steep topographic highs and lows near the top edge of the Medicine Hat Valley. The study area is located on the

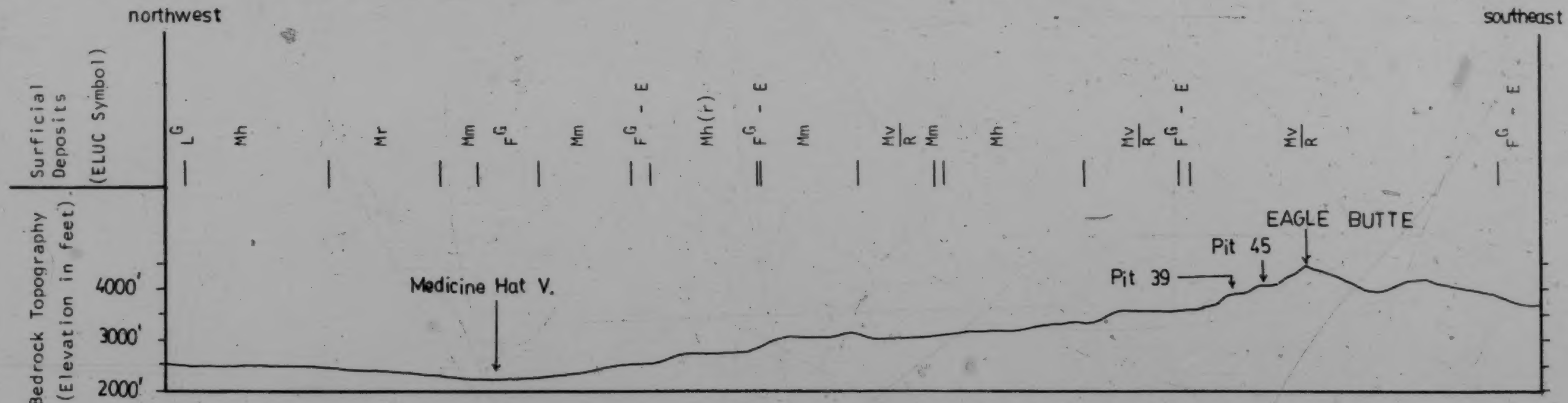

Horizontal Scale: 1: 250,000
Vertical Scale: 1: 30,480

(Source: Westgate, 1968, fig. 6, map29)
Vertical Exaggeration: 8.2 x

Figure I.5 : Bedrock Topographic Cross-Section, Cypress Hills Area (cross-section drawn at N45° W with respect to the section measured at Pit 45 of the Area)

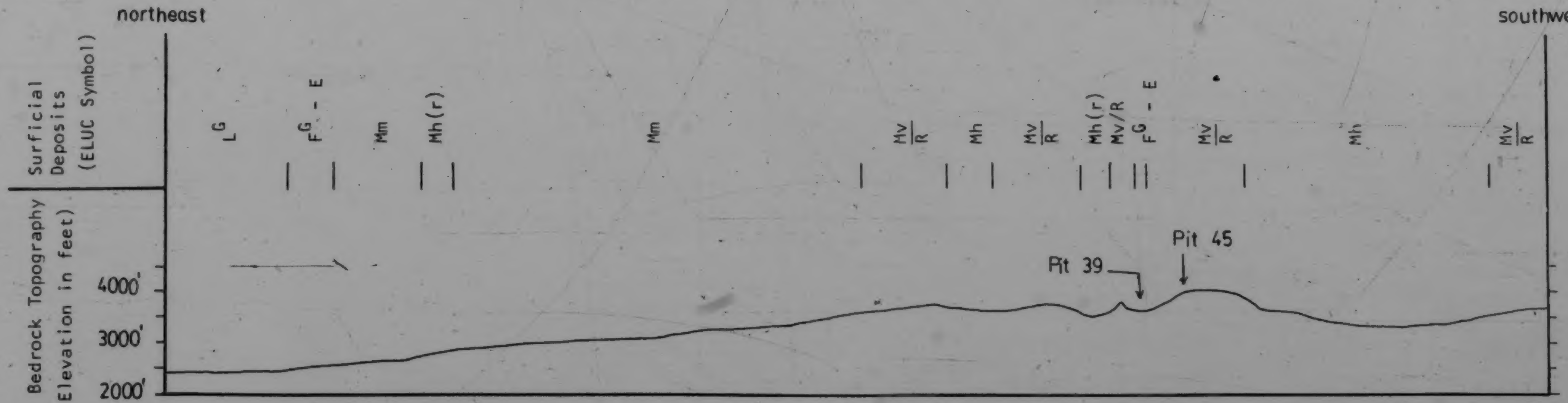

Horizontal Scale: 1: 250,000
Vertical Scale: 1: 30,480

(Source: Westgate, 1968, fig. 6, map29)
Vertical Exaggeration: 8.2 x

Figure I.6 : Bedrock Topographic Cross-Section, Cypress Hills Area (cross-section drawn at N45°E with respect to the section measured at Pit 45 of the Area)

northeast-facing slope of one of these highs and lows with a gradient of about 52.3 m/km. Away from these highs and lows, the bedrock surface dips gently northeastward with a gradient of about 11.6 m/km. Plate I.1 shows the change in slope gradient near the Eagle Butte district, Cypress Hills area. Although the study area is located on a terrain of bedrock veneered with till, hummocky disintegration moraine is found at about 7.5 km northwest, 1.5 km northeast and 2.8 km southwest of the study area (Appendix C, Figure C.28).

The study area is considered as an Escarpment Type glaciotectonic facies.

I.2 Valley Facies

I.2.1 Edmonton City Area

Figures I.7 and I.8 are the bedrock topographic cross-sections of the area drawn perpendicular to the thalweg of the preglacial valley (trending NE-SW) and its tributaries (trending NW-SE). Bedrock topographic cross-sections show that ice-thrust features appear on one or both sides of the walls of the preglacial valleys in the city of Edmonton (Figures I.7 and I.8).

At the location where the cross-section is drawn, the Beverly Valley has a width of about 8.5 km between its top edges and 3.75 km at its bottom. The gradients of the northwest-facing and southeast-facing slopes are 23 m/km and 32 m/km respectively (Figure I.7). Suspected ice-thrust

Plate I.1 Looking South Toward Eagle Butte District, Cypress Hills Area

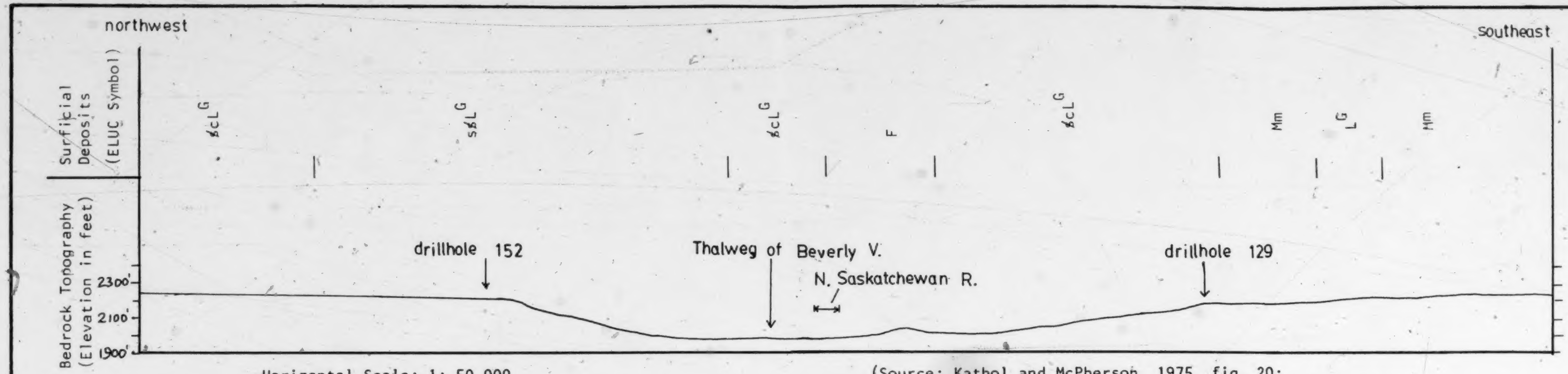
northwest
southeast
Surficial Deposits (ELUC Symbol)
Bedrock Topography (Elevation in feet)
ℓcL G
sℓL G
ℓcL G
F
ℓcL G
Mm
L G
Mm
drillhole 152
Thalweg of Beverly V.
N. Saskatchewan R.
drillhole 129
2300'
2100'
1900'

Horizontal Scale: 1: 50,000
Vertical Scale: 1: 7,620

(Source: Kathol and McPherson, 1975, fig. 20;
McPherson and Kathol, 1972; Bayrock, 1972)
Vertical Exaggeration: 6.6 x

Figure I.7 : Bedrock Topographic Cross-Section, Edmonton Area (cross-section drawn at N54° W with respect to drill holes 129 and 152 and is also perpendicular to the Thalweg of the Beverly Valley)

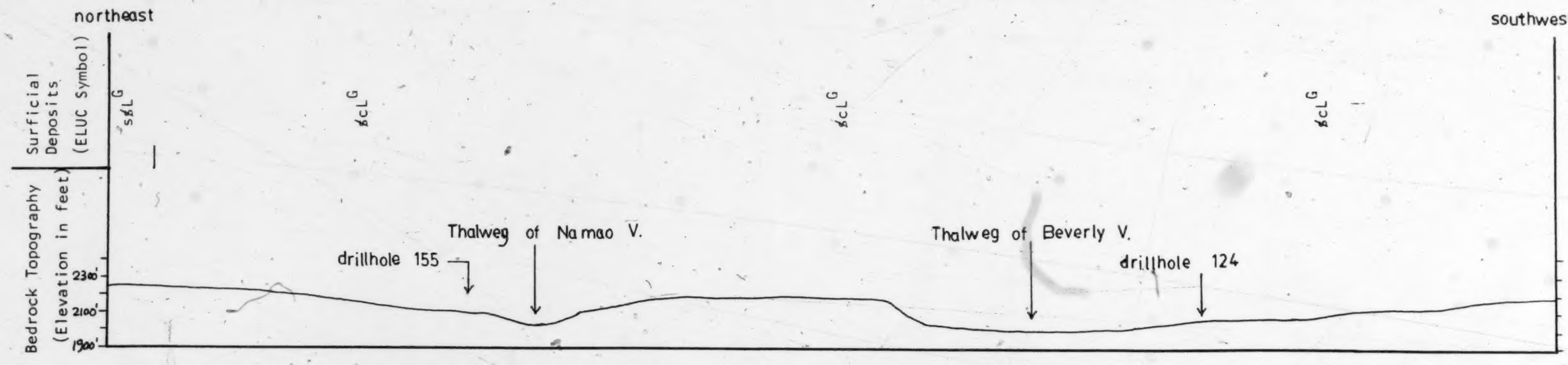
northeast
southwest
Surficial Deposits (ELUC Symbol)
Bedrock Topography (Elevation in feet)
sℓL G
ℓcL G
ℓcL G
ℓcL G
Thalweg of Namao V.
drillhole 155
Thalweg of Beverly V.
drillhole 124
2300'
2100'
1900'

Horizontal Scale: 1: 50,000
Vertical Scale: 1: 7,620

(Source: as above)
Vertical Exaggeration: 6.6 x

Figure I.8 : Bedrock Topographic Cross-Section, Edmonton Area (cross-section drawn at N52° E with respect to drillholes 124 and 155 and is also perpendicular to the Thalweg of the Beverly Valley)

features are found on the top edge of the northwest-facing slope (drillhole 129). They are situated 5 km southeast and 61 m higher than the thalweg of the Beverly Valley. On the top edge of the southeast-facing slope (drillhole 152), suspected ice-deformed bedrock is noticed at 3.3 km northwest and 69 m higher than the thalweg of the valley.

Figure I.8 indicates that suspected ice-thrust features are observed in drillholes on the northeast-facing slope of the Beverly Valley which has a gradient of 11 m/km. The Valley is at least 7.5 km wide at its top and 2 km wide at its bottom. These features are found at 1.9 km southwest and 15 m higher than the thalweg of the Beverly Valley. Suspected ice-thrust features are also found in drillholes located in the southwest-facing slope of the Namao Valley which has a gradient of 28 m/km. The features are about 0.75 km northeast and 21 m higher than the thalweg of the Namao Valley. The widths of the top and bottom of the Namao Valley are about 4 km and 0.35 km respectively.

In the Edmonton city vicinity, the appearance of ice-thrust features on both sides of the preglacial valleys, the trend of these valleys, and the general ice flow direction (NE-SW) in the area suggest that the last glacier entered the area and flowed along the preglacial valleys. The location of the ice-thrust features in these preglacial valleys which show on the bedrock topographic cross-sections strongly support this view (Figures I.7 and I.8). In this case, the Edmonton city area has a Valley Type glaciotectonic facies.

I.3 Plains Facies

I.3.1 Hanna - Sedgewick Area

The bedrock surface of the Alliance - Galahad - Hardisty district dips gently toward northeast with a gradient of about 2.2 m/km except that, in the spillway (which is occupied by the Battle River) and its tributary, the surface becomes rolling and undulatory. The north-facing slope of the tributary has a gradient of 27 m/km with ice-thrust features located at its base (Figure I.9).

The bedrock surface of the Castor - Coronation - Brownfield district is featureless and flat as shown in Figure I.10. Northeast of Highway 36 in the area, the surface has a gradient of about 2.6 m/km toward the northeast; while southwest of the highway, the surface dips southwestward with a gradient of 4.6 m/km. The above districts are mainly covered by ground moraine and glaciofluvial deposits.

It is known that ice thrusting tends to occur on upland slopes such as escarpments and valley walls (Chapter 2, Section 2.3.2). The occurrence of ice-thrust features in the study area which is located on a relatively flat to very gently inclined bedrock surface suggests that ice thrusting could occur on relatively flat surface. The districts are considered as a Plains Type glaciotectonic facies.

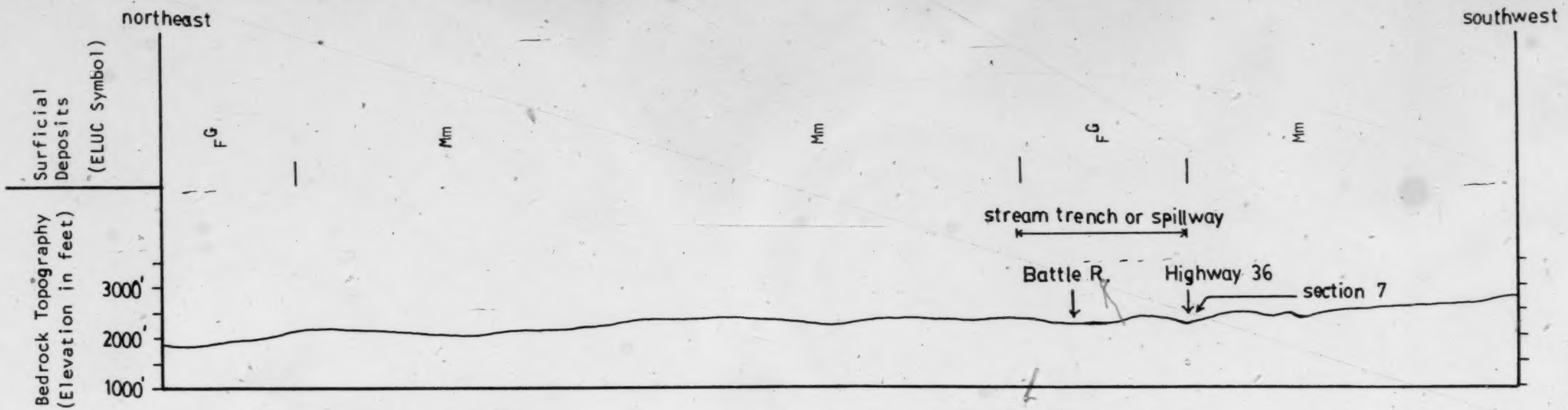
northeast
southwest
Surficial Deposits (ELUC Symbol)
F^G
Mm
Mm
F^G
Mm
stream trench or spillway
Battle R.
Highway 36
section 7
Bedrock Topography (Elevation in feet)
3000'
2000'
1000'

Horizontal Scale: 1: 250,000
Vertical Scale : 1: 30,480

(Source: Carlson and Topp, 1972; Bayrock, 1958a, map 57-2A; Bayrock, 1958b, maps 57-3A, 57-3B)
Vertical Exaggeration: 8.2 x

Figure I.9 : Bedrock Topographic Cross-Section, Alliance-Galahad-Hardisty Districts

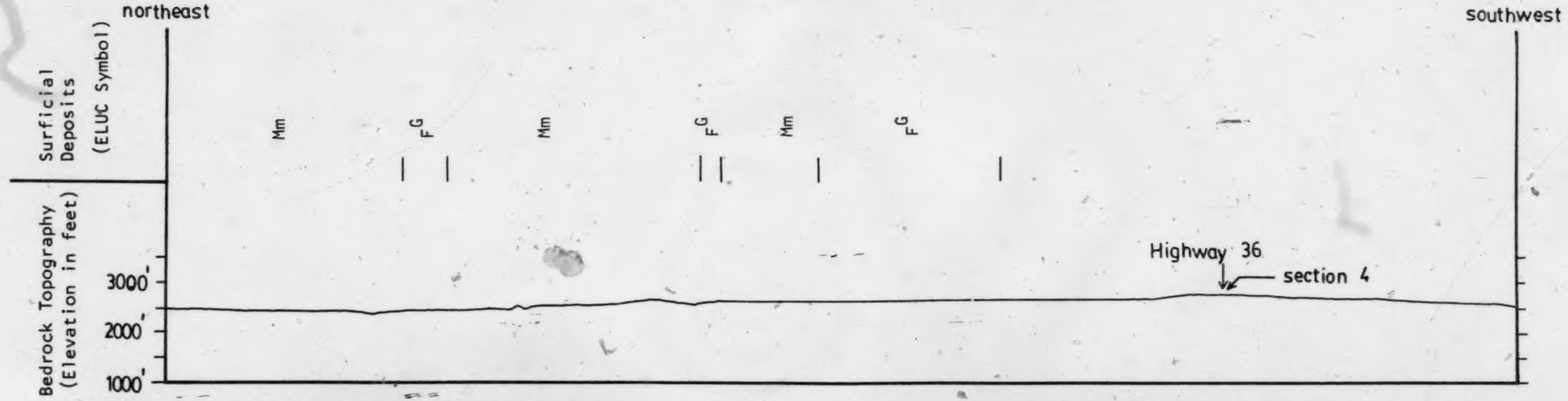
northeast
southwest
Surficial Deposits (ELUC Symbol)
Mm
F^G
Mm
F^G
Mm
F^G
Highway 36
section 4
Bedrock Topography (Elevation in feet)
3000'
2000'
1000'

Horizontal Scale: 1: 250,000
Vertical Scale: 1: 30,480

(Source: Carlson, 1970; Carlson and Topp, 1972; Gravenor and Bayrock, 1955, mapp 55-1; Gravenor, 1956, map 56-2; Bayrock, 1958a, map57-2B)
Vertical Exaggeration: 8.2 x

Figure I.10 : Bedrock Topographic Cross-Section, Castor-Coronation-Brownfield Districts (cross-section drawn at N45° E with respect to section 4 measured in the Area)

I.3.2 Northwest of Sullivan Lake Area

The bedrock topographic map shows that the study area is situated at the northwest-facing valley of the Buffalo Lake bedrock preglacial channel and the Halkirk Divide. This is a ridge with very gentle and rounded crest that separates the Battle Plain and the Endiang Plain, and is located just south of the study area (Farvolden, 1963a, fig. 14). The Buffalo Lake bedrock channel is one of the many preglacial bedrock channels in southern Alberta which are mature river valleys that occupy broad lowland areas between widely separated low and rounded upland areas (Farvolden, 1963b, p. 66). These preglacial valleys are usually 3 - 16 km wide with gently sloping valley walls (Stalker, 1961). The bedrock surface of the region around the study area has a gradinet of 3.0 and 4.4 m/km toward northwest and northeast respectively and can be approximated as a flat surface.

The study area is referred to as a Plains Type glaciotectonic facies. Figure 8.4 is a fabric diagram of this facies observed in the Hanna - Sedgewick area and the area northwest of Sullivan Lake.